UC San Diego

UC San Diego Electronic Theses and Dissertations

Title

Enzyme Activity, Bacteria, and Pollution in Sea Spray Aerosol

Permalink

https://escholarship.org/uc/item/4q54639s

Author

Pendergraft, Matthew Allen

Publication Date

2022

Peer reviewed|Thesis/dissertation

eScholarship.org Powered by the California Digital Library
University of California

UNIVERSITY OF CALIFORNIA SAN DIEGO

Enzyme Activity, Bacteria, and Pollution in Sea Spray Aerosol

A dissertation submitted in partial satisfaction of the requirements

for the degree Doctor of Philosophy

in

Oceanography

by

Matthew Allen Pendergraft

Committee in charge:

Professor Kimberly Prather, Chair
Professor Lihini Aluwihare
Professor Rommie Amaro
Professor Farooq Azam
Professor Susan Giddings
Professor Francesca Malfatti

2022

Copyright

Matthew Allen Pendergraft, 2022

All rights reserved.

The Dissertation of Matthew Allen Pendergraft is approved, and it is acceptable in quality and form for publication on microfilm and electronically.

University of California San Diego

2022

DEDICATION

To my family, who are my friends, and to my friends, who are family.

.

EPIGRAPH

"Our work suggests that viruses are carried by the aerosol created by the surf as well as the open ocean, and suggests that seawater in which raw sewage is present may produce an airborne health hazard."

- E. R. Baylor, M. B. Baylor, Duncan C. Blanchard, Lawrence D. Syzdek, Curtis Appel, *Virus Transfer from Surf to Wind (1977)*

"Like Farooq would say, simplify, whatever that means."

- Prof. Francesca Malfatti

"Knowledge without sharing is not really knowledge."

- Kumeyaay elder, as told to, and re-told by, Dr. Stanley Rodriguez

TABLE OF CONTENTS

LIST OF ABBREVIATIONS

AF	aerosolization factor
ALK	alkaline phosphatase
AMP	aminopeptidase
APS	aerodynamic particle sizer
ASV	amplicon sequencing variant
CCN	cloud condensation nuclei
CSIDE	Cross Surfzone/Inner-shelf Dye Exchange Study
chl-a	chlorophyll a
CWP	coastal water pollution
DOM	dissolved organic matter
EDTA	ethylenediaminetetraacetic acid
FASW	filtered autoclaved seawater
HB	heterotrophic bacteria
HEPA	high efficiency particulate air
IBa	Imperial Beach aerosol
IBPw	Imperial Beach Pier seawater
IMP	impinger
IN	ice nucleus
INP	ice nucleating particle
LC-MS/MS	liquid chromatography tandem mass spectrometry
LIP	lipase
LoD	limit of detection

LPM	liters per minute
MART	marine aerosol reference tank
MS	mass spectrometry
MS/MS	product ion mass spectrometry
OM	organic matter
PBS	phosphate buffer solution
PCR	polymerase chain reaction
PGE	1x PBS at 20% (v/v) glycerol and 20 mM EDTA
RA	relative abundance
RPCA	Robust Aitchinson principal component analysis
RWT	rhodamine water tracer dye
SIOPa	Scripps Institution of Oceanography Pier aerosol
SIOPw	Scripps Institution of Oceanography Pier seawater
SMA	secondary marine aerosol
SML	surface microlayer
SPE	solid phase extraction
SPOT	Aerosol Devices Inc. Series 100 Universal Spot Sampler
SR	sampling round
SSA	sea spray aerosol
ST2	SourceTracker2
SW	seawater
TJRW	Tijuana River water

LIST OF FIGURES

LIST OF TABLES

ACKNOWLEDGEMENTS

I thank my advisor, Professor Kimberly Prather, for bringing me into her research group and providing me with the opportunity to pursue research I found both interesting and important. I am very grateful to her for giving me the chance to work on an issue that matters a lot to my hometown and I, and also affects many people globally. I am also grateful for being given decision making roles, because it is rewarding to design the research one conducts. The research design is perhaps the most important part.

I thank my thesis committee for giving me their time and attention. I wish I spent still more time with them. Professor Lihini Aluwihare helped me transition to the Marine Chemistry and Geochemistry curricular group and allowed me to join her research group meetings. This provided me with additional opportunities to discuss my research with others, see other people's research, and to strengthen my academic community. These meetings also sprouted the productive collaboration with Dr. Daniel Petras. Thank you Professor Rommie Amaro; I wish I had bugged you more. Professor Farooq Azam met with me on multiple occasions to provide valuable insight into the marine microbial research I conducted. He also allowed me to use his lab to conduct parts of my research. His group provided additional support. Thank you very much to Professor Sarah Giddings for spending time with me as if I was your student. I greatly appreciate your willingness to assist me with my data analysis/coding, which is such an important part of the research, and also my writing. I am very grateful to you and Professor Falk Feddersen for allowing our group to join the Cross Surfzone Inner Shelf Dye Exchange Experiment (CSIDE). This completely changed my PhD, and allowed me to benefit from your guidance. Professor Francesca Malfatti has been something like a secondary advisor. She guided

my research and was someone who would work out the details with me. The time we spent making measurements and discussing data was invaluable.

I thank the Prather research group for working as a team and shouldering significant responsibilities. I got to work with very talented people here. Thank you to: Kevin Axelrod, Hashim Al-Mashat, Nicole Campbell, Lucia Cancelada, Dr. Richard Cochran, Adriana Corrales, Dr. Douglas Collins, Josh Cox, Dr. Gavin Cornwell, Sierra DeAngelo, Dr. Charlotte Dewald (née Beall), Dr. Julie Dinasquet, Dr. Abby Dommer, Lee Elmont, Dr. Luisa Galgani, James Garrafa-Luna, Wyeth Gibson, Dr. Charbel Harb, Maile Heyer, Ikran Ibrahim, Young Jeong, Ke'La Kimble, Tricia Light, Dolan Lucero, Dr. Louise Kristensen, Dr. Totti Laitinen, Dr. Christopher Lee, Raymond Leibensperger III, Joseph Manson, James Mayer, Dr. Kathryn Mayer, Dr. Brock Mitts, Alexia Moore, Kathryn Moore, Alma Anides Morales, Clare Morris, Dr. Daniel Petras, Brooke Rasina, Robin Richardson, Ben Rico, Dr. Olivia Ryder, Greg Sandstrom, Dr. Mitchell Santander, Bas Schapp, Dr. Jamie Schiffer, Dr. Rebecca Simpson, Dr. Camille Sultana, Sabrina Ufer, Dr. Xiaofei Wang, and Jake Weber. Special thanks to Joe Mayer and Monica Castrejon for being especially adept and making things happen.

Many thanks to all of my collaborators, including the Knight Lab, the Dorrestein Lab, the Aluwihare Lab, the Azam Lab, Brian Seegers and Alan Saluk at the TSRI flow core facility. I greatly appreciate all the students at SIO, and previously at Tulane University, that I got to know and work with. The students are the fabric of SIO; they are carrying out the work; they are initiating collaborations; they often originate the ideas for the research; and their doors are always open; thank you SIO students. Thank you in particular to the 2014 cohort, my MCG friends, and my CASPO friends. I’m lucky to have spent time with you. Thank you Keiara Auzenne for taking on a problem greater than our walls and having great success. I thank all my

professors at SIO. I struggled in the coursework at times and only value it more and more. Thank you for giving me your time and giving me a chance, or two.

I thank all those from whom I learned prior to starting my PhD: my master's advisor Professor Brad Rosenheim and the Stable Isotope Lab at Tulane University; Maria dos Santos Afonso, Enrique San Roman, Horacio Bogo, the group at YPF, and my friends in Buenos Aires; Professors Jane Teranes and Mark Thiemens from UCSD Environmental Systems; David Merks, Eileen Maher, Damon LaCasella, Phil Gibbons and everyone else at the Port of San Diego Environmental Services Department from my internship there.

I thank my family. I could not have been raised in a better environment. My Mom and Dad, Julie and Kim, provided me with everything necessary to succeed in life and be happy, both tangible and intangible things. Thank you for setting a good example, across the board, from how to treat others to how to work hard. My siblings Breanne, Jeanette, and Vernon: you mean so much to me. Thank you to Cynthia and Beatrice for joining me for this last 18.75 months. Lastly, I benefit from great privilege, and I hope to use it to help others.

Chapter 2, in full, is currently being prepared for submission: Pendergraft, M.A., Malfatti, F., Morris, C.K., Santander, M.V., DeAngelo, S., Mayer, K.J., Sauer, J.S., Wang, X., Azam, F., Prather, K.A. (in prep) Sea Spray Aerosol Enzyme Activity is Qualitatively Distinct from its Source Waters. The dissertation author is the primary investigator and author of this manuscript.

Chapter 3, in full, is currently being prepared for submission for publication of the material. Pendergraft, M.A., Minich, J.J., Belda-Ferre, P., Morris, C.K., Malfatti, F., Knight, R., Prather, K. (*in prep*), *Advances in Sea Spray Aerosol 16S Sequencing Reveal a Dynamic*

Community. The dissertation author and Dr. Jeremiah J. Minich are co-first authors of this manuscript.

Chapter 4, in full, is a reprint of material that has been published in PeerJ. Pendergraft, M.A., Grimes, D.J., Giddings, S.N., Feddersen, F., Beall, C.M., Lee, C., Santander, C., Prather, K.A. (2021). Airborne Transmission Pathway for Coastal Water Pollution. PeerJ 9:e11358 DOI: 10.7717/peerj.11358. The dissertation author is the primary investigator and author of this publication.

Chapter 5, in full, has been submitted to Environmental Science & Technology for publication, where it is currently in review. Pendergraft, M. A., Belda-Ferre, P., Petras, D., Morris, C. K., Mitts, B. A., Aron, A. T., Bryant, M., Schwartz, T., Ackermann, G., Humphrey, G., Kaandorp, E., Dorrestein, P. C., Knight, R., Prather, K. A. Bacterial and chemical evidence of coastal water pollution from the Tijuana River in sea spray aerosol. The dissertation author is the primary author of the manuscript.

VITA

2007 Bachelor of Science, University of California San Diego

2007 Bachelor of Arts, University of California San Diego

2013 Masters of Science, Tulane University

2021 Masters of Science, University of California San Diego

2022 Doctor of Philosophy, University of California San Diego

PUBLICATIONS

Pendergraft, M.A., Beldá-Ferre, P., Petras, D., Morris, C.K., Mitts, B.A., Aron, A.T., Bryant, M., Schwartz, T., Ackermann, G., Humphrey, G., Kaandorp, E., Dorrestein, P.C., Knight, R., Prather, K.A. (in review at *Environmental Science & Technology*) Bacterial and chemical evidence of coastal water pollution from the Tijuana River in sea spray aerosol.

Sauer, J.S., Mayer, K.J., Lee, C., Alves, M.R., Amiri, S., Bahaveolos, C.J., Franklin, E.B., Crocker, D.R., Dang, D., Dinasquet, J., Garofalo, L.A., Kaluarachchi, C.P., Kilgour, D.B., Mael, L.E., Mitts, B.A., Moon, D.R., Moore, A.N., Morris, C.K., Mullenmeister, C.A., Ni, CM., Pendergraft, M.A., Petras, D., Simpson, R.M.C., Smith, S., Tumminello, P.R., Walker, J.L., DeMott, P.J., Farmer, D.P., Goldstein, A.H., Grassian, V.H., Jaffe, J.J., Malfatti, F., Martz, T.R., Slade, J.H., Tivanski, A.V., Bertram, T.H., Cappa, C.D., Prather, K.A. (2022). The Sea Spray Chemistry and Particle Evolution study (SeaSCAPE): overview and experimental methods. *Environmental Science: Processes & Impacts*, 24, 290-315

Schmid, R., Petras, D., Nothias, L.F., Wang, M., Aron, A.T., Jagels, A., Tsugawa, H., Rainer, J., Garcia-Aloy, M., Duhrkop, M., Korf, A., Pluskal, T., Kamenik, Z., Jarmusch, A.K., Caraballo-Rodriguez, A.M., Weldon, K.C., Nothias-Esposito, M., Akssenov, A.A., Bauermeister, A., Albarracin Orio, A., Grundmann, C.O., Vargas, F., Koester, I., Gauglitz, J.M., Gentry, E.C., Hovelmann, Y., Kalinina, S.A., Pendergraft, M.A., Panitchpakdi, M., Tehan, R., Le Gouellec, A., Aleti, G., Mannochio Russo, H., Arndt, B., Hubner, F., Hayen, H., Zhi, H. Raffatellu, M., Prather, K.A., Aluwihare, L.I., Bocker, S., McPhail, K.L., Humpf, H.U., Karst, U., Dorrestein, P.C. (2021). Ion identity molecular networking for mass spectrometry-based metabolomics in the GNPS environment. *Nature Communications*, 12, 3832.

Pendergraft, M.A., Grimes, D.J., Giddings, S.N., Feddersen, F., Beall, C.M., Lee, C., Santander, C., Prather, K.A. (2021). Airborne transmission pathway for coastal water pollution. *PeerJ* 9:e11358

Santander, M.V.; Mitts, B.A.; Pendergraft, M.A.; Dinasquet, J.; Lee, C.; Moore, A.N.; Cancelada, L.B.; Kimble, K.A.; Malfatti, F.; Prather, K.A. (2021) Tandem fluorescence measurements of organic matter and bacteria released in sea spray aerosols. *Environmental Science & Technology*, 55, 5171–5179.

Crocker, D.R., Hernandez, R.E., Huang, H.D., Pendergraft, M.A., Cao, R., Dai, J., Morris, C.K., Deane, G.B., Prather, K.A., Thiemens, M.H., (2020) Biological influence on $\delta^{13}C$ and organic composition of nascent sea spray aerosol. *ACS Earth & Space Chemistry*, 4(9), 1686-1699.

Hasenecz, E.S., Jayarathne, T., Pendergraft, M.A., Santander, M.V., Mayer, K.J., Sauer, J.S., Lee, C., Gibson, W., Kruse, S., Malfatti, F., Prather, K.A. and Stone, E. (2020). Marine bacteria affects saccharide enrichment in sea spray aerosol during a phytoplankton bloom, *ACS Earth & Space Chemistry*, 4(9), 1638–1649.

Malfatti, F., Lee, C., Tinta, T., Pendergraft, M.A., Celussi, M., Zhou, Y., Sultana, C.M., Rotter, A., Axson, J.L., Collins, D.B., Santander, M.V., Anides Morales, A.L., Aluwihare, L.I., Riemer, N., Grassian, V.H., Azam, F., Prather, K.A. (2019). Detection of active microbial enzymes in nascent sea spray aerosol: Implications for atmospheric chemistry and climate. *Environ. Sci. Technol. Lett*., 6(3), 171–177.

Nandy, L., Liu, S., Gunsbury, C., Wang, X., Pendergraft, M.A., Prather, K.A., Dutcher, C.S. (2019) Multistep phase transitions in sea surface microlayer droplets and aerosol mimics using microfluidic wells. *ACS Earth & Space Chemistry*, 3(7), 1260-1267.

Schiffer, J.M., Luo, M., Dommer, A.C., Thoron, G., Pendergraft, M.A., Santander, M.V., Lucero, D., Pecora de Barros, E., Prather, K.A., Grassian, V.H., Amaro, R.E. (2018). Impacts of lipase enzyme on the surface properties of marine aerosols. *J. Phys. Chem. Lett*., 9(14), 3839–3849.

Jayarathne, T., Sultana, C.M., Lee, C., Malfatti, F., Cox, J.L., Pendergraft, M.A., Moore, K.A., Azam, F., Tivanski, A.V., Cappa, C.D., Bertram, T.H., Grassian, V.H., Prather, K.A., Stone, E.A. (2016). Enrichment of saccharides and divalent cations in sea spray aerosol during two phytoplankton blooms. *Environmental Science & Technology*, 50(21), 11511–11520.

Rosenheim, B.E., Pendergraft, M.A., Flowers, G.C., Carney,R., Sericano, J.L., Amer, R.M., Chanton, J., Dincer, Z., Wade, T.L. (2016). Employing extant stable carbon isotope data in Gulf of Mexico sedimentary organic matter for oil spill studies. *Deep Sea Research Part II: Topical Studies in Oceanography*, 129, 249-258.

Wang, X., Sultana, C.M., Trueblood, J., Hill, T.C.J., Malfatti, F., Lee, C., Laskina, O., Moore, K.A., Beall, C.M., McCluskey, C.S., Cornwell, G.C., Zhou, Y., Cox, J.L., Pendergraft, M.A., Santander, M.V., Bertram, T.H., Cappa, C.D., Azam, F., DeMott, P.J., Grassian, V.H., Prather, K.A. (2015). Microbial control of sea spray aerosol composition: A tale of two blooms. *ACS Central Science*, 1(3), 124–131.

Fernandez, A., Santos, G.M., Williams, E.K., Pendergraft, M.A., Vetter, L., Rosenheim, B.E. (2014) Blank corrections for ramped pyrolysis radiocarbon dating of sedimentary and soil organic carbon. *Analytical Chemisty*, 86(24), 12085–12092

Pendergraft, M.A., Rosenheim, B.E. (2014) Varying relative degradation rates of oil in different forms and environments revealed by ramped pyrolysis. *Environmental Science & Technology*, 48(18), 10966-10974.

Pendergraft, M.A., Dincer, Z., Sericano, J.L., Wade, T.L., Kolasinski, J., Rosenheim, B.E. (2013) Linking ramped pyrolysis isotope data to oil content through PAH analysis. *Environmental Research Letters*, 8, 044038

PRESENTATIONS

Pendergraft, M., Grimes, D.J., Giddings, S.N., Feddersen, F., Santander, M., Lee, C., Beall, C., Prather, K.A. (2016) A water mass tracer detected in aerosols demonstrates ocean-atmosphere mass transfer and links sea spray aerosol to source waters. Poster presentation. American Geophysical Union Fall Meeting 2016. AGU.

Pendergraft, M., Malfatti, F., Petras, D., Minich, J.J., Belda-Ferre, P., DeAngelo, S., Morris, C.K., Santander, M., Dorrestein, P., Aluwihare, L., Knight, R., Azam, F., Prather, K.A. (2020) Exploring links between bacteria, enzymes, and organic compounds in seawater and sea spray aerosol. Hybrid oral and poster presentation. Ocean Sciences Meeting 2020. AGU.

ABSTRACT OF THE DISSERTATION

Enzyme Activity, Bacteria, and Pollution in Sea Spray Aerosol

by

Matthew Allen Pendergraft

Doctor of Philosophy in Oceanography

University of California San Diego, 2022

Professor Kimberly A. Prather, Chair

Atmospheric aerosols are microscopic solid and liquid particles that influence Earth's climate and impact human health. Sea spray aerosol is the most abundant atmospheric aerosol by mass. Sea spray aerosol composition controls its atmospheric roles and is a function of seawater composition. Seawater composition is determined by abundant marine microorganisms, but can also be heavily impacted by pollution, especially in coastal waters. This dissertation investigates the transfer of enzymes, bacteria, and contamination from seawater to sea spray aerosol. Heterotrophic bacteria significantly shape ocean carbon cycling and the composition of marine organic material by expressing extracellular enzymes. These enzymes transfer to the atmosphere in sea spray aerosol where they can continue to catalyze chemical reactions. This dissertation demonstrates that sea spray aerosol enzyme activity is qualitatively distinct from that of its source waters. Aminopeptidase, lipase, and alkaline phosphatase show similar activity levels in

sea spray aerosol despite aminopeptidase being dominant in seawater. This illustrates that the enzyme activity in sea spray aerosol prioritizes different chemical reactions than in seawater. Along with the enzymes they produce, bacteria themselves also transfer in sea spray aerosol. This dissertation coupled high efficiency aerosol sampling with a low biomass 16S gene amplicon sequencing protocol to produce a novel workflow for the sampling and sequencing of bacteria in sea spray aerosol. Detection limits for successful sequencing were established at 4.1 million aerosols and 1046 airborne bacteria. The results demonstrate that different water masses with different bacteria communities produce different airborne bacteria communities. Along the many populated coastlines worldwide, water pollution is prevalent and has the potential to reach people on land by transferring in sea spray aerosol. To investigate this potential, three dye releases were conducted to mimic coastal water pollution at full scale in the environment. Coordinated aerosol sampling detected the dye in the coastal aerosol up to 668 m inland and 720 m downwind of the dyed coastal waters. These findings demonstrate that coastal water pollution transfers to the atmosphere in sea spray aerosol and reaches many people on land through this airborne exposure pathway. Subsequently, non-targeted high resolution tandem mass spectrometry and 16S gene amplicon sequencing were applied to investigate chemical and bacterial signs of coastal water pollution in coastal aerosol. Chemicals and bacteria identified in a major pollution source were also found in coastal aerosol in onshore winds. The selected bacteria comprised up to 76% of the identified airborne bacteria community and included members independently linked to sewage pollution. Although they had multiple sources to the atmosphere, specific chemical contaminants were identified in aerosols coming from the ocean. This dissertation provides new insight into enzyme activity, bacteria, and coastal water pollution transferring in sea spray aerosol, with implications for atmospheric chemistry and human health.

Chapter 1. Introduction

1.1 Atmospheric Aerosols

Atmospheric aerosols regulate the Earth's temperature, clouds, hydrological cycle, weather, and climate. An aerosol is defined as a solid or liquid suspended in a gas. The air we breathe contains hundreds to thousands of aerosols per cubic centimeter (cm^3). These particles generally range in size from tens of nanometers (nm) to tens of micrometers (or "microns", μm). There are natural and anthropogenic sources of aerosols. Common natural aerosol types and sources include dust from the land, especially deserts; pollen released by plants and other biological particles; and sea spray aerosol (SSA) (Pöschl, 2005). Smoke and soot particles can be considered natural or anthropogenic depending on the source, with combustion from engines comprising a major source of anthropogenic aerosols (Seinfeld & Pandis, 2016). Primary aerosols are those that are directly emitted to the atmosphere as particles, whereas secondary aerosols form when atmospheric gases condense to form new particles or coat existing particles (Kroll & Seinfeld, 2008; Shiraiwa et al., 2013).

1.2 Climate Roles of Atmospheric Aerosols

Atmospheric aerosols influence the Earth's climate by interacting with radiation and nucleating clouds and ice. The aerosol "direct effect" is the net effect on Earth's radiative budget from interactions between aerosols and radiation; it is estimated to be a cooling effect of -0.3 W m^{-2} (Zhang et al. 2021). Particle composition influences the direct effect, and some aerosol types, like black carbon aerosols emitted by humans, can have a warming effect. Aerosols also influence the Earth's radiative balance through cloud formation. Every cloud droplet is the result of water vapor condensing on an aerosol. Indirect aerosol radiative effects are the interactions between radiation and clouds and have a net radiative forcing of -1.0 W m^{-2} (Zhang et al. 2021).

Not all aerosols are able to nucleate clouds, and the ability to do so is determined by particle size and composition (Farmer et al., 2015).

1.3 Sea Spray Aerosol

With roughly 70% of the Earth's surface covered by the ocean, SSA is the most abundant aerosol type in the atmosphere by mass (Lewis & Schwartz, 2004). Most SSA forms from waves breaking and bubbles bursting at the ocean surface and ejecting aerosols of seawater (SW) (Leeuw et al., 2011). Recent research highlights the importance of secondary marine aerosol, which is formed from the condensation of gases emitted by marine microbes, because it significantly influences marine cloud formation (Mayer et al., 2020). Just as SW has a complex chemical composition, SSA too contains diverse chemical compounds, including salts, lipids, fatty acids, and polysaccharides (Quinn et al., 2015). Bacteria, viruses, and other marine microorganisms also transfer in SSA (Baylor et al., 1977; Blanchard & Syzdek, 1970; Patterson et al., 2016). The diverse composition of SSA can influence its climate relevant properties. For example, the ability of SSA to nucleate ice in the atmosphere depends on aerosol composition, and the formation of ice in the atmosphere can influence how much precipitation falls from a storm (Creamean et al., 2013; DeMott et al., 2016; Wilson et al., 2015).

1.4 Bacteria Shape Seawater and SSA Composition

The ocean is full of microscopic life that shapes the composition of seawater and SSA. Marine phytoplankton carry out half of global primary production and much of the organic matter (OM) produced gets respired back to carbon dioxide (CO_2) by marine heterotrophic bacteria (HB). (Azam, 1998; Falkowski et al., 1998; Field et al., 1998). HB accomplish this through their abundance, numbering 10^4-10^6 ml^{-1}, and because they express extracellular enzymes that rapidly process OM (Azam & Malfatti, 2007). This releases molecules small

enough for the HB to incorporate into their cells to meet their nutritional demands (Arnosti, 2011). HB release "free" enzymes into SW and have "cell-associated" enzymes attached to their cell exterior. HB and their enzymes are prolific enough to respire approximately 50% of new marine OM created by photosynthesis back to the atmosphere as CO_2 (Azam, 1998). Thus, HB and their enzymatic activity chemically alter a large fraction of marine OM. By shaping SW composition, enzymes also influence SSA composition, and signs of this have been observed in a coupled ocean-atmosphere system (Wang et al., 2015). Major marine exoenzyme types include proteases, which liberate short amino acids and oligomers; lipases, which free up lipids and fatty acids; glucosidases, which liberate small sugars; chitinases and other carbohydrate active enzymes (CAZymes); and phosphatases that release chemical species containing phosphate (Arnosti, 2011). Marine proteases include aminopeptidases (AMP), trypsin, chymotrypsin, and elastase type enzymes (Obayashi & Suzuki, 2005).

1.5 Bacteria and Enzymes Transfer to the Atmosphere in SSA

HB commonly transfer to the atmosphere in SSA (Patterson et al., 2016). In the marine boundary layer roughly 0.3-2x10^4 prokaryote cells m^{-3} air and 0.02-1x10^4 eukaryote cells m^{-3} air come from the ocean (Mayol et al., 2014; 2017). Fluxes from the tropical and subtropical ocean to the atmosphere are reported at 0.001-2x10^6 cells m^{-2} day^{-1} for prokaryotes and 1-2x10^3 cells m^{-2} d^{-1} for eukaryotes (Mayol et al., 2014; 2017). HB hydrophobic cell surfaces are attracted to the gas-liquid interface of ascending bubbles, resulting in HB accumulation at the ocean's surface microlayer, where bursting bubbles then eject them into the atmosphere (Blanchard et al., 1981; Carlucci & Williams, 1965). Aerosolization rates of HB have been observed to follow taxonomic groupings, known as taxon specific aerosolization (TSA) (Fahlgren et al., 2015; Harb et al., 2021; Hejkal et al., 1980; Michaud et al., 2018). Drivers of HB aerosolization rates include

SW properties, such as salinity and OM composition, and cell properties, including shape, lipid content, and lipophilicity (Harb et al., 2021; Hejkal et al., 1980; Kjelleberg et al., 1976; Manabe et al., 2020).

1.6 Coastal Water Composition is Influenced by Contamination

Coastal water pollution alters seawater composition and has the potential to transfer in SSA. Roughly half of the human population lives near the coast, resulting in human waste in the local waters (Boehm et al., 2002; Halpern et al., 2012; Howarth et al., 2002; Singh et al., 2004). CWP causes approximately 120 million cases of gastrointestinal illness, 50 million cases of respiratory illness, and tens of thousands of deaths each year (Halpern et al., 2012; Shuval, 2003). Sewage, urban stormwater runoff, agricultural effluents, and industrial discharges are common sources of coastal water pollution (Gersberg et al., 2004; Halpern et al., 2012; Howarth et al., 2002; Singh et al., 2004; Steele et al., 2018). Chemical contaminants in CWP include oils, fuels, metals, plastics, pharmaceuticals, personal care products, pesticides, herbicides, detergents, solvents, and fire retardants (Kolpin et al., 2002; Petras et al., 2021). Pathogens - microorganisms that cause illness - are biological contaminants of concern and include enteroviruses, human norovirus, hepatitis A virus, and SARS-CoV2 (Boehm et al., 2009; Gersberg et al., 2006; Griffin et al., 2003; Rocha et al., 2022; Steele et al., 2018). It has been demonstrated that entering contaminated coastal waters increases the incidence of multiple illnesses (Arnold et al., 2017; Haile et al., 1999).

1.7 Goals of Dissertation

This dissertation investigates the transfer of enzyme activity, bacteria, and pollution from the ocean to the atmosphere in sea spray aerosol. Isolated SW and SSA systems are used in the

laboratory to investigate enzyme activity and bacteria in SSA. The aerosolization of coastal water pollution is investigated in the field.

The main questions addressed in the studies presented in this dissertation are:

1. How does selective transfer shape SSA enzyme activity and bacteria community?
2. Which bacteria and chemicals from coastal water pollution transfer to the atmosphere in SSA?

1.8 Synopsis of Dissertation

This dissertation includes results from laboratory and field studies which were performed to answer these questions. Chapter 2 investigated in the laboratory isolated SSA and source waters to make qualitative comparisons between their enzyme activities. In three separate experiments, enzyme activities in seawater and aerosol were tracked across nutrient-stimulated phytoplankton and HB growth cycles in a marine aerosol reference tank (MART; Stokes et al., 2013). Whereas seawater enzyme activity is dominated by aminopeptidase activity, SSA shows similar aminopeptidase, lipase, and alkaline phosphatase enzyme activities. These results demonstrate that the enzyme activity of SSA undergoes different chemical reactions in the atmosphere relative to seawater.

Chapter 3 of this dissertation applies novel aerosol sampling and sequencing methods to gain new insight into bacteria transfer in SSA. The findings from chapter 2 called for an improvement in the ability to sequence bacteria in SSA so that enzyme activities in SSA may be linked to bacteria in SSA. In three iterations the seawater and aerosol bacteria communities were tracked in a MART. Combining high efficiency aerosol sampling with a low biomass 16S gene amplicon sequencing workflow achieved sequencing limits of detection at 4.1×10^6 SSA particles containing 1046 airborne heterotrophic bacteria cells. The multiple experiment iterations

demonstrate that different bacteria communities in seawater produce different airborne bacteria communities in SSA.

Chapter 4 of this dissertation replicated coastal water pollution events at full scale in the environment in order to demonstrate coastal water pollution transferring to the atmosphere in SSA. Three dye releases in the Imperial Beach, USA surfzone mimicked pollution and were tracked in the ocean with hyperspectral aerial observations. Dye was detected in the air for two days following two of three dye releases, up to 668 m inland and 720 m downwind of the surfzone. Local winds were used to relate dye concentrations in the ocean and atmosphere. Wind direction and dye concentration in the upwind waters determined when dye was detected. This research demonstrates that coastal water pollution can aerosolize in SSA and reach many people on land, and that coastal currents and winds combine to determine pollution's pathway through the ocean and atmosphere.

Chapter 5 of this dissertation applies 16S rRNA gene amplicon sequencing and non-targeted tandem mass spectrometry to identify bacteria and chemicals from CWP transferring to the atmosphere in SSA. Bacteria identified in the Tijuana River, a major source of coastal water pollution, were detected in coastal aerosol in onshore winds. These bacteria were independently linked to sewage pollution from the Tijuana River and accounted for up to 76% of the bacteria detected in the coastal air. Mass spectrometry identified specific chemicals that aerosolized in SSA from CWP along with the bacteria. The bacteria and chemical results combined to provide evidence of CWP reaching people on land by aerosolizing in SSA.

Chapter 6 of this dissertation provides conclusions and future directions.

1.9 Acknowledgements

Thank you Dr. Rebecca Simpson, Dr. Victoria Steck, and Dr. Jon Sauer for editing this chapter.

1.10 References

Arnold, B.F., Schiff, K.C., Ercumen, A., Benjamin-Chung, J., Steele, J.A., Griffith, J.F., Steinberg, S.J., Smith, P., McGee, C.D., Wilson, R., Nelsen, C., Weisberg, S.B., Colford, J.M., Jr. (2017). Acute illness among surfers after exposure to seawater in dry- and wet-weather conditions. *American Journal of Epidemiology*, 186(7), 866–875.

Arnosti, C. (2011). Microbial extracellular enzymes and the marine carbon cycle. *Annual Review of Marine Science*, 3, 401–425.

Azam, F. (1998). Microbial control of oceanic carbon flux: the plot thickens. *Science*, 280(5364), 694–696. DOI: 10.1126/science.280.5364.694

Azam, F., Malfatti, F. (2007). Microbial structuring of marine ecosystems. *Nature Reviews Microbiology*, 5(10), 782–791.

Baylor, E.R., Baylor, M.B., Blanchard, D.C., Syzdek, L.D., Appel, C. (1977). Virus transfer from surf to wind. *Science*, 198(4317), 575–580.

Blanchard, D.C., Syzdek, L. (1970). Mechanism for the water-to-air transfer and concentration of bacteria. *Science*, 170(3958), 626–628.

Blanchard, D.C., Syzdek, L.D., Weber, M.E. (1981). Bubble scavenging of bacteria in freshwater quickly produces bacterial enrichment in airborne jet drops. *Limnology and Oceanography*, 26(5), 961–964.

Boehm, A.B., Grant, S.B., Kim, J.H., Mowbray, S.L., McGee, C.D., Clark, C.D., Foley, D.M., Wellman, D.E. (2002). Decadal and shorter period variability of surf zone water quality at Huntington Beach, California. *Environmental Science & Technology*, 36(18), 3885–3892.

Boehm, A.B., Yamahara, K.M., Love, D.C., Peterson, B.M., McNeill, K., Nelson, K.L. (2009). Covariation and photoinactivation of traditional and novel indicator organisms and human viruses at a sewage-impacted marine beach. *Environmental Science & Technology*, 43(21), 8046–8052.

Carlucci, A.F., Williams, P.M. (1965). Concentration of bacteria from sea water by bubble scavenging. *ICES Journal of Marine Science*, 30(1), 28–33. DOI: 10.1093/icesjms/30.1.28

Creamean, J.M., Suski, K.J., Rosenfeld, D., Cazorla, A., DeMott, P.J., Sullivan, R.C., White, A.B., Ralph, F.M., Minnis, P., Comstock, J.M., Tomlinson, J.M., Prather, K.A. (2013). Dust and biological aerosols from the Sahara and Asia influence precipitation in the Western U.S. *Science*, 339(6127), 1572–1578.

DeMott, P.J., Hill, T.C.J., McCluskey, C.S., Prather, K.A., Collins, D.B., Sullivan, R.C., Ruppel, M.J., Mason, R.H., Irish, V.E., Lee, T., Hwang, C.Y., Rhee, T.S., Snider, J.R., McMeeking, G.R., Dhaniyala, S., Lewis, E.R., Wentzell, J.J.B., Abbatt, J., Lee, C.,

Sultana, C.M., Ault, A.P., Axson, J.L., Diaz Martinez, M., Venero, I., Santos-Figueroa, G., Stokes, M.D., Deane, G.B., Mayol-Bracero, O.L., Grassian, V.H., Bertram, T.H., Bertram, A.K., Moffett, B.F., Franc, G. D. (2016). Sea spray aerosol as a unique source of ice nucleating particles. *Proceedings of the National Academy of Sciences of the United States of America*, 113(21), 5797–5803.

Fahlgren, C., Gómez-Consarnau, L., Zábori, J., Lindh, M.V., Krejci, R., Mårtensson, E.M., Nilsson, D., Pinhassi, J. (2015). Seawater mesocosm experiments in the Arctic uncover differential transfer of marine bacteria to aerosols. *Environmental Microbiology Reports*, 7(3), 460–470.

Falkowski, P.G., Barber, R.T., Smetacek, V.V. (1998). Biogeochemical controls and feedbacks on ocean primary production. *Science*, 281(5374), 200–207.

Farmer, D.K., Cappa, C.D., Kreidenweis, S.M. (2015). Atmospheric processes and their controlling influence on cloud condensation nuclei activity. *Chemical Reviews*, 115(10), 4199–4217.

Field, C.B., Behrenfeld, M.J., Randerson, J.T., Falkowski, P. (1998). Primary production of the biosphere: integrating terrestrial and oceanic components. *Science*, 281(5374), 237–240.

Gersberg, R.M., Daft, D., Yorkey, D. (2004). Temporal pattern of toxicity in runoff from the Tijuana River watershed. *Water Research*, 38(3), 559–568.

Gersberg, R.M., Rose, M.A., Robles-Sikisaka, R., Dhar, A.K. (2006). Quantitative detection of Hepatitis A virus and enteroviruses near the United States-Mexico border and correlation with levels of fecal indicator bacteria. *Applied and Environmental Microbiology*, 72(12), 7438–7444.

Griffin, D.W., Donaldson, K.A., Paul, J.H., Rose, J.B. (2003). Pathogenic human viruses in coastal waters. *Clinical Microbiology Reviews*, 16(1), 129–143.

Haile, R.W., Witte, J.S., Gold, M., Cressey, R., McGee, C., Millikan, R.C., Glasser, A., Harawa, N., Ervin, C., Harmon, P., Harper, J., Dermand, J., Alamillo, J., Barrett, K., Nides, M., Wang, G. (1999). The health effects of swimming in ocean water contaminated by storm drain runoff. *Epidemiology*, 10(4), 355–363.

Halpern, B.S., Longo, C., Hardy, D., McLeod, K.L., Samhouri, J.F., Katona, S.K., Kleisner, K., Lester, S.E., O'Leary, J., Ranelletti, M., Rosenberg, A.A., Scarborough, C., Selig, E.R., Best, B.D., Brumbaugh, D.R., Chapin, F.S., Crowder, L.B., Daly, K.L., Doney, S.C., Elfes, F., Fogarty, M.J., Gaines, S.D., Jacobsen, K.I., Karrer, L.B., Leselie, H.M., Neeley, E., Pauly, D., Polasky, S., Ris, B., St Martin, K., Stone, G.S., Sumalia, U.R., Zeller, D. (2012). An index to assess the health and benefits of the global ocean. *Nature*, 488(7413), 615–620.

Harb, C., Pan, J., DeVilbiss, S., Badgley, B., Marr, L.C., Schmale, D.G., 3rd, Foroutan, H. (2021). Increasing freshwater salinity impacts aerosolized bacteria. *Environmental Science & Technology*, 55(9), 5731–5741.

Hejkal, T.W., Larock, P.A., Winchester, J.W. (1980). Water-to-air fractionation of bacteria. *Applied and Environmental Microbiology*, 39(2), 335–338.

Howarth, R.W., Sharpley, A., Walker, D. (2002). Sources of nutrient pollution to coastal waters in the United States: implications for achieving coastal water quality goals. *Estuaries*, 25(4), 656–676. DOI: 10.1007/bf02804898

Kjelleberg, S., Norkrans, B., Löfgren, H., Larsson, K. (1976). Surface balance study of the interaction between microorganisms and lipid monolayer at the air/water interface. *Applied and Environmental Microbiology*, 31(4), 609–611.

Kolpin, D.W., Furlong, E.T., Meyer, M.T., Thurman, E.M., Zaugg, S.D., Barber, L.B., Buxton, H.T. (2002). Pharmaceuticals, hormones, and other organic wastewater contaminants in U.S. streams, 1999-2000: a national reconnaissance. *Environmental Science & Technology*, 36(6), 1202–1211.

Kroll, J.H., Seinfeld, J.H. (2008). Chemistry of secondary organic aerosol: formation and evolution of low-volatility organics in the atmosphere. *Atmospheric Environment*, 42(16), 3593–3624.

de Leeuw, G., Andreas, E.L., Anguelova, M.D., Fairall, C.W., Lewis, E.R., O'Dowd, C., Schulz, M., Schwartz, S.E. (2011). Production flux of sea spray aerosol. *Reviews of Geophysics*, 49(2). DOI: 10.1029/2010rg000349

Lewis, E.R., Schwartz, S.E. (2004). Sea salt aerosol production: mechanisms, methods, measurements, and models. American Geophysical Union.

Malfatti, F., Lee, C., Tinta, T., Pendergraft, M.A., Celussi, M., Zhou, Y., Sultana, C.M., Rotter, A., Axson, J.L., Collins, D.B., Santander, M.V., Anides Morales, A.L., Aluwihare, L.I., Riemer, N., Grassian, V.H., Azam, F., Prather, K.A. (2019). Detection of active microbial enzymes in nascent sea spray aerosol: Implications for atmospheric chemistry and climate. *Environmental Science & Technology Letters*, 6(3), 171–177.

Manabe, J., Omori, T., Ishikawa, T. (2020). Shape matters: entrapment of a model ciliate at interfaces. *Journal of Fluid Mechanics*, 892(A15). DOI: 10.1017/jfm.2020.160

Mayer, K.J., Wang, X., Santander, M.V., Mitts, B.A., Sauer, J.S., Sultana, C.M., Cappa, C.D., Prather, K.A. (2020). Secondary marine aerosol plays a dominant role over primary sea spray aerosol in cloud formation. *ACS Central Science*, 6(12), 2259–2266.

Mayol, E., Arrieta, J.M., Jiménez, M.A., Martínez-Asensio, A., Garcias-Bonet, N., Dachs, J., González-Gaya, B., Royer, S.-J., Benítez-Barrios, V.M., Fraile-Nuez, E., Duarte, C.M. (2017). Long-range transport of airborne microbes over the global tropical and subtropical ocean. *Nature Communications*, 8(1), 201.

Mayol, E., Jiménez, M.A., Herndl, G.J., Duarte, C.M., Arrieta, J.M. (2014). Resolving the abundance and air-sea fluxes of airborne microorganisms in the North Atlantic Ocean. *Frontiers in Microbiology*, 5, 557.

Michaud, J.M., Thompson, L.R., Kaul, D., Espinoza, J.L., Richter, R.A., Xu, Z.Z., Lee, C., Pham, K.M., Beall, C.M., Malfatti, F., Azam, F., Knight, R., Burkart, M.D., Dupont, C. L., Prather, K.A. (2018). Taxon-specific aerosolization of bacteria and viruses in an experimental ocean-atmosphere mesocosm. *Nature Communications*, 9(1), 2017.

Patterson, J.P., Collins, D.B., Michaud, J.M., Axson, J.L., Sultana, C.M., Moser, T., Dommer, A. C., Conner, J., Grassian, V.H., Stokes, M.D., Deane, G.B., Evans, J.E., Burkart, M.D., Prather, K.A., Gianneschi, N.C. (2016). Sea spray aerosol structure and composition using cryogenic transmission electron microscopy. *ACS Central Science*, 2(1), 40–47.

Petras, D., Minich, J.J., Cancelada, L.B., Torres, R.R., Kunselman, E., Wang, M., White, M.E., Allen, E.E., Prather, K.A., Aluwihare, L.I., Dorrestein, P.C. (2021). Non-targeted tandem mass spectrometry enables the visualization of organic matter chemotype shifts in coastal seawater. *Chemosphere*, 271, 129450.

Pöschl, U. (2005). Atmospheric aerosols: composition, transformation, climate and health effects. *Angewandte Chemie*, 44(46), 7520–7540.

Quinn, P.K., Collins, D.B., Grassian, V.H., Prather, K.A., Bates, T. S. (2015). Chemistry and related properties of freshly emitted sea spray aerosol. *Chemical Reviews*, 115(10), 4383–4399.

Rocha, A.Y., Verbyla, M.E., Sant, K.E., Mladenov, N. (2022). Detection, quantification, and simplified wastewater surveillance model of SARS-CoV-2 RNA in the Tijuana River. *ACS ES&T Water*, 2(11), 2134–2143.

Seinfeld, J.H., Pandis, S.N. (2016). Atmospheric chemistry and physics: from air pollution to climate change. John Wiley & Sons. 3rd Edition.

Shiraiwa, M., Zuend, A., Bertram, A.K., Seinfeld, J.H. (2013). Gas-particle partitioning of atmospheric aerosols: interplay of physical state, non-ideal mixing and morphology. *Physical Chemistry Chemical Physics: PCCP*, 15(27), 11441–11453.

Shuval, H. (2003). Estimating the global burden of thalassogenic diseases: human infectious diseases caused by wastewater pollution of the marine environment. *Journal of Water and Health*, 1(2), 53–64.

Singh, K.P., Mohan, D., Sinha, S., Dalwani, R. (2004). Impact assessment of treated/untreated wastewater toxicants discharged by sewage treatment plants on health, agricultural, and environmental quality in the wastewater disposal area. *Chemosphere*, 55(2), 227–255.

Steele, J.A., Denene Blackwood, A., Griffith, J.F., Noble, R.T., Schiff, K.C. (2018). Quantification of pathogens and markers of fecal contamination during storm events along popular surfing beaches in San Diego, California. *Water Research*, 136, 137–149. doi.org/10.1016/j.watres.2018.01.056

Stokes, M.D., Deane, G.B., Prather, K., Bertram, T.H., Ruppel, M.J., Ryder, O.S., Brady, J.M., Zhao, D. (2013). A Marine Aerosol Reference Tank system as a breaking wave analogue

for the production of foam and sea-spray aerosols. *Atmospheric Measurement Techniques*, 6(4), 1085–1094.

Wang, X., Sultana, C.M., Trueblood, J., Hill, T.C.J., Malfatti, F., Lee, C., Laskina, O., Moore, K.A., Beall, C.M., McCluskey, C.S., Cornwell, G.C., Zhou, Y., Cox, J.L., Pendergraft, M.A., Santander, M.V., Bertram, T.H., Cappa, C.D., Azam, F., DeMott, P.J., Grassian, V.H., Prather, K.A. (2015). Microbial control of sea spray aerosol composition: a tale of two blooms. *ACS Central Science*, 1(3), 124–131.

Wilson, T.W., Ladino, L.A., Alpert, P.A., Breckels, M.N., Brooks, I.M., Browse, J., Burrows, S.M., Carslaw, K.S., Huffman, J.A., Judd, C., Kilthau, W.P., Mason, R.H., McFiggans, G., Miller, L.A., Nájera, J.J., Polishchuk, E., Rae, S., Schiller, C.L., Si, M., Vergara Temprado, J., Whale, T.F., Wong, J.P.S., Wurl, O., Yakobi-Hancock, J.D., Abbatt, J.P.D., Aller, J.Y., Bertram, A.K., Knopf, D.A., Murray, B.J. (2015). A marine biogenic source of atmospheric ice-nucleating particles. *Nature*, 525(7568), 234–238.

Chapter 2. Enhanced Lipase and Alkaline Phosphatase Enzyme Activities in Sea Spray Aerosol

2.1 Abstract

Enzymes shape seawater composition and drive global carbon cycling. Heterotrophic bacteria express extracellular enzymes to liberate small molecules from marine organic matter they can incorporate into their cells to meet their nutritional demands. Enzymes also transfer into sea spray aerosol, allowing them to continue their chemistry in the atmosphere. This work investigates isolated seawater and SSA in the laboratory to show that SSA enzyme activity has a distinct profile from its source waters. Whereas aminopeptidase activity is dominant in SW, SSA shows similar lipase, alkaline phosphatase, and aminopeptidase activities. Lipase-to-aminopeptidase activity ratios in SSA and seawater show a 10x enhancement of lipase activity in SSA. Enzyme activity profiles of seawater and SSA show alkaline phosphatase has a similar 10x enhancement in SSA. These results agree with other observations that have shown marine microenvironments, like aggregates, to have unique enzyme signatures. The discovery of active enzymes in SSA identified a previously unknown atmospheric reaction pathway. This study demonstrates that SSA prioritizes different enzymatic reactions compared to seawater. This research yields further insight into how ocean microbiology can drive atmospheric chemistry.

2.2 Introduction

The ocean is full of microscopic life that shapes SW composition and regulates ocean uptake of atmospheric carbon dioxide. Phytoplankton convert sunlight, CO_2, and nutrients into biomass. Following phytoplankton exudation and death, their organic matter is processed by abundant heterotrophic bacteria (HB) that number 10^4-10^6 cells ml^{-1} (Azam et al., 1983). HB are osmotrophs and can only incorporate into their cells molecules smaller than ~600-800 Da, which

means that large macromolecules, like proteins, lipids, complex polysaccharides, are too large to be ingested (Weiss et al., 1991). To be able to utilize the diverse forms of marine organic matter, including macromolecules, gels, aggregates, and particulate organic material (POM), HB need enzymes to cleave and release their small molecule building blocks (Arnosti, 2011; Azam & Malfatti, 2007; Smith et al., 1992). Using enzymes, HB respire roughly 50% of new OM created by marine primary production and significantly influence marine OM composition in the process (Azam, 1998). Enzyme activities are measured as reaction rates: the rate at which the enzyme processes its respective substrate (Arnosti, 2011). The high enzyme activities HB use to degrade POM as it falls through the water column determines what fraction of fixed carbon reaches the seafloor for long term storage (Smith et al. 1992). HB are understood to be the largest source of EA in the ocean (Arnosti, 2011). Changes in SW composition and enzymes have been linked to changes in the HB community (Teeling et al., 2012). Cell-associated enzymes exist on the external cellular surface of HB and "free enzymes" are individual enzymes released into the water (Azam & Malfatti, 2007). Common marine enzyme classes include proteases, which cleave short amino acids and oligomers from marine OM; lipases (LIP), which liberate lipids and fatty acids; glucosidases, which liberate small sugars; chitinases and other carbohydrate active enzymes (CAZymes); and phosphatases, which release chemical species containing phosphate (Martinez et al., 1996). Marine proteases include aminopeptidases (AMP), trypsin, chymotrypsin, and elastase type enzymes (Obayashi and Suzuki 2005). Different enzyme types show significantly different activities, with protease actiivty often highest in SW (Smith et al., 1992; Arnosti, 2011; Martinez et al., 1996). A single type of enzyme activity can show significant changes over time, and it has been shown that individual HB isolates can vary their expression of different enzymes (Martinez et al., 1996). Comparing enzyme activities associated

with POM vs. the surrounding waters has shown that different microenvironments can have qualitatively different EAs (Smith et al., 1992). Qualitative differences in enzyme activity imply different enzyme activities being expressed at different levels.

Marine HB and enzymes transfer to the atmosphere in SSA produced by high winds and bubbles rupturing at the ocean surface (Lewis & Schwartz, 2004; Quinn et al., 2015; Malfatti & Lee et al., 2019; Schiffer et al., 2018). In marine air, roughly 0.3-2 $x10^4$ prokaryote cells m^{-3} air and 0.02-1 $x10^4$ eukaryote cells m^{-3} air come from the ocean (Mayol et al. 2014, 2017). Recent work has demonstrated SSA to be enzymatically active (Malfatti & Lee et al., 2019). That work identified activity from oleate- and stearate-lipases, alkaline phosphatases (ALKs), and leucine- and serine-aminopeptidases. When normalizing by sample volume, enzyme activities showed faster reaction rates in SSA than in SW. Enzyme activity in SSA can come from enzymes attached to bacteria and/or from free enzymes detached from cells. Active enzymes in SSA can hydrolyze substrates within their own particle and in other particles they encounter during collisions (Malfatti & Lee et al., 2019). The presence of lipase in SSA can affect SSA surface properties and could influence the climate relevant properties of the particles, like water vapor uptake and ice nucleation (Schiffer et al., 2018). The initial detection of EA in SSA also reported qualitative differences in EA between SSA and its source waters, which is investigated further here (Malfatti & Lee et al., 2019).

This study tests the hypothesis that SSA enzyme activity is qualitatively distinct from that of its source waters. Nascent SSA is investigated using the MART, which isolates SSA and its source waters, allowing for direct comparison between enzyme activities in the water and aerosol (Stokes et al., 2013). First, LIP and AMP activities are compared in SW and SSA to show enhanced LIP activity in SSA. Then, EA profiles are employed to show that ALK is also

enhanced in SSA, and AMP is less prominent in SSA than in SW. These observations show specific enzymatic reaction pathways that come from the ocean but are enhanced in the atmosphere.

2.3 Materials and Methods

2.3.1 Microcosm Experiments

To compare enzyme activities in seawater and SSA, this study includes three experiments from 2016 and 2018. Additional information on the methods used in these experiments has been previously described in detail (Trueblood et al., 2019; Lee et al., 2015; Hasenecz et al., 2020). Here a summary is provided. In each experiment, coastal seawater was collected from the Ellen Browning Scripps Memorial Pier at Scripps Institution of Oceanography. The SW was filtered with a 50 μm mesh (Sefar Nitex 03-100/32) to remove zooplankton grazers and debris. Algae growth medium (Proline F2, Pentair AES Aquatic Ecosystems) and sodium metasilicate was added to the SW to promote phytoplankton growth (Lee et al., 2015; Guillard, 1975). The SW was placed in a 2400 liter PTFE tank kept outdoors to receive ambient levels of sunlight to promote phytoplankton growth, which was tracked by chlorophyll-a (chl-a) measurements made with a calibrated Aquafluor fluorometer (Turner Designs, San Jose, CA, USA). Nascent SSA was generated in the lab from isolated source waters using the MART (Stokes et al., 2013). The MART holds 120 liters of SW and 90 liters of headspace and uses a plunging sheet of water to generate SSA with bubble and particle size distributions similar to those measured on breaking waves. The 2016 experiment was conducted in one MART on Aug 20-26, 2016. The 2018-1 experiment was conducted in triplicate, using 3 MARTs, on Aug 4-16, 2018. The 2018-2 experiment was conducted in duplicate in 2 MARTs on Aug 21-30, 2018. While chl-a in the tank was increasing, the MARTs were filled with water from the tank each morning and the water

was returned to the tank after each day of measurements. This allowed the phytoplankton community to grow by only subjecting a fraction of the SW to the plunging of the MART. Once chl-a decreased in the tank, water was transferred to the MARTs one final time and remained for the remaining days of measurements, without daily exchange with the tank. In 2018-1, 3 marine bacteria isolates - AltSIO, ATW7, and BBFL7 - were added to 2 of 3 MARTS, but not in high enough concentrations to affect SW HB counts nor enzyme activities. In 2018-2, the isolates were added to 1 of 2 MARTs at high enough levels to generate increases in SW HB counts and ALK EA. The data from the multiple MARTs for 2018-1 and, separately, 2018-2, were averaged to generate an average system for each.

2.3.2 Seawater and SSA Sampling

Seawater was sampled from the MART from a stainless steel port below the water surface. We did not sample the surface microlayer (SML) from the MART to preserve and not deplete it, as its presence is important in SSA formation (Cochran et al., 2016; Quinn et al., 2015). Nascent SSA was sampled into liquid for measuring EA. In 2016 SSA was sampled with impingers (Chemglass CG-1820; heretofore "IMP") and the Spot sampler (Aerosol Devices Inc; model SS110A; heretofore "SPOT") using the liquid sampling configuration (Pan et al., 2016). Both the IMP and SPOT sampled SSA into filtered and autoclaved SW (FASW) and their EA data were averaged. In 2018 SSA was sampled into FASW using only the SPOT. SSA blanks for EA and HB enumeration were collected by sampling through a HEPA filter.

2.3.3 Extracellular Enzyme Activity Measurements and HB Enumeration

Extracellular EA was measured on SW and SSA samples using fluorogenic substrate analogs at 20 µM concentrations (Malfatti & Lee et al., 2019; Martinez et al., 1996; Hoppe, 1983). Samples of SSA in FASW were diluted to sufficient volume for multiple 250-300 µl

replicates for each substrate. LIP activity was assessed by measuring the rates of hydrolysis of 4-methylumbelliferone oleate and 4-methylumbelliferone stearate. AMP activity was assessed by measuring the rates of hydrolysis of leucine and serine from L-Leucine-7-amido-4-methylcoumarin hydrochloride and L-Serine-7-amido-4-methylcoumarin hydrochloride. AMPs are exopeptidases, which hydrolyze the peptide bond adjacent to the terminal amino acid (Obayashi & Suzuki, 2005). ALP activity was measured using 4-methylumbelliferone phosphate. These enzyme activities are commonly investigated in the ocean and include the four enzyme activities previously detected in SSA (Arnosti 2011; Martinez et al. 1996; Malfatti & Lee et al. 2019). Substrates were dissolved in varying combinations of 2-methoxy ethanol (methyl cellosolve) and deionized water. For each measurement, 6 µl of a fluorogenic substrate solution was placed in a 330 µl well in a 96 well plate (Costar product # 3915). 250-300 µl of SW or SSA in FASW was then added to the well containing substrates. Each sample-substrate combination consisted of 4-6 replicates. Using a multimode plate reader (2016: SpectraMax M3, Molecular Devices, 355/460 nm excitation/emission; 2018: Synergy H1, BioTek, 360/460 nm excitation/emission), fluorescence was read immediately after combining samples and substrates on the plate, then again after a 45-60 min incubation period. Calibration curves of the free fluorophores are used to convert the increase in fluorescence to concentration of substrate hydrolyzed per hour of incubation. The equivalent air volume for each aliquot measured was determined by relating total air sample volume to total liquid sample volume.

HB in SW were counted using flow cytometry (Gasol and Del Giorgio, 2000). Samples were fixed with glutaraldehyde (1% final concentration) prior to flash freezing in liquid nitrogen, then thawed, diluted 100x in TE buffer (Invitrogen/Thermo Fisher), and stained with SYBR

green I nucleic acid stain (Invitrogen/Thermo Fisher) with a final stain concentration of 1x (from 10,000x stain stock) (Noble & Fuhrman, 1998).

2.3.4 Data Analysis

EA data presented here represents the average of 4-6 replicates after removal of outliers determined using Dixon's Q test, excluding at most one outlier and using the 99% confidence interval because variability is expected within SW and SSA. For 2016 the IMP & SPOT activities were averaged for all EAs. For 2018, SW and SSA EAs from the multiple MARTs were averaged. SSA activities were blank-subtracted using daily HEPA-SSA blank activities. Values below the blank are reported as not detected. SSA activities were divided by the equivalent air volume sampled to achieve activities per liter of air (nM hr^{-1} l-air^{-1}), as previously reported (Malfatti & Lee et al., 2019). Leucine- and serine-AMP activities were summed to characterize AMP activity. Oleate- and stearate-LIP activities were summed to characterize LIP activity. For each SW and SSA sample, the summed LIP activity was divided by the summed AMP activity to achieve a LIP:AMP ratio. For each paired SW-SSA sampling, the SSA LIP:AMP was divided by SW LIP:AMP to achieve a SSA:SW LIP:AMP factor. Using ratios within each experiment facilitates comparing across experiments. The standard deviations associated with the replicate samples and blanks were propagated through all calculations to arrive at final standard deviations.

2.4 Results and Discussion

2.4.1 Microbiological Dynamics in Seawater and SSA

Chl-a showed a significant rise and fall in 2016 and 2018-2, but not in 2018-1, indicating different phytoplankton dynamics across the three experiments (Fig. 2.1). Chl-a reached the highest values in 2018-2, with max chl-a levels of 4.4, 2.4, and 12.1 µg/l in 2016, 2018-1, and

2018-2, respectively. The SW HB population increased significantly in each experiment and also reached the highest level ($1.95x10^7$ ml^{-1}) in 2018-2, compared to peaks of $0.82x10^7$ ml^{-1} and $1.06x10^7$ ml^{-1} in 2016 and 2018-1 (Fig. 2.1 G-I). In 2016 and 2018-2, the HB maximum followed the chl-a peak, yet in 2018-1 HB showed a significant rise and fall without a chl-a peak. Chl-a levels fall within the range of values observed for phytoplankton blooms observed in the ocean and generated in the lab (O'Reilly et al., 1998; Riemann et al., 2000; Teeling et al. 2012). HB concentrations were higher than some nutrient amended phytoplankton studies and comparable to others (Wang et al., 2015; Riemann et al., 2000). Thus, the levels and trends observed in chl-a and HB are typical of ocean and laboratory phytoplankton blooms.

2.4.2 Lipase and Aminopeptidase Activities in Seawater and SSA

Seawater AMP activities were much higher than LIP activities, in agreement with past research (Arnosti 2011; Riemann, Steward, and Azam 2000; Wang et al. 2015). AMP followed the HB trends and, like chl-a and HB, was highest in 2018-2, reaching 2400 nM hr^{-1}, compared to max values of 619 nM hr^{-1} in 2016 and 730 nM hr^{-1} in 2018-1 (Fig. 2.1 D-F). The SW AMP activity falls within the range of values measured in the ocean and in nutrient amendment studies (Riemann et al., 2000; Fukuda et al., 2000; Balmonte et al., 2019; Wang et al., 2015). Seawater LIP activity was much lower than AMP activity in the three experiments, with max LIP values of 48, 190, and 167 nM hr^{-1} in 2016, 2018-1, and 2018-2. (Fig. 2.1 D-F). The SW LIP activity falls within the 5-80 nM hr^{-1} range commonly observed for SW and is lower than max values of 150-200 nM hr^{-1} observed in other nutrient amended phytoplankton studies (Riemann et al., 2000; Arnosti 2011; Wang et al., 2015).

Whereas AMP activity greatly exceed LIP activity in the seawater, LIP activity was close to or greater than AMP activity in SSA. LIP and AMP activities in the SSA ranged between 0

and 100 nM hr^{-1} $l\text{-}air^{-1}$. SSA LIP activity exceeded SSA AMP activity in 2016 and 2018-1, whereas AMP activity was greater than lipase activity in 2018-2. LIP and AMP activities in SSA exceeded previously reported max values of ~1 nM hr^{-1} $l\text{-}air^{-1}$ despite lower chl-a and SW HB reached here (Malfatti & Lee et al., 2019). SSA activities were measured on much smaller sample amounts compared to SW, resulting in a lower signal:noise ratio in SSA EAs. Significant variability has been previously observed over time in SW and HB isolates (Martinez et al., 1996; Teeling et al., 2012). Selective and variable aerosolization of enzymes and HB in SSA likely contribute additional variability to SSA EA on top variability in SW EA. Together these three experiments show varying EA levels in both SW and SSA and different relationships between LIP and AMP EA in SSA, which is examined further.

2.4.3 Lipase-to-Aminopeptidase Ratios in Seawater and SSA

Comparing LIP and AMP activities provides their relative strengths in SW and SSA and describes EA in terms of two major enzyme classes. Previously, AMP to glucosidase EA ratios were used to show gradients in EA across ocean basins (Fukuda et al. 2000; Misic et al. 2006). Here, comparing LIP:AMP in SW and SSA allows comparison of the two different sample types. In all three experiments, SW LIP activity is much lower than SW AMP activity (Fig. 1 D-F), yielding SW LIP:AMP ratios below 1 (Fig. 2 A-C). In SSA, LIP activity exceeded AMP activity in 2016 and 2018-1 (Fig. 1 A-B), and consequently SSA LIP:AMP is above 1 for both (Fig. 2 A-B). Elevated SSA AMP activities in 2018-2 SSA produced SSA LIP:AMP ratios below 1. Thus, LIP:AMP ratios in SW and SSA succinctly demonstrate their relative strengths, with lower LIP:AMP ratios in SW and higher LIP:AMP ratios in SSA.

2.4.4 Enhanced Lipase Activity in SSA

Comparing LIP:AMP ratios across SW and SSA reveals SSA is a distinct enzymatic environment due to LIP enhancement. A great advantage of the MART is that it allows direct comparison between SSA and its source waters, which is not possible to do in the field. To compare LIP and AMP in SW and SSA, SSA LIP:AMP was divided by SW LIP:AMP, analogous to an enrichment factor (Jayarathne et al., 2016; Michaud et al., 2018). The resulting SSA:SW LIP:AMP ratios show consistent LIP enhancement in SSA (Fig. 2.2). 2016 presented the only value below 1 (0.86; Fig. 2.2 A), from a day when SSA LIP activity dropped and SSA AMP activity increased (Fig. 2.1 A). All other values for this factor are greater than one, demonstrating consistently elevated LIP activity in SSA. Presenting the highest SSA EA, 2016 also presented the highest individual (63.8) and mean (25) SSA:SW LIP:AMP values (Fig. 2.2 A). 2018-1 produced values consistently in the vicinity of 10x, with a mean value of 12 (Fig. 2.2 B). 2018-2 had the competing effects of the highest SW AMP activities and SSA LIP:AMP consistently below 1. The net result of these effects was a mean SSA LIP:AMP : SW LIP:AMP value of 3. Although SSA LIP:AMP < 1, taking into consideration the SW EAs shows SSA in SSA to be enriched in lipase activity. Taking the mean of the three experiments yields an average LIP:AMP enhancement factor of 13. These results show LIP activity to be over 10x enhanced in SSA when compared to AMP in SW and SSA, demonstrating that SSA greatly prioritizes the hydrolysis of lipids.

2.4.5 Alkaline Phosphatase Activity is also Elevated in SSA

In addition to LIP, SSA shows elevated ALK activity relative to its source waters. Five enzyme activities were measured in all three experiments: leucine- and serine-AMP, oleate- and stearate-LIP, and ALK. These activities were compiled and are presented as their average fractional contribution to SW and SSA in each experiment, and for all three experiments

combined (Fig. 3). These activities are not the total EA of each system, which would be comprised of many different EAs, but they are useful for comparing fractional contributions in SSA and SW. With the addition of ALK, AMP is still dominant in the SW, comprising on average 82% of these five EAs (Fig. 2.3, bottom row). Yet AMP accounts for just 37% of these five activities measured in SSA (Fig. 2.3 D). LIP accounts for 10% of the SW activities (Fig. 2.3 H) and 34% in SSA (Fig. 2.3 D), again showing LIP enhancement in SSA. Figure 3 provides the average relative contributions of the individual EAs that were summed in LIP and AMP in Figure 1. Leucine-AMP activity is ~6.5x the serine-AMP activity in the SW (Fig. 2.3 H). Stearate-LIP showed a ~15x SSA:SW enhancement in 2016 (Fig. 2.3 A, E), but this did not occur in 2018 (Fig. 2.3 B, C, F, G), when oleate-LIP showed greater enhancement than stearate-LIP, but much lower than 15x. ALK shows an equally strong enhancement in SSA as LIP, comprising on average 8% of the SW activity (Fig. 2.3 H) and 30% in SSA (Fig. 2.3 D). Using the combined values to calculate a SSA ALK:AMP to SW ALK:AMP ratio, as done for LIP, yielded a mean value of 8.3 for ALK. Calculating the value for LIP this way yielded a mean value of 7.5, therefore ALK enrichment in SSA is equal to or greater than LIP enhancement in SSA. The first report of SSA EA used non-metric multidimensional scaling (NMDS) to show qualitative differences in the EAs of SSA, SW, and the surface microlayer (Malfatti & Lee et al., 2019). But those results did not identify how SSA and SW EAs are different. Here we identify specific ways in which SSA EA is distinct from the EA of its source waters. Whereas AMP accounted for 72% of these five EAs in SW, ALK, LIP, and AMP showed similar activities in SSA (Fig. 2.3 D, H). This demonstrates that SSA is a distinct enzymatic environment from its source waters by being enhanced in ALK and LIP.

2.4.6 Mechanisms for LIP and ALK Enhancement in SSA

Enhanced lipase and alkaline phosphatase enzyme activities in SSA is an example of selective transfer in SSA. Lipids and their fatty acid building blocks have elevated transfer rates in SSA and this could result in elevated transfer of LIP embedded in lipids (Cochran et al., 2016; Mochida et al., 2002). The majority of ALK activity in SW comes from free ALK (not attached to cells), therefore ALK enhancement in SSA may stem from selective transfer of free ALK (Hoppe, 2003). Selective aerosolization of HB and cell associated enzymes could cause differences between SW and SSA enzyme profiles. Multiple factors, including HB cell properties, cause preferential transfer of certain bacteria in SSA, and those taxa could have more LIP and ALK attached (Hejkal et al., 1980; Fahlgren et al., 2015; Perrott et al., 2017; Rastelli et al., 2017; Michaud et al. 2018). Aerosol generation - rupturing bubble caps and jet drop ejection - could also cause different SW and SSA EA profiles. These processes could disproportionately damage certain enzymes as they transfer in SSA. Aerosolization processes could potentially stress HB and induce enzyme expression, as it has been shown that HB isolates can significantly modulate their EA (Martinez et al., 1996). It is assumed that the observed differences in SW and SSA EA profiles are not due to HB expressing different enzymes in SSA because the data come from nascent SSA with a short particle lifetime between particle and sampling, on the order of 10 min (Stokes et al., 2013).

2.4.7 Implications

The presence of different enzymes in SSA could influence the climate relevant roles of the particles in the atmosphere. Particle composition can affect water uptake and ice nucleation, and enzymes can change the chemical species that determine these particle properties. LIP has been shown to affect SSA surface properties, which becomes more significant in light of these results showing LIP to be an important SSA EA (Schiffer et al., 2018). The initial detection of

EA identified that enzymatically active SSA can collide and react with other particles in the atmosphere, a newly identified atmospheric reaction pathway (Malfatti & Lee et al., 2019). With equal LIP, ALK and AMP EAs, SSA is equally "tuned" for the hydrolysis of lipids, fatty acids, phosphate groups, proteins, and amino acids in the atmosphere. This differs from SW EA in which AMP is much higher than LIP and ALK. Therefore HB and enzymes influence the chemistry of both the ocean and atmosphere, but prioritize reactions differently in each.

2.5 Conclusions

Here SSA is shown to prioritize different enzymes than the source waters. Comparing LIP to AMP in SW and SSA reveals a ~10x enhancement of LIP activity in SSA. LIP, AMP, and ALK activities in SW and SSA show ALK to be equally enhanced in SSA as LIP. LIP, ALK, and AMP show roughly equal activities in SSA despite AMP being dominant in SW. Whereas the detection of active enzymes identified a previously undetected atmospheric chemical reaction pathway, this research shows specific enzymatic reactions that elevated in SSA. SSA prioritizes lipase and alkaline phosphatase reactions much more than seawater. The causes for this SW-SSA enzymatic shift may include the selective transfer of free enzymes, of cells with enzymes attached, or effects to enzymes or cells in the aerosolization process. Future work may gain insight into contributions of free vs. attached enzymes in SSA by sampling SSA by particle size and measuring enzyme activity. Advances in method sensitivity may be necessary to achieve such resolution. Such advances could be applied to test whether the variable stearate-LIP enhancement observed here between 2016 and 2018 is a function of SW chemical or microbial composition. Additional studies could also apply advances in sequencing to SW and SSA and relate SSA EA to SW and SSA HB community composition. Whereas these observations are from nascent SSA, the aging of particles in the atmosphere will further shape the enzyme profile

of SSA, which merits further investigation. Bacteria can release enzymes in SSA for as long as they remain alive, and after, following death and cell lysis. Much work remains to reveal the total atmospheric impact of active enzymes in SSA.

2.6 Acknowledgements

The authors gratefully acknowledge the support of the National Science Foundation through the Centers of Chemical Innovation Program via the Center for Aerosol Impacts on Chemistry of the Environment (CHE-1801971).

Chapter 2, in full, is currently being prepared for resubmission to ACS Earth & Space Chemistry: Pendergraft, M.A., Malfatti, F., Morris, C.K., Santander, M.V., DeAngelo, S., Mayer, K.J., Sauer, J.S., Wang, X., Azam, F., Prather, K.A. (*in prep*) Enhanced Lipase and Alkaline Phosphatase Enzyme Activities in Sea Spray Aerosol. The dissertation author is the primary investigator and author of this manuscript.

2.7 Figures

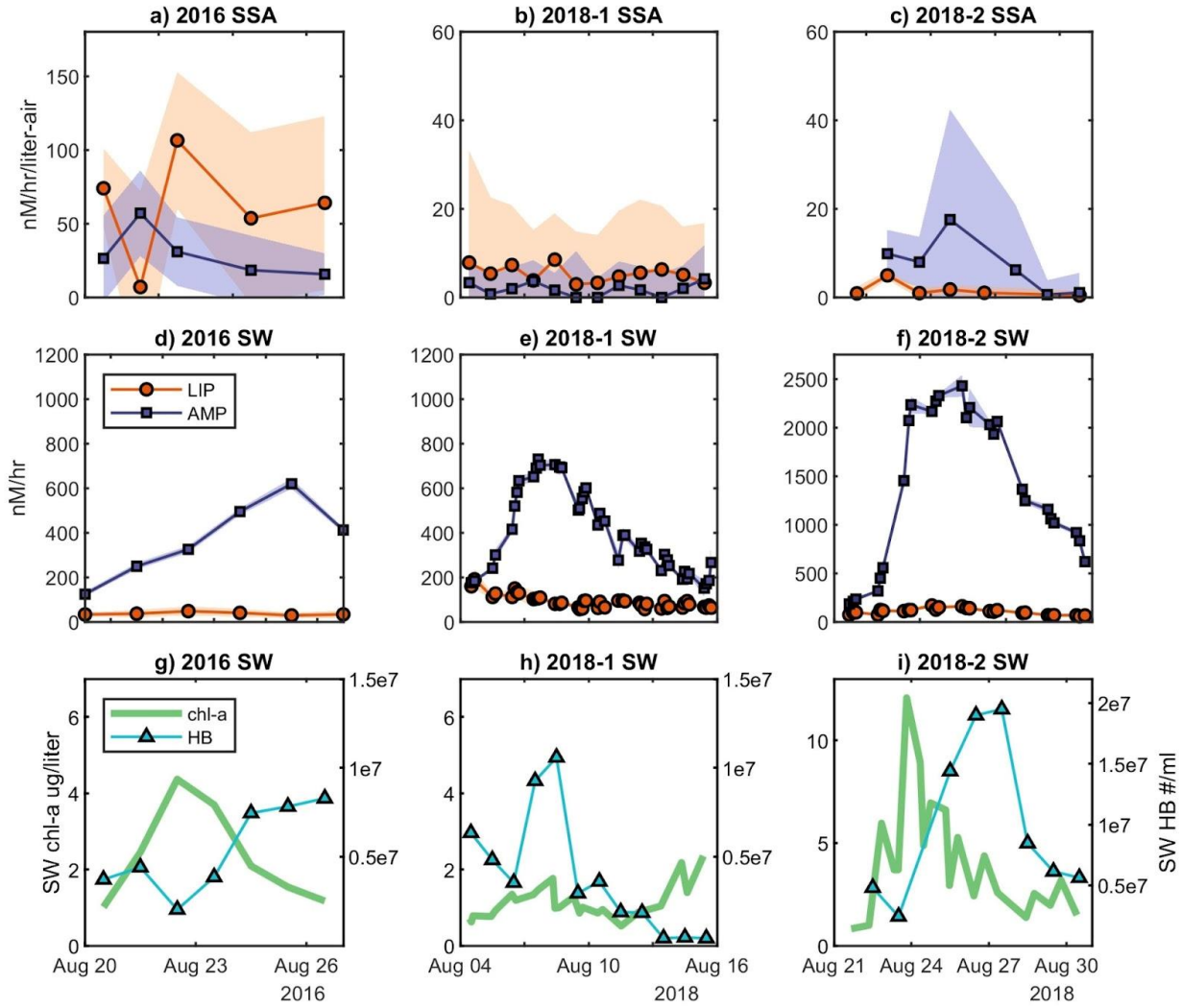

Figure 2.1 Enzyme activities, chl-a, and heterotrophic bacteria counts across the three experiments. Left column: 2016. Middle column: 2018-1. Right column: 2018-2. Top row (a-c) shows LIP and AMP EA in SSA. Middle row (d-f) shows LIP and AMP EA in SW. Bottom row (g-i) shows chl-a and HB concentrations in SW. Points denote measured values. Lines assist in linking the points. Shaded regions present one standard deviation.

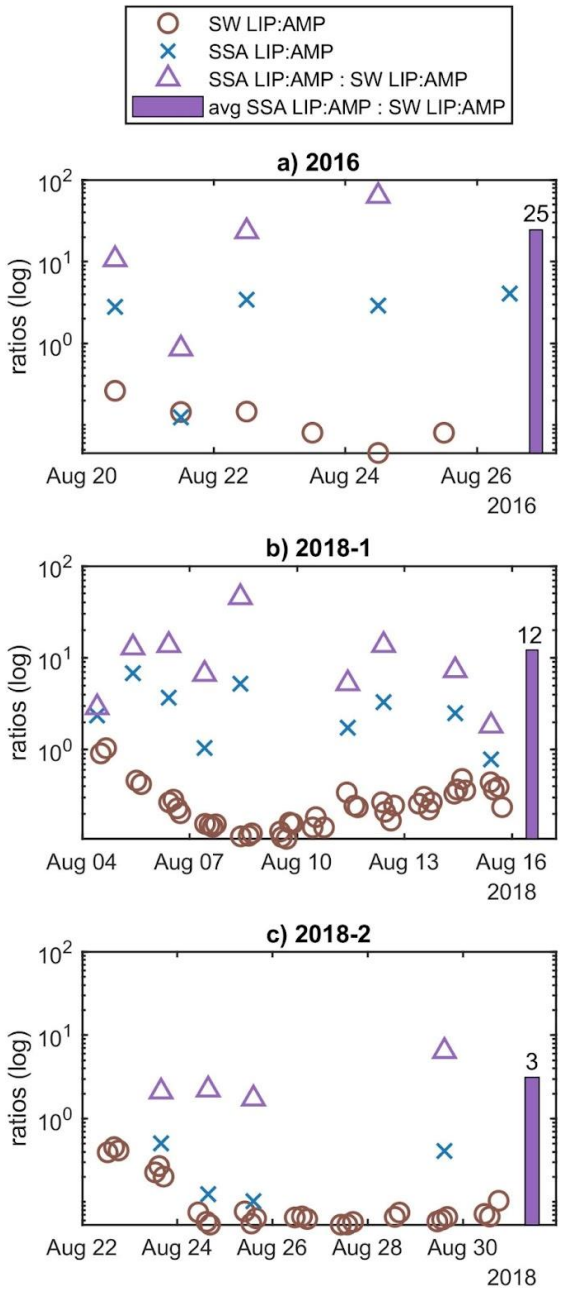

Figure 2.2 Lipase-to-aminopeptidase ratios (LIP:AMP) within and across SW and SSA. Individual SSA LIP:AMP : SW LIP:AMP points (purple triangles) are calculated from the SSA LIP:AMP value and the SW LIP:AMP value(s), interpolated to the SSA timepoints. The purple bar presents the average SSA LIP:AMP : SW LIP:AMP for each experiment and is labeled with its value.

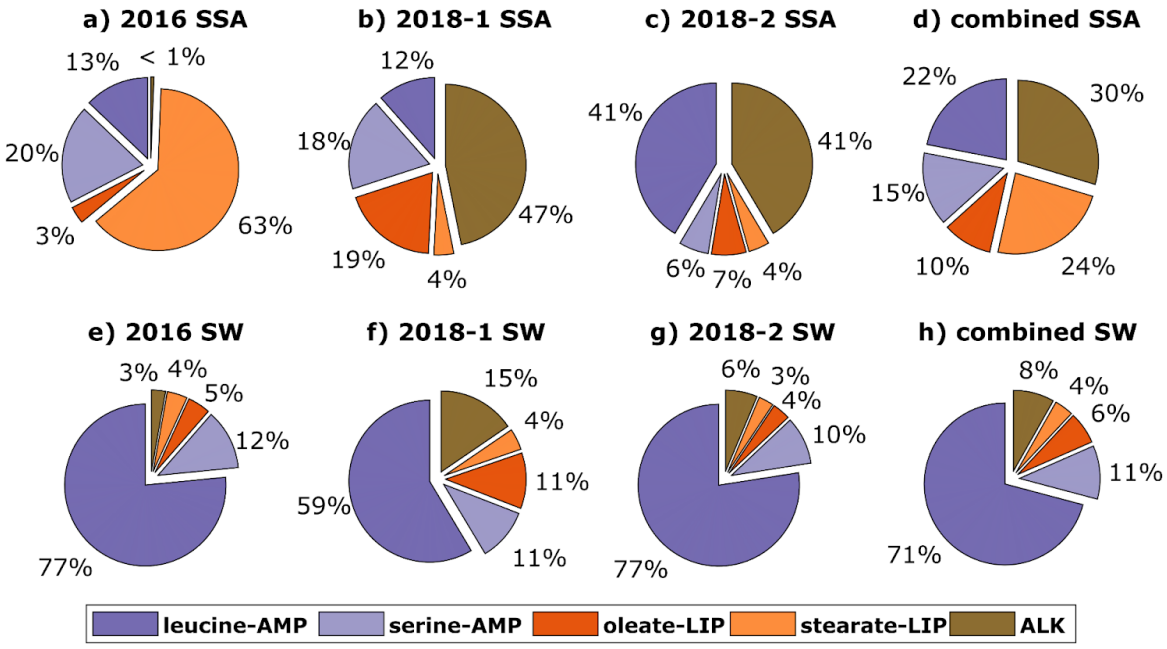

Figure 2.3 Fractional contributions of 5 enzymes show lipase (LIP) and alkaline phosphatase (ALK) enhancement in SSA. The average fractional contribution of each of five enzymes to SW (bottom) and SSA (top) is displayed for each experiment (columns) and for the average of the 3 experiments combined (d & h).

2.8 References

Arnosti, C. (2011). Microbial extracellular enzymes and the marine carbon cycle. *Annual Review of Marine Science*, 3, 401–425.

Azam, F., Fenchel, T., Field, J. G., Gray, J. S., Meyer-Reil, L. A., Thingstad, F. (1983). The ecological role of water-column microbes in the sea. *Marine Ecology Progress Series*, 10, 257–263. doi.org/10.3354/meps010257

Azam, F., Malfatti, F. (2007). Microbial structuring of marine ecosystems. *Nature Reviews Microbiology*, 5(10), 782–791.

Balmonte, J.P., Buckley, A., Hoarfrost, A., Ghobrial, S., Ziervogel, K., Teske, A., Arnosti, C. (2019). Community structural differences shape microbial responses to high molecular weight organic matter. *Environmental Microbiology*, 21(2), 557–571.

Cochran, R.E., Jayarathne, T., Stone, E.A., Grassian, V.H. (2016). Selectivity across the interface: a test of surface activity in the composition of organic-enriched aerosols from bubble bursting. *Journal of Physical Chemistry Letters*, 7(9), 1692–1696.

Cochran, R.E., Laskina, O., Jayarathne, T., Laskin, A., Laskin, J., Lin, P., Sultana, C., Lee, C., Moore, K.A., Cappa, C.D., Bertram, T.H., Prather, K.A., Grassian, V.H., Stone, E.A. (2016). Analysis of organic anionic surfactants in fine and coarse fractions of freshly emitted sea spray aerosol. *Environmental Science & Technology*, 50(5), 2477–2486.

Fahlgren, C., Gómez-Consarnau, L., Zábori, J., Lindh, M. V., Krejci, R., Mårtensson, E. M., Nilsson, D., Pinhassi, J. (2015). Seawater mesocosm experiments in the Arctic uncover differential transfer of marine bacteria to aerosols. *Environmental Microbiology Reports*, 7(3), 460–470.

Fukuda, R., Sohrin, Y., Saotome, N., Fukuda, H., Nagata, T., Koike, I. (2000). East-west gradient in ectoenzyme activities in the subarctic Pacific: possible regulation by zinc. *Limnology and Oceanography*, 45(4), 930–939. doi.org/10.4319/lo.2000.45.4.0930

Gasol, J.M., Del Giorgio, P.A. (2000). Using flow cytometry for counting natural planktonic bacteria and understanding the structure of planktonic bacterial communities. *Scientia Marina*, 64(2), 197–224. doi.org/10.3989/scimar.2000.64n2197

Guillard, R.R.L. (1975). Culture of phytoplankton for feeding marine invertebrates. *Culture of Marine Invertebrate Animals*, 29–60. Springer US.

Hasenecz, E.S., Jayarathne, T., Pendergraft, M.A., Santander, M.V., Mayer, K.J., Sauer, J., Lee, C., Gibson, W.S., Kruse, S.M., Malfatti, F., Prather, K.A., Stone, E.A. (2020). Marine

bacteria affect saccharide enrichment in sea spray aerosol during a phytoplankton bloom. *ACS Earth and Space Chemistry*, 4(9), 1638–1649. doi.org/10.1021/acsearthspacechem.0c00167

Hejkal, T.W., Larock, P.A., Winchester, J.W. (1980). Water-to-Air Fractionation of Bacteria. *Applied and Environmental Microbiology*, 39(2), 335–338.

Hoppe, H.-G. (1983). Significance of exoenzymatic activities in the ecology of brackish water: measurements by means of methylumbelliferyl-substrates. *Marine Ecology Progress Series*, 11, 299–308. doi.org/10.3354/meps011299

Hoppe, H.-G. (2003). Phosphatase activity in the sea. *Hydrobiologia*, 493(1/3), 187–200.

Jayarathne, T., Sultana, C.M., Lee, C., Malfatti, F., Cox, J.L., Pendergraft, M.A., Moore, K.A., Azam, F., Tivanski, A.V., Cappa, C.D., Bertram, T.H., Grassian, V.H., Prather, K.A., Stone, E.A. (2016). Enrichment of saccharides and divalent cations in sea spray aerosol during two phytoplankton blooms. *Environmental Science & Technology*, 50(21), 11511–11520.

Lee, C., Sultana, C.M., Collins, D.B., Santander, M.V., Axson, J.L., Malfatti, F., Cornwell, G.C., Grandquist, J.R., Deane, G.B., Stokes, M.D., Azam, F., Grassian, V.H., Prather, K.A. (2015). Advancing model systems for fundamental laboratory studies of sea spray aerosol using the microbial loop. *The Journal of Physical Chemistry A*, 119(33), 8860–8870.

Lewis, E.R., Schwartz, S.E. (2004). Sea salt aerosol production: mechanisms, methods, measurements, and models. American Geophysical Union.

Malfatti, F., Lee, C., Tinta, T., Pendergraft, M. A., Celussi, M., Zhou, Y., Sultana, C.M., Rotter, A., Axson, J.L., Collins, D.B., Santander, M.V., Anides Morales, A.L., Aluwihare, L.I., Riemer, N., Grassian, V.H., Azam, F., Prather, K.A. (2019). Detection of active microbial enzymes in nascent sea spray aerosol: implications for atmospheric chemistry and climate. *Environmental Science & Technology Letters*, 6(3), 171–177.

Martinez, J., Smith, D.C., Steward, G.F., Azam, F. (1996). Variability in ectohydrolytic enzyme activities of pelagic marine bacteria and its significance for substrate processing in the sea. *Aquatic Microbial Ecology: International Journal*, 10(3), 223–230.

Mayol, E., Arrieta, J.M., Jiménez, M.A., Martínez-Asensio, A., Garcias-Bonet, N., Dachs, J., González-Gaya, B., Royer, S.-J., Benítez-Barrios, V.M., Fraile-Nuez, E., Duarte, C.M. (2017). Long-range transport of airborne microbes over the global tropical and subtropical ocean. *Nature Communications*, 8(1), 201.

Mayol, E., Jiménez, M.A., Herndl, G.J., Duarte, C.M., Arrieta, J.M. (2014). Resolving the abundance and air-sea fluxes of airborne microorganisms in the North Atlantic Ocean. *Frontiers in Microbiology*, 5, 557.

Michaud, J.M., Thompson, L.R., Kaul, D., Espinoza, J.L., Alexander Richter, R., Xu, Z.Z., Lee, C., Pham, K.M., Beall, C.M., Malfatti, F., Azam, F., Knight, R., Burkart, M.D., Dupont, C.L., Prather, K.A. (2018). Taxon-specific aerosolization of bacteria and viruses in an experimental ocean-atmosphere mesocosm. *Nature Communications*, 9(1). doi.org/10.1038/s41467-018-04409-z

Misic, C., Castellano, M., Fabiano, M., Ruggieri, N., Saggiomo, V., Povero, P. (2006). Ectoenzymatic activity in surface waters: a transect from the Mediterranean Sea across the Indian Ocean to Australia. *Deep-Sea Research Part I: Oceanographic Research Papers*, 53(9), 1517–1532.

Mochida, M., Kitamori, Y., Kawamura, K., Nojiri, Y., Suzuki, K. (2002). Fatty acids in the marine atmosphere: factors governing their concentrations and evaluation of organic films on sea-salt particles. *Journal of Geophysical Research: Atmospheres*, 107(D17). doi.org/10.1029/2001jd001278

Noble, R.T., Fuhrman, J.A. (1998). Use of SYBR Green I for rapid epifluorescence counts of marine viruses and bacteria. *Aquatic Microbial Ecology*, 14, 113–118. doi.org/10.3354/ame014113

Obayashi, Y., Suzuki, S. (2005). Proteolytic enzymes in coastal surface seawater: significant activity of endopeptidases and exopeptidases. Limnology and Oceanography, 50(2), 722–726.

O'Reilly, J.E., Maritorena, S., Mitchell, B.G., Siegel, D.A., Carder, K.L., Garver, S.A., Kahru, M., McClain, C. (1998). Ocean color chlorophyll algorithms for SeaWiFS. *Journal of Geophysical Research: Oceans*, 103(C11), 24937–24953. doi.org/10.1029/98jc02160

Pan, M., Eiguren-Fernandez, A., Hsieh, H., Afshar-Mohajer, N., Hering, S.V., Lednicky, J., Hugh Fan, Z., Wu, C.-Y. (2016). Efficient collection of viable virus aerosol through laminar-flow, water-based condensational particle growth. *Journal of Applied Microbiology*, 120(3), 805–815.

Perrott, P., Turgeon, N., Gauthier-Levesque, L., Duchaine, C. (2017). Preferential aerosolization of bacteria in bioaerosols generated in vitro. *Journal of Applied Microbiology*, 123(3), 688–697.

Quinn, P.K., Collins, D.B., Grassian, V.H., Prather, K.A., Bates, T.S. (2015). Chemistry and related properties of freshly emitted sea spray aerosol. *Chemical Reviews*, 115(10), 4383–4399.

Rastelli, E., Corinaldesi, C., Dell'Anno, A., Lo Martire, M., Greco, S., Cristina Facchini, M., Rinaldi, M., O'Dowd, C., Ceburnis, D., Danovaro, R. (2017). Transfer of labile organic matter and microbes from the ocean surface to the marine aerosol: an experimental approach. *Scientific Reports*, 7(1), 11475.

Riemann, L., Steward, G.F., Azam, F. (2000). Dynamics of bacterial community composition and activity during a mesocosm diatom bloom. *Applied and Environmental Microbiology*, 66(2), 578–587.

Schiffer, J.M., Luo, M., Dommer, A.C., Thoron, G., Pendergraft, M.A., Santander, M.V., Lucero, D., Pecora de Barros, E., Prather, K.A., Grassian, V.H., Amaro, R.E. (2018). Impacts of lipase enzyme on the surface properties of marine aerosols. *Journal of Physical Chemistry Letters*, 9(14), 3839–3849.

Smith, D.C., Simon, M., Alldredge, A. L., Azam, F. (1992). Intense hydrolytic enzyme activity on marine aggregates and implications for rapid particle dissolution. *Nature*, 359(6391), 139–142.

Stokes, M.D., Deane, G.B., Prather, K., Bertram, T.H., Ruppel, M.J., Ryder, O.S., Brady, J.M., Zhao, D. (2013). A Marine Aerosol Reference Tank system as a breaking wave analogue for the production of foam and sea-spray aerosols. *Atmospheric Measurement Techniques*, 6(4), 1085–1094.

Teeling, H., Fuchs, B.M., Becher, D., Klockow, C., Gardebrecht, A., Bennke, C.M., Kassabgy, M., Huang, S., Mann, A.J., Waldmann, J., Weber, M., Klindworth, A., Otto, A., Lange, J., Bernhardt, J., Reinsch, C., Hecker, M., Peplies, J., Bockelmann, F. D., Callies, U., Gerdts, G., Wichels, A., Wiltshire, K.H., Glockner, F.O., Schweder, T., Amann, R. (2012). Substrate-controlled succession of marine bacterioplankton populations induced by a phytoplankton bloom. *Science*, 336(6081), 608–611.

Trueblood, J.V., Wang, X., Or, V.W., Alves, M.R., Santander, M.V., Prather, K.A., Grassian, V.H. (2019). The old and the new: aging of sea spray aerosol and formation of secondary marine aerosol through OH oxidation reactions. *ACS Earth and Space Chemistry*, 3(10), 2307–2314. doi.org/10.1021/acsearthspacechem.9b00087

Wang, X., Sultana, C.M., Trueblood, J., Hill, T.C.J., Malfatti, F., Lee, C., Laskina, O., Moore, K.A., Beall, C.M., McCluskey, C.S., Cornwell, G.C., Zhou, Y., Cox, J.L., Pendergraft, M.A., Santander, M.V., Bertram, T.H., Cappa, C.D., Azam, F., DeMott, P.J., Grassian, V.H., Prather, K.A. (2015). Microbial control of sea spray aerosol composition: a tale of two blooms. *ACS Central Science*, 1(3), 124–131.

Weiss, M.S., Abele, U., Weckesser, J., Welte, W., Schiltz, E., Schulz, G.E. (1991). Molecular architecture and electrostatic properties of a bacterial porin. *Science*, 254(5038), 1627–1630.

Chapter 3. Advances in Sea Spray Aerosol 16S Sequencing Reveal a Dynamic Community

3.1 Abstract

The airborne microbiome affects global ecosystems and human health by distributing species across the planet, influences weather and climate by interacting with radiation and cloud formation, and is understudied due to its low biomass and unique sampling requirements. Rich with microbial life and covering ~70% of the Earth, the ocean is a major source of microorganisms to the atmosphere. Marine bacteria number 10^4-10^6 ml^{-1}, accumulate at the ocean surface, and readily transfer to the atmosphere in sea spray aerosol. Sensitive aerosol sampling and sequencing is necessary to better understand the atmospheric roles of marine bacteria. This work develops and details a low biomass workflow for the sampling and 16S amplicon sequencing of SSA. By combining efficient aerosol sampling with the Katharoseq 16S method, detection limits for sequencing success were achieved at 3.9 hs sampling time, 37 liters of air, $4.1x10^6$ supermicron SSA, and 1046 heterotrophic bacteria cells. The resulting data confirm previous observations that the SSA bacteria community is distinct from the community of its source waters. Furthermore, the data show for the first time that different seawater communities produce different SSA communities. Bacteria aerosolization varied within taxonomic groupings and across different water masses, showing intermittent taxons specific aerosolization to be dominant. By improving the sequencing of aerosols and our understanding of the controls on bacteria transfer from the ocean to the atmosphere, the scientific community can improve our collective understanding of how the ocean and atmosphere interact to shape the global microbiome and impact the health of people and the planet.

3.2 Introduction

The atmosphere is home to diverse microorganisms and the ocean is a significant source. High winds, breaking waves, and bubbles popping at the ocean surface eject sea spray aerosol (SSA) from the ocean's surface (Quin et al., 2015). These particles range in size from tens of nanometers to tens of microns and are large enough to contain marine bacteria (~1 µm), viruses (~0.1 µm), and other microorganisms (Patterson et al., 2016; Michaud et al., 2018). In the marine boundary layer, approximately 0.3-2 $x10^4$ prokaryotes (bacteria and archaea) and 0.02-$1x10^4$ eukaryotes per m^3 of air come from the ocean (Mayol et al., 2014, 2017). Fluxes from the tropical and subtropical ocean to the atmosphere are reported at $1x10^3$ to $2x10^6$ cells m^{-2} day^{-1} for prokaryotes and 1-2 $x10^3$ cells m^{-2} d^{-1} for eukaryotes (Mayol et al., 2014; 2017). Microorganisms comprise a significant fraction of the global aerosol population and play important roles in the atmosphere. Atmospheric ice formation influences precipitation amounts, and the oceans are a significant source of ice nuclei to the atmosphere (Wilson et al., 2015; DeMott et al., 2016; Creamean et al., 2013). Clouds require aerosols to form and the ~0.5-1 µm size of many airborne marine prokaryotes and eukaryotes implies they are effective cloud condensation nuclei (Möhler et al., 2007). Aerosolization in SSA is an important dispersal mechanism for marine microbes. Viruses (phages) transfer to the atmosphere in SSA and can infect distant phytoplankton after re-entering the ocean (Sharoni et al., 2015). It is also possible for microbes from coastal water pollution to aerosolize in SSA and reach large numbers of people on land (Baylor et al., 1977; Graham et al., 2018; Michaud et al., 2018).

Bacteria are abundant throughout the ocean and commonly transfer to the atmosphere SSA. In oceanic surface waters they commonly number 10^6 ml^{-1}, with higher concentrations possible in productive waters (Azam et al., 1983). Using enzymes bacteria carry out much of marine respiration and chemically alter marine organic matter (Azam, 1998; Azam & Malfatti,

2007). Approximately 50% of carbon fixed in the oceans by photosynthesis is respired back to CO_2 by marine bacteria (Azam et al., 1983). They have been detected in marine and coastal air and in SSA generated in the laboratory (Cho and Hwang, 2011; Xia et al., 2015; Michaud et al., 2018; Archer et al., 2020; Uetake et al., 2020). The ~0.5-1 μm diameter of marine bacteria is conducive to aerosolization, cloud formation, and potential precipitation, implying bacteria readily cycle between ocean and atmosphere (Farmer et al., 2015).

Investigating community composition of airborne marine bacteria presents an analytical challenge. Genetic sequencing of aerosols is complicated by low biomass and relatively high sample contamination. This work develops a SSA sampling and sequencing workflow by applying high efficiency aerosol sampling with a low biomass 16S sequencing protocol.

3.3 Materials and Methods

3.3.1 Sea Spray Aerosol Generation

Three sampling rounds (SR) were conducted in which seawater (SW) and isolated, nascent sea spray aerosol (SSA) were sampled using the MART (Stokes et al., 2013; Lee et al., 2015). The MART (120 liters SW, 90 liters headspace) uses a plunging waterfall to generate nascent SSA with bubble and particle size distributions that match those observed for breaking waves (Stokes et al., 2013). A challenge of studying SSA in the atmosphere is that there are many particle types from different sources present. The MART exclusively generates SSA from isolated source waters, which allows for direct comparison between SSA and source waters. In the present study, the MART was filled with SW from the Ellen Browning Scripps Memorial Pier at Scripps Institution of Oceanography, filtered through 50 μm Nitex mesh to remove phytoplankton predators, as done before (Lee et al., 2015). For each SR, recently collected SW was added to the MART to provide a community of marine bacteria. For SR's 2 and 3,

Guillard's algae growth medium (Proline/Pentaires, Apopka, FL) was added at the f/20 level with sodium metasilicate to indirectly bolster the bacteria community by supporting phytoplankton growth. Figure 3.1 provides a visual summary of the methods.

3.3.2 SSA Sizing and Counting

Aerosols were sized and counted using an aerodynamic particle sizer (APS; TSI Inc. model 3321) for particles with aerodynamic diameters 0.5-20 μm. This is the size range where we expect to find marine bacteria (~0.5-1 μm) in SSA. For the sake of simplicity we refer to this size range as supermicron. The aerosols were not dried prior to being sized in order to capture their sizes at the MART's ambient relative humidity (~90%).

3.3.3 SSA Sampling

Nascent SSA was sampled using the Series 100 Universal Spot Sampler (model SS110A; Aerosol Devices Inc, Fort Collins, CO; heretofore "SPOT"), using the liquid sampling configuration. The SPOT uses a condensation growth tube to increase particle size and sampling efficiency. It has shown ~90% sampling efficiency for particles smaller than 100 nm, appropriate for collecting marine bacteria (~0.5-1 μm) (Pan et al., 2016). Following condensational growth, the particles are impacted into liquid. Sampling aerosols into liquid facilitates downstream procedures such as cell counting and DNA extraction by avoiding extraction from a filter, and also allows direct aerosol collection into liquid preservatives. MART SSA was sampled simultaneously into two SPOTs: one sampled SSA into 0.2 μm filtered and autoclaved seawater (FASW); the other sampled SSA into PGE: 1x phosphate buffer solution (PBS) at 20% (v/v) glycerol and 20 mM ethylenediaminetetraacetic acid (EDTA). PBS provides salinity to reduce osmotic lysis of marine cells, glycerol reduces evaporation and protects cells in frozen storage, and EDTA chelates divalent cations required by DNA-degrading nucleases (Seutin et al., 1991;

Sharpe et al., 2020). 0.75 ml of the solution was used in the SPOT cup, then upon sample retrieval the total volume was brought to 1.6 ml. Replicate aliquots (0.1-0.3 ml) for DNA extraction were pipetted into cryovial tubes or directly into extraction tubes (Qiagen PowerSoil kit, Cat#12888-50). Aliquots for cell counts (0.4 ml) were pipetted into cryovial tubes and immediately fixed with glutaraldehyde. Varying amounts of SSA were collected from the MART by varying the sampling durations in order to test sequencing success against the amount of aerosol collected. Blanks were collected by connecting a HEPA filter to the inlet of the SPOTs to sample particle free air for varying periods of time (Fig. 3.1; Table 3.1).

3.3.4 Bacteria Cell Counts

Samples of SW and SSA from the MART were processed for estimation of heterotrophic bacteria abundance by flow cytometry using ZE5 Cell Analyzer (BioRad, Hercules, CA) at The Scripps Research Institute (TSRI) Flow Core Facility facility (Gasol and Del Giorgio, 2000). SSA samples and blanks were diluted 1:1 into 1×TE buffer (pH 8) then stained with SYBR™ Green I (Invitrogen, Waltham, MA) at room temperature for 10 min in the dark. SW was diluted 1:10 in the 1×TE buffer (pH 8) then stained with SYBR™ Green I at room temperature for 10 min in the dark. The SYBR™ Green I stock (10,000x) was diluted by 100 and then 5 µl was added to the 500 µl samples, incubated for 10 minutes at room temperature, and then analyzed. Cells with autofluorescence (from chl-a) were excluded, generating counts of heterotrophic bacteria.

3.3.5 DNA Extraction

The Katharoseq ultra low biomass method for 16S amplicon sequencing of SSA was applied to SSA (Minich et al., 2018). Katharoseq uses a positive addition of a control to establish a read count lower limit for each sequencing run. The method also uses ultraclean laboratory

practices and single tube extractions to minimize sample contamination and carryover. Briefly, samples were processed following the Earth Microbiome Project protocols (EMP) (earthmicrobiome.org) (Thompson et al., 2017). A 100 µl aliquot of SW or SSA was processed for DNA extraction. For the EMP extraction method, which implements an additional lysis step where tubes are incubated for 10 min at 65 °C prior to bead beating, 100 µl of liquid sample was placed into 2 ml bead beating tubes sourced from the Qiagen PowerSoil kit (Qiagen, Cat# 12888-50) and then processed according to the Qiagen PowerMag kit (Qiagen, Cat# 27200-4). Performing lysis in single tubes rather than a plate based method helps reduce the amount of well-to-well contamination (Minich et al., 2019). For all extractions, a titration of positive controls using the zymo mock community (Cat# D6300, Zymo Research, Irvine CA) was used to determine the limit of detection of the assay which is critical for low biomass samples (Minich et al., 2018a).

3.3.6 Library Preparation and Sequencing

Library preparation for 16S sequencing utilized the 515F/806R 16S primers from the EMP protocols (Apprill et al., 2015; Walters et al., 2016). All libraries were processed in triplicate reactions. Two different PCR reaction volumes were used (5 µl or 25 µl) to evaluate if DNA volume (0.2 µl vs. 5 µl) had a positive impact on ultra-low biomass samples. A large volume (25 µl) PCR reaction using 5 µl of gDNA was used following guidance from the Katharoseq protocol (Minich et al., 2018a). The second PCR reaction followed the ‘miniaturized protocol’ which uses a PCR reaction volume of 5 µl composed of 0.2 µl of gDNA (Minich et al., 2018b). All PCR reactions followed the standard EMP 16S thermocycler procedure. All PCR reactions had equal volumes (2 µl per sample) pooled to ensure compatibility for sample success

comparisons (Minich et al., 2018a). The final pool was then processed through a PCR cleanup kit and then sequenced on a MiSeq (Caporaso et al., 2011; 2012).

3.3.7 Microbiome Analysis

The sequencing run was uploaded to Qiita (Qiita study ID: 12544; 16S artifact 13246) and processed using Qiime2 (version 2021.11) (Gonzalez et al., 2018; Bolyen et al., 2019). Samples were demultiplexed and processed using the deblur (version 2019.09) pipeline to generate Amplified Sequence Variants (ASVs) which represent unique sequence variants (Amir et al., 2017). The primary analysis was conducted in Qiita (Qiita Analysis ID: 52421). The dataset was annotated in Qiita using the pre-fitted sklearn SILVA-138-99-515-806 classifier. For the limit of detection (read count cutoff), only the positive controls (control_type=Zymo) were included. The features were collapsed and analyzed at the genus level (level 6). Each PCR reaction volume protocol was independently analyzed (25 µl vs 5 µl). The limit of detection for the assay was calculated for each of the two PCR strategies by comparing the total reads vs. the relative abundance of target sequences amongst the titration of positive controls. For the zymo mock community, the table 3.2 lists the taxa that were included and summed to determine the total reads mapping to the target. All known members of the mock community were found. Salmonella enterica is the f__Enterobacteriaceae;__. The distribution is fit using the allosteric sigmoidal equation in Prism9.0 (GraphPad) following the Katharoseq protocol (Minich et al., 2018a). We determine a minimum read cutoff at the number of reads present when 90% of reads represent and map to the known control. Samples with less reads are excluded because contaminants may account for more than 10% of their reads. Microbial biomass of each sample was estimated using the 16S rRNA read counts from the titrations of known Zymo mock community controls following the Katharoseq protocol [Host biology, ecology and the

environment influence microbial biomass and diversity in 101 marine fish species DOI : 10.1038/s41467-022-34557-2]. Briefly, one uses the positive control titrations (Zymo mock community) to plot the total reads (post deblur) against the relative abundance of the controls (% of reads which match the target). One fits the allosteric sigmoidal equation which can be done in the Katharoseq Qiime2 plugin or using Prism9. One must then solve the equation where y=0.9. We choose 0.9 so that 90% of the reads map back to the control and erroneous reads from contamination or otherwise are at 10% or less. The equation is: Y=Vmax * X^h(Kprime + X^h). For alpha diversity, richness, Shannon, and Faith's phylogenetic diversity were calculated while both Weighted normalized UniFrac and Unweighted UniFrac distances were used for beta diversity comparisons (Faith, 1992; Lozupone et al., 2011).

3.3.8 Final Sample Set

For the comparison of SW and SSA communities, samples from experiments 'MARTC_2', 'SIO Pier', and the filter blanks were excluded as they were part of a different study. The final dataset for this study contains only samples processed with the PowerSoil MAG attract DNA purification method and the 25 µl PCR reaction volume (5 µl of DNA as template). In total, there were 49 samples (19 SW, 30 SSA) and 10 spot sampler blanks.

3.3.9 Data Availability

The primary data set is publicly available (Qiita ID 12544) along with the analysis (Qiita analysis ID: 52421).

3.4 Results

3.4.1 Limits of Detection: Katharoseq Read Cutoff

Samples from this study were processed in Qiita (Qiita study ID: 12544). After applying the deblur positive hit filter, a total of 330 samples and 11,772 features were included in the raw

biom table (Qiita analysis ID: 52406). A total of 30 positive controls (Zymo mock community titrations) were processed using the Power Mag extraction kit and then amplified in either a 5 µl or 25 µl PCR reaction. The limit of detection (LoD) sample threshold for each method was calculated: 3673 reads for the 25 µl reaction and 1600 reads for the 5 µl reaction (Fig. 3.2 a-b). When applied to the dataset, the 25 µl PCR reaction had a higher sample retention (success) rate (45 out of 49 samples) as compared to the 5 µl PCR reaction (36 out of 49 samples) for SW and SSA samples combined. Both PCR reaction volumes retained all 19 sea water samples, whereas the 25 µl reaction retained 26 out of 30 SSA, and the 5 µl reaction only retained 17 out of 30 SSA samples (Fig. 3.2 c, d). Thus, for the purposes of the biomass estimation, we use samples processed with the 25 µl PCR reaction (5 µl of DNA) (Vmax = 1.047, h=0.9776, K1/2=575.6, Kprime=499.1) with the calculated threshold of 3673 reads (Fig. 3.2 b). For the microbiome analysis, samples with less than 3673 reads were excluded. Figure 3.2 e shows that total reads increase with increasing amounts of positive control cells input. The biomass estimation used all of the Katharoseq positive controls. The estimation of biomass from reads positively correlates (R^2=0.7696) with HB cell counts from flow cytometry Figure 3.2 f. The remainder of the analyses only use the samples that were extracted with the PowerMag method and processed using the 25 µl PCR reaction with 5 µl of DNA.

Two storage solutions for SSA, FASW and PGE, were tested for their sequencing success. Out of FASW samples 7 were successful (per read counts) whereas 11 of 13 PGE samples sequenced successfully. A total of 7 SSA samples had successful sequencing of both FASW and PGE samples. This included two samples from experiment 1 (12-02-18 1145; 12-04-18 1615), three samples from experiment 2 (12-13-18 0900; 12-13-18 1330; 12-14-18 0740), and two samples from experiment 3 (12-20-18 0800; 12-20-18 1810). Because there were no

noticeable differences in success rate and therefore storage stability, we pooled data from both solutions for subsequent analyses.

3.4.2 Limits of Detection: SSA Sample Size

Read counts were compared to sample size in order to test the hypothesis that SSA sequencing success is determined by SSA sample size. Logistic regression and generalize linear (GLM) models were constructed to estimate sequencing success in terms of total SSA sampling time, volume of air into DNA extraction, number of supermicron aerosols into DNA extraction, and heterotrophic bacteria cells into DNA extraction. From the modeling, sampling success was reached, on average, at: 3.92 hs of total aerosol sampling time; 37.2 liters of air in each aliquot sent into DNA extraction; $4.1x10^6$ supermicron SSA extracted, and 1046 HB extracted (Fig. 3.3). These are effectively the limits of detection achieved by the combined SSA sampling and sequencing approach in terms of those parameters. Estimated biomass was similarly modeled against these parameters (Fig. 3.4) and demonstrate that estimated biomass increases with SSA sampling time, air volume, particle counts, and cell counts. Table 3.1 summarizes metrics on sequencing success for all samples with data for all of the included fields.

3.4.3 Effects of SSA Collection Duration and Amount

Long sampling times spanning multiple hours are often required to obtain sufficient microbial biomass for SSA sequencing. A concern with long sampling times is the stability of the microbial community in the sample. SSA microbial diversity did not significantly vary across sampling times (Fig. 3.5 a-d), volumes of air extracted (Fig. e-h), nor number of aerosols extracted (Fig. 3.5 i-l). In addition, SSA bacterial diversity did not vary with increasing counts of HB (Fig. 3.5 m-o). Estimated biomass increased with increasing sampling time, air volume sampled, and aerosols sampled (Fig. 3.5 m-o), but the relationship was not significant. HB

counts in SSA were positively and significantly associated with estimated biomass (Fig. 3.5 p). Why the relationships in Fig. 3.5 m-p were not stronger may be due to inconsistent HB aerosolization, errors in HB counts, and/or variability in the relationship between read counts and biomass. Overall, these results demonstrate that smaller SSA samples are effective at capturing microbial diversity, community composition remains stable over longer sampling times, biomass estimated from read counts correlates with HB cell counts.

3.4.4 SW and SSA Community Composition

Figure 3.6 reports the fractional contribution of the 12 most abundant families to each SSA (Fig. 3.6 a) and SW (Fig. 3.6 b) sampling. Alteromonadaceae, Flavobacteraceae, and Nitrincolaceae comprised the top 3 families in both SW and SSA and are common marine prokaryotes (Ivanova & Mikhaĭlov, 2001; Liu et al., 2020). We were not able to determine why the SSA community on day 1 of SR 3 was different from other days, which influences subsequent community analyses. Figure 3.7 provides a community overview at the phylum level.

3.5 Discussion

3.5.1 Method Evaluation

This research aimed to establish sensitivities for sampling and 16S sequencing of isolated, nascent SSA. The MART was ideal for this application because it generated isolated SSA - without other particle types present - using a mechanism that mimicked a breaking wave and produced the corresponding bubble and particle sizes, including supermicron SSA (Stokes et al., 2013). Investigations into the SSA community in the open atmosphere inevitably collect non-SSA because they are ubiquitous, even over the remote ocean (Urbano et al., 2011; Mayol et al., 2017; Graham et al., 2018). One disadvantage of the MART is that its fixed volume contains a limited amount of surface microlayer (SML). We did not sample the SML in order to not deplete

it because it is important in SSA formation and bacteria transfer. Sampling SSA with the SPOT was appropriate for this application for multiple reasons. The SPOT has a high collection efficiency (>90%) for particle sizes down to ~30 nm, making it appropriate to collect airborne bacteria (Pan et al., 2016). Sampling into liquid allowed sampling SSA directly into a preservative. The low flow rate (1-2 lpm) of the SPOT was appropriate for sampling SSA from the MART, which requires low flow sampling.

The positive correlation between read counts and each of our four measures of SSA sample size verify that sampling success increases with increasing SSA sample size (Fig. 3.3). Sampling time, air volume, and number of supermicron SSA show weak correlations to read counts (Fig. 3.3 a-c). The variability observed here indicates bacteria transfer in SSA is irregular with respect to time, air volume, and SSA counts, even with controlled aerosol production. The correlation between read counts and cell counts is greatest (Fig. 3.3 d) because cell counts are a direct measure of biomass.

Similar sequencing success rates from sampling SSA into PGE vs. FASW show that PGE can be used in place of FASW for SSA collection and storage. PGE is easier to prepare than FASW and poses improvements for reproducibility and contaminant DNA in reagents. PGE is produced from reagent grade commercial products, whereas FASW is prepared from seawater, which is rich with life. Although filtering (0.2 um) and autoclaving combined is effective at sterilization, they do not necessarily remove all DNA. Qualitative, visual inspection of the flow cytometry data from the aerosol blanks shows a cleaner background for PGE vs. FASW, suggesting a lower background and better signal-to-noise ratio. The inclusion of viscous glycerol in the PGE appears to be effective at slowing evaporation from the SPOT cup during extended sampling periods in the lab and field. Evaporation lowers the level of the liquid in the SPOT

collection cup, which may impact collection efficiency; total evaporation of the liquid is a lost sample. Additionally, at 20% glycerol, PGE may be more conducive than FASW for culturing SSA microbes from frozen samples, although the 20 mM EDTA may require dilution or centrifugation and washing.

3.5.2 *Family* Level Comparison of Seawater and SSA Communities

Beyond metrics on the sampling and sequencing of SSA, this dataset provides an opportunity to investigate SSA community composition. Looking at community composition at the family level (Fig. 3.6), the SSA community shows similarities to and differences from the SW community. The same 3 families - *Alteromonadaceae*, *Flavobacteriaceae*, and *Nitrincolaceae* - comprise the top 3 families in both SW and SSA. Differences in their relative abundances in the SW mark the three SR. Their combined relative abundance is generally lower in the SSA than in the SW, with relatively greater fractional contributions to the SSA community by other families. Within each experiment their relative abundances vary more in the SSA than in the SW, indicating greater community variability in SSA vs. SW. For instance, Cryomorphaceae is the ninth most abundant family in the SW and the fourth most abundant family in SSA, indicating preferential aerosolization of this family, which we investigate in greater detail further on.

3.5.3 Different Seawater Communities Produce Different SSA Communities

Generating SSA from three batches of SW with different prokaryotic communities reveals that as the SW community varied, so did the SSA community. The *Flavobacteriaceae* family is prominent in both SW and SSA in SR1 (Fig. 3.6). When *Flavobacteriaceae* are rare in SR2 SW, they are also rare in the SSA (Fig. 3.6). *Flavobacteriaceae* increase in relative abundance in both SW and SSA over the course of SR3 (Fig. 3.6). Analysis of whole community

composition better reveals the coupling of SW and SSA communities (Fig. 3.8). Here again it is evident that SW from each sampling round contained a different bacteria community, shown by the separate clustering of SW points from each SR (Fig. 3.8 a, b). Similar to the SW, there is separation in the SSA data from each SR, with some overlap. Further statistical analysis shows the coupling of SW and SSA communities (Fig. 3.9). Those results show that the SSA community from each round is more similar to the SW community from that round than it is to the SW community of other rounds (Fig. 3.9). This demonstrates that different SW communities produce different SSA communities, and changes in the SW community yield changes in the SSA community. Other work has shown that the SW community at a given location can change over time (Morris et al., 2005; Fuhrman et al., 2006; Carlson et al., 2009; Treusch et al., 2009; Gilbert et al., 2012; Chow et al., 2013; Vergin et al., 2013; Cram et al., 2015). The SW microbial community is shaped by a combination of bottom-up and top-down controls. Bottom-up controls include abiotic properties like seawater temperature, oxygen, salinity, and nutrients (Fuhrman et al., 2006). Top-down controls include the shaping of marine microbial assemblages by viruses, protists, and zooplankton like copepods (Franks, 2002; Azam & Malfatti, 2007).

3.5.4 Intermittent Taxon Specific Aerosolization

Taxon specific aerosolization was investigated as a mechanism for why different SW communities produced different SSA communities. TSA is the observation that different bacteria taxa show different tendencies to transfer in SSA. TSA has been identified multiple times in isolated, nascent SSA, as investigated here (Fahlgren et al., 2015; Hejkal et al., 1980; Michaud et al., 2018; Perrott et al., 2017; Rastelli et al., 2017). TSA implies that the SSA community is different than, but also a function of, the SW community, which is seen in the present study (Fig. 3.8). The aerosolization factor (AF) is a measure of the propensity of each type of bacteria to

aerosolize in SSA. The AF is commonly used in TSA studies and has also been called the concentration factor and enrichment factor (Fahlgren et al., 2015; Hejkal et al., 1980; Michaud et al., 2018; Perrott et al., 2017; Rastelli et al., 2017). The AF is simply the ratio of the relative abundance (RA) in SSA to the RA in SW. It can be calculated for each ASV in each paired sampling of SW and SSA. Here, RA is the reads of the ASV in the sample (SW or SSA) divided by the total reads in the sample. At AF = 1, RA in SSA equals RA in SW, and a consistent AF = 1 implies increases or decreases in RA in SW are matched with equal changes in SSA RA. AF values significantly above (or below) 1 mean that RA in SSA is greater (or less) than in SW. In previous observations of TSA, bacteria in the same taxonomic groups, namely orders and classes, showed similar aerosolization AFs (Fahlgren et al., 2015; Harb et al., 2021; Hejkal et al., 1980; Michaud et al., 2018; Rastelli et al., 2017). Bacteria taxa can show constituent (consistent) or intermittent (variable) aerosolization rates and either could result in different SW communities producing different SSA communities.

To determine if constituent or intermittent TSA is dominant in the data, the AFs from the 12 most abundant families in SSA were examined across taxa and SR (Fig. 3.10). Each point reports the AF and SSA RA for a single ASV from a paired sampling of SW and SSA. AF was plotted against SSA RA in order to 1) investigate whether AF varies with SSA RA, and 2) distinguish AF values at low vs. high SSA RA. Relatively low or high SW RA can be inferred from the SSA RA and AF values. For each family (Fig. 3.10 A-L), the data were plotted twice: in each left plot the points are colored by genera, and in each right plot the points are colored by SR. The plots of *families* and *genera* were grouped and colored by shared taxonomic *class* and *order* to look for trends at multiple taxonomic levels. Variation may come from higher taxonomic levels (*species*, strains) that are unable to be resolved with our methods. Some

individual AFs are very high (~100-200), but these are generally rare points with relatively low SSA RA values; the high AF comes from very low SW RA. More important are individual AF values at elevated SSA RA, and the average (AFa) and median (AFm) AF values that summarize each taxon. For example, *Rhodobacteraceae* shows the highest AF value, but it is a single point at a relatively low SSA RA value (Fig. 3.10 A). Its multiple points of AF = 1 at elevated SSA RA show that when *Rhodobacteraceae* increased in relative abundance in SSA, its AF did not. Thus, *Rhodobacteraceae* aerosolize in SSA at a rate equivalent to its SW RA (AF = 1). The AFa and AFm values fall within the range of values produced by multiple investigations into taxon specific AFs for isolated, nascent SSA (Fahlgren et al., 2015; Harb et al., 2021; Hejkal et al., 1980; Michaud et al., 2018; Rastelli et al., 2017).

In this dataset, intermittent TSA that varied within taxa and across SR was more common than constituent TSA. Among the *Alphaproteobacteria*, *Rhodobacteraceae*'s consistently low AFs demonstrate constituent TSA (Fig. 3.10 A), whereas *Sphingomonadaceae's* variable AFs show intermittent TSA (Fig. 3.10 C). *Flavobacteriaceae* and *Cryomorphaceae* fall under the same *class* and *order* and show intermittent TSA that varied within taxa and across SRs (Fig. 3.10 E, G). Both *families* show one *genus* elevated in SSA RA, with an AF of ~20, but this only happened in SR3, and therefore was intermittent. The *Bacillaceae family* distinguishes itself with high AF values that increase with increasing SSA RA, showing significant variability, with signs of possible influence from the SRs (Fig. 3.10 I). The *Chloroplast family* also shows intermittent TSA in a trend of increasing AF with increasing SSA RA, but with much lower values than *Bacillaceae*, showing taxon specificity (Fig. 3.10 I, K). The *Gammaproteobacteria class* shows intermittent TSA in AFa values of 1-9 (Fig. 3.10 B, D, F, H, J, L). Its *Alteromonadales* and *Oceanospirillales* orders show variability with weak influence by both taxonomy and SR; in

multiple cases one *genus* shows elevated AF values that also vary according to SR (Fig. 3.10 B, D, F). The *Methylophilaceae family* shows general separation between its two *genera*; the *genus* represented by yellow points separates out by SR (Fig. 3.10 L).

3.5.5 Multiple Controls on Bacteria Aerosolization

Controls on bacteria aerosolization in SSA explain drivers behind intermittent TSA. Bubble scavenging and accumulation in the ocean surface microlayer (SML) are major drivers of bacteria aerosolization rates (Blanchard et al., 1981; Carlucci & Williams, 1965). These processes are controlled both by cell properties, like surface hydrophobicity, and SW properties, like salinity, OM content and SML lipid concentration. Hydrophobic bacteria accumulate at the surface more than hydrophilic bacteria, which may be influenced by SW properties like salinity (Schäfer et al., 1998). Different types of bacteria have different affinities for lipids, which accumulate in the SML (Kjelleberg et al., 1976). The shape of bacteria may influence their accumulation at the SML (Manabe et al., 2020). The presence of gas vesicles and storage vacuoles can affect buoyancy and, thus, accumulation in the SML (Alvarez et al., 1997; Kalscheuer et al., 2007; Shively, 2006; Walsby, 1994; Walsby et al., 1995). By generating aerosols using bacteria cultures at 1.5 d and 5 d of growth, it was found that not only does cellular lipid content affect surface accumulation and aerosolization, but so does culture age (Hejkal et al., 1980). This implies that the physiological state of bacteria can cause variability in their TSA. The aerosolization of freshwater bacteria was sensitive to added salinity, another demonstration of the influence of water composition on bacteria aerosolization (Harb et al., 2021). Bacteria associations with gels, transparent exopolymer substances (TEP) and other particle types might also influence bacteria aerosolization (Aller et al., 2005). Many microbes have a particle-attached lifestyle and being bound to a large particle might inhibit aerosolization

(D'Ambrosio et al., 2014; Mestre et al., 2018). Fahlgren et al. hypothesized that different SW communities not only produce different SSA communities but also different taxon specific AFs (Fahlgren et al., 2015). In sum, bacteria transfer in SSA is influenced by variable attributes of the bacteria and variations in SW composition. A combination of these factors produced variations in SSA community via variations in TSA.

3.6 Conclusions

Sequencing aerosols has been a longstanding analytical challenge for the scientific community. This work applied the Katharoseq low biomass 16S amplicon sequencing workflow to isolated SSA collected with the high collection efficiency Spot sampler. This achieved sequencing success at 3.9 hs of sampling, 37 liters of air, $4.1x10^6$ aerosols, and 1046 heterotrophic bacteria. For future sampling of the open atmosphere, other samplers with high flow rates can be used to allow high frequency sampling of the airborne microbiome. Increasing the sensitivity of our techniques to reveal the atmospheric microbiome enables better research into the roles microorganisms play in the atmosphere.

These methodological advances demonstrated that the SSA community changes as the SW community changes. This work confirmed that different bacteria taxa have different propensities for transfer in SSA. Significant variability in the aerosolization taxa was observed, analogous to the intermittent aerosolization previously identified (Michaud et al., 2018). It was also observed that total bacteria aerosolization in SSA is irregular over time, air volume, and SSA counts, even with controlled SSA production. These findings agree with prior work that states bacteria aerosolization varies across individual taxa (e.g. TSA) and their cellular properties, the SW community, as well as SW composition. More work is needed to identify which cellular and seawater properties - such as cell surface net charge, the presence or absence

of flagella, a polysaccharide matrix that can increase the surface to volume ratio - control bacteria aerosolization in SSA, as well as their underlying mechanisms. The magnitude of importance that cell surface lipophilicity has on aerosolization merits further research. From a microscale perspective, marine microbes might have developed strategies to regulate their AF propensity, allowing a sort of "SSA ballooning" to move to a new marine niche. Being able to reliably model taxon specific aerosolization as a function of community and SW properties would allow prediction of the SSA community in global models.

3.7 Acknowledgements

The authors gratefully acknowledge the support of the National Science Foundation through the Centers of Chemical Innovation Program via the Center for Aerosol Impacts on Chemistry of the Environment (CHE-1801971).

Chapter 3, in full, is currently being prepared for resubmission to mSystems: Pendergraft, M.A., Minich, J.J., Belda-Ferre, P., Morris, C.K., Malfatti, F., Knight, R., Prather, K.A. (in prep). Advances in Sea Spray Aerosol Sequencing Reveal a Dynamic Community. Jeremiah J. Minich and the dissertation author are co-first authors of this manuscript.

3.8 Figures

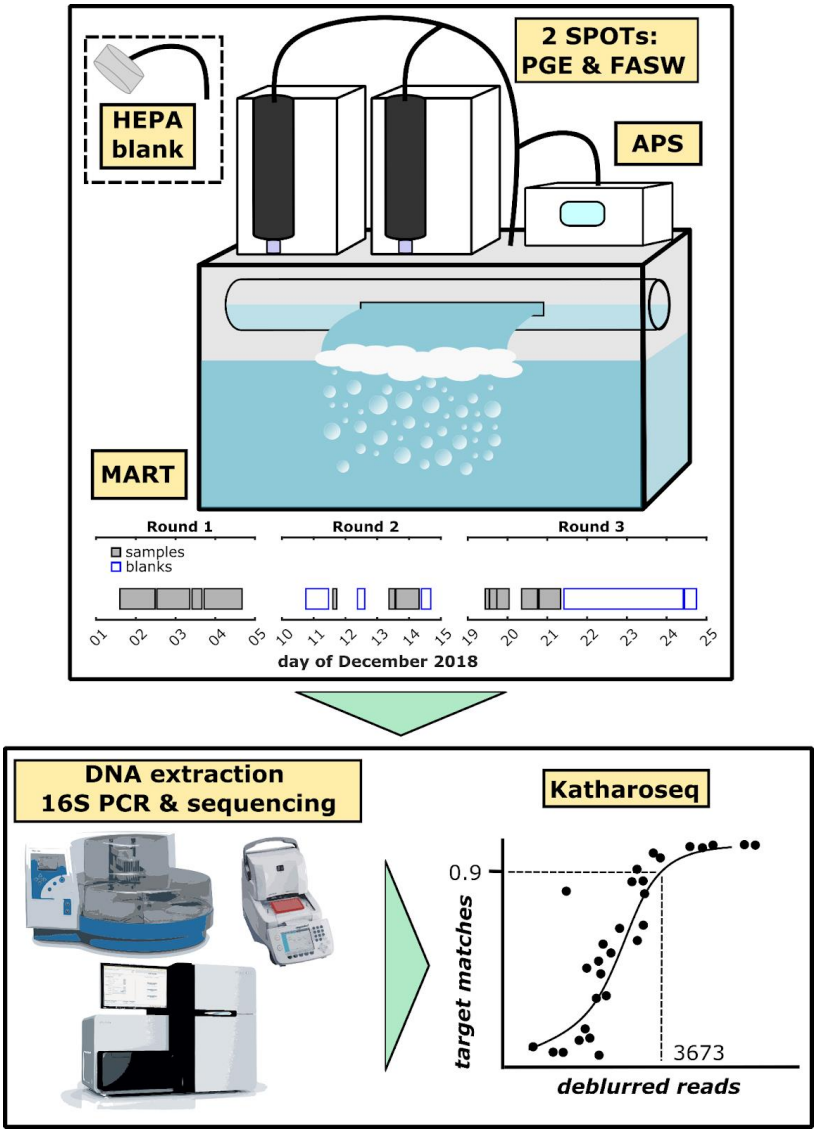

Figure 3.1 Graphic experimental design. SSA was generated with a MART and sampled with 2 Aerosol Devices Inc. Spot samplers into two different solutions: PGE and FASW. Electrically conductive tubing (McMaster Carr Cat# 1909T(x); mcmaster.com/catalog/126/161) was used for sampling lines. A timeline shows sampling durations for the three sampling rounds. DNA extraction, 16S rRNA gene PCR, and Sequencing followed. Then the Katharoseq low biomass method was applied.

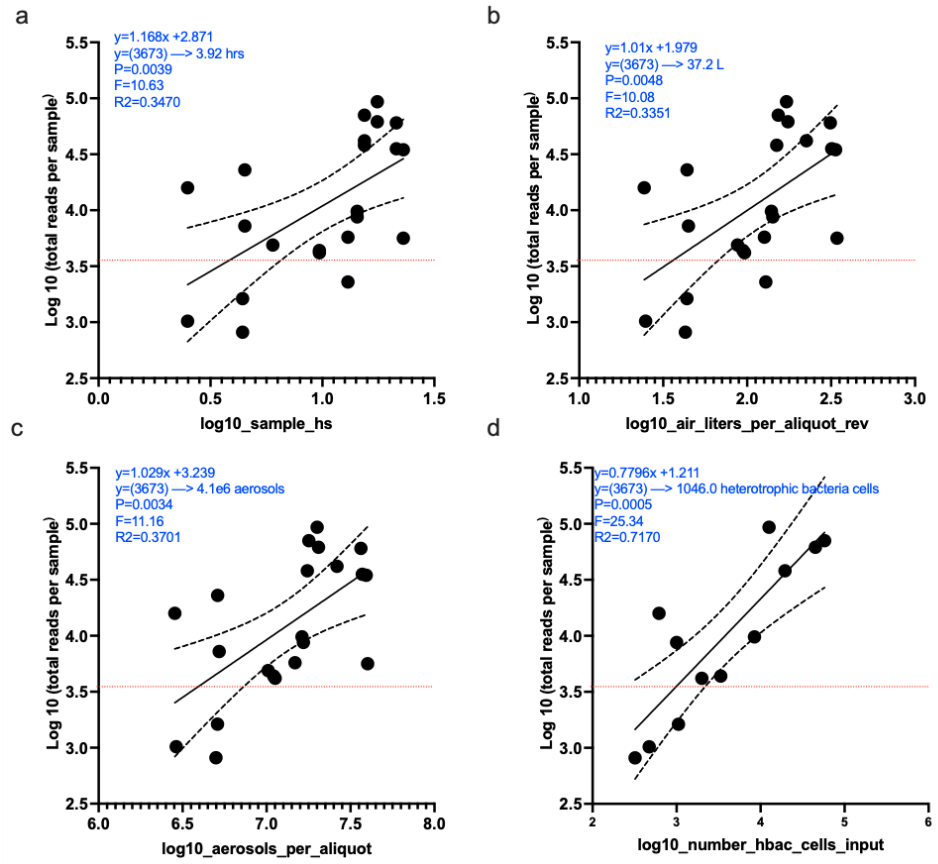

Figure 3.3 Modeling minimum sampling requirements for successful 16S sequencing of SSA, in terms of a) SSA sampling duration, b) air volume c) aerosol counts, and d) SSA heterotrophic bacteria cells. a) is for the total sampling period and b), c) and d) are for the fraction of the liquid sample that was extracted. Axes are both log 10 transformed. The red dashed line on each figure indicates the limit of detection for the assay such that samples (black dots) under this line are considered failures. The limit of detection - where 90% of the reads map to the control - is 3673 reads. X is solved using the log 10 of 3673 followed by a conversion back to the original units.

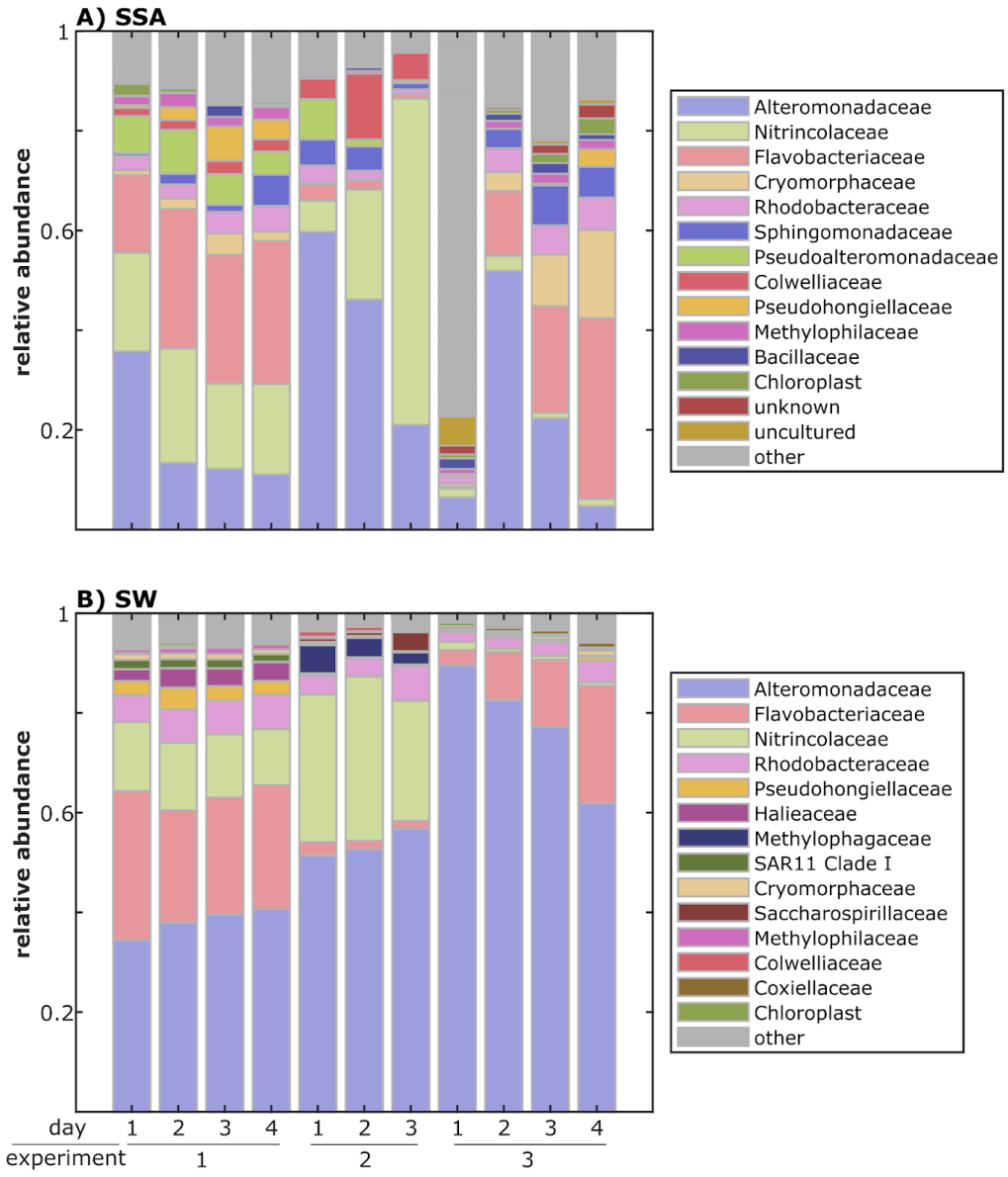

Figure 3.6 SSA (A) and SW (B) community composition at the family level. Shown are the cumulative relative abundances for each of the 14 families with the highest cumulative relative abundances. Family colors are consistent between A) and B).

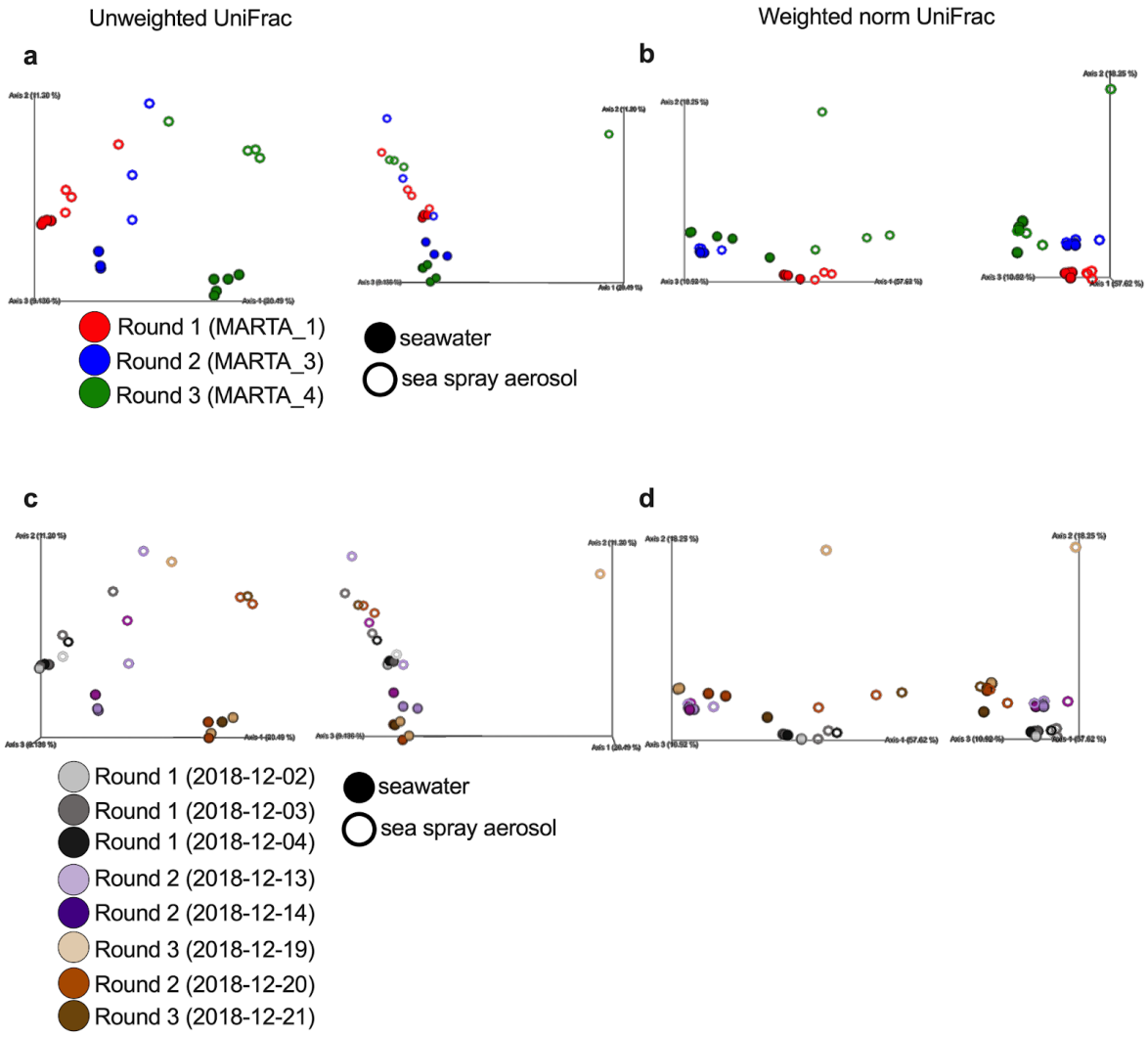

Figure 3.8 Combined beta diversity of SW and SSA from all three experiments. PCoA plots depicting a) Unweighted UniFrac and b) Weighted normalized UniFrac whereby samples are formatted according to sampling round (color) and sample type (shape). Each panel a)-c) shows the same data from two different angles, rotated 90° on the vertical axis. The same plots c) Unweighted UniFrac and d) Weighted normalized Unifrac are also colored by collection date.

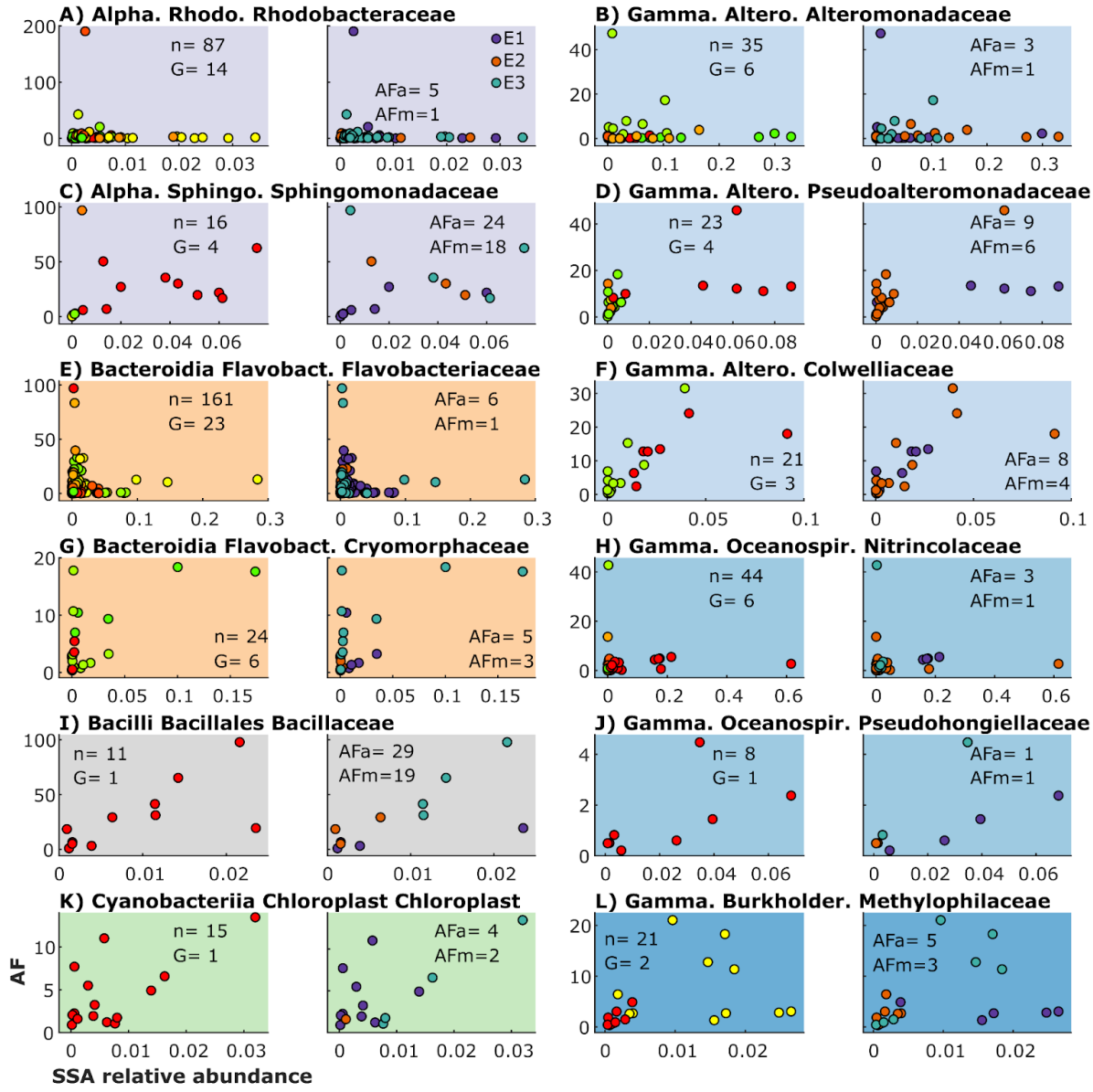

Figure 3.10 Aerosolization factor (AF) vs. SSA relative abundance (RA) for the 12 most abundant families in SSA. Each point is the data from a single ASV detected in both SW and SSA at a single time point. For each family A-L there are two plots: in the left plot points are colored by genus; in the right plot points are colored by sampling round (SR). Subplot titles provide the taxonomic class, order, and family. Plots of multiple families from the same class or order are grouped and colored accordingly. Annotations are: n - the number of points in each plot; G - the number of genera; AFa - average AF; AFm - median AF. Taxonomic abbreviations are: *order: Alpha. - Alphaproteobacteria; Gamma. - Gammaproteobacteria; family: Rhodo. - Rhodobacterales; Sphingo. - Sphingomonadales; Flavobact. - Flavobacteriales; Altero. - Alteromonadales; Oceanospir. - Oceanospirillales; Burkholder. - Burkholderiales.*

3.9 Supplementary figures

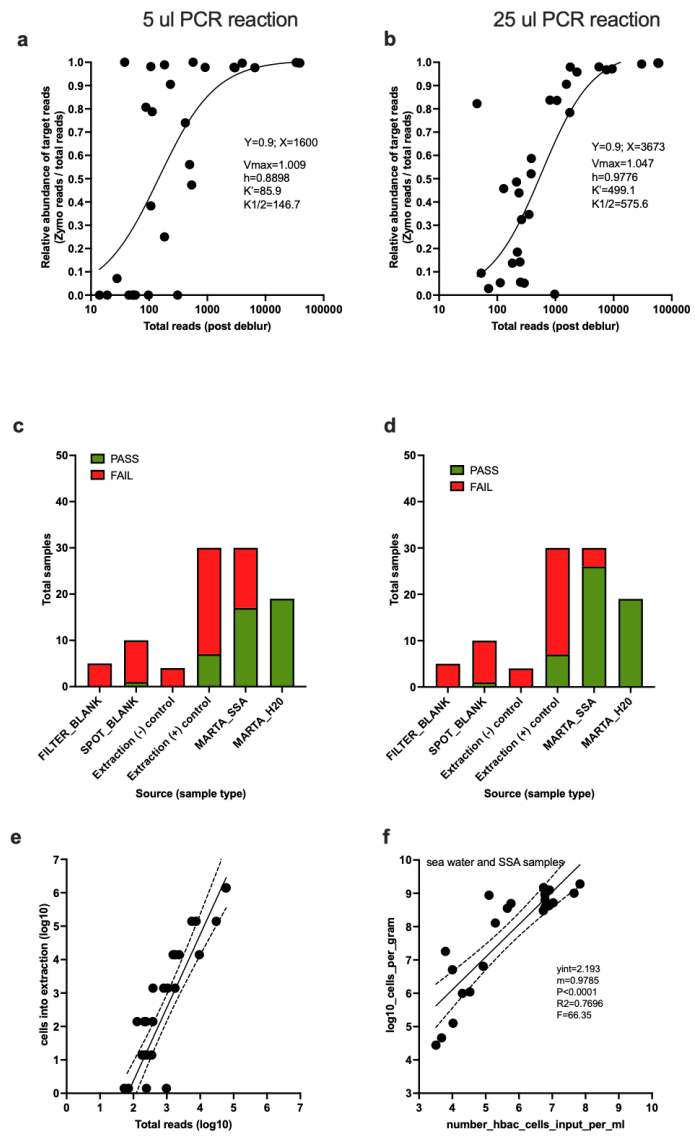

Figure 3.2 Impact of PCR reaction volume and subsequent DNA input on sample success rate. Samples included are from the PowerMag DNA extraction. Katharoseq limit of detection calculation applied to the a) 5 µl reaction with and b) 25 µl PCR reaction. Sample success rate across a variety of sampling negative controls, DNA extraction controls, and actual samples (water and sea spray aerosol) for c) 5 µl PCR reaction volume and d) 25 µl PCR reaction volume. e) The association of read counts to cell counts from the positive controls from the 25 µl PCR reaction (linear model with 95% CI). Biomass estimates applied to the broad dataset and then f) compared to known heterotrophic bacteria cell counts from flow cytometry in water and sea spray aerosol samples from the 25 µl PCR reaction (linear model with 95% CI).

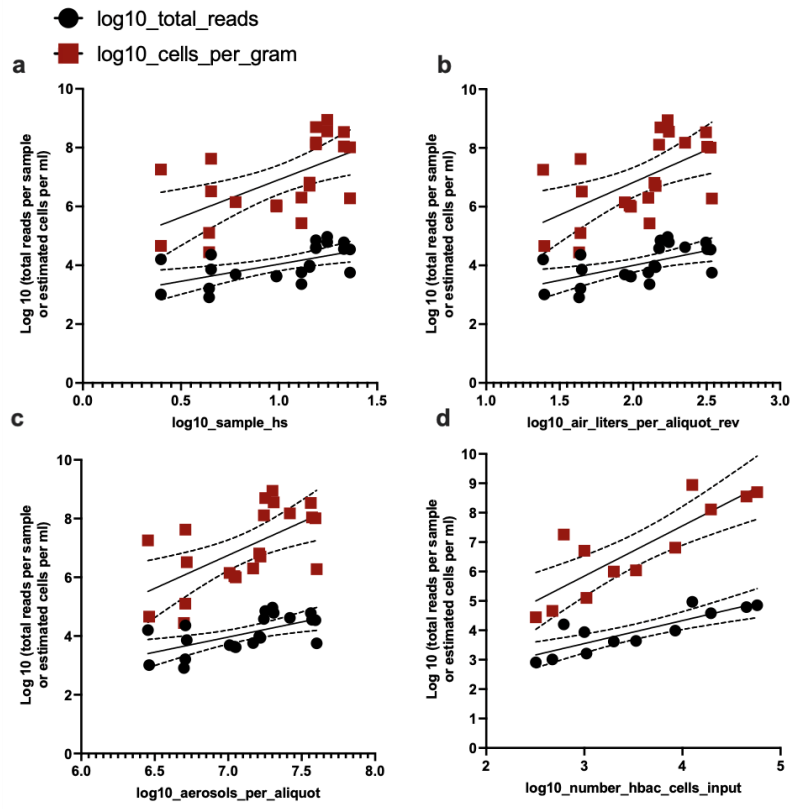

Figure 3.4 Estimated cell biomass added to the Modeling minimum sampling requirements for successful 16S sequencing of SSA, in terms of a) SSA sampling duration (hours), b) air volume c) aerosol counts, and d) SSA heterotrophic bacteria cells. a) is for the total sampling period and b), c) and d) are for the aliquot extracted: 25% of each liquid sample recovered from the SPOT sampler. Data is from Powermag extraction samples using 5 µl of input DNA into 25 µl PCR reaction. Axes are both log transformed. The limit of detection - where 90% of the reads map to the control - is 3673 reads. X is solved using the log 10 of 3673 followed by a conversion back to the original units.

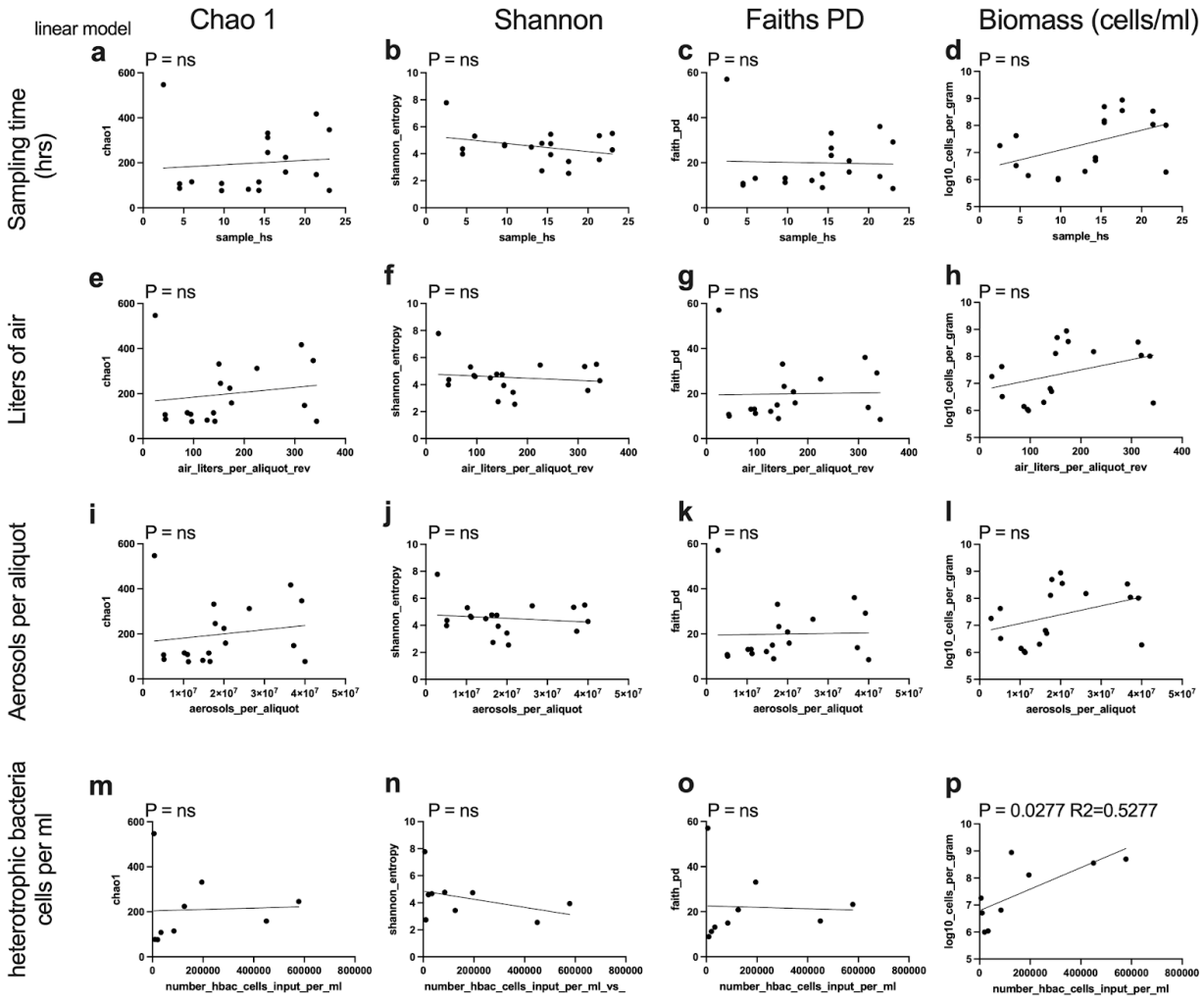

Figure 3.5 Determining the effects of SSA sampling durations and amounts on alpha diversity and microbial biomass. Effects of prolonged sampling time (in hours) on a) Chao1, b) Shannon, c) Faiths PD, and d) microbial biomass per ml. Effects of the total volume of air sampled (liters of air per aliquot) on e) Chao1, f) Shannon, g) Faiths PD, and h) microbial biomass per ml. Effects of the number of aerosols per aliquot on i) Chao1, j) Shannon, k) Faiths PD, and l) microbial biomass per ml.

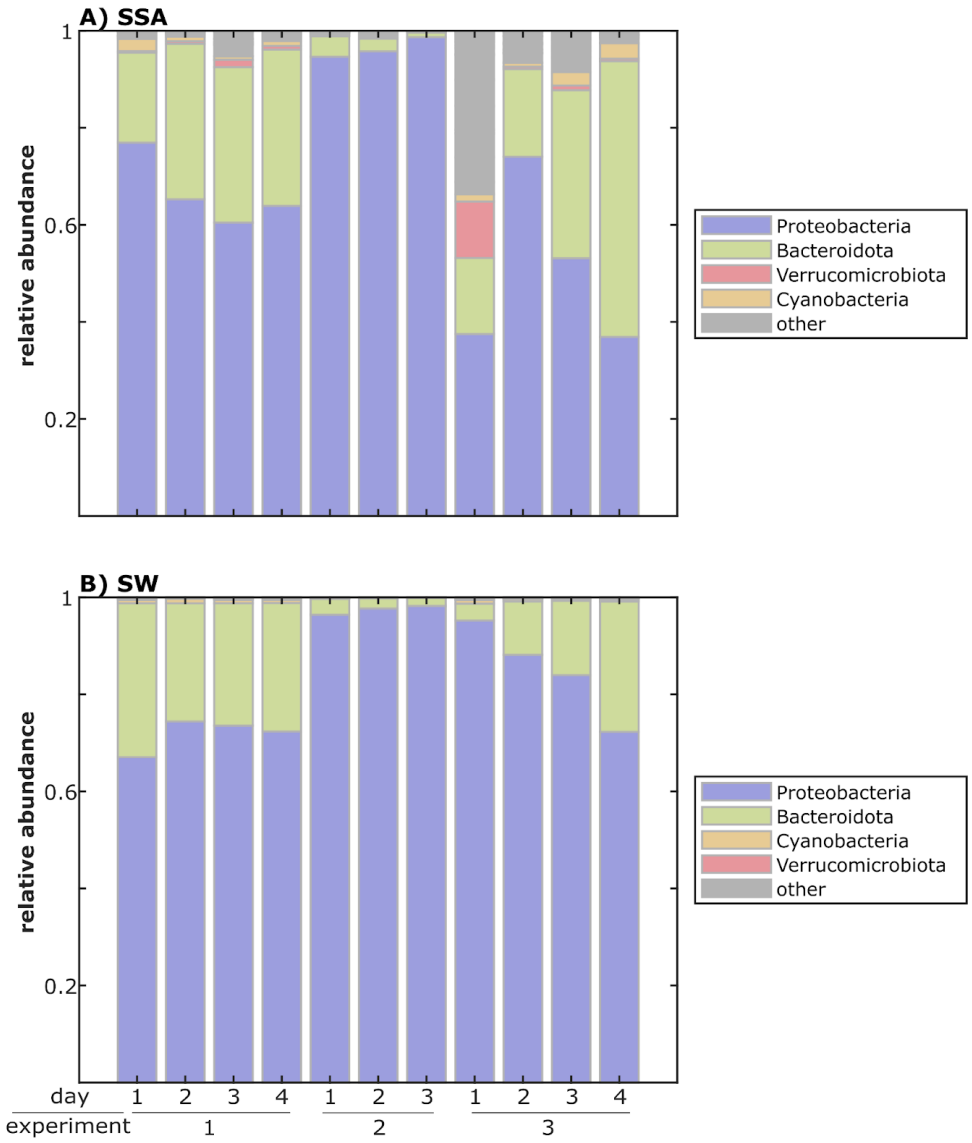

Figure 3.7 SSA (A) and SW (B) community composition at the phylum level.

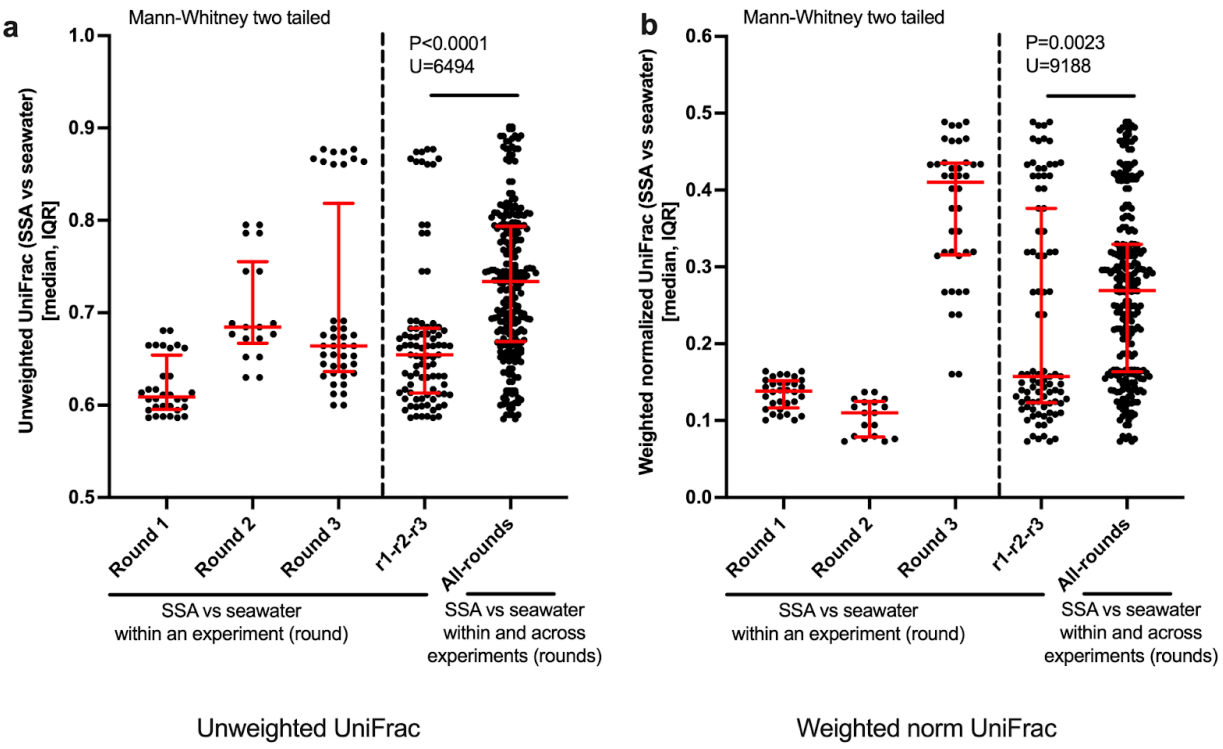

Figure 3.9 SSA community is more similar to SW community within an experiment as compared to across experiments. Distance comparisons of SW vs. SSA for samples collected within a sampling round/experiment and across rounds. a) Unweighted Unifrac distances and b) Weighted normalized UniFrac distances. All samples were from PowerSoil MAG attract DNA extraction and 25 µl PCR reaction volume with 5 µl DNA input. All SSA samples were from SPOT2 with SSA sampled into PGE.

3.10 Supplementary tables

Table 3.1 Summary table on sample success and failure metrics. Only samples with data for all of the fields were included; i.e. samples missing cell counts.

#	type	collection	frozen storage	sample hs	air liters extracted	# SSA extracted	cells extracted	reads	success
1	SW	SW	neat	0	not applicable	not applicable	6810000	132040	1
2	SW	SW	extraction tube	0	not applicable	not applicable	550000	117804	1
3	SW	SW	neat	0	not applicable	not applicable	825000	109236	1
4	SW	SW	extraction tube	0	not applicable	not applicable	608000	105417	1
5	SW	SW	extraction tube	0	not applicable	not applicable	4540000	98626	1
6	SW	SW	extraction tube	0	not applicable	not applicable	606000	94200	1
7	SW	SW	extraction tube	0	not applicable	not applicable	608000	79610	1
8	SW	SW	extraction tube	0	not applicable	not applicable	1070000	72748	1
9	SW	SW	neat	0	not applicable	not applicable	810000	67044	1
10	SW	SW	extraction tube	0	not applicable	not applicable	608000	63349	1
11	SW	SW	extraction tube	0	not applicable	not applicable	540000	56834	1
12	SSA	PGE	extraction tube	17.6	172	20008560	12600	92339	1
13	SSA	FASW	extraction tube	15.4	153	17857640	57800	71317	1
14	SSA	FASW	extraction tube	17.6	175	20408731	45000	61376	1
15	SSA	PGE	extraction tube	15.4	150	17507490	19500	38448	1
16	SSA	PGE	extraction tube	2.5	24	2842125	618	15684	1
17	SSA	PGE	extraction tube	14.3	139	16256955	8460	9815	1
18	SSA	FASW	extraction tube	14.3	142	16582094	1002	8786	1
19	SSA	PGE	extraction tube	9.7	95	11027445	3360	4373	1
20	SSA	PGE	extraction tube	9.7	96	11247994	2000	4178	1
21	SSA	FASW	extraction tube	4.4	44	5102183	1052	1629	0
22	SSA	FASW	extraction tube	2.5	25	2898968	472	1027	0
23	SSA	PGE	extraction tube	4.4	43	5002140	320	816	0
24	SSA_blank	PGE	extraction tube	17.2	252	0	6.87	6866	1
25	SSA_blank	FASW	extraction tube	7.2	72	0	3880	1801	0
26	SSA_blank	PGE	extraction tube	7.2	70	0	41	566	0
27	SSA_blank	PGE	extraction tube	0	0	0	22.8	171	0
28	SSA_blank	FASW	extraction tube	17.2	257	0	280.8	154	0

Table 3.2. Taxa in the mock community used in the Katharoseq method to determine total reads mapping to the target.

Taxa
1. d__Bacteria;p__Proteobacteria;c__Gammaproteobacteria;o__Enterobacterales;f__Enterobacteriaceae;g_Escherichia-Shigella
2. d__Bacteria;p__Proteobacteria;c__Gammaproteobacteria;o__Pseudomonadales;f__Pseudomonadaceae;g__Pseudomonas
3. d__Bacteria;p__Proteobacteria;c__Gammaproteobacteria;o__Enterobacterales;f__Enterobacteriaceae;__
4. d__Bacteria;p__Firmicutes;c__Bacilli;o__Lactobacillales;f__Lactobacillaceae;g__Lactobacillus
5. d__Bacteria;p__Firmicutes;c__Bacilli;o__Staphylococcales;f__Staphylococcaceae;g__Staphylococcus
6. d__Bacteria;p__Firmicutes;c__Bacilli;o__Lactobacillales;f__Enterococcaceae;g__Enterococcus
7. d__Bacteria;p__Firmicutes;c__Bacilli;o__Bacillales;f__Bacillaceae;g__Bacillus
8. d__Bacteria;p__Firmicutes;c__Bacilli;o__Lactobacillales;f__Listeriaceae;g__Listeria

3.11 References

Aller, J.Y., Kuznetsova, M.R., Jahns, C.J., Kemp, P.F. (2005). The sea surface microlayer as a source of viral and bacterial enrichment in marine aerosols. *Journal of Aerosol Science*, 36(5-6), 801–812.

Alvarez, H.M., Pucci, O.H., Steinbüchel, A. (1997). Lipid storage compounds in marine bacteria. *Applied Microbiology and Biotechnology*, 47(2), 132–139.

Amir, A., McDonald, D., Navas-Molina, J.A., Kopylova, E., Morton, J.T., Zech Xu, Z., Kightley, E.P., Thompson, L.R., Hyde, E.R., Gonzalez, A., Knight, R. (2017). Deblur rapidly resolves single-nucleotide community sequence patterns. mSystems, 2(2). doi.org/10.1128/mSystems.00191-16

Anderson, M.J. (2001). A new method for non-parametric multivariate analysis of variance. *Austral Ecology*, 26(1), 32–46. doi.org/10.1111/j.1442-9993.2001.01070.pp.x

Apprill, A., McNally, S., Parsons, R., Weber, L. (2015). Minor revision to V4 region SSU rRNA 806R gene primer greatly increases detection of SAR11 bacterioplankton. *Aquatic Microbial Ecology*, 75(2), 129–137. doi.org/10.3354/ame01753

Archer, S.D.J., Lee, K.C., Caruso, T., King-Miaow, K., Harvey, M., Huang, D., Wainwright, B.J., Pointing, S.B. (2020). Air mass source determines airborne microbial diversity at the ocean–atmosphere interface of the Great Barrier Reef marine ecosystem. *The ISME Journal*, 14(3), 871–876. doi.org/10.1038/s41396-019-0555-0

Azam, F. (1998). Microbial control of oceanic carbon flux: the plot thickens. *Science*, 280(5364), 694–696. doi.org/10.1126/science.280.5364.694

Azam, F., Fenchel, T., Field, J.G., Gray, J.S., Meyer-Reil, L.A., Thingstad, F. (1983). The ecological role of water-column microbes in the sea. *Marine Ecology Progress Series*, 10, 257–263. doi.org/10.3354/meps010257

Azam, F., Malfatti, F. (2007). Microbial structuring of marine ecosystems. *Nature Reviews Microbiology*, 5(10), 782–791. doi.org/10.1038/nrmicro1747

Baylor, E.R., Baylor, M.B., Blanchard, D.C., Syzdek, L.D., Appel, C. (1977). Virus transfer from surf to wind. *Science*, 198(4317), 575–580.

Blanchard, D.C., Syzdek, L.D., Weber, M.E. (1981). Bubble scavenging of bacteria in freshwater quickly produces bacterial enrichment in airborne jet drops. *Limnology and Oceanography*, 26(5), 961–964. doi.org/10.4319/lo.1981.26.5.0961

Bolyen, E., Rideout, J.R., Dillon, M.R., Bokulich, N.A., Abnet, C.C., Al-Ghalith, G.A., Alexander, H., Alm, E.J., Arumugam, M., Asnicar, F., Bai, Y., Bisanz, J.E., Bittinger, K.,

Brejnrod, A., Brislawn, C.J., Brown, C.T., Callahan, B.J., Caraballo-Rodríguez, A.M., Chase, J., Cope, E.K., DaSilva, R., Diener, C., Dorrestein, P.C., Douglas, G.M., Durrall, D.M., Duvallet, C., Edwardson, C.F., Ernst, M., Estaki, M., Fouquier, J., Gauglitz, J.M., Gibbons, S.M., Gibson, D.L., Gonzalez, A., Gorlick, K., Guo, J., Hillmann, B., Holmes, S., Holste, H., Huttenhower, C., Huttley, G.A., Janssen, S., Jarmusch, A.K., Jiang, L., Kaehler, B.D., Kang, K.B., Keefe, C.R., Keim, P., Kelley, S.T., Knights, D., Koester, I., Kosciolek, T., Kreps, J., Langille, M.G.I., Lee, J., Ley, R., Liu, Y.-X., Lotfield, E., Lozupone, C., Maher, M., Marotz, C., Martin, B.D., McDonald, D., McIver, L.J., Melnik, A.V., Metcalf, J.L., Morgan, S.C., Morton, J.T., Naimey, A.T., Navas-Molina, J.A., Nothias, L.F., Orchanian, S.B., Pearson, T., Peoples, S.L., Petras, D., Preuss, M.L., Pruesse, E., Rasmussen, L.B., Robeson 2nd, M.S., Rosenthal, P., Segata, N., Shaffer, M., Shiffer, A., Sinha, R., Song, S.J., Spear, J.R., Swafford, A.D., Thompson, L.R., Torres, P.J., Trinh, P., Tripathi, A., Turnbaugh, P.J., Ul-Hassan, S., vander Hooft, J.J.J., Vargas, F., Vazquez-Baeza, Y., Vogtmann, E., von Hippel, M., Walters, W., Wan, Y., Wang, M., Warren, J., Weber, K.C., Williamson, C.H.D., Willis, A.D., Xu, Z.Z., Zaneveld, J.R., Zhang, Y., Zhu, Q., Knight, R., Caporaso, J. G. (2019). Reproducible, interactive, scalable and extensible microbiome data science using QIIME 2. *Nature Biotechnology*, 37(8), 852–857.

Caporaso, J.G., Lauber, C.L., Walters, W.A., Berg-Lyons, D., Huntley, J., Fierer, N., Owens, S. M., Betley, J., Fraser, L., Bauer, M., Gormley, N., Gilbert, J.A., Smith, G., Knight, R. (2012). Ultra-high-throughput microbial community analysis on the Illumina HiSeq and MiSeq platforms. *The ISME Journal*, 6(8), 1621–1624.

Caporaso, J.G., Lauber, C.L., Walters, W.A., Berg-Lyons, D., Lozupone, C.A., Turnbaugh, P.J., Fierer, N., Knight, R. (2011). Global patterns of 16S rRNA diversity at a depth of millions of sequences per sample. *Proceedings of the National Academy of Sciences*, 108, 4516–4522. doi.org/10.1073/pnas.1000080107

Carlson, C.A., Morris, R., Parsons, R., Treusch, A.H., Giovannoni, S.J., Vergin, K. (2009). Seasonal dynamics of SAR11 populations in the euphotic and mesopelagic zones of the northwestern Sargasso Sea. *The ISME Journal*, 3(3), 283–295.

Carlucci, A.F., Williams, P.M. (1965). Concentration of Bacteria from Sea Water by Bubble Scavenging. *ICES Journal of Marine Science*, 30(1), 28–33. doi.org/10.1093/icesjms/30.1.28

Cho, B.C., Hwang, C.Y. (2011). Prokaryotic abundance and 16S rRNA gene sequences detected in marine aerosols on the East Sea (Korea). *FEMS Microbiology Ecology*, 76(2), 327–341.

Chow, C.-E.T., Sachdeva, R., Cram, J.A., Steele, J.A., Needham, D.M., Patel, A., Parada, A.E., Fuhrman, J.A. (2013). Temporal variability and coherence of euphotic zone bacterial communities over a decade in the Southern California Bight. *The ISME Journal*, 7(12), 2259–2273. doi.org/10.1038/ismej.2013.122

Cram, J.A., Chow, C.-E.T., Sachdeva, R., Needham, D.M., Parada, A.E., Steele, J.A., Fuhrman, J.A. (2015). Seasonal and interannual variability of the marine bacterioplankton community throughout the water column over ten years. *The ISME Journal*, 9(3), 563–580.

Creamean, J.M., Suski, K.J., Rosenfeld, D., Cazorla, A., DeMott, P.J., Sullivan, R.C., White, A.B., Ralph, F.M., Minnis, P., Comstock, J.M., Tomlinson, J.M., Prather, K.A. (2013). Dust and biological aerosols from the Sahara and Asia influence precipitation in the western U.S. *Science*, 339(6127), 1572–1578.

D'Ambrosio, L., Ziervogel, K., MacGregor, B., Teske, A., Arnosti, C. (2014). Composition and enzymatic function of particle-associated and free-living bacteria: a coastal/offshore comparison. *The ISME Journal*, 8(11), 2167–2179.

DeMott, P.J., Hill, T.C.J., McCluskey, C.S., Prather, K.A., Collins, D.B., Sullivan, R.C., Ruppel, M.J., Mason, R.H., Irish, V.E., Lee, T., Hwang, C.Y., Rhee, T.S., Snider, J.R., McMeeking, G.R., Dhaniyala, S., Lewis, E.R., Wentzell, J.J.B., Abbatt, J., Lee, C., Sultana, C.M., Ault, A.P., Axson, J.L., Diaz Martinez, M., Venero, I., Santos-Figueroa, G., Stokes, M.D., Deane, G.B., Mayol-Bracero, O.L., Grassian, V.H., Bertram, T.H., Bertram, A.K., Moffett, B.F., Franc, G. D. (2016). Sea spray aerosol as a unique source of ice nucleating particles. *Proceedings of the National Academy of Sciences of the United States of America*, 113(21), 5797–5803.

Dixon, P. (2003). VEGAN, a package of R functions for community ecology. Journal of Vegetation Science, 14(6), 927–930. doi.org/10.1111/j.1654-1103.2003.tb02228.x

Fahlgren, C., Gómez-Consarnau, L., Zábori, J., Lindh, M.V., Krejci, R., Mårtensson, E.M., Nilsson, D., Pinhassi, J. (2015). Seawater mesocosm experiments in the Arctic uncover differential transfer of marine bacteria to aerosols. *Environmental Microbiology Reports*, 7(3), 460–470.

Faith, D. P. (1992). Conservation evaluation and phylogenetic diversity. *Biological Conservation*, 61(1), 1–10. doi.org/10.1016/0006-3207(92)91201-3

Farmer, D.K., Cappa, C.D., Kreidenweis, S.M. (2015). Atmospheric processes and their controlling influence on cloud condensation nuclei activity. *Chemical Reviews*, 115(10), 4199–4217.

Franks, P.J.S. (2002). NPZ models of plankton dynamics: their construction, coupling to physics, and application. *Journal of Oceanography*, 58(2), 379–387. doi.org/10.1023/A:1015874028196

Fuhrman, J.A., Hewson, I., Schwalbach, M.S., Steele, J.A., Brown, M.V., Naeem, S. (2006). Annually reoccurring bacterial communities are predictable from ocean conditions. *Proceedings of the National Academy of Sciences of the United States of America*, 103(35), 13104–13109.

Gasol, J.M., Del Giorgio, P.A. (2000). Using flow cytometry for counting natural planktonic bacteria and understanding the structure of planktonic bacterial communities. *Scientia Marina*, 64(2), 197–224. doi.org/10.3989/scimar.2000.64n2197

Gilbert, J.A., Steele, J.A., Caporaso, J.G., Steinbrück, L., Reeder, J., Temperton, B., Huse, S., McHardy, A.C., Knight, R., Joint, I., Somerfield, P., Fuhrman, J.A., Field, D. (2012). Defining seasonal marine microbial community dynamics. *The ISME Journal*, 6(2), 298–308.

Gonzalez, A., Navas-Molina, J.A., Kosciolek, T., McDonald, D., Vázquez-Baeza, Y., Ackermann, G., DeReus, J., Janssen, S., Swafford, A.D., Orchanian, S.B., Sanders, J.G., Shorenstein, J., Holste, H., Petrus, S., Robbins-Pianka, A., Brislawn, C.J., Wang, M., Rideout, J.R., Bolyen, E., Dillon, M., Caporaso, J.G., Dorrestein, P.C., Knight, R. (2018). Qiita: rapid, web-enabled microbiome meta-analysis. *Nature Methods*, 15(10), 796–798.

Graham, K.E., Prussin, A.J., 2nd, Marr, L.C., Sassoubre, L.M., Boehm, A. B. (2018). Microbial community structure of sea spray aerosols at three California beaches. *FEMS Microbiology Ecology*, 94(3). doi.org/10.1093/femsec/fiy005

Harb, C., Pan, J., DeVilbiss, S., Badgley, B., Marr, L.C., Schmale, D.G., 3rd, Foroutan, H. (2021). Increasing freshwater salinity impacts aerosolized bacteria. *Environmental Science & Technology*, 55(9), 5731–5741.

Hejkal, T.W., Larock, P.A., Winchester, J.W. (1980). Water-to-air fractionation of bacteria. *Applied and Environmental Microbiology*, 39(2), 335–338.

Ivanova, E.P., Mikhaĭlov, V.V. (2001). A new family of Alteromonadaceae fam. nov., including the marine proteobacteria species Alteromonas, Pseudoalteromonas, Idiomarina i Colwellia]. Mikrobiologiia, 70(1), 15–23.

Ivanova, E.P., Mikhailov, V.V. (2001). A new family, Alteromonadaceae fam. nov., including marine proteobacteria of the genera Alteromonas, Pseudoalteromonas, Idiomarina, and Colwellia. *Microbiology*, 70, 10–17. doi.org/10.1023/A:1004876301036

Kalscheuer, R., Stöveken, T., Malkus, U., Reichelt, R., Golyshin, P.N., Sabirova, J.S., Ferrer, M., Timmis, K.N., Steinbüchel, A. (2007). Analysis of storage lipid accumulation in Alcanivorax borkumensis: evidence for alternative triacylglycerol biosynthesis routes in bacteria. *Journal of Bacteriology*, 189(3), 918–928.

Kjelleberg, S., Norkrans, B., Löfgren, H., Larsson, K. (1976). Surface balance study of the interaction between microorganisms and lipid monolayer at the air/water interface. Applied and Environmental Microbiology, 31(4), 609–611. doi.org/10.1128/aem.31.4.609-611.1976

Lee, C., Sultana, C.M., Collins, D.B., Santander, M.V., Axson, J.L., Malfatti, F., Cornwell, G.C., Grandquist, J.R., Deane, G.B., Stokes, M.D., Azam, F., Grassian, V.H., Prather, K.A.

(2015). Advancing model systems for fundamental laboratory studies of sea spray aerosol using the microbial loop. *The Journal of Physical Chemistry A*, 119(33), 8860–8870. doi.org/10.1021/acs.jpca.5b03488

Liu, Y., Blain, S., Crispi, O., Rembauville, M., Obernosterer, I. (2020). Seasonal dynamics of prokaryotes and their associations with diatoms in the Southern Ocean as revealed by an autonomous sampler. *Environmental Microbiology*, 22(9), 3968–3984.

Lozupone, C., Lladser, M.E., Knights, D., Stombaugh, J., Knight, R. (2011). UniFrac: an effective distance metric for microbial community comparison. The ISME Journal, 5(2), 169–172.

Manabe, J., Omori, T., Ishikawa, T. (2020). Shape matters: entrapment of a model ciliate at interfaces. *Journal of Fluid Mechanics*, 892. doi.org/10.1017/jfm.2020.160

Mayol, E., Arrieta, J.M., Jiménez, M.A., Martínez-Asensio, A., Garcias-Bonet, N., Dachs, J., González-Gaya, B., Royer, S.-J., Benítez-Barrios, V.M., Fraile-Nuez, E., Duarte, C.M. (2017). Long-range transport of airborne microbes over the global tropical and subtropical ocean. *Nature Communications*, 8(1), 201.

Mayol, E., Jiménez, M.A., Herndl, G.J., Duarte, C.M., Arrieta, J.M. (2014). Resolving the abundance and air-sea fluxes of airborne microorganisms in the North Atlantic Ocean. *Frontiers in Microbiology*, 5, 557.

Mestre, M., Ruiz-González, C., Logares, R., Duarte, C.M., Gasol, J.M., Sala, M.M. (2018). Sinking particles promote vertical connectivity in the ocean microbiome. *Proceedings of the National Academy of Sciences of the United States of America*, 115(29), E6799–E6807.

Michaud, J.M., Thompson, L.R., Kaul, D., Espinoza, J.L., Alexander Richter, R., Xu, Z.Z., Lee, C., Pham, K.M., Beall, C.M., Malfatti, F., Azam, F., Knight, R., Burkart, M.D., Dupont, C.L., Prather, K.A. (2018). Taxon-specific aerosolization of bacteria and viruses in an experimental ocean-atmosphere mesocosm. *Nature Communications*, 9(1). doi.org/10.1038/s41467-018-04409-z

Minich, J.J., Zhu, Q., Janssen, S., Hendrickson, R., Amir, A., Vetter, R., Hyde, J., Doty, M.M., Stillwell, K., Benardini, J., Kim, J. H., Allen, E.E., Venkateswaran, K., Knight, R. (2018a). KatharoSeq enables high-throughput microbiome analysis from low-biomass samples. *mSystems*, 3(3). doi.org/10.1128/mSystems.00218-17

Minich, J.J., Humphrey, G., Benitez, R.A.S., Sanders, J., Swafford, A., Allen, E.E., Knight, R. (2018b). High-throughput miniaturized 16S rRNA amplicon library preparation reduces costs while preserving microbiome integrity. *mSystems*, 3(6). doi.org/10.1128/msystems.00166-18

Minich, J.J., Sanders, J.G., Amir, A., Humphrey, G., Gilbert, J.A., Knight, R. (2019). Quantifying and understanding well-to-well contamination in microbiome research. *mSystems*, 4(4). doi.org/10.1128/mSystems.00186-19

Möhler, O., DeMott, P.J., Vali, G., Levin, Z. (2007). Microbiology and atmospheric processes: the role of biological particles in cloud physics. Biogeosciences, 4(6), 1059–1071. doi.org/10.5194/bg-4-1059-2007

Morris, R. M., Vergin, K.L., Cho, J.-C., Rappé, M.S., Carlson, C.A., Giovannoni, S.J. (2005). Temporal and spatial response of bacterioplankton lineages to annual convective overturn at the Bermuda Atlantic Time-series Study site. *Limnology and Oceanography*, 50(5), 1687–1696). doi.org/10.4319/lo.2005.50.5.1687

Pan, M., Eiguren-Fernandez, A., Hsieh, H., Afshar-Mohajer, N., Hering, S.V., Lednicky, J., Hugh Fan, Z., Wu, C.-Y. (2016). Efficient collection of viable virus aerosol through laminar-flow, water-based condensational particle growth. *Journal of Applied Microbiology*, 120(3), 805–815.

Patterson, J.P., Collins, D.B., Michaud, J.M., Axson, J.L., Sultana, C.M., Moser, T., Dommer, A.C., Conner, J., Grassian, V.H., Stokes, M.D., Deane, G.B., Evans, J.E., Burkart, M.D., Prather, K.A., Gianneschi, N.C. (2016). Sea spray aerosol structure and composition using cryogenic transmission electron microscopy. *ACS Central Science*, 2(1), 40–47.

Pendergraft, M.A., Grimes, D.J., Giddings, S.N., Feddersen, F., Beall, C.M., Lee, C., Santander, M.V., Prather, K. A. (2021). Airborne transmission pathway for coastal water pollution. *PeerJ*, 9, e11358. doi.org/10.7717/peerj.11358

Perrott, P., Turgeon, N., Gauthier-Levesque, L., Duchaine, C. (2017). Preferential aerosolization of bacteria in bioaerosols generated in vitro. *Journal of Applied Microbiology*, 123(3), 688–697.

Quinn, P.K., Collins, D.B., Grassian, V.H., Prather, K.A., Bates, T.S. (2015). Chemistry and related properties of freshly emitted sea spray aerosol. *Chemical Reviews*, 115(10), 4383–4399.

Rastelli, E., Corinaldesi, C., Dell'Anno, A., Lo Martire, M., Greco, S., Cristina Facchini, M., Rinaldi, M., O'Dowd, C., Ceburnis, D., Danovaro, R. (2017). Transfer of labile organic matter and microbes from the ocean surface to the marine aerosol: an experimental approach. *Scientific Reports*, 7(1), 11475.

Schäfer, A., Harms, H., Zehnder, A. J. B. (1998). Bacterial accumulation at the air−water interface. *Environmental Science & Technology*, 32(23), 3704–3712. doi.org/10.1021/es980191u

Seutin, G., White, B.N., Boag, P.T. (1991). Preservation of avian blood and tissue samples for DNA analyses. *Canadian Journal of Zoology*, 69(1), 82–90. doi.org/10.1139/z91-013

Sharoni, S., Trainic, M., Schatz, D., Lehahn, Y., Flores, M.J., Bidle, K.D., Ben-Dor, S., Rudich, Y., Koren, I., Vardi, A. (2015). Infection of phytoplankton by aerosolized marine viruses. *Proceedings of the National Academy of Sciences of the United States of America*, 112(21), 6643–6647.

Sharpe, A., Barrios, S., Gayer, S., Allan-Perkins, E., Stein, D., Appiah-Madson, H.J., Falco, R., Distel, D.L. (2020). DESS deconstructed: Is EDTA solely responsible for protection of high molecular weight DNA in this common tissue preservative? *PloS One*, 15(8), e0237356.

Shively, J.M. (2006). Complex intracellular structures in prokaryotes. Springer Science & Business Media.

Stokes, M.D., Deane, G.B., Prather, K., Bertram, T.H., Ruppel, M.J., Ryder, O.S., Brady, J.M., Zhao, D. (2013). A Marine Aerosol Reference Tank system as a breaking wave analogue for the production of foam and sea-spray aerosols. *Atmospheric Measurement Techniques*, 6(4), 1085–1094. doi.org/10.5194/amt-6-1085-2013

Thompson, L.R., Sanders, J.G., McDonald, D., Amir, A., Ladau, J., Locey, K.J., Prill, R.J., Tripathi, A., Gibbons, S.M., Ackermann, G., Navas-Molina, J.A., Janssen, S., Kopylova, E., Vázquez-Baeza, Y., González, A., Morton, J.T., Mirarab, S., Xu, Z.Z., Jiang, L., Haroon, M.F., Kanbar, J., Zhu, Q., Song, S.E., Kosciolek, T., Bokulich, N.A., Lefler, J., Brislawn, C.J., Humphrey, G., Owens, S.M., Hampton-Marcell, J., Berg-Lyons, D., McKenzie, V., Fierer, N., Fuhrman, J.A., Clauset, A., Stevens, R.L., Shade, A., Pollard, K.S., Goodwin, K.D., Jansson, J.K., Gilbert, J.A., Knight, R., The Earth Microbiome Project Consortium. (2017). A communal catalogue reveals Earth's multiscale microbial diversity. *Nature*, 551(7681), 457–463. doi.org/10.1038/nature24621

Treusch, A.H., Vergin, K.L., Finlay, L.A., Donatz, M.G., Burton, R.M., Carlson, C.A., Giovannoni, S.J. (2009). Seasonality and vertical structure of microbial communities in an ocean gyre. *The ISME Journal*, 3(10), 1148–1163. doi.org/10.1038/ismej.2009.60

Uetake, J., Hill, T.C.J., Moore, K.A., DeMott, P.J., Protat, A., Kreidenweis, S.M. (2020). Airborne bacteria confirm the pristine nature of the Southern Ocean boundary layer. *Proceedings of the National Academy of Sciences of the United States of America*, 117(24), 13275–13282.

Urbano, R., Palenik, B., Gaston, C.J., Prather, K.A. (2011). Detection and phylogenetic analysis of coastal bioaerosols using culture dependent and independent techniques. *Biogeosciences*, 8(2), 301–309. doi.org/10.5194/bg-8-301-2011

Vergin, K.L., Done, B., Carlson, C.A., Giovannoni, S.J. (2013). Spatiotemporal distributions of rare bacterioplankton populations indicate adaptive strategies in the oligotrophic ocean. *Aquatic Microbial Ecology*, 71(1), 1–13. doi.org/10.3354/ame01661

Walsby, A.E. (1994). Gas vesicles. *Microbiological Reviews*, 58(1), 94–144.

Walsby, A.E., Hayes, P.K., Boje, R. (1995). The gas vesicles, buoyancy and vertical distribution of cyanobacteria in the Baltic Sea. *European Journal of Phycology*, 30(2), 87–94.

Walters, W., Hyde, E.R., Berg-Lyons, D., Ackermann, G., Humphrey, G., Parada, A., Gilbert, J.A., Jansson, J.K., Caporaso, J.G., Fuhrman, J.A., Apprill, A., Knight, R. (2016). Improved bacterial 16S rRNA gene (V4 and V4-5) and fungal internal transcribed spacer marker gene primers for microbial community surveys. *mSystems*, 1(1). doi.org/10.1128/msystems.00009-15

Wilson, T.W., Ladino, L.A., Alpert, P.A., Breckels, M.N., Brooks, I.M., Browse, J., Burrows, S.M., Carslaw, K.S., Huffman, J.A., Judd, C., Kilthau, W.P., Mason, R.H., McFiggans, G., Miller, L.A., Nájera, J.J., Polishchuk, E., Rae, S., Schiller, C.L., Si, M., Vergara Temprado, J., Whale, T.F., Wong, J.P.S., Wurl, O., Yakobi-Hancock, J.D., Abbatt, J.P.D., Aller, J.Y., Bertram, A.K., Knopf, D.A., Murray, B.J. (2015). A marine biogenic source of atmospheric ice-nucleating particles. *Nature*, 525(7568), 234–238.

Xia, X., Wang, J., Ji, J., Zhang, J., Chen, L., Zhang, R. (2015). Bacterial communities in marine aerosols revealed by 454 pyrosequencing of the 16S rRNA gene. *Journal of the Atmospheric Sciences*, 72(8), 2997–3008. doi.org/10.1175/jas-d-15-0008.1

Chapter 4. Airborne Transmission Pathway for Coastal Water Pollution

4.1 Abstract

Each year, over one hundred million people become ill and tens of thousands die from exposure to viruses and bacteria from sewage transported to the ocean by rivers, estuaries, stormwater, and other coastal discharges. Water activities and seafood consumption have been emphasized as the major exposure pathways to coastal water pollution. In contrast, relatively little is known about the potential for airborne exposure to pollutants and pathogens from contaminated seawater. The Cross Surfzone/Inner-shelf Dye Exchange (CSIDE) study was a large-scale experiment designed to investigate the transport pathways of water pollution along the coast by releasing dye into the surfzone in Imperial Beach, CA. Additionally, we leveraged this ocean-focused study to investigate potential airborne transmission of coastal water pollution by collecting complementary air samples along the coast and inland. Aerial measurements tracked sea surface dye concentrations along 5+ km of coast at 2 m x 2 m resolution. Dye was detected in the air over land for the first two days during two of the three dye releases, as far as 668 m inland and 720 m downwind of the ocean. These coordinated water/air measurements, comparing dye concentrations in the air and upwind source waters, provide insights into the factors that lead to the water-to-air transfer of pollutants. These findings show that coastal water pollution can reach people through an airborne pathway and this needs to be taken into account when assessing the full impact of coastal ocean pollution on public health. This study sets the stage for further studies to determine the details and importance of airborne exposure to sewage-based pathogens and toxins in order to fully assess the impact of coastal pollution on public health.

4.2 Introduction

Roughly half of the global population lives in coastal regions (U.S. Comission on Ocean Policy, 2004). The discharge of treated and untreated sewage, industrial effluents, agricultural drainage, and urban stormwater into coastal waters is a global public health concern (Halpern et al., 2012; Shuval, 2003; U.S. Comission on Ocean Policy, 2004). Chemical contaminants include metals, chlorinated pesticides, oil, fuel, soot, and butyltins, amongst others (NOAA, 2016). The United States Environmental Protection Agency lists 126 Priority Pollutants in industrial discharges, in addition to the many emerging contaminants of concern (Hutchinson et al., 2013; US EPA). But it is untreated sewage in coastal waters that is of primary concern because it often contains pathogens that can cause illness from a single exposure (Gersberg et al., 2006; Griffin et al., 2003; Shuval, 2003). Pathogenic viruses cause most cases of illness from contact with sewage contaminated waters (Griffin et al., 2003; Shuval, 2003). Serious illness can result from exposure to low numbers of viruses (i.e. 1's-10's) which have been shown to remain infectious in seawater longer than bacteria (Fong & Lipp, 2005; Gersberg et al., 2006; Griffin et al., 2003; Munn, 2011; Schiff et al., 1983). Over 100 enteric viruses - those affecting the gut - have been detected in contaminated waters, including hepatitis A virus (HAV) and norovirus, and SARS-CoV-2 virus is present in sewage (Gersberg et al., 2006; Lodder & de Roda Husman, 2020; Munn, 2011). Globally, over 120 million cases of gastrointestinal disease and more than 50 million cases of respiratory disease are estimated to be caused each year by people entering contaminated coastal waters (Shuval, 2003).

Coastal water quality is an increasing challenge for developed and developing countries alike. San Diego County, CA, USA, has 50 miles of coastline, much of which is impacted by seasonal stormwater runoff that enters the ocean untreated, a common occurrence in coastal cities worldwide (Dwight et al., 2011; Gersberg et al., 2006; Griffin et al., 2003; Steele et al.,

2018). Human fecal pollution associated with stormwater runoff has been documented at San Diego beaches (Gersberg et al., 2006; Steele et al., 2018). The problem is compounded at Imperial Beach, San Diego County's most southwesterly city, which lies across the border from Tijuana, Mexico. Rainfall in Tijuana River watershed results in both stormwater and sewage being discharged untreated into the Tijuana River, which empties into the ocean 2 km north of the US/Mexico border and pollutes the coastal waters on both sides. Specific infrastructure failures have resulted in additional releases of untreated sewage in recent years (Dibble & Smith, 2017; Hernandez, 2017). Moreover, other point sources of untreated sewage further south broaden the problem. The health risks are significant, with HAV having been detected in Imperial Beach's coastal waters following rainfall (Gersberg et al., 2006). Beach water quality is monitored in San Diego on a weekly basis; when poor water quality is detected, beaches are closed to direct water contact (i.e. swimming, surfing) (San Diego County, n.d.). But other forms of exposure to polluted water are possible, including atmospheric exposure, as we aim to demonstrate in this study.

Sea spray aerosol produced by breaking waves in the open ocean and surfzone transfers microscopic droplets of seawater into the atmosphere (Gantt and Meskhidze, 2013; Lenain & Melville, 2017; Lewis & Schwartz, 2004). Sea spray aerosol comprises a significant fraction of total aerosol at the coast and 20+ km downwind, especially during elevated winds, whitecaps, and surf (Clarke et al., 2006; Van Eijk et al., 2011; de Leeuw et al., 2000). The majority of SSA particles have diameters ranging between 10's of nm to 10 μm (Fröhlich-Nowoisky et al., 2016). SSA particles contain various chemical compounds and microorganisms, including bacteria and viruses (Patterson et al., 2016; Quinn et al., 2015). Airborne microorganisms have been found to be most abundant in SSA particles greater than 2 μm in diameter (Montero et al., 2016; Patterson

et al., 2016; Shaffer & Lighthart, 1997). Genetic sequencing efforts have shown that coastal air contains a mixture of microorganisms from the ocean and land (Graham et al., 2018; Li et al., 2011; Urbano et al., 2011). Culturing approaches have demonstrated the presence of viable bacteria and viruses in coastal and marine aerosol (Baylor et al., 1977; Fahlgren et al., 2010; Ladino et al., 2019; Li et al., 2011; Shaffer & Lighthart, 1997; Smith et al., 2013; Urbano et al., 2011). Hazardous chemicals and microorganisms have been detected in SSA (Cheng et al., 2005; Fleming et al., 2011; Graham et al., 2018; Kirkpatrick et al., 2010; Michaud et al., 2018; Pierce et al., 2003).The detection of brevetoxins in coastal air downwind of harmful algal blooms confirmed reports of naturally occurring marine toxins reaching humans on land via airborne transport (Cheng et al., 2005; Fleming et al., 2011; Kirkpatrick et al., 2010; Pierce et al., 2003). Genetic sequencing of coastal aerosol has identified potentially pathogenic bacteria at the species and genera levels (Graham et al., 2018). Whole genome shotgun sequencing identified potentially pathogenic bacteria in isolated SSA (Michaud et al., 2018).

Coastal water pollution has the potential to transfer into the atmosphere in SSA and reach people inland, a growing public health concern (O'Mullan et al., 2017). Baylor and colleagues demonstrated sea-to-air virus transfer by releasing non-native viruses into coastal waters and recovering the same virus strains on the beach (Baylor et al., 1977). Exposure to aerosolized microorganisms has also been identified as a risk in other environments, including solid waste treatment facilities, wastewater treatment plants, and agricultural sites using wastewater for spray irrigation (Brisebois et al., 2018; Carducci et al., 1995; Fannin, K.F., Gannon et al., 1977; Li et al., 2021; Malakootian et al., 2013; Teltsch & Katzenelson, 1978). This risk has been demonstrated for aerosols from sewage impacted rivers using aeration remediation (Dueker et al., 2012; Dueker & O'Mullan, 2014). Aerosols released into the air from rivers have been linked

with illness (Pickup et al., 2005). The objectives of the present study were to: a) use a nontoxic dye to simulate large-scale coastal water pollution events; b) determine the conditions leading to the transfer of the dye to the atmosphere; and c) relate dye concentrations between the ocean and atmosphere. This study is the first to examine the potential for inland transport of airborne water pollution in coastal regions. The detection of the dye in the air inland from the beach demonstrates that coastal water pollution transfers to the air in SSA and reaches communities via an airborne exposure pathway.

4.3 Materials and Methods

4.3.1 Tracer Dye as a Water Pollution Mimic

The CSIDE study simulated the impacts of coastal water pollution events on coastal air quality by releasing rhodamine WT (RWT) dye into the surfzone at Imperial Beach, CA, USA (Fig. 4.1) (Grimes et al., 2019). Rhodamine WT (molecular weight 566.99 g/mol) is a water soluble, non-toxic, fluorescent dye used as a semi-conservative water mass tracer, having no known oceanic sources and a minor sink in the form of photodegradation (Clark et al., 2009; Smart & Laidlaw, 1977; Suijlen & Buyse, 1994; Wilson et al., 1986). It is a non-volatile, solid compound at room temperature with maximum fluorescence at excitation/emission wavelengths of 558/582 nm (Mackay et al., 1981; Wilson et al., 1986). We simulated three pollution events by releasing roughly 30 gallons of concentrated RWT solution into the surfzone on September 23 (early morning, 3.2 h release), October 8 (early morning, 3.8 h release), and October 12 (mid morning, 1.8 h release into estuary outflow on ebb tide), 2015 (Fig. 4.1). Sea surface concentrations of the fluorescent dye (Fig. 4.1, Table 4.1) were measured with a hyperspectral camera mounted on an airplane that flew over the study site multiple times each hour on the first two days of each dye release (DR) (Melville et al., 2016). The hyperspectral camera was

calibrated with in-situ near-surface dye measurements to provide dye concentrations in surface waters with high spatial resolution (2 m x 2 m) (Clark et al., 2014; Feddersen et al., 2016; Grimes et al., 2019; Melville et al., 2016). This method is limited to daylight hours, and therefore no nighttime sea surface dye concentrations are reported.

4.3.2 Aerosol Sampling

Atmospheric aerosols were sampled at up to 3 sites over 2-4 days following each DR, at a total of 9 locations (Fig. 4.1 and Table 4.1). Aerosol sampling began the morning of each DR and continued into the afternoon, when samples were recovered and new sampling periods began, yielding ~6 hs daytime and ~16 hs overnight collection periods. Aerosol sampling locations were selected each morning based on the current dye observations (aerial and in-situ) in an effort to sample downwind of the ocean dye. The oceanic dye plume continued to evolve over time such that the aerosol sampling sites did not always remain downwind, and the downwind distance varied. Aerosols were collected using a PAS450-10 SpinCon I (heretofore "SpinCon I"), which utilizes a swirling technique to transfer aerosols and water soluble compounds from the air into a fixed volume of sterile water (Michaud et al., 2018; Yooseph et al., 2013). The SpinCon I samples air at 450 lpm and can sample continuously for hours, greatly concentrating airborne constituents into a 10 ml liquid sample. Internal surfaces of the SpinCon I were cleaned with 70% ethanol and tubing was flushed with 10% bleach followed by sodium thiosulfate to neutralize the bleach. In between samples, rinse cycles, in which the instrument is run for 30 seconds and then the sample is discarded, were used to flush surfaces. Field blanks were collected on October 7-8, between the first and second DRs, after the dye had dissipated in the coastal waters for two weeks.

4.3.3 RWT Measurements on Aerosol Samples

Samples were analyzed for RWT using fluorescence spectroscopy, normalizing to the water Raman peak (Lawaetz & Stedmon, 2009; Murphy, 2011). The fluorescence measurements were made the day the samples were recovered, using the Horiba Aqualog fluorescence spectrometer (Aqualog UV 800C, Horiba Ltd.), at 425-625 nm excitation wavelengths, at 5 nm increments, and reading at emission wavelengths of 248-827 nm, at ~4.5 nm increments. A calibration curve was generated to quantitatively relate fluorescence to RWT concentration, which also provided the RWT fluorescence pattern in the excitation-emission matrix, which we used to identify RWT in aerosol samples (Fig. 4.2). Positive detection of RWT in the aerosol samples are those that showed the RWT fluorescence pattern and a RWT fluorescence intensity above that of our limit of detection derived from the field blanks (Equation 1) (Armbruster & Pry 2008):

(1) limit of detection = $\alpha - 3.29\beta$

where α is the mean of the field blanks and β is the standard deviation of the field blanks. The RWT fluorescence pattern was not detected in any aerosol field blanks nor any sampler rinses.

4.3.4 Atmospheric Dye Concentrations

The average concentration of RWT in the air during each sampling period was determined by dividing the amount of RWT in the SpinCon I liquid sample by the total volume of air sampled. Figure 4.3 shows fluorescence spectra from a RWT standard (Fig. 4.3 A), from aerosol samples with strong and weak RWT signatures (Fig. 4.3 B & C), and from a field blank (Fig. 4.3 D), as well as the peaks used for quantitation and the region for background correction. RWT concentrations are reported for all air samples and those which met both criteria for RWT detection are noted (Table 4.1).

4.3.5 Dye Concentrations in Upwind Waters

To determine sea surface dye concentrations upwind of the aerosol samplers ([dye] (ppb)); Table 4.1), wind vectors were used from a local meteorological station (KNRS, Fig. 4.1) and interpolated to the time intervals of sea surface dye measurements. No lag between source and wind times was imposed because the observed ~5 m/s winds advected material from the surfzone to the furthest sampler (~1.5 km) in ~5 min, much shorter than the multi-hour sampling intervals. The intersection of the interpolated upwind vector with the tidally varying shoreline location, estimated using the 2012 NOAA Tsunami DEM and local water-level (including tides, but neglecting wave set-up), provided the center location for the upwind dye source in the ocean. A 200 m alongshore by 100 m offshore sea surface dye concentration window was extracted for each sea surface dye measurement taken during each aerosol sampling period. This box was limited to 100 m in the offshore direction because SSA was mainly generated in the surfzone region of depth-limited breaking waves (van Eijk et al. 2011; de Leeuw et al. 2000). The spatial and temporal average of the sea surface dye concentration in those windows was taken for each aerosol sampling period ([dye]sea (ppb)). This allowed us to precisely define the RWT aerosol source waters and quantitatively relate RWT concentrations in the ocean and atmosphere.

4.4 Results

4.4.1 RWT Transport by Ocean Currents

The three DRs demonstrated different ocean transport pathways of the RWT, driven by the coastal ocean currents. Figure 4.1 A–C show the maximum sea surface dye concentration at each point in the ocean on the first day of each dye release as measured from the air with the hyperspectral camera (Melville et al., 2016; Clark et al., 2014). Although temporal information such as persistence/transience is obscured in these figures, they provide a broad visual

comparison of the major dye distribution for each DR. At the broadest level, the three DRs showed that the pollution mimic did not immediately disperse offshore, but instead remained within 1 km of the shoreline during the first day of each release, consistent with multiple studies showing surfzone trapping (Boehm, 2003; Grant et al., 2005; Clark, Feddersen & Guza, 2010; Rodriguez, Giddings & Kumar, 2018). For DRs 1 and 3 (Figs. 1A & 1C), the dye remained within ~2 km alongshore of the release location. For DR2 (Fig. 4.1 B) a strong, wave-driven, alongshore current rapidly advected the dye ~10 km northward along the coast (Grimes et al., 2020; Wu et al., 2020). Thus for DR2, although high sea surface dye concentrations are seen along the coast, they only persisted at any given location for a short time due to the rapid northward advection. Sea surface dye concentrations are overall much lower for DR3, likely a result of localized mixing and, to a lesser extent, missing aerial measurements due to flight access limitations in the first few hours following the DR. Combined, the three DRs show the variability in water and pollution transport expected for the coastal ocean and the motivation for the CSIDE study. The ocean transport aspects of the CSIDE study are discussed in greater depth in other publications (Grimes et al., 2020; Wu et al., 2020).

4.4.2 RWT Detected in Coastal Aerosol

Dye was detected in coastal aerosols on days 1 and 2 of DRs 1 and 3 in four total aerosol samples (Figs. 4.1 A, C; Table 4.1). Dye was detected as far as 668 m inland and 720 m downwind from source waters. Wind rose plots (Figs. 4.1 D–F) for daytime winds show that onshore winds, typical of coastal meteorology patterns, were common. Wind data link the oceanic source waters with locations of atmospheric dye detection over land. Figure 1 broadly shows that atmospheric dye was detected downwind of the dye plume. The well characterized

distribution of RWT in coastal waters allows quantitative comparison between dye concentrations in the air and in the source waters.

4.4.3 Comparing Ocean and Atmosphere Observations

Repeated measurements of dye in the coastal waters allow us to examine dye concentrations in the source waters during the atmospheric sampling periods. Figure 4.4 shows the comparison of ocean dye data from two exemplary samples for when dye was and was not detected in the air. The mean sea surface dye concentration in the upwind waters during the aerosol sampling period is presented relative to the aerosol sampling location on land. The inset dotted box shows a 200 m × 100 m region centered where the mean wind direction during the aerosol sampling period intersected the coastal waters. Sample 2 (Fig. 4.4, left panel) was collected on the first day of DR1 and sample 4 (Fig. 4.4, right panel) was collected the day after, i.e. day 2 of DR1. Dye was detected in sample 2, which was collected downwind of waters with high dye concentrations. Dye was not detected in sample 4, which was collected downwind of waters with little to no detectable dye. Analogous plots for all air samples with coupled ocean measurements are provided in the Supplemental Materials (Fig. 4.5).

4.5 Discussion

4.5.1 Atmospheric Transfer of RWT in SSA

Surfzone production of SSA transferred RWT from the ocean to the atmosphere. Rhodamine WT's transfer in SSA is consistent with the detection of other chemical species in SSA (Fleming et al., 2011; Cheng et al., 2005; Hawkins & Russell, 2010; Cochran et al., 2017; Kuznetsova, Lee & Aller, 2005) and larger entities including viruses and bacteria (Patterson et al., 2016; Baylor et al., 1977; Michaud et al., 2018; Aller et al., 2005). Dissolved RWT has a low surface activity, therefore it acts as a tracer of bulk seawater, which transfers to SSA primarily in

jet drops. Sea spray aerosol production, specifically from depth-limited waves breaking in the surfzone, must have been the dominant RWT transfer mechanism because surfzone production of SSA has been shown to be dominant for low to moderate wind speeds (van Eijk et al., 2011; de Leeuw et al., 2000). Dye transfer outside the surfzone was negligible because whitecap conditions were not common during the study period, due to low wind speeds often below 6 m/s.

4.5.2 Atmospheric Transport of RWT SSA

We understand that the major factors influencing atmospheric concentrations of RWT SSA include: dye concentrations in aerosol source waters, which depends on advection and dispersion of the dye in the ocean, driven by waves, regional pressure gradients, buoyant plumes, winds, tides, and internal tides; ocean-to-atmosphere RWT SSA flux, which occurred primarily through SSA production by surfzone depth-limited wave breaking; downwind advection and horizontal and vertical dispersion in the atmosphere, driven by coastal winds and atmospheric boundary layer dynamics; and dry deposition (gravitational settling) of RWT SSA. We understand that dye was not detected in most aerosol samples due to high variability in ocean and air transport patterns. Photobleaching of RWT is negligible on our <4 d timescales (Suijlen & Buyse, 1994). We compare dye concentrations in the ocean and atmosphere to test whether source water dye concentrations influenced airborne dye concentrations (Fig. 4.6). Dye was not always detected when upwind waters contained elevated dye concentrations, due to downwind distance, 3D atmospheric dispersion, and the lack of a vertical sampling array. When RWT dye was detected in the aerosol (Fig. 4.6, magenta points), the data suggest dye concentrations in the air are proportional to dye concentrations in source waters. Importantly, there were no false positive atmospheric dye values because higher RWT concentrations in the air correspond to higher RWT concentrations in the ocean; there are no data points high in air RWT and low in

ocean RWT (Fig. 4.6). More experiments with sampling at higher temporal and vertical/horizontal spatial resolution are needed to confirm a robust, quantitative relationship between SSA and upwind source waters, and to better understand the role of atmospheric dispersion.

4.5.3 Implications

Our results demonstrate the ability to trace SSA back to its source waters with high spatial and temporal resolution, and to quantitatively relate dye concentrations in source waters and air masses. More importantly, this study confirms coastal water pollution can be transferred from the surf into the atmosphere by releasing a tracer dye into the ocean and detecting it in the air inland from the beach. These observations highlight an under-appreciated airborne exposure pathway to coastal water pollution. We expand on the pioneering work of Baylor et al. (1977) by simulating large-scale artificial water pollution events, measuring sea surface dye concentrations at high spatio-temporal resolution (2 m × 2 m, hourly), tightly constraining RWT SSA source waters, and making quantitative ocean-atmosphere comparisons that extend inland beyond the beach. Whereas many atmospheric aerosol studies detect particles from distant sources, and aerosol dispersion models provide insight into particle origin at regional level resolution (~100 km), we were able to pinpoint SSA source waters on the <1 km scale. Although we were unable to detect RWT SSA beyond 668 m inland (Fig. 4.1, Table 4.1), it is well documented that SSA can travel much further (Smith et al., 2013; Bondy et al., 2017; Prospero et al., 2005; Smith et al., 2012). A 2 μm SSA particle has a predicted dry deposition residence time of ~1.5 weeks with an estimated travel distance of 10,000 km (Lewis & Schwartz, 2004). SSA particles this size have been detected hundreds to thousands of km from their oceanic source region (Bondy et al., 2017). Bacteria can remain viable after travelling thousands of km in the atmosphere (Prospero

et al., 2005; Smith et al., 2012). Our findings emphasize that species transfer from the ocean to the atmosphere includes not just natural seawater components but also pollutants. This study also demonstrates that coastal water pollution reaches people beyond the shoreline through atmospheric transport. These results detail a promising approach for linking pollution in source waters, including the surfzone, estuaries, and other outflows, to atmospheric pollutants and health impacts downwind.

4.6 Conclusions

In summary, this study confirms that coastal water pollution can be transferred from the surf to the atmosphere by measuring tracer dye concentrations in the ocean and air. Airborne transport of coastal water pollution can expose people beyond the water and beach, including entire coastal communities, to biological and chemical pollutants. The magnitude of this risk is a function of various parameters. Dispersion in the atmosphere dilutes airborne pollution, and pathogens can die or deactivate in the atmosphere, but exposure to a relatively small number of viruses have been shown to cause illness (Schiff et al., 1983; Fong & Lipp, 2005; Munn, 2011). This study draws attention to an underappreciated airborne exposure pathway and sets the stage for future studies to better quantify the magnitude of the airborne exposure. Additional work is needed to assess public health threats from known coastal pathogens and emerging pathogens, like SARS-CoV-2, which is present in wastewater (Lodder & de Roda Husman, 2020; Colwell, 1996). Coastal water pollution is an increasing global problem that will only worsen as the human population grows and climate change leads to more extreme precipitation events. Ultimately, a thorough understanding of how pathogens and toxins are transported by coastal water currents and wind patterns will allow timely predictions of potential health risks to coastal communities and beyond.

4.7 Acknowledgements

Any opinions, findings, and conclusions or recommendations expressed in this material are those of the authors and do not necessarily reflect the views of the National Science Foundation. The authors thank NSF and the Dankberg Family Foundation for financial support. We thank Ken Melville, Luc Lenain, Nick Statom, and Stephen Holleman for acquisition and preliminary processing of MASS data and SIO CDIP for wave data. We thank YMCA: Camp Surf for providing a base of operations; the cities of Imperial Beach and Coronado, the Imperial Beach lifeguards, the Tijuana River National Estuary Research Reserve, Mar Vista High School, and CA State Parks for accommodating our research activities. We thank the US Navy and Naval Base Coronado for their support during the CSIDE experiment. Extra thanks to CA Border Patrol, Adriana Corrales, Josh Cox, Jeff Crooks, Chris Peregrin, Julio Lorda, Capt. Robert Stabenow, Sgts. Ayala & Lindquist, Kevin Willard, Randy Rosenheim, the Blake/Giardina household, and the Pendergraft household for sampling assistance and access.

Chapter 4, in full, is a reprint of material that has been published in PeerJ. Pendergraft, M.A., Grimes, D.J., Giddings, S.N., Feddersen, F., Beall, C.M., Lee, C., Santander, C., Prather, K.A. (2021). Airborne Transmission Pathway for Coastal Water Pollution. PeerJ 9:e11358 https://doi.org/10.7717/peerj.11358

4.8 Figures

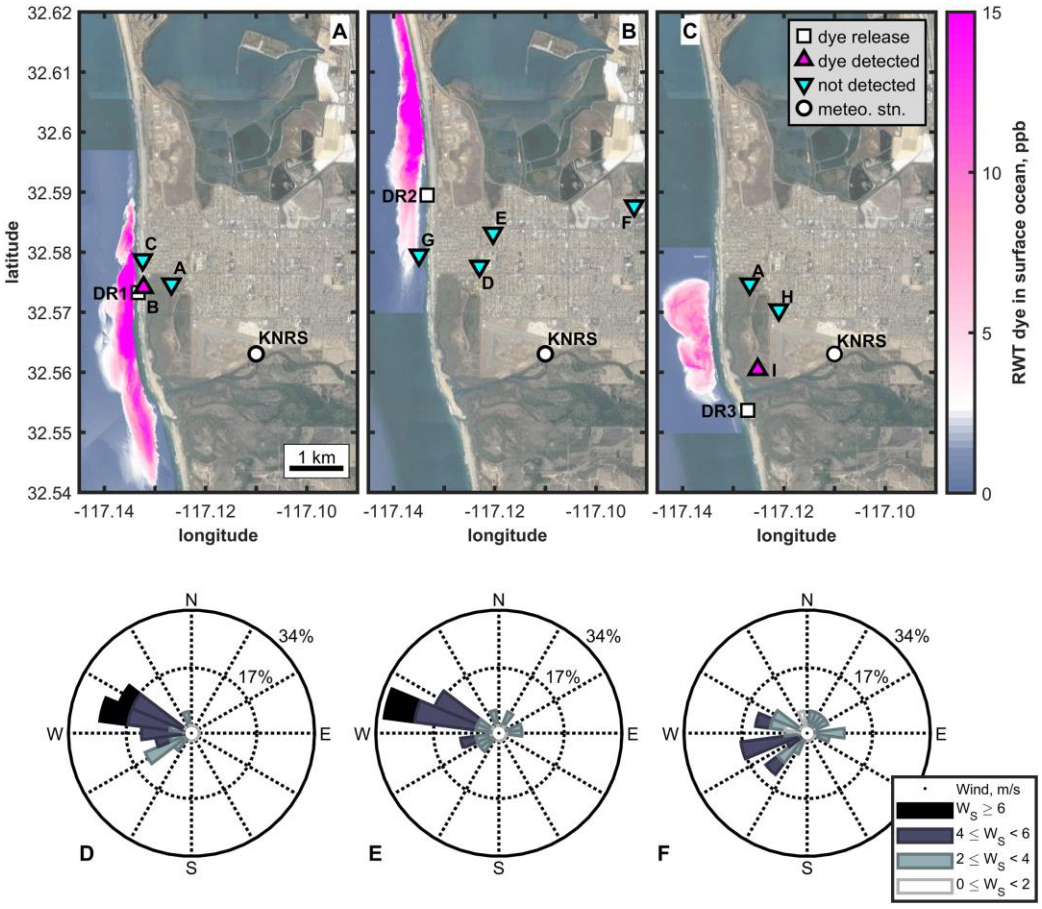

Figure 4.1 Overview of the three dye releases of the CSIDE study. (A)–(C) present maximum RWT dye concentrations in coastal waters and aerosol sampling locations and results from each dye release (1–3). Magenta triangles pointing up indicate locations where dye was detected in the aerosol. Cyan triangles pointing down show the locations where aerosol was sampled and dye was not detected. (D)–(F) contain wind roses presenting daytime winds, responsible for onshore transport, for the first 2 days of each DR, when most aerosol samples were collected (4). Stacked bars in the wind roses indicate the percent of the time period the wind blew from the indicated direction and at the indicated speed (represented by color). (1) Zohar Bar-Yehuda (2017). zoharby/plot_google_map (https://github.com/zoharby/plot_google_map), GitHub. Retrieved June 1, 2017. (2) Map data: Imagery ©2020 Google. Data USGS, Data SIO, NOAA, U.S. Navy, NGA, GEBCO, Data LDEO-Columbia, NSF, NOAA, Imagery ©2020 TerraMetrics, Map data ©2020 INEGI. (3) Jonathan Sullivan (2017). Automatic Map ScaleGeneration (https://www.mathworks.com/matlabcentral/fileexchange/33545-automatic-map-scale-generation), MATLAB Central File Exchange. Retrieved June 1, 2017. (4) Daniel Pereira (2017). Wind Rose (https://www.mathworks.com/matlabcentral/fileexchange/47248-wind-rose), MATLAB Central File Exchange. Retrieved June 1, 201

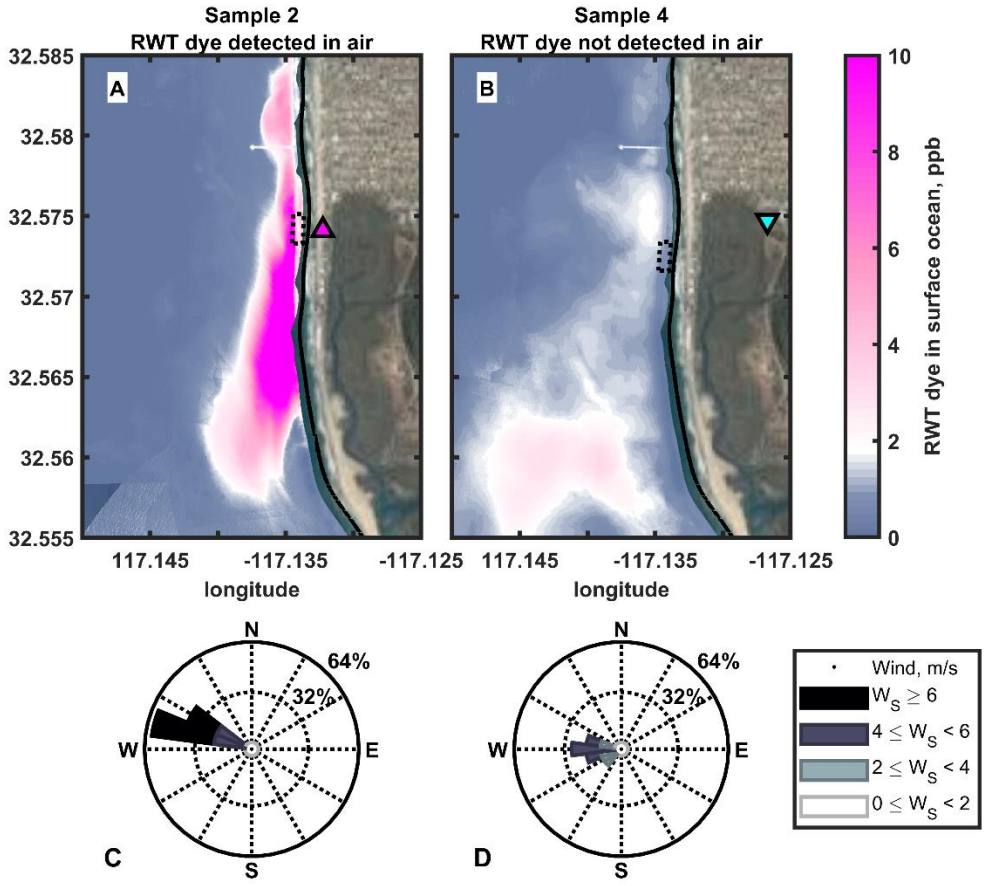

Figure 4.4 Conditions during two aerosol sampling periods. (A) and (B): average sea surface dye concentrations during the period each aerosol sample was collected at the location on land indicated by the triangle . The dotted black box indicates where the average wind direction during each sampling interval intersected the coastal waters, and the box over which the source water concentrations shown in Fig. 3 are calculated. (C) and (D) are wind roses for the winds observed at the KNRS meteorological station during the aerosol sampling periods. Aerosol sample 2 (A) contained dye and was collected downwind of high dye concentrations in coastal water. Aerosol sample 4 (B) did not contain detectable dye and was collected downwind of seawater containing very low dye concentrations near the detection limit.

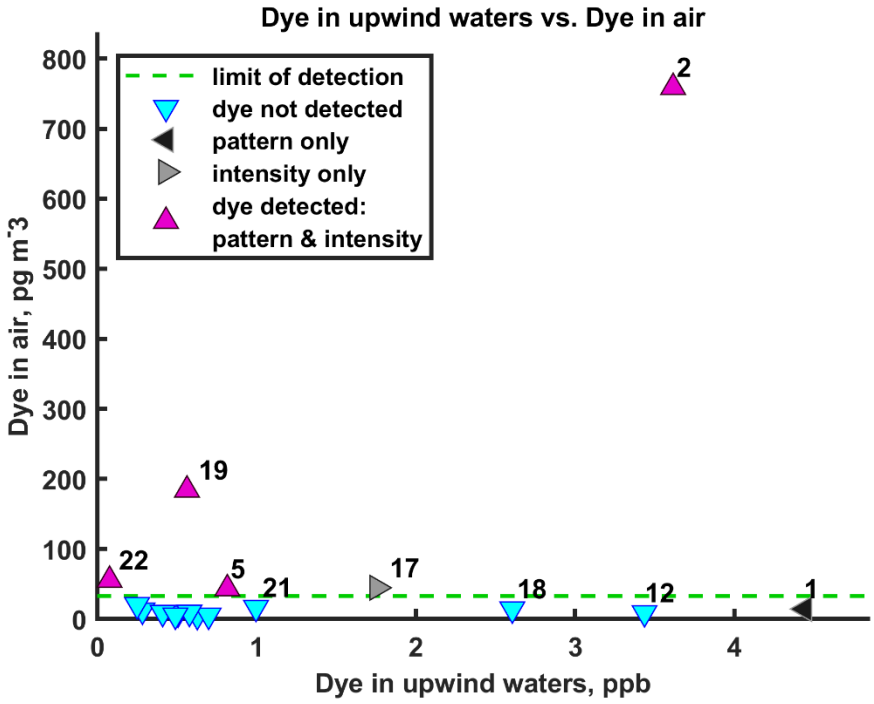

Figure 4.6 Dye concentrations in air and upwind waters. For aerosol samples that were collected during periods of hyperspectral measurements of ocean dye concentrations (primarily daytime), the RWT concentration in the air (vertical axis) is compared against the dye concentration in the upwind source waters (horizontal axis). Symbol labels are sample numbers. A dye concentration in the air can be calculated whether dye was detected (magenta) or not (cyan) as dye detection relies both on values being above the blank and containing the RWT signature. The green dashed line indicates the limit of detection determined from the air field blanks and eqn. 1 (32.8 pg/m3). False positives would show up along a vertical line near 0 on the horizontal axis. Here, two air samples met one of two criteria for dye detection and two other air samples did as well, but do not appear here because sea surface RWT concentrations are not available for them.

4.9 Tables

Table 4.1 Data for the aerosol samples collected following the 3 dye releases. Distance inland is the distance from the air sampling location to the nearest point along the shoreline. Distance downwind is the mean distance along the wind vector from the center of the 200 m x 100 m ocean source window to the aerosol sampling site. Distance inland is fixed, whereas distance downwind is subject to the relevant wind directions. [dye]air (pg/m3) is the concentration of dye in the air calculated from the fluorescence intensity and the volume of air sampled. The four samples which match our criteria for dye detection are highlighted in bold. The values for the samples that did not meet our criteria for dye detection are provided in parentheses. [dye]sea (ppb) indicates the sea surface dye concentration measured by the hyperspectral camera and are available for most daylight hours on the day of each dye release and the following day and are not available for aerosol samples collected at night.

#	DR	date start	sample period	Site	inland (m)	downwind (m)	sampled air (m^3)	dye pattern	above LoD	$[dye]_{air}$ (pg/m^3)	$[dye]_{sea}$, (ppb)
1	1	9/23	day	A	615	678	198	Yes	No	(14.3)	4.4
2	**1**	**9/23**	**day**	**B**	**101**	**154**	**135**	**Yes**	**Yes**	**759.0**	**3.6**
3	1	9/23	night	A	615	653	398	No	No	(4.8)	0.6
4	1	9/24	day	A	615	664	226	No	No	(5.2)	0.7
5	**1**	**9/24**	**day**	**B**	**101**	**148**	**162**	**Yes**	**Yes**	**43.3**	**0.8**
6	1	9/24	night	C	122	NA	422	No	No	(5.0)	NA
7	1	9/24	night	A	615	NA	377	No	No	(11.3)	NA
8	1	9/25	day	C	122	NA	116	No	No	(20.0)	NA
9	1	9/25	day	A	615	NA	137	No	No	(4.8)	NA
10	2	10/8	day	D	976	1057	241	No	No	(8.3)	0.5
11	2	10/8	day	E	1256	1310	216	No	No	(9.4)	0.6
12	2	10/8	day	F	3867	3953	181	No	No	(8.9)	3.4
13	2	10/8	night	E	1256	1284	428	No	No	(12.5)	0.3
14	2	10/8	day	D	976	1037	54	No	No	(20.4)	0.3
15	2	10/9	day	G	108	57	140	No	No	(9.2)	0.4
16	2	10/9	24 h	E	1256	1288	691	No	No	(5.3)	0.5
17	3	10/12	day	A	615	712	211	No	Yes	(44.6)	1.8
18	3	10/12	day	H	1193	1275	234	No	No	(14.1)	2.6
19	**3**	**10/12**	**day**	**I**	**668**	**720**	**178**	**Yes**	**Yes**	**184.2**	**0.6**
20	3	10/12	night	H	1193	NA	347	No	No	(15.2)	NA
21	3	10/12	night	A	615	NA	376	No	No	(16.4)	1.0
22	**3**	**10/13**	**day**	**I**	**668**	**694**	**169**	**Yes**	**Yes**	**55.5**	**0.1**
23	3	10/14	day	I	668	NA	135	No	Yes	(60.9)	NA
24	3	10/15	day	I	668	NA	152	No	Yes	(34.0)	NA
25	blank	10/7	night	D	976	NA	192	No	NA	(2.0)	NA
26	blank	10/7	night	C	122	NA	383	No	NA	(7.3)	NA
27	blank	10/7	day	D	976	NA	119	No	NA	(18.9)	NA
28	blank	10/7	day	C	122	NA	224	No	NA	(10.0)	NA
29	rinse	9/23	NA	rinse	NA	NA	NA	No	NA	NA	NA
30	rinse	10/9	NA	rinse	NA	NA	NA	No	NA	NA	NA
								blanks mean		**9.5**	
								blanks SD		**7.1**	
									LoD	**32.8**	

4.10 Supplementary Methods

4.10.1 Rhodamine WT Identification and Quantification in Aerosol Samples

Analyzing a RWT standard provided the RWT fluorescence pattern for visual detection in the samples (Fig. 4.3). The maximum fluorescence from the five highest calibration curve concentrations (15 total scans) occurred at a total of 3 excitation/emission wavelength pairs (555/580, 560/580, and 560/585 nm), all in the vicinity of the reported wavelengths of maximum RWT fluorescence (558/582 nm). Fluorescence quantification used the mean fluorescence intensity from these three wavelength pairs for each sample.

Four aerosol field blanks were collected Oct. 7-8, 2015, after dye from the first dye release had dissipated for 2 weeks. None of the four blanks presented the RWT fluorescence signature. They were processed identically as the aerosol samples to generate dye concentrations in air, which provided values for measurement error (Table 4.1). This produced a mean and standard deviation of 9.5±7.1 pg/m3 which was used along with eqn. (1) to generate our limit of detection of 32.8 pg/m3 which serves as one of two criteria for detecting dye in air samples (Armbruster & Pry, 2008). We observed significant variability in the background fluorescence of our air samples and field blanks, as evidenced by varying fluorescence intensities between features in the excitation-emission matrices, which we attribute to atmospheric particle loads that varied across different samples. To account for this variability, a background subtraction was applied to all standards and samples to remove scatter off the 1/1 excitation/emission line and other noise, so as to not be quantified as RWT fluorescence. After reviewing all spectra, an excitation/emission region was selected which did not show strong signal in any samples or standards, but did include the 1/1 excitation/emission line (see boxes in Fig. 4.3). For each spectrum, the mean fluorescence intensity from this region was subtracted from the entire

spectrum. Then RWT fluorescence was calculated from the fluorescence intensity at the three excitation/emission pairs as described.

4.10.2 RWT Concentrations Near the Surfzone Upwind of the Aerosol Samplers

To determine the sea surface dye concentrations upwind of the aerosol samplers ([dye]sea (ppb); Table 4.1 and x axis in Fig. 4.5), upwind vectors were derived using wind data from a local meteorological station (KNRS, Fig. 4.1) and interpolated to the time intervals of aerial dye measurements. No lag between source and wind times was imposed because the observed ~5 m/s winds advected material from surfzone to sampler (~1.5 km) in ~5 min, much shorter than the multi-hour aerosol sampling intervals. The intersection of the interpolated upwind vector with the tidally varying shoreline location, estimated using the 2012 NOAA Tsunami DEM and local water-level (including tides, but neglecting wave set-up), provided the center location for the upwind dye source. A 200 m alongshore by 100 m offshore sea surface dye concentration window, relative to the upwind shoreline intersection location, was extracted for each remote sea surface dye measurement taken during each aerosol sampling period. The spatial and temporal average of the sea surface dye concentration windows provided an approximate average upwind sea surface dye concentration over each aerosol sampling period (SS dye (ppb); Table 4.1). This allowed us to accurately define the RWT aerosol source waters and quantitatively relate RWT concentrations in the ocean and atmosphere. This box was limited to 100 m in the offshore direction as SSA generation was mainly expected to occur in the surfzone region of depth-limited breaking waves.

4.11 Supplementary Figures

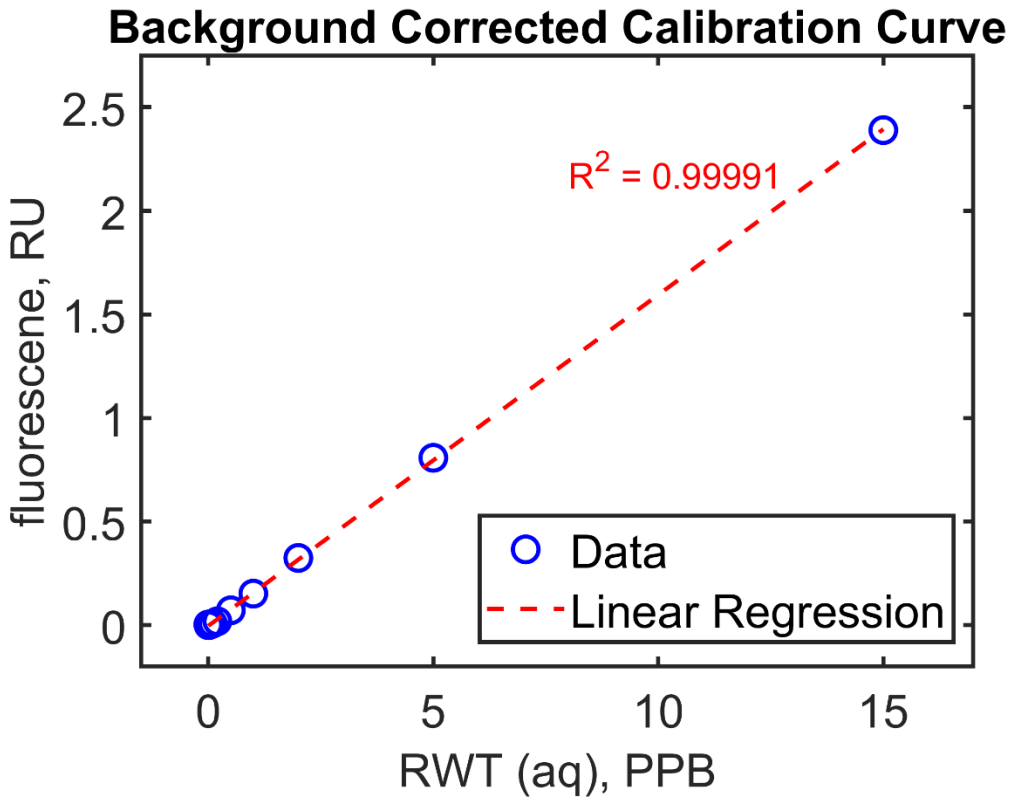

Figure 4.2 RWT fluorescence calibration curve for aerosol measurements. Calibration curve produced by measuring the fluorescence of RWT solutions at known concentrations. The data were background corrected using the same technique used for the collected samples.

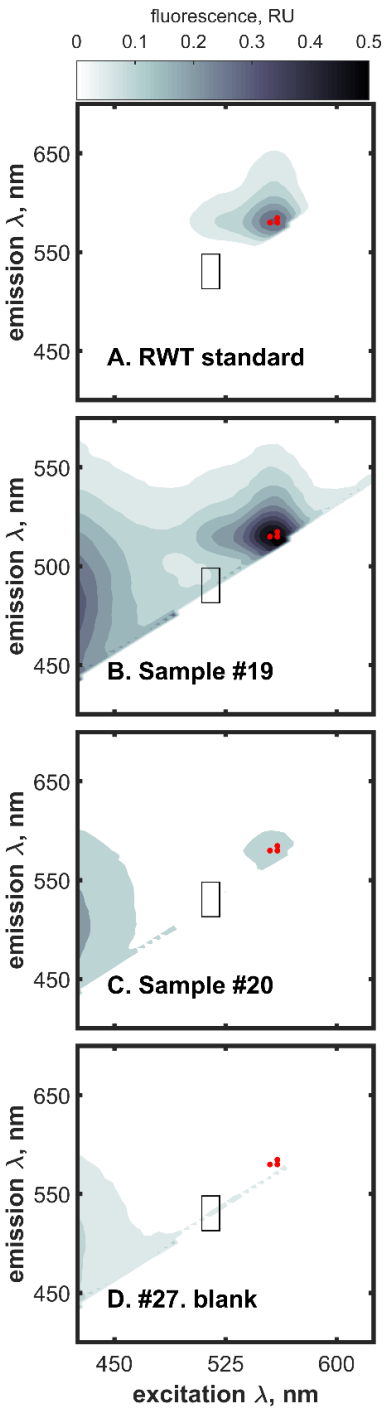

Figure 4.3 Example excitation-emission matrices (EEMs) displaying fluorescence intensity in Raman Units (RU). (A) a 2 PPB RWT standard, (B) sample #19 - dye detected, (C) sample #20 - dye not detected, and (D) sample #27 - aerosol field blank; dye not detected Red dots indicate the 3 excitation/emission pairs determined from the calibration to be used for RWT dye quantification. The mean fluorescence intensity from the black rectangle was subtracted from the entire spectrum as an internal background correction.

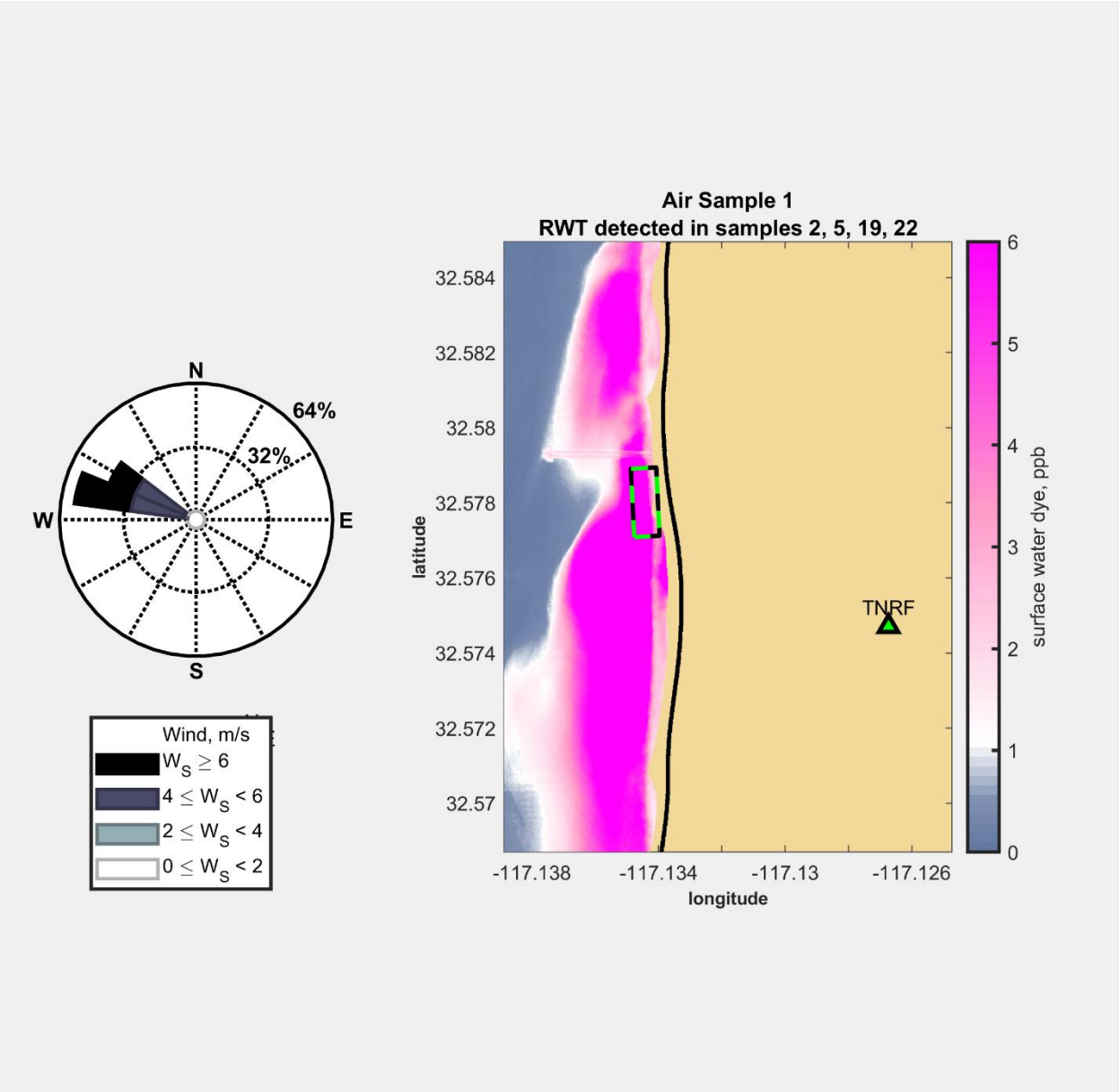

Figure 4.5 (A) Mean sea surface dye concentrations upwind of aerosol sample #1. Like Figure 2, for all aerosol samples with data available (day samples). Right: Average sea surface dye concentrations during the period each aerosol sample was collected at the location on land indicated by the triangle. The 200 m x 100 m dotted box indicates where the average wind direction during each sampling interval intersected the coastal waters from the sampling site. Figure 3 finds the location of that box and its mean dye value for each hourly sea surface dye measurement. Here we show the mean dye field during each air sampling period and the mean upwind location (box). Left: wind rose for the winds observed at the KNRS meteorological station during the aerosol sampling periods.

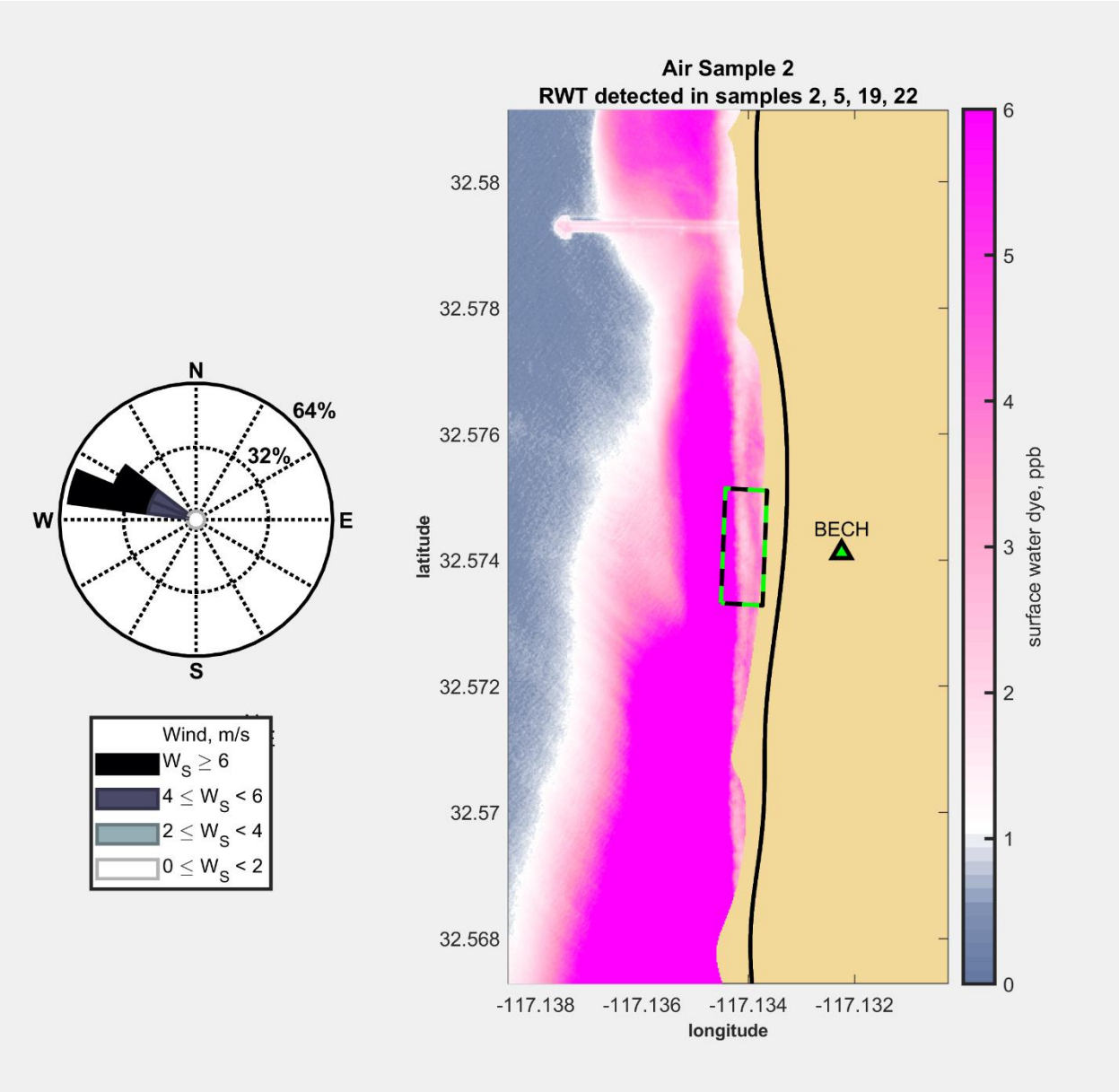

Figure 4.5 (continued) (B) Mean sea surface dye concentrations upwind of aerosol sample #2.

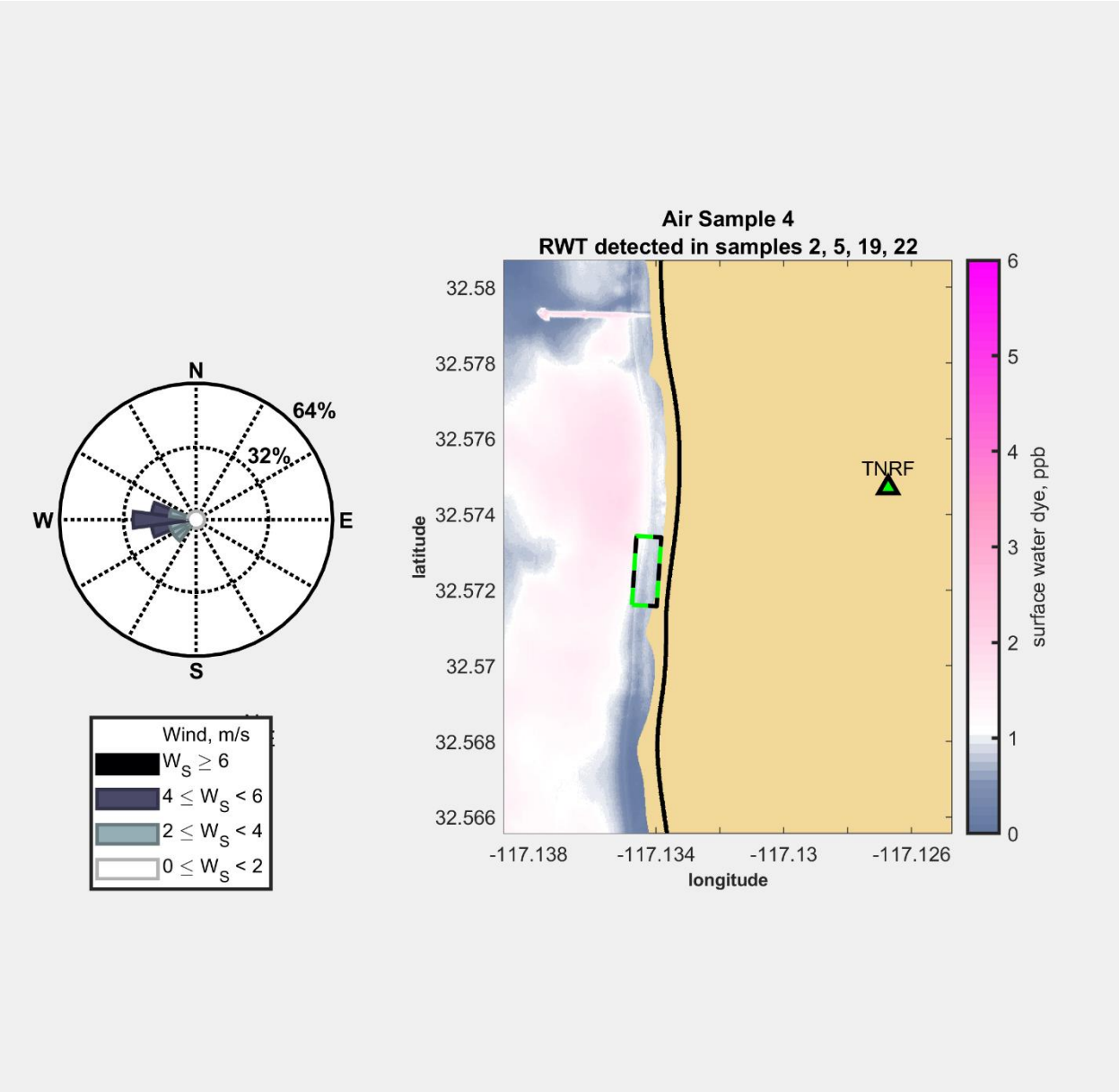

Figure 4.5 (continued) (C) Mean sea surface dye concentrations upwind of aerosol sample #4.

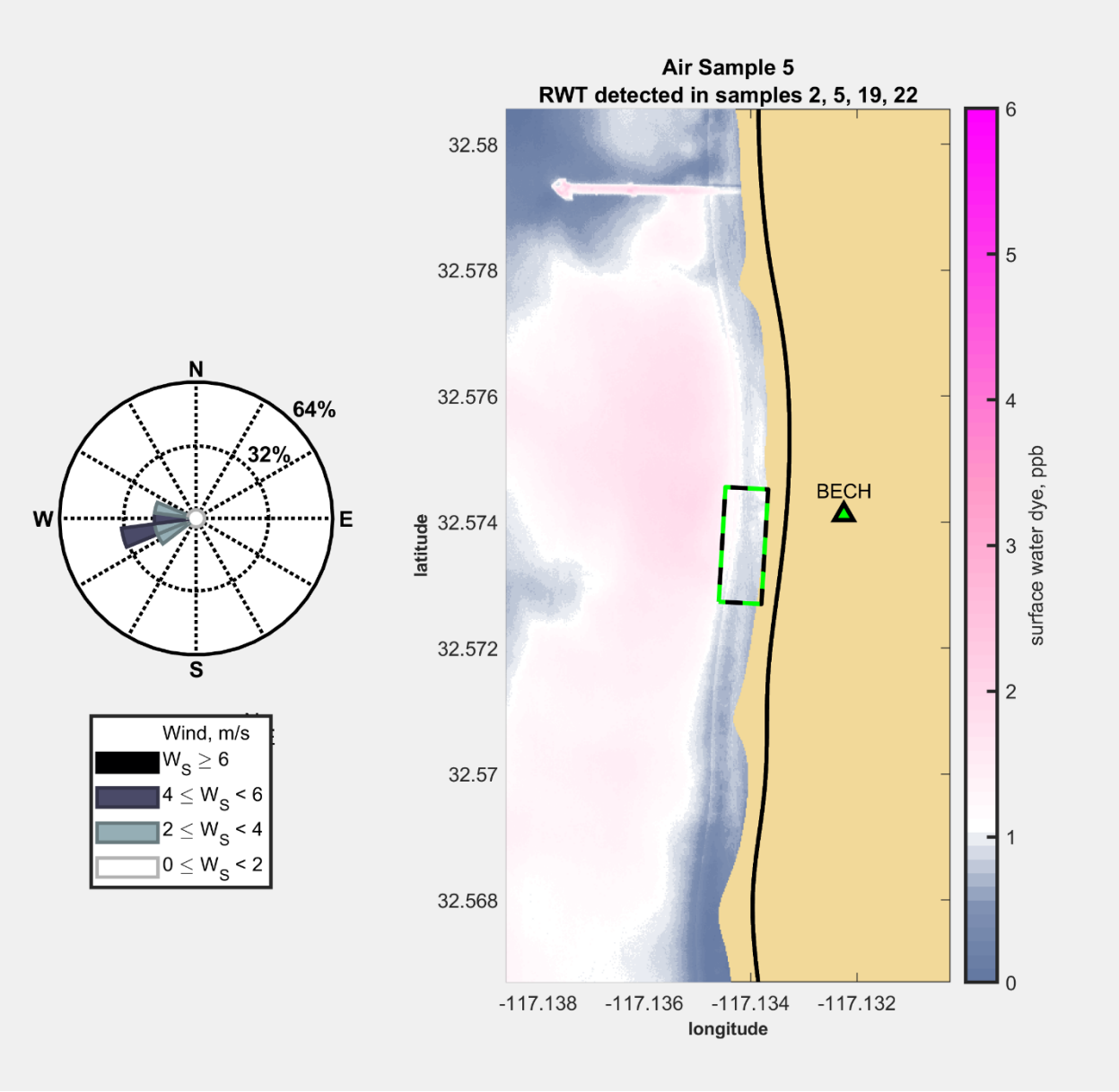

Figure 4.5 (continued) (D) Mean sea surface dye concentrations upwind of aerosol sample #5.

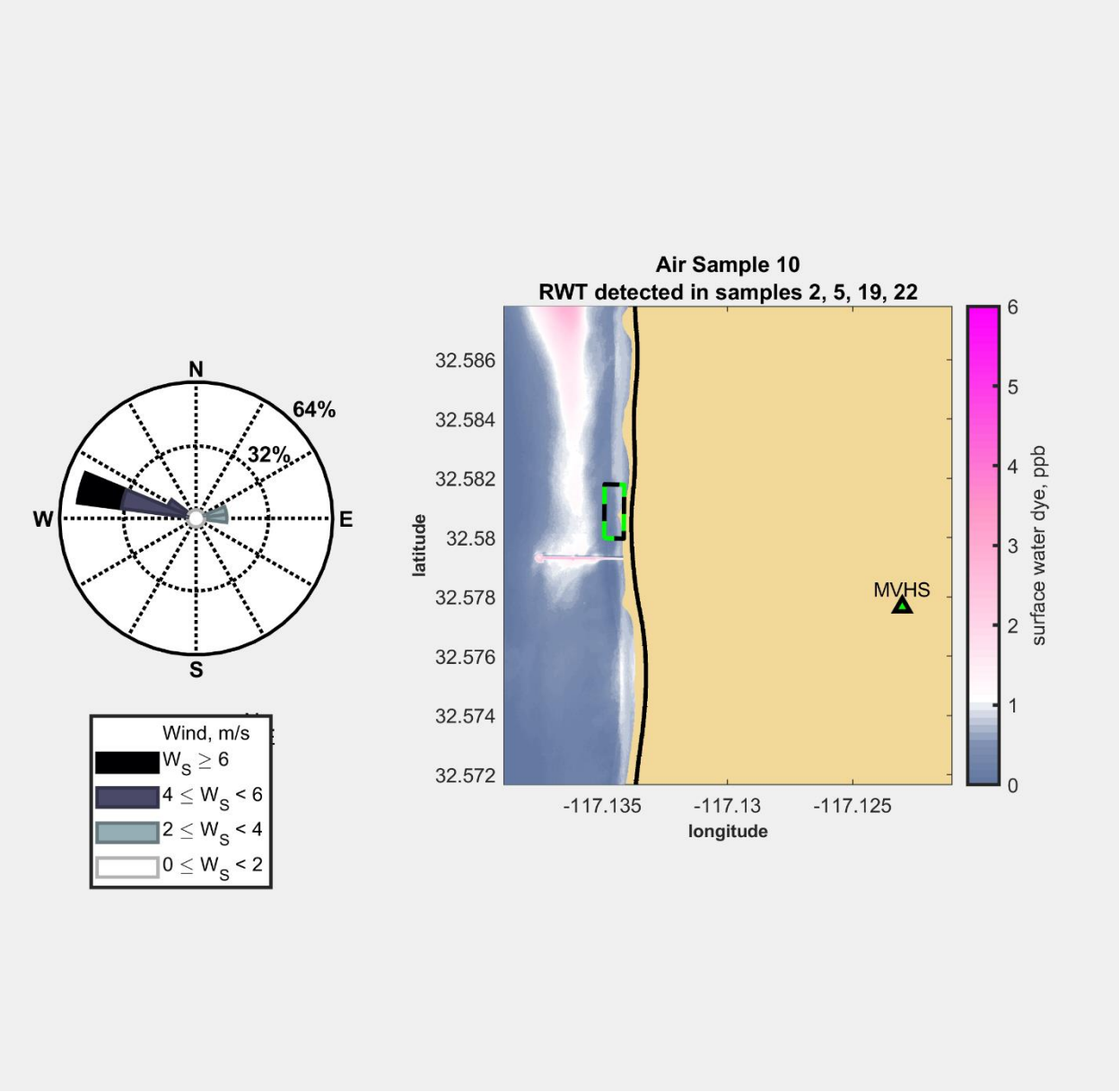

Figure 4.5 (continued) (E) Mean sea surface dye concentrations upwind of aerosol sample #10.

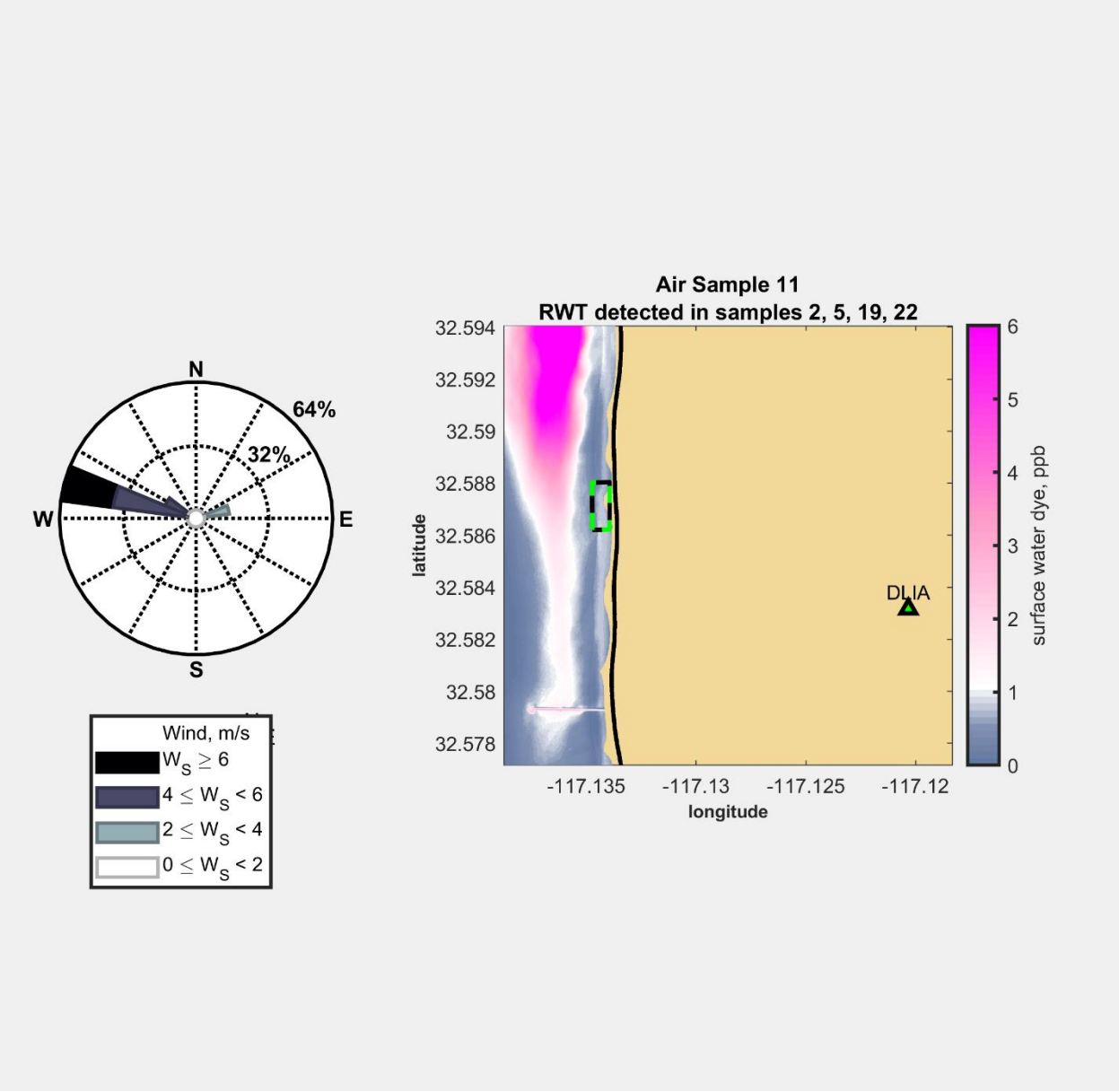

Figure 4.5 (continued) (F) Mean sea surface dye concentrations upwind of aerosol sample #11.

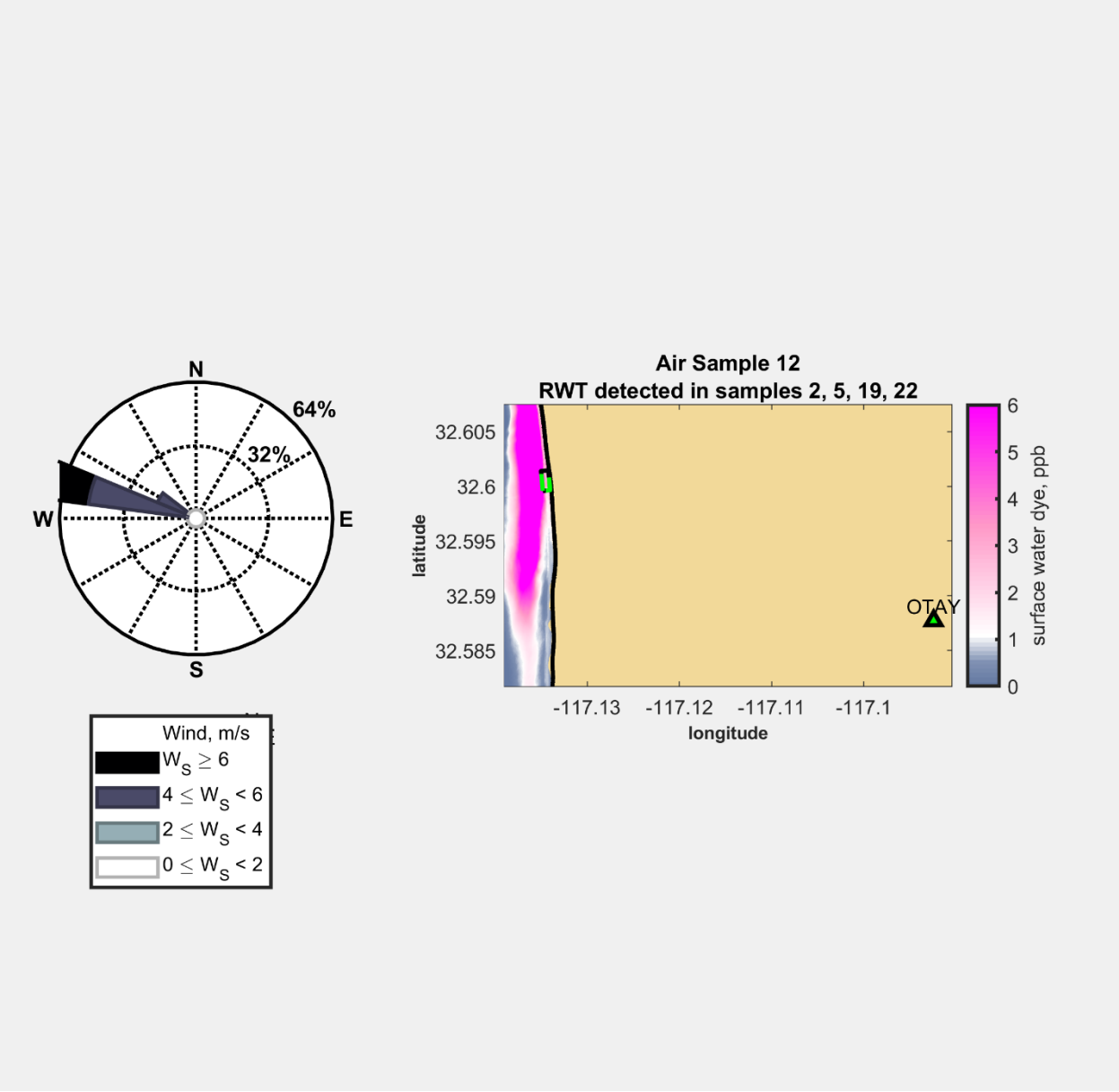

Figure 4.5 (continued) (G) Mean sea surface dye concentrations upwind of aerosol sample #12.

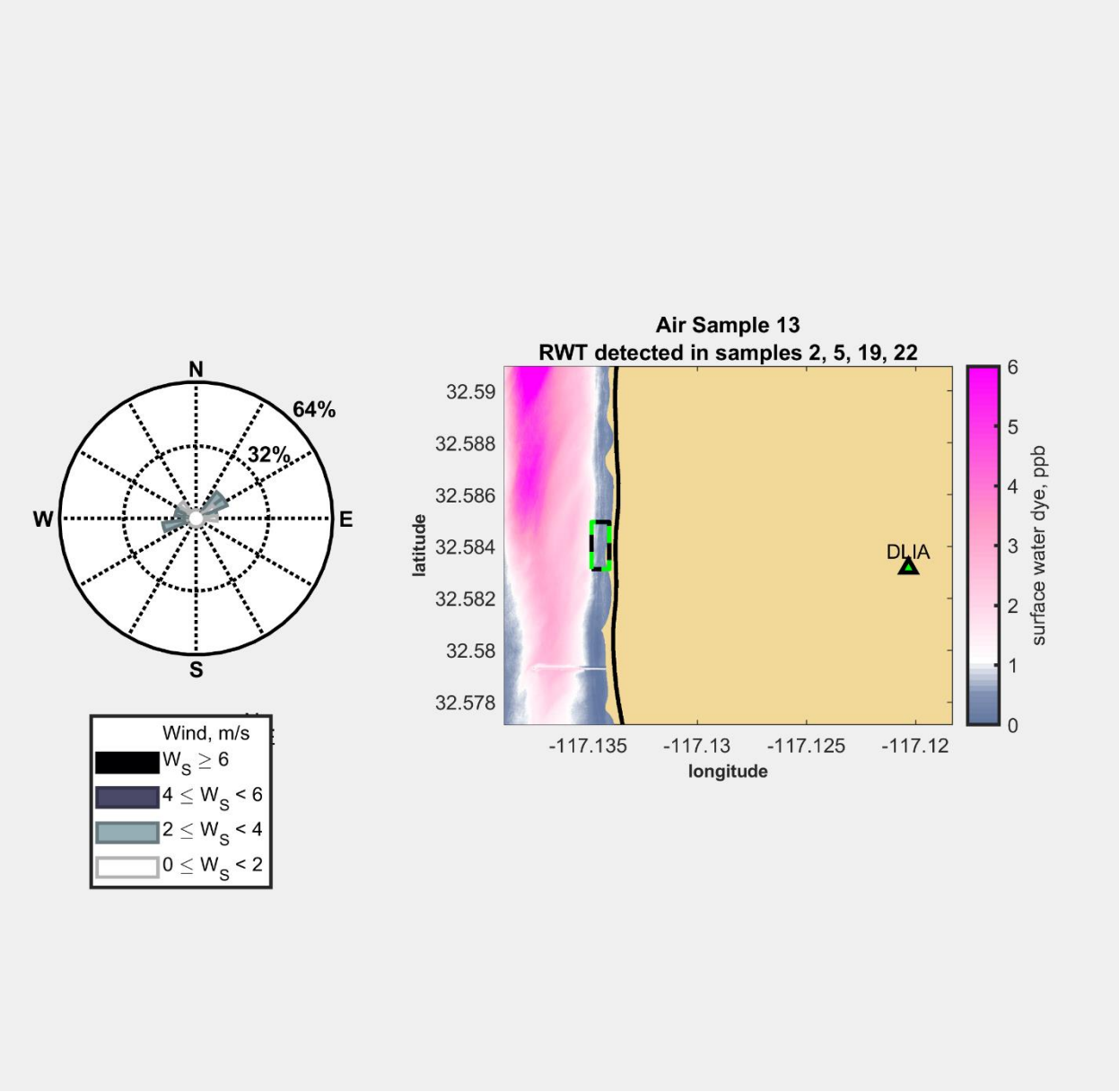

Figure 4.5 (continued) (H) Mean sea surface dye concentrations upwind of aerosol sample #13.

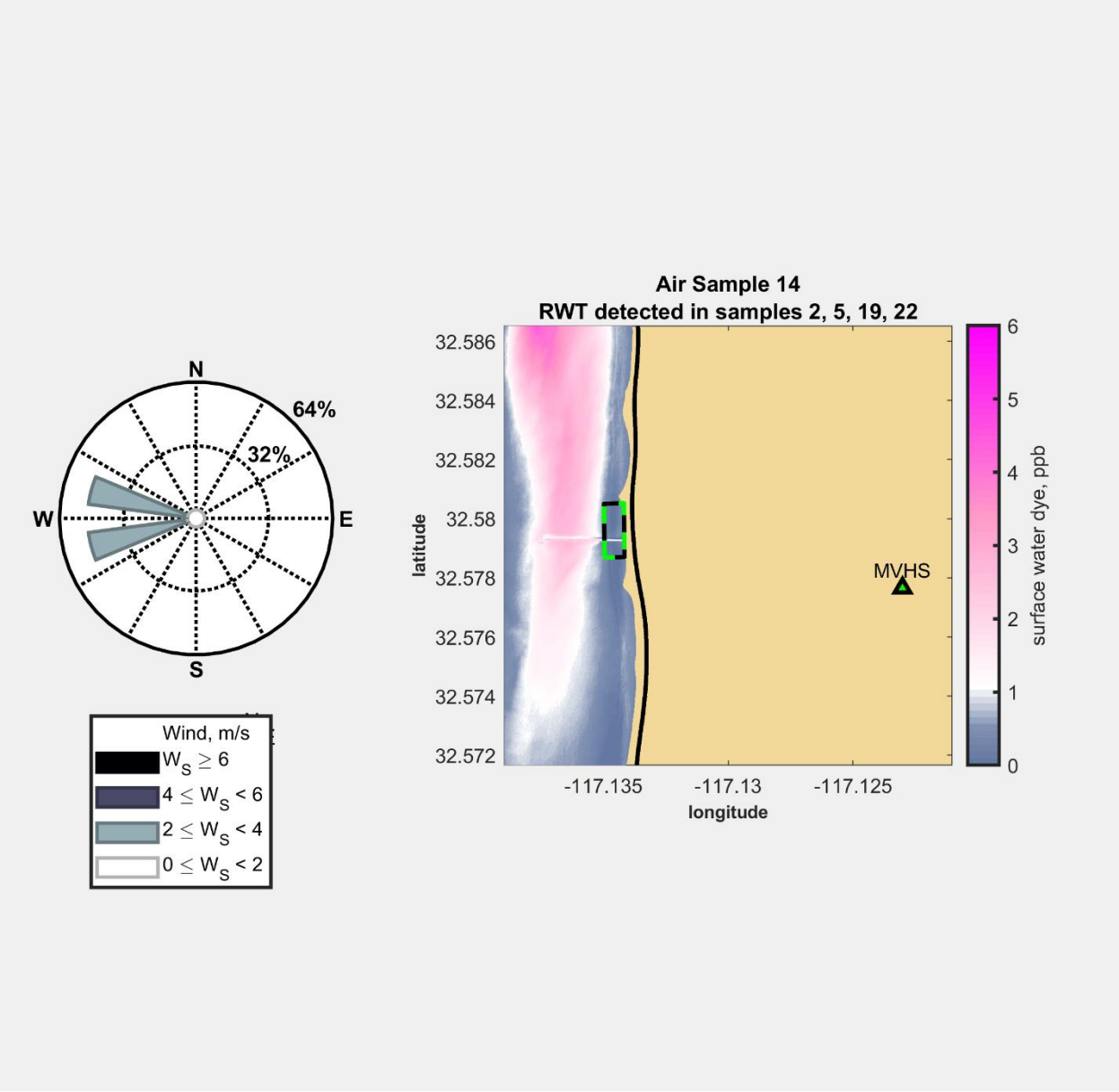

Figure 4.5 (continued) (I) Mean sea surface dye concentrations upwind of aerosol sample #14.

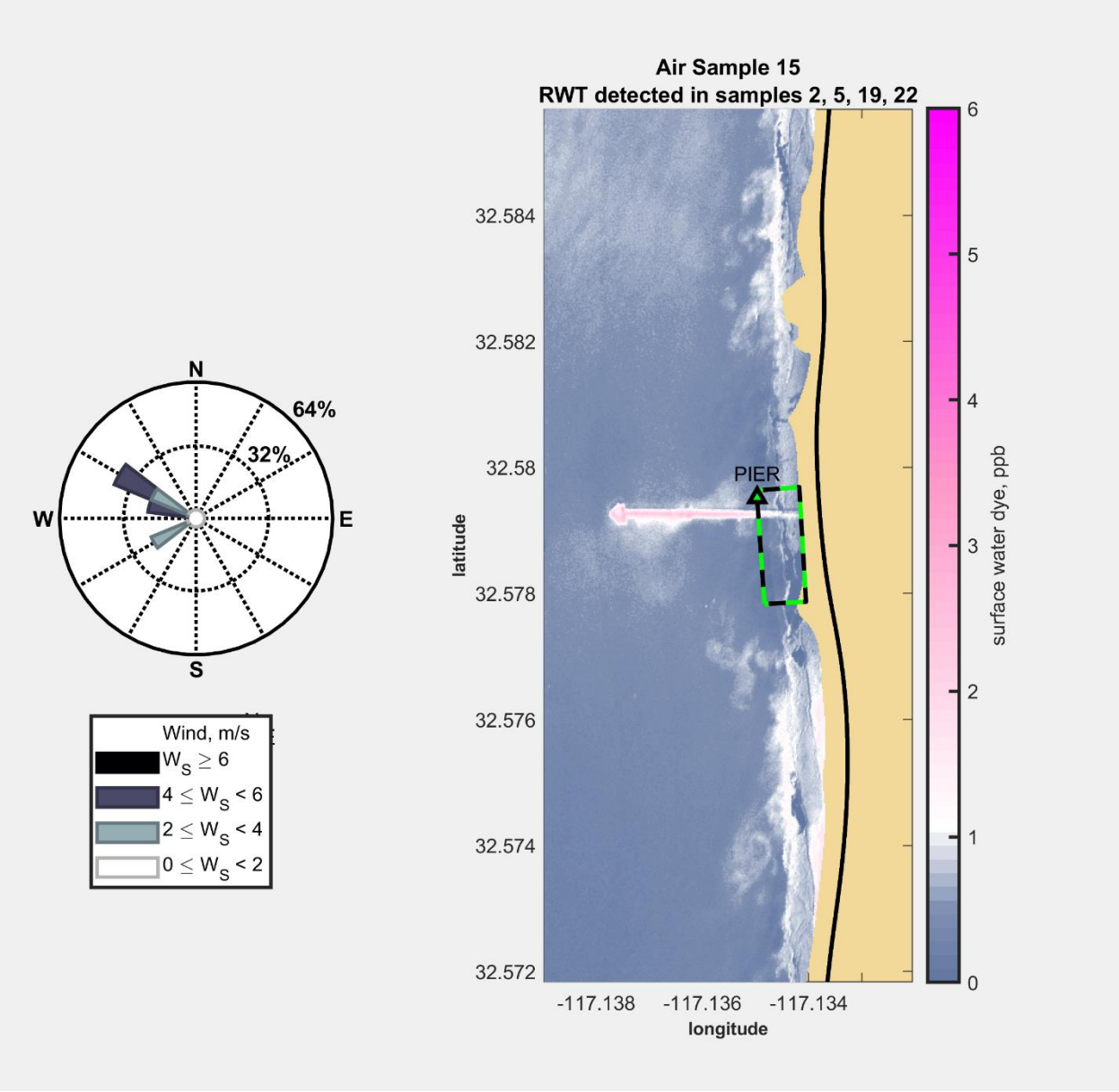

Figure 4.5 (continued) (J) Mean sea surface dye concentrations upwind of aerosol sample #15.

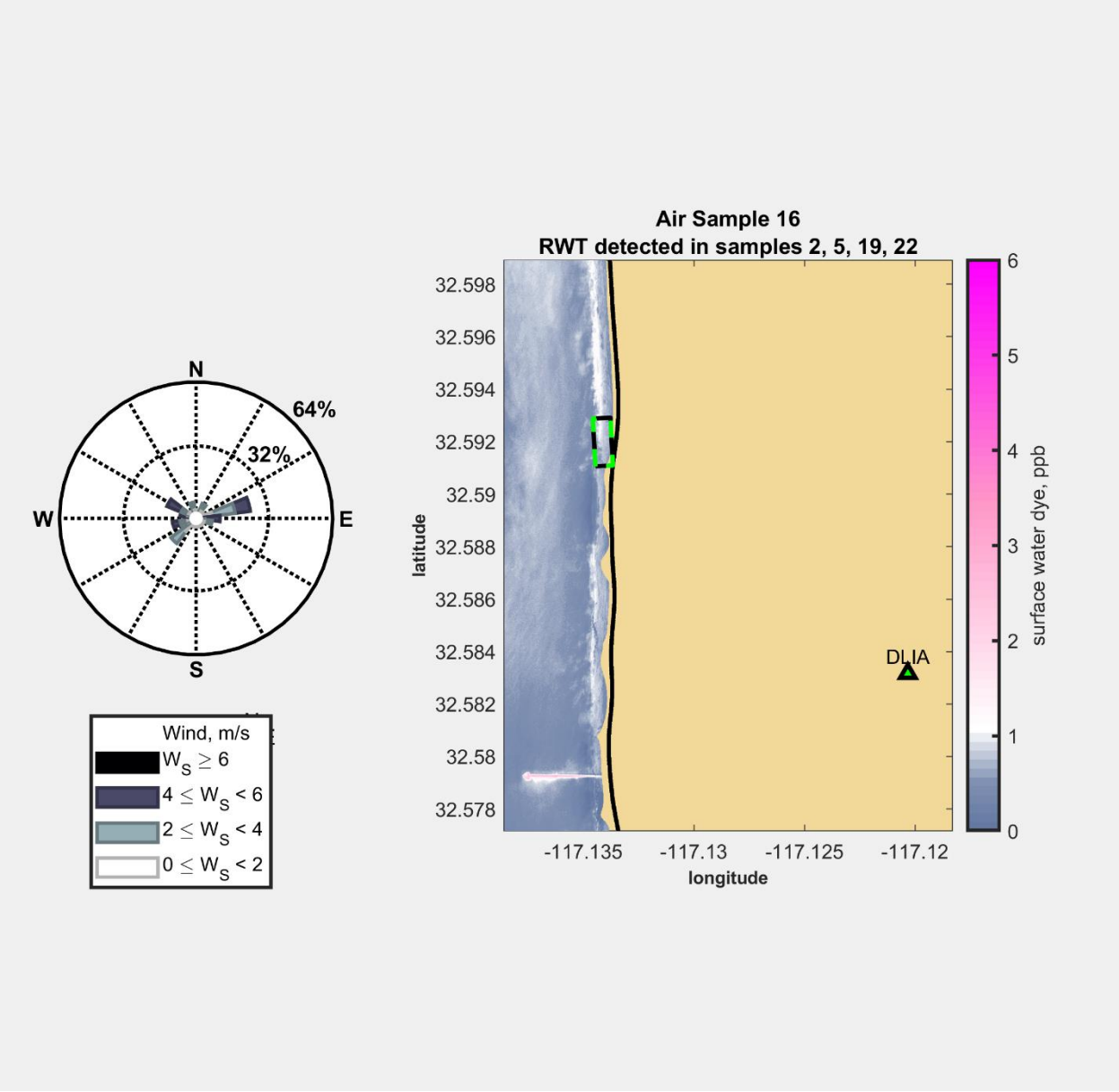

Figure 4.5 (continued) (K) Mean sea surface dye concentrations upwind of aerosol sample #16.

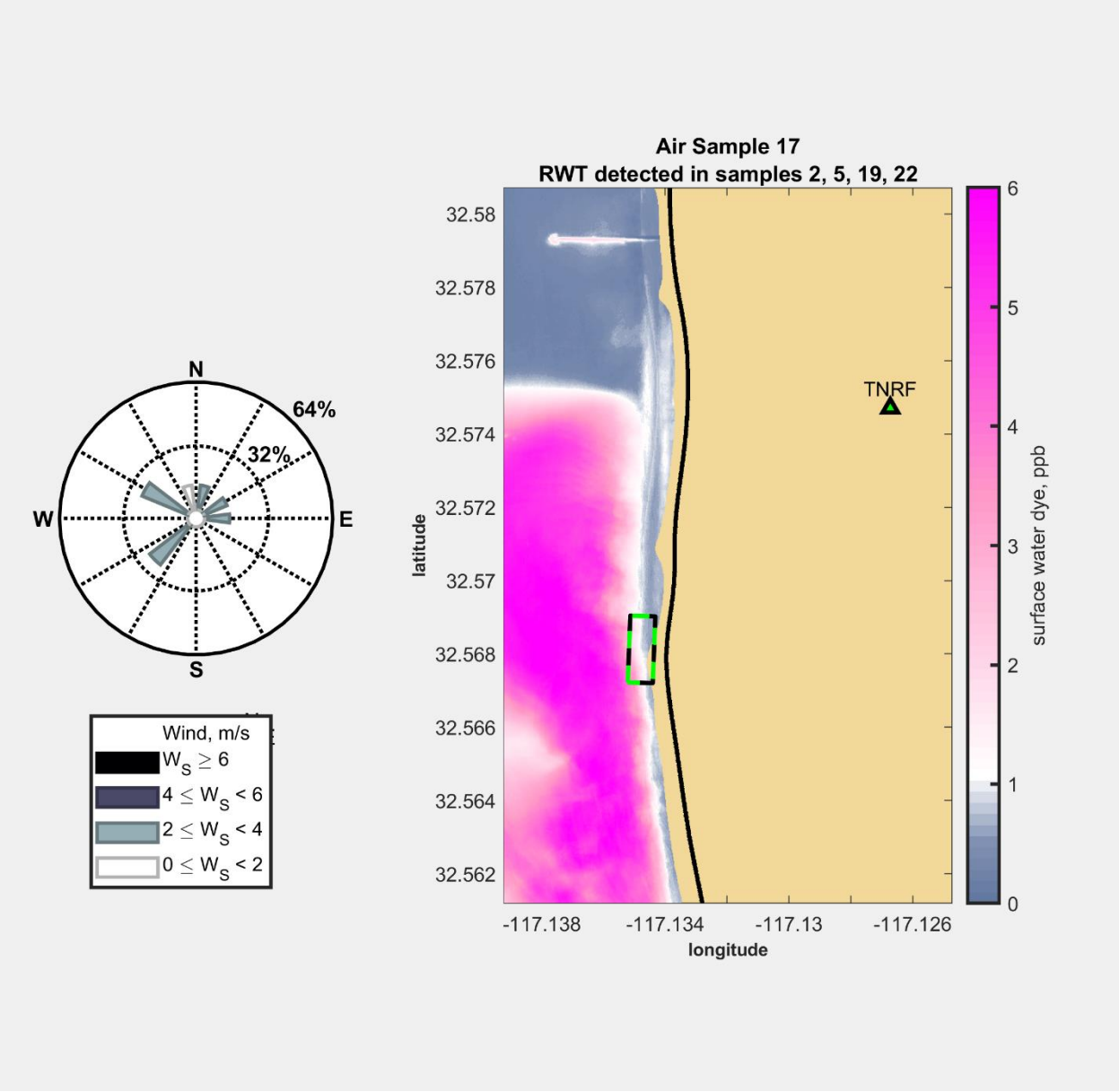

Figure 4.5 (continued) (L) Mean sea surface dye concentrations upwind of aerosol sample #17.

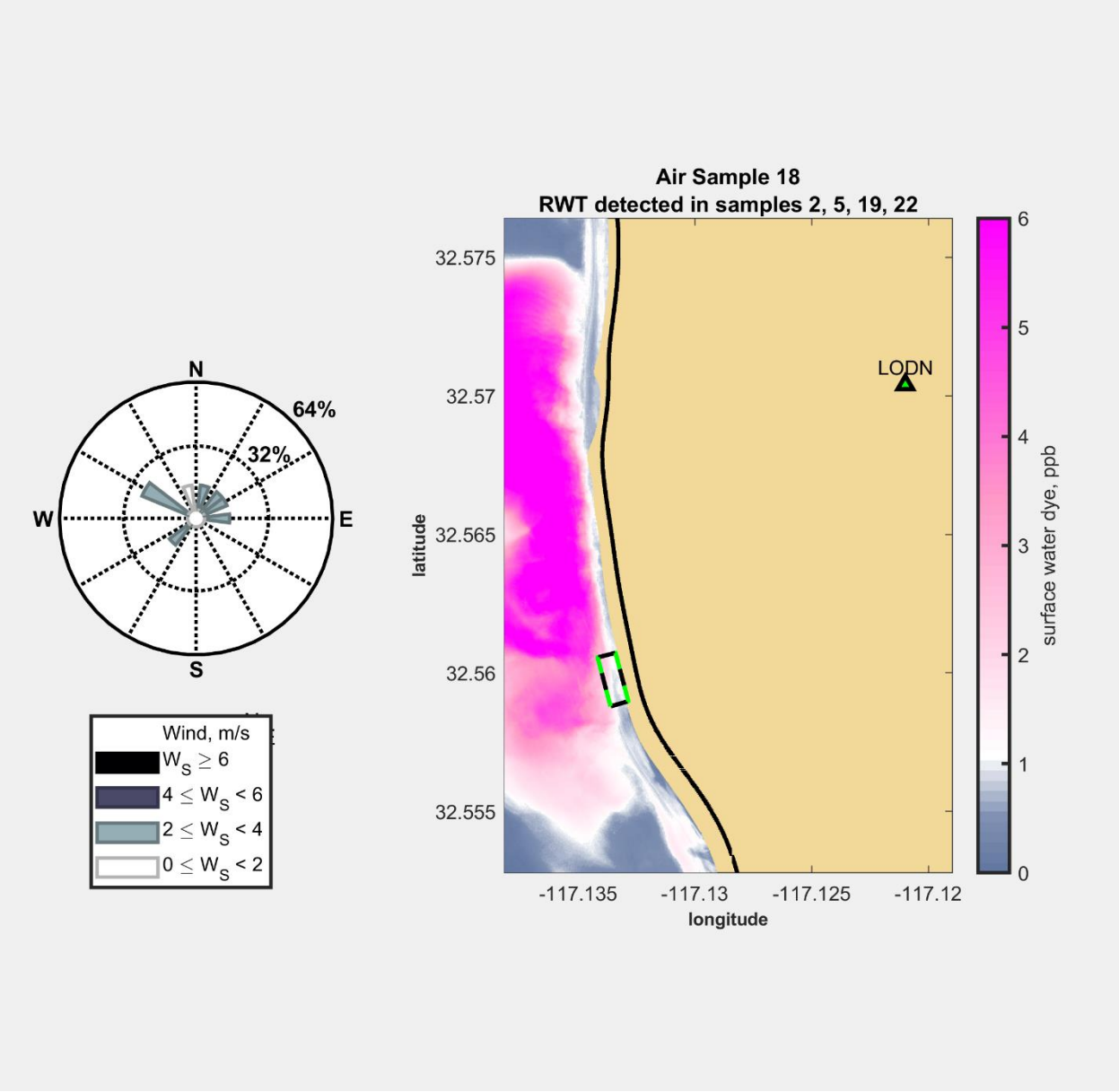

Figure 4.5 (continued) (M) Mean sea surface dye concentrations upwind of aerosol sample #18.

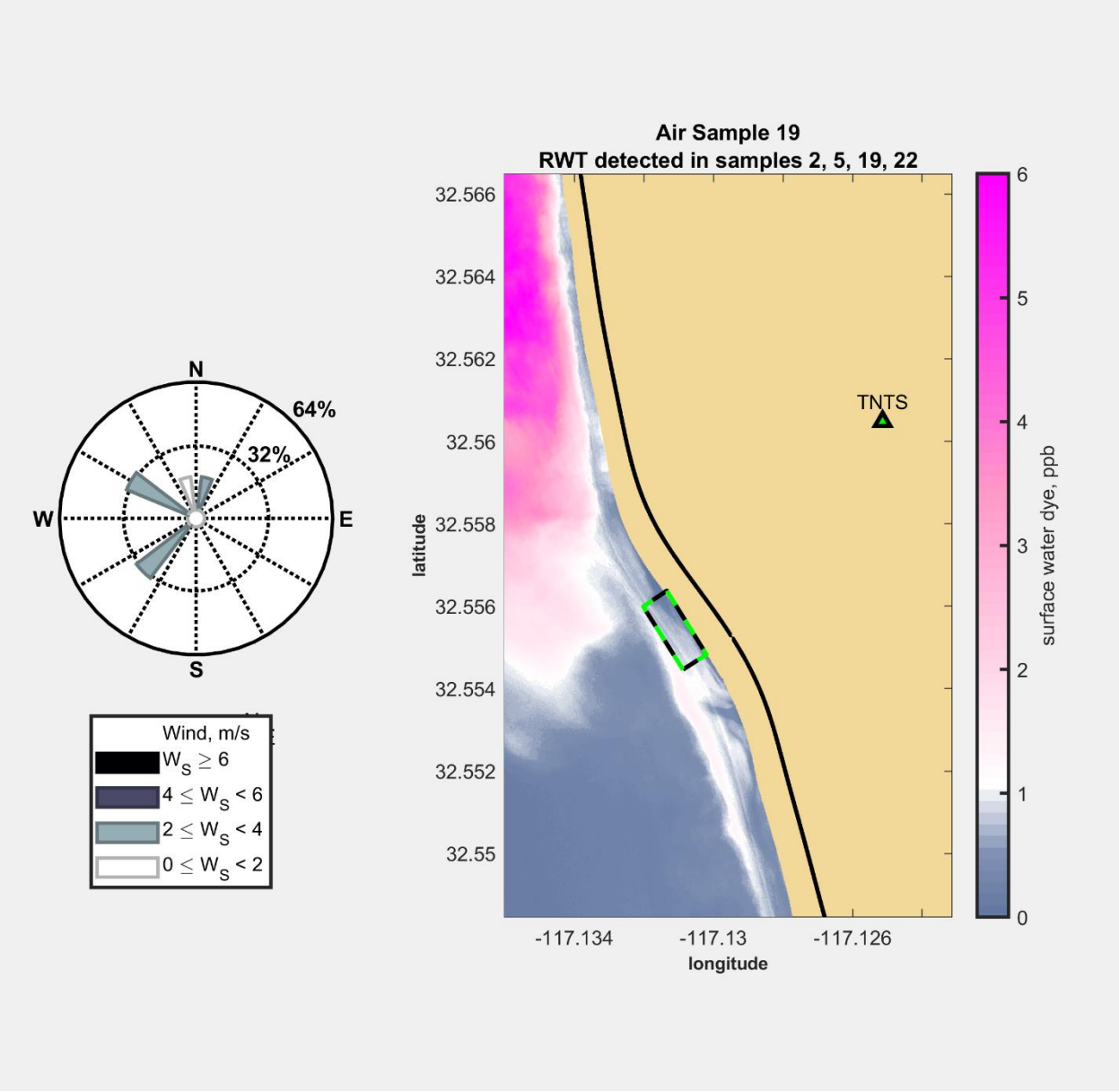

Figure 4.5 (continued) (N) Mean sea surface dye concentrations upwind of aerosol sample #19.

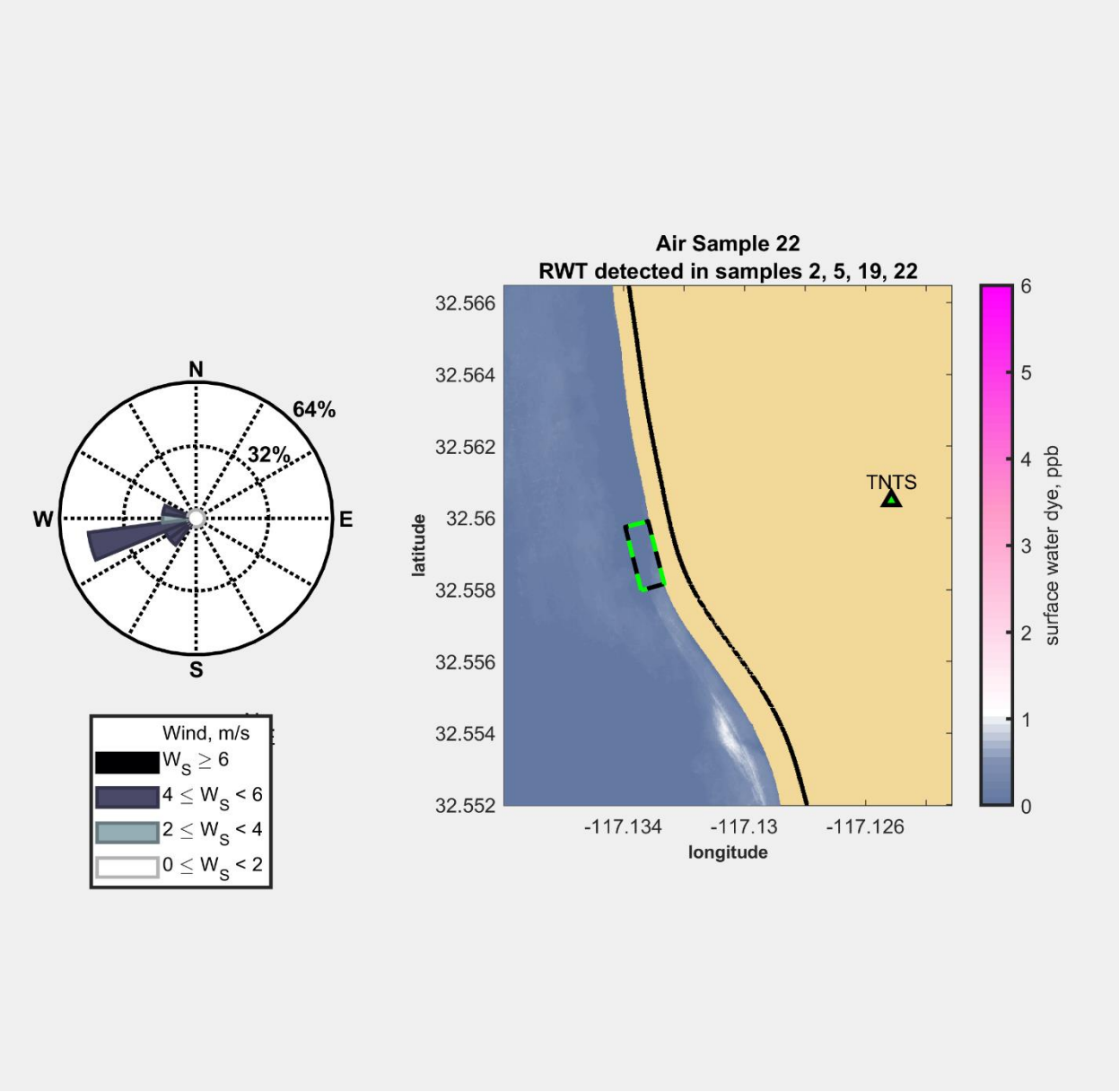

Figure 4.5 (continued) (O) Mean sea surface dye concentrations upwind of aerosol sample #22.

4.12 References

Aller, J.Y., Kuznetsova, M.R., Jahns, C.J., Kemp, P.F. (2005). The sea surface microlayer as a source of viral and bacterial enrichment in marine aerosols. *Journal of Aerosol Science*, 36(5–6), 801-812

Armbruster D.A., Pry, T. (2008). Limit of blank, limit of detection and limit of quantitation. *Clinical Biochemist Reviews*, 29(Suppl 1), S49-52.

Baylor, A.E.R., Baylor, M.B., Blanchard, D.C., Syzdek, L.D. (1977). Virus transfer from surf to wind. *Science*, 198(4317), 575-580

Boehm, A.B. (2003). Model of microbial transport and inactivation in the surf zone and application to field measurements of total coliform in Northern Orange County, California. *Environmental Science & Technology*, 37(24), 5511-5517

Bondy, A.L., Wang, B., Laskin, A., Craig, R.L., Nhliziyo, M.V., Bertman, S.B., Pratt, K.A., Shepson, P.B., Ault, A.P. (2017). Inland sea spray aerosol transport and incomplete chloride depletion: varying degrees of reactive processing observed during SOAS. *Environmental Science & Technology*, 51(17), 9533-9542

Brisebois, E., Veillette, M., Dion-Dupont, V., Lavoie, J., Corbeil, J., Culley, A., Duchaine, C. (2018). Human viral pathogens are pervasive in wastewater treatment center aerosols. *Journal of Environmental Sciences (China)*, 67(10), 45-53.

Carducci, A., Arrighi, S., Ruschi, A. (1995). Detection of coliphages and enteroviruses in sewage and aerosol from an activated sludge wastewater treatment plant. *Letters in Applied Microbiology*, 21(3), 207-209.

Cheng, Y.S., Zhou, Y., Irvin, C.M., Pierce, R.H., Naar, J., Backer, L.C., Fleming, L.E., Kirkpatrick, B., Baden, D.G. (2005). Characterization of marine aerosol for assessment of human exposure to brevetoxins. *Environmental Health Perspectives*, 113(5), 638-643.

Clark, D.B., Feddersen, F., Guza, R.T. (2010). Cross-shore surfzone tracer dispersion in an alongshore current. Journal of Geophysical Research: Oceans 115(10):1-18

Clark, D.B., Feddersen, F., Omand, M.M., Guza, R.T. (2009). Measuring fluorescent dye in the bubbly and sediment-laden surfzone. *Water, Air, and Soil Pollution*, 204(1–4), 103-115.

Clark, D.B., Lenain, L., Feddersen, F., Boss, E., Guza, R.T. (2014). Aerial imaging of fluorescent dye in the near shore. *Journal of Atmospheric and Oceanic Technology*, 31(6), 1410-1421

Clarke, A.D., Owens, S.R., Zhou, J. (2006). An ultrafine sea-salt flux from breaking waves: implications for cloud condensation nuclei in the remote marine atmosphere. *Journal of Geophysical Research Atmospheres*, 111(6), 1-14.

Cochran, R.E., Laskina, O., Trueblood, J.V., Estillore, A.D., Morris, H.S., Jayarathne, T., Sultana, C.M., Lee, C., Lin, P., Laskin, J., Laskin, A., Dowling, J.A., Qin, Z., Cappa, C.D., Bertram, T.H., Tivanski, A.V., Stone, E.A., Prather, K.A., Grassian. V.H. (2017). Molecular diversity of sea spray aerosol particles: impact of ocean biology on particle composition and hygroscopicity. *Chem*, 2(5), 655-667

Colwell, R.R. (1996). Global climate and infectious disease: the cholera paradigm. *Science*, 274(5295), 2025-2031.

County of San Diego Department of Environmental Health and Quality. (2017). Beach and Bay Water Quality Program. (accessed 1 January 2017).

de Leeuw, G., Neele, F.P., Hill, M., Smith, M.H., Vignati, E. (2000). Production of sea spray aerosol in the surf zone. *Journal of Geophysical Research*, 105(D24), 29397-29409

Dibble, S., Smith, J.E.. (2017). Massive Tijuana Sewage Spill That Polluted San Diego Beaches Part of Larger Problem. San Diego Union Tribune. (accessed 6 June 2018).

Dueker, M.E., O'Mullan, G.D. (2014). Aeration remediation of a polluted waterway increases near-surface coarse and culturable microbial aerosols. *Science of the Total Environment*, 478, 184-189.

Dueker, M.E., O'Mullan, G.D., Juhl, A.R., Weathers, K.C., Uriarte M. (2012). Local environmental pollution strongly influences culturable bacterial aerosols at an urban aquatic superfund site. *Environmental Science & Technology*, 46(20), 10926-10933.

Dwight, R.H., Caplan, J.S., Brinks, M.V., Catlin, S.N., Buescher, G., Semenza, J.C. (2011). Influence of variable precipitation on coastal water quality in Southern California. *Water Environment Research*, 83(12), 2121-2130

Fahlgren, C., Hagström, Å., Nilsson, D., Zweifel, U.L. (2010). Annual variations in the diversity, viability, and origin of airborne bacteria. *Applied and Environmental Microbiology*, 76(9), 3015-3025.

Fannin, K.F., Gannon, J.J., Cochran, K.W., Spendlove, J.C. (1977). Field studies on coliphages and coliforms as indicators of airborne animal viral contamination from wastewater treatment facilities. *Water Research*, 11(2), 181-188.

Feddersen, F., Olabarrieta, M., Guza, R.T., Winters, D., Raubenheimer, B., Elgar, S. (2016). Observations and modeling of a tidal inlet dye tracer plume. *Journal of Geophysical Research: Oceans*, 121(10), 7819-7844.

Fleming, L.E., Kirkpatrick, B., Backer, L.C., Walsh, C.J., Nierenberg, K., Clark, J., Reich, A., Hollenbeck, J., Benson, J., Cheng, Y.S., Naar, J., Pierce, R., Bourdelais, A.J., Abraham, W.M., Kirkpatrick, G., Zaias, J., Wanner, A., Mendes, E., Shalat, S., Hoagland, P., Stephan, W., Bean, J., Watkins, S., Clarke, T., Byrne, M., Baden, D.G. (2011). Review of Florida Red Tide and Human Health Effects. *Harmful Algae*, 10(2), 224-233. doi.org/10.1016/j.hal.2010.08.006.

Fong, T.-T., Lipp, E.K. (2005). Enteric viruses of humans and animals in aquatic environments: health risks, detection, and potential water quality assessment tools. *Microbiology and Molecular Biology Reviews*, 69(2), 357-371.

Fröhlich-Nowoisky, J., Kampf, C.J., Weber, B., Huffman, J.A., Pöhlker, C., Andreae, M.O., Lang-Yona, N., Burrows, S.M., Gunthe, S.S., Elbert, W., Su, H., Hoor, P., Thines, E., Hoffmann, T., Després, V.R., Pöschl, U. (2016). Bioaerosols in the earth system: climate, health, and ecosystem interactions. *Atmospheric Research*, 182, 346-376.

Gantt, B., Meskhidze, N. (2013). The physical and chemical characteristics of marine primary organic aerosol: a review. *Atmospheric Chemistry and Physics*, 13(8), 3979-3996.

Gersberg, R.M., Rose, M.A., Robles-Sikisaka, R., Dhar, A.K. (2006). Quantitative detection of hepatitis a virus and enteroviruses near the United States-Mexico border and correlation with levels of fecal indicator bacteria. *Applied and Environmental Microbiology*, 72(12), 7438-7444.

Graham, K.E., Prussin, A.J., Marr, L.C., Sassoubre, L.M., Boehm, A.B. (2018). Microbial community structure of sea spray aerosols at three California beaches. *FEMS Microbiology Ecology*, 94(3), 1-10.

Grant, S.B., Kim, J.H., Jones, B.H., Jenkins, S.A., Wasyl, J., Cudaback, C. (2005). Surf zone entrainment, along-shore transport, and human health implications of pollution from tidal outlets. *Journal of Geophysical Research C: Oceans*, 110(10), 1-20.

Griffin, D.W., Donaldson, K.A., Paul, J.H., Rose, B., Griffin, D.W., Donaldson, K.A., Paul, J.H., Rose, J.B. (2003). Pathogenic human viruses in coastal waters. *American Society for Microbiology*, 16(1), 129-143.

Grimes, D.J., Feddersen, F., Giddings, S.N., Pawlak, G. (2020). Cross-shore deformation of a surfzone released dye plume by an internal tide on the inner-shelf. *Journal of Physical Oceanography*, 50(1), 35-54.

Halpern, B.S., Longo, C., Hardy, D., McLeod, K.L., Samhouri, J.F., Katona, S.K., Kleisner, K., Lester, S.E., O'Leary, J., Ranelletti, M., Rosenberg, A.A., Scarborough, C., Selig, E.R., Best, B.D., Brumbaugh, D.R., Chapin, F.S., Crowder, L.B., Daly, K.L., Doney, S.C., Elfes, F., Fogarty, M.J., Gaines, S.D., Jacobsen, K.I., Karrer, L.B., Leselie, H.M., Neeley, E., Pauly, D., Polasky, S., Ris, B., St Martin, K., Stone, G.S., Sumalia, U.R., Zeller, D.

(2012). An index to assess the health and benefits of the global ocean. *Nature*, 488(7413), 615–620.

Hawkins, L.N., Russell, L.M. (2010). Polysaccharides, proteins, and phytoplankton fragments: four chemically distinct types of marine primary organic aerosol classified by single particle spectromicroscopy. *Advances in Meteorology*, 3642, 1-14.

Hernandez, D. (2017). 143 Million Gallons of Sewage Spill into Tijuana River. San Diego Union Tribune. (accessed 6 June 2018).

Hutchinson, T.H., Lyons, B.P., Thain, J.E., Law, R.J. (2013). Evaluating legacy contaminants and emerging chemicals in marine environments using adverse outcome pathways and biological effects-directed analysis. *Marine Pollution Bulletin*, 74(2), 517-525.

Kirkpatrick, B., Pierce, R., Cheng, Y.S., Henry, M.S., Blum, P., Osborn, S., Nierenberg, K., Pederson, B.A., Fleming, L.E., Reich, A., Naar, J., Kirkpatrick, G., Backer, L.C., Baden, D. (2010). Inland transport of aerosolized Florida red tide toxins. *Harmful Algae*, 9(2), 186-189.

Kuznetsova, M., Lee, C., Aller, J. (2005). Characterization of the proteinaceous matter in marine aerosols. *Marine Chemistry*, 96(3–4), 359-377.

Ladino, L.A., Raga, G.B., Alvarez-Ospina, H., Andino-Enríquez, M.A., Rosas, I., Martínez, L., Salinas, E., Miranda, J., Ramírez-Díaz, Z., Figueroa, Chou, C., Bertram, A.K., Quintana, E.T., Maldonado, L.A., Garcia-Reynoso, A., Si, M., Irish, V.E. (2019). Ice-nucleating particles in a coastal tropical site. *Atmospheric Chemistry and Physics*, 19(9), 6147-6165.

Lawaetz, A.J., Stedmon, C.A. (2009). Fluorescence intensity calibration using the Raman Scatter Peak of Water. *Applied Spectroscopy*, 63(8), 936-940.

Lenain, L., Melville, W.K. (2017). Evidence of sea-state dependence of aerosol concentration in the marine atmospheric boundary layer. *Journal of Physical Oceanography*, 47(1), 69-84.

Lewis, E.R., Schwartz, S.E. (2004). Sea salt aerosol production: mechanisms, methods, measurements and models - a critical review. Washington D.C.: American Geophysical Union.

Li, P., Li, L., Yang, K., Zheng, T., Liu, J., Wang, Y. (2021). Characteristics of microbial aerosol particles dispersed downwind from rural sanitation facilities: size distribution, source tracking, and exposure risk. *Environmental Research*, 195, 110798.

Li, M., Qi, J., Zhang, H., Huang, S., Li, L., Gao, D. (2011). Concentration and size distribution of bioaerosols in an outdoor environment in the Qingdao Coastal Region. *Science of the Total Environment*, 409(19), 3812-3819.

Lodder, W., de Roda Husman, A.M. (2020). SARS-CoV-2 in wastewater: potential health risk, but also data source. *The Lancet Gastroenterology and Hepatology*, 5(6), 533-534.

Mackay, D., Shiu, W.Y. (1981). A critical review of Henry's Law constants for chemicals of environmental interest. *Journal of Physical Chemistry*, 10(4), 1175.

Malakootian, M., Radhakrishna, N., Mazandarany, M.P., Hossaini, H. (2013). Bacterial-aerosol emission from wastewater treatment plant. *Desalination and Water Treatment*, 51(22–24), 4478-4488.

Melville, W.K., Lenain, L., Cayan, D.R., Kahru, M., Kleissl, J.P., Linden, P.F., Statom, N.M. (2016). The modular aerial sensing system. *Journal of Atmospheric and Oceanic Technology*, 33(6), 1169-1184.

Michaud, J.M., Thompson, L.R., Kaul, D., Espinoza, J.L., Richter, R.A., Xu, Z.Z., Lee, C., Pham, K.M., Beall, C.M., Malfatti, F., Azam, F., Knight, R., Burkart, M.D., Dupont, C. L., Prather, K.A. (2018). Taxon-specific aerosolization of bacteria and viruses in an experimental ocean-atmosphere mesocosm. *Nature Communications*, 9(1), 2017.

Montero, A., Dueker, M.E., O'Mullan, G.D. (2016). Culturable bioaerosols along an urban waterfront are primarily associated with coarse particles. *PeerJ*, 2016(12), 1-18.

Munn, C. (2011). Marine microbiology: ecology and applications. New York: Taylor & Francis.

Murphy, K.R. (2011). A note on determining the extent of the water Raman Peak in Fluorescence Spectroscopy. *Applied Spectroscopy*, 65(2), 233-236.

National Oceanic and Atmospheric Administration. (2016). Bioeffects Program. National Centers for Coastal Ocean Science. (accessed 1 January 2017).

O'Mullan, G.D., Dueker, E.M., Juhl, A.R. (2017). Challenges to managing microbial fecal pollution in coastal environments: extra-enteric ecology and microbial exchange among water, sediment, and air. *Current Pollution Reports*, 3(1), 1-16.

Patterson, J.P., Collins, D.B., Michaud, J.M., Axson, J.L., Sultana, C.M., Moser, T., Dommer, A. C., Conner, J., Grassian, V.H., Stokes, M.D., Deane, G.B., Evans, J.E., Burkart, M.D., Prather, K.A., Gianneschi, N.C. (2016). Sea spray aerosol structure and composition using cryogenic transmission electron microscopy. *ACS Central Science*, 2(1), 40–47.

Pickup, R.W., Rhodes, G., Arnott, S., Sidi-Boumedine, K., Bull, T.J., Weightman, A., Hurley, M., Hermon-Taylor, J. (2005). Mycobacterium avium subsp. paratuberculosis in the catchment area and water of the River Taff in South Wales, United Kingdom, and its potential relationship to clustering of Crohn's Disease cases in the City of Cardiff. *Applied and Environmental Microbiology*, 71(4), 2130-2139.

Pierce, R.H., Henry, M.S., Blum, P.C., Lyons, J., Cheng, Y.S., Yazzie, D., Zhou, Y. (2003). Brevetoxin concentrations in marine aerosol. Human Exposure Levels During a Karenia Brevis Harmful Algal Bloom. *Bulletin of Environmental Contamination and Toxicology*, 70(1), 161-165.

Prospero, J.M., Blades, E., Mathison, G., Naidu, R. (2005). Interhemispheric transport of viable fungi and bacteria from Africa to the Caribbean with soil dust. *Aerobiologia*, 21(1), 1-19.

Quinn, P.K., Collins, D.B., Grassian, V.H., Prather, K.A., Bates, T.S. (2015). Chemistry and related properties of freshly emitted sea spray aerosol. *Chemical Reviews*, 115(10), 4383-4399.

Rodriguez, A.R., Giddings, S.N., Kumar, N. (2018). Impacts of nearshore wave-current interaction on transport and mixing of small-scale buoyant plumes. *Geophysical Research Letters*, 45(16), 8379-8389.

Schiff, G., Stefanovic, G., Young, E., Pennekamp, J.K. (1983). Determination of Minimal Infectious Dose of an Enterovirus in Drinking Water. U.S. Environmental Protection Agency, Washington, D.C., EPA/600/1-83/004.

Shaffer, B.T., Lighthart, B. (1997). Survey of culturable airborne bacteria at four diverse locations in Oregon: urban, rural, forest, and coastal. *Microbial Ecology*, 34(3), 167-177.

Shuval, H. (2003). Estimating the global burden of thalassogenic diseases: human infectious diseases caused by wastewater pollution of the marine environment. *Journal of Water and Health*, 1(2), 53-64.

Smart, P.L., Laidlaw, I.M.S. (1977). An evaluation of some fluorescent dyes for water tracing. *Water Resources Research*, 13(1), 15-33.

Smith, D.J., Jaffe, D.A., Birmele, M.N., Griffin, D.W., Schuerger, A.C., Hee, J., Roberts, M.S. (2012). Free tropospheric transport of microorganisms from Asia to North America. *Microbial Ecology*, 64(4), 973-985.

Smith, D.J., Timonen, H.J., Jaffe, D.A., Griffin, D.W., Birmele, M.N., Perry, K.D., Ward, P.D., Roberts, M.S. (2013). Intercontinental dispersal of bacteria and archaea by transpacific winds. *Applied and Environmental Microbiology*, 79(4), 1134-1139.

Steele, J.A., Blackwood, A.D., Griffith, J.F., Noble, R.T., Schiff, K.C. (2018). Quantification of pathogens and markers of fecal contamination during storm events along popular surfing beaches in San Diego, California. *Water Research*, 136(2), 137-149.

Suijlen, J.M., Buyse, J.J. (1994). Potentials of photolytic rhodamine WT as a large-scale water tracer assessed in a long-term experiment in the Loosdrecht Lakes. *Limnology and Oceanography*, 39(6), 1411-1423.

Teltsch, B., Katzenelson, E. (1978). Airborne enteric bacteria and viruses from spray irrigation with wastewater. *Applied and Environmental Microbiology*, 35(2), 290-296.

Urbano, R., Palenik, B., Gaston, C.J., Prather, K.A. (2011). Detection and phylogenetic analysis of coastal bioaerosols using culture dependent and independent techniques. *Biogeosciences*, 8(2), 301-309.

U.S. Comission on Ocean Policy. (2004). An Ocean Blueprint for the 21st Century. Final Report.

United States Environmental Protection Agency. 2014. Toxic and Priority Pollutants Under the Clean Water Act. (accessed 1 January 2017)

van Eijk, A.M.J., Kusmierczyk-Michulec, J.T., Francius, M.J., Tedeschi, G., Piazzola, J., Merrittm D.L., Fontana, J.D. (2011). Sea-spray aerosol particles generated in the surf zone. *Journal of Geophysical Research Atmospheres*, 116(19), 1-20.

Wilson, J.F., Cobb, E.D., Kilpatrick, F.A. (1986). Fluorometric Procedures for Dye Tracing. In: U.S. Geological Survey, Techniques of Water-Resources Investigations, 03-A12. Washington D.C.: US Government Printing Office.

Wu, X., Feddersen, F., Giddings, S.N., Kumar, N., Gopalakrishnan, G. (2020). Mechanisms of mid-to outer-shelf transport of shoreline-released tracers. *Journal of Physical Oceanography*, 50(7), 1813-1837.

Yooseph, S., Andrews-Pfannkoch, C., Tenney, A., McQuaid, J., Williamson, S., Thiagarajan, M., Brami, D., Zeigler-Allen, L., Hoffman, J., Goll, J.B., Fadrosh, D., Glass, J., Adams, M.D., Friedman, R., Venter, J.C. (2013). A metagenomic framework for the study of airborne microbial communities. *PLoS One*, 8(12), e81862.

Chapter 5. Bacterial and Chemical Evidence of Coastal Water Pollution from the Tijuana River in Sea Spray Aerosol

5.1 Abstract

Roughly half of the human population lives near the coast and coastal water pollution is widespread. Coastal waters along Tijuana, Mexico and Imperial Beach, USA are frequently polluted by millions of gallons of untreated sewage and stormwater runoff. These waters are often closed to human contact, but CWP has the potential to reach many people on land via transfer in sea spray aerosol. Using 16S rRNA gene amplicon sequencing, we found sewage associated bacteria in the polluted Tijuana River flowing into coastal waters and returning in marine aerosol. Tentative chemical identification from non-targeted tandem mass spectrometry identified anthropogenic compounds as chemical indicators of aerosolized CWP. These compounds were found in the same aerosol populations as our tracer bacteria, but were ubiquitous and present in highest concentrations in continental aerosol. Bacteria proved to be more effective tracers of airborne CWP, and our 40 tracer bacteria comprised up to 76% of the airborne bacteria community in Imperial Beach air. These findings confirm that CWP transfers in SSA and can reach many people along the coast. Our changing climate may exacerbate CWP with more extreme storms and our findings call for minimizing CWP and investigating the health effects of airborne exposure.

5.2 Introduction

A Coastal water pollution (CWP) is an ever-growing global environmental problem and public health threat. Over one hundred thousand cases of illness and tens of thousands of deaths occur annually worldwide due to people entering contaminated waters or eating tainted seafood (Shuval, 2003). Swimming and surfing in polluted waters increases the incidence of multiple

types of illness (Arnold et al., 2017; Haile et al., 1999). Untreated sewage and stormwater runoff are common causes of CWP. Oils, fuels, metals, plastics, drugs, insecticides, detergents, solvents, and fire retardants are common chemical contaminants (Kolpin et al., 2002; Petras et al., 2021). Escherichia coli (E. coli) and Enterococcus spp. are bacteria used as sewage indicators, whereas enteroviruses, human norovirus, hepatitis A virus, and SARS-CoV2 are actual pathogens found in sewage contaminated waters (Griffin et al., 2003; Gersberg et al., 2006; Boehm et al., 2009; Rocha et al., 2022). Pathogens in coastal waters pose an immediate health threat because illness can occur from a single exposure (Shuval, 2003; Griffin, 2003).

CWP at the Mexico-USA border between Tijuana (TJ), Mexico and Imperial Beach (IB), USA has persisted for decades and has been officially declared a state of emergency (Gersberg et al. 2006; Council Resolution R-2022-79; Orozco-Borbon et al., 2006). Whereas fecal and chemical pollution from stormwater runoff have been detected at various beaches in SD, there is persistent and severe CWP at IB and TJ (Petras et al., 2021; Gersberg et al., 2006; Steele et al., 2018; Orozco-Borbon et al., 2006). Rains and inadequate infrastructure result in untreated sewage flowing into TJ-IB coastal waters. Hepatitis A virus and bacteria from TJ sewage have been detected in IB coastal waters 7,12. The Tijuana River (TJR) is a major pollution conduit that sends 100-million-gallon sewage spills into South IB coastal waters 12,13,72. SARS-CoV-2 has been detected in TJR waters at concentrations matching those at wastewater treatment plants (Rocha et al., 2022). These problems caused IB beaches to be closed to water contact for 295 days in 2020 (Smith & Fry, 2021). This problem will likely persist after implementation of planned infrastructure due to multiple sources and continued diversion of high flow stormwater and sewage directly to the ocean (Feddersen et al., 2021). Climate change is expected to cause

more extreme precipitation events, which may further exacerbate the problem (Curriero et al., 2001).

CWP has the potential to transfer to the atmosphere in sea spray aerosol (SSA) and reach people on land through airborne transport (Pendergraft et al., 2021). SSA is formed by breaking waves and bursting bubbles that eject microscopic seawater aerosol into the atmosphere, ranging in size from tens of nanometers to tens of microns (Lewis & Schwartz, 2004). SSA contains diverse chemical compounds and microorganisms from the source waters, including bacteria (~1 μm diameter) and viruses (~0.1 μm diameter) (Baylor et al., 1977; Quinn et al., 2015). Microbes and chemical compounds can become greatly enriched in SSA by bubble scavenging and bursting through the ocean's surface microlayer (Blanchard et al., 1970; Aller et al., 2005; Wurl et al., 2011). Once in the atmosphere, SSA can travel hundreds of kilometers 17. Prior research used a tracer dye to demonstrate the transfer of CWP in SSA 16. Here we present evidence from non-targeted tandem mass spectrometry and 16S amplicon sequencing of CWP transferring to the atmosphere in SSA.

5.3 Materials and Methods

5.3.1 Sampling

To investigate airborne transport of CWP, we sampled coastal water and aerosol in IB and at Scripps Institution of Oceanography (SIO) in five sampling rounds (SR) following rain events from January to May of 2019 (Figs. 5.1, 5.2). We chose IB for its frequent and severe water quality issues, and SIO served as a reference site. Coastal water quality at both IB and SIO can be impacted by stormwater runoff, so by comparing IB to SIO we investigate signs of CWP that are above common levels for the region 10. We collected coastal water daily from the West (seaward) ends of the IB and SIO piers (IBPw & SIOPw, SR 1-5, Fig. 5.1), into acid cleaned

buckets and bottles. CWP is transported by ocean currents and is a challenge to sample (Wu et al., 2021). We overcame this by directly sampling the TJR (TJRw in Fig. 5.1; SR 2-5), which was actively flowing into IB coastal waters throughout the study (Fig. 5.2) and is a major pathway of CWP in the area (Zimmer-Faust et al., 2021; Rocha et al., 2022; Hernandez, 2017).

Coastal aerosol was sampled at one location each day in IB during SR 1-4 and at SIO for SR 5. Aerosol was sampled at two locations along the IB coast: from a second floor deck at the Dempsey Holder Safety Center (IBSCa, SR 1-2), at an elevation of 5 m above sea level (MASL) and 50 m from the shoreline; and at Border Field State Park (IBBFa, SR 3-4) at 20 MASL and 100 m from the shoreline (Fig. 5.1). Aerosol was sampled at SIO near the East (landward) end of the Ellen Browning Scripps Memorial Pier at SIO (SIOPa, Fig. 5.1). IBSCa, IBBFa, and SIOPa lie 3 km North, 2 km South, and 37 km North of the Tijuana River mouth, respectively (Fig. 5.1). During typical onshore winds, all aerosol sampling sites were downwind of an active surfzone with abundant wave breaking, an important source of SSA (van Eijk, 2011). We also observed whitecaps in the local coastal waters on multiple occasions and they were an additional source of local SSA. Aerosol (total suspended particles) was collected in triplicate onto 47 mm quartz fiber filters in filter holders (2500 QAT-UP & 2220, Pall Corporation, New York) at 30 liters per minute (lpm) for 22 hours. To minimize contamination, filters were combusted at 500°C for 2 hours prior to sampling and stored in combusted aluminum foil before deployment and after recovery. Laboratory blanks were combusted filters; field blanks were filters taken into the field, placed into filter holders, and then immediately removed. Across five rounds of sampling, we sampled coastal waters on 26 days and coastal aerosol for 21 one-day periods.

5.3.2 Non-targeted Chemical and Microbial Analyses

Aerosol and water samples were analyzed using liquid chromatography high-resolution tandem mass spectrometry (LC-MS/MS) to identify chemical species and 16S rRNA gene amplicon sequencing (16S) to identify bacteria taxa. Detailed methods are provided in the Supplementary Methods. LC-MS/MS was acquired as described before (Petras et al., 2021; Cancelada et al., 2022). To apply the method to aerosol samples, one 47 mm aerosol filter was extracted with 0.5 ml of methanol followed by 2 ml of ultrapure water and sonication. Filter extracts and seawater samples were desalted via solid phase extraction (SPE), followed by chromatographic separation with a C18 reversed phase column, then two technical replicates were analyzed with a Q-Exactive quadrupole orbitrap mass spectrometer (Thermo Fisher Scientific, Bremen, Germany) in top5 data dependent acquisition mode. For 16S, ¼ of an aerosol filter or 400 μl of a water sample was extracted and sequenced using the KatharoSeq method for low biomass samples (Minich et al., 2018).

5.3.3 Data Analysis

The 16S data were processed through the QIIME 2 workflow using Qiita 27,28. Processing with Deblur resulted in the identification of 7627 amplicon sequencing variants (ASVs) that were annotated using GreenGenes (McDonald et al., 2012; Amir et al., 2017). For simplicity we refer to the ASVs as bacteria. The LC-MS/MS data were processed using MZMine2 and the Global Natural Products Social Molecular Networking (GNPS) ion identity networking workflow, producing 16822 chemical features (Schmid et al., 2021). 2028 Level 2 compound annotations were determined from matches to mass spectral libraries, yielding an annotation rate of 0.12 (Sumner et al., 2007; Schymanski et al., 2014). Mass spectra were matched against the GNPS and NIS17 libraries using a minimum cosine score of 0.7 to define spectral similarity. Precursor and Fragment Ion Mass Tolerances were set to 0.01 Da, Minimum

Matched Fragment Ions was set to 4, and Minimum Cluster Size was set to 1 (MS Cluster off). The maximum mass difference was set to 100 Da for Analog Search. The Level 2 annotations provide tentative compound identifications, but definite confirmation requires chemical standards.

SourceTracker2 (ST2) was employed to identify potential contributions to the aerosol from the sampled waters (Knights et al., 2011). ST2 is a Bayesian statistical method that assigns sources to sinks on a feature-by-feature basis. ST2 was run with the aerosol samples as sinks and the water samples as sources.

In order to assess if it was possible that the air masses we sampled contained SSA from the local waters, a local particle origin for each sampling period was derived from local winds and a particle dispersion model. We used FLEXPART version 9.0, a Lagrangian particle dispersion model that simulates the release of particles into the atmosphere and uses gridded wind speeds and directions to estimate transport forwards or backwards in time (Stohl, 2003; Stohl et al., 1998). Input data were the National Centers for Environmental Protection (NCEP) Climate Forecast System Version 2 (CFSv2) 6-hourly products. Data were accessed from the Research Data Archive (RDA) at the National Center for Atmospheric Research (NCAR) (https://rda.ucar.edu/datasets/ds094.0/?hash=access). The parameters selected were the FLEXPART Model Input: 1-hour to 6-hour Forecasts including wind speeds, temperature, planetary boundary layer height, pressure, pressure reduced to MSL, and relative humidity, on a 0.5° x 0.5° grid. We ran FLEXPART in back trajectory mode starting at the end of each aerosol sampling period and running back to 24 hr before the start of the sampling period, for a total of 46 hr, sufficient to evaluate whether the sampled air mass traveled over local waters or passed over land (Fig. 5.3). For each sampling period, 500 simulated particles were released from the

sampling site at an elevation of 5 m and transported backwards in time and space. Local particle origins (and aerosol samples) were classified as coming from the sea (IBa-sea; n=5) or from the land (IBa-land; n=5) when winds and back trajectories agreed on either; otherwise, mixed (IBa-mixed; n=7) was assigned (Fig. 5.3). A potential downside of sampling IBa from two locations on separate days is that atmospheric conditions were not identical: IBSCa sampling periods were 1 sea, 1 mixed, and 4 land; IBBFa periods were 4 sea, 6 mixed, and 1 land. Therefore, we do not compare the two IBa locations. Instead, we group the IBa data according to local particle origin and we target IBa-sea samples for signs of CWP in SSA. We assume the sampled aerosol includes SSA and non-SSA during sea and mixed periods, and we refer to the sea particle populations as coastal aerosol coming from the direction of the ocean. Land periods from both IBa locations characterize continental aerosol of the region and are used for comparison. Aerosol sampling at SIO (SIOPa) had 3 sea periods and one mixed (Fig. 5.3), and are used to compare against the IBa-sea and IBa-mixed samples.

5.3.4 Identifying Potential Tracers of CWP

The ST2 outputs and relative abundances were used to identify potential tracers of TJRw in the sampled aerosol. Features from LC-MS/MS (chemicals) and 16S (bacteria) were ranked from IBa-sea samples, which are most likely to contain the largest SSA:non-SSA ratio. Features were not selected from IBPw because they would not necessarily be pollution associated. In the ST2 source apportionments, for each feature in each IBa-sea sample, the SIOPw contribution was subtracted from the TJRw contribution, to prioritize features abundant in TJRw but not in SIOPw. These differences were then summed across the five IBa-sea samples to provide an initial ranking. Then we removed features that did not meet the following criteria based on estimated, relative abundance, using MS1 peak areas for LC-MS/MS and read counts for 16S: a)

TJRw > SIOPw; b) IBa-sea > SIOPa; and c) IBa-sea > blank. Criterion (a) was a check on the subtraction done in the ST2 tracer ranking to identify features associated with the TJRw; (b) removed features more abundant at our reference location; and (c) excluded sample contaminants. Mean values were used due to the small number of samples in each of these subsets. In the 16S data, criteria (a), (b), and (c) did not remove any of the top 40 bacteria from the initial ST2 ranking. This analysis was carried out using MATLAB version 9.10.0.1602886 (R2021a) (MATLAB, 2021).

5.4 Results and Discussion

5.4.1 Sample Types Differ in Chemical and Bacterial Compositions

For an initial evaluation of compositional similarities and differences across the sample types, we applied Robust Aitchinson principal component analysis (RPCA) to their chemical compositions and bacteria communities (Fig. 5.4 A, B). Samples that are closer together in RPCA space have more similar compositions than samples further apart 38. In both LC-MS/MS (Fig. 5.4 A) and 16S (Fig. 5.4 B) RPCA spaces, points plot along PC2 according to broad sample type: water or aerosol. IBPw groups with SIOPw and separates out from TJRw (Fig. 5.4 A, B), indicating that after entering IB coastal waters, TJRw did not travel North to substantially impact IBPw, although sampling the surfzone may have revealed TJRw influence there, due to alongshore transport specific to the surfzone (Rodriguez et al., 2018). PC1 appears to separate out samples according to chemical composition (Fig. 5.4 A) or bacteria community (Fig. 5.4 B), and IBa plots closer to TJRw, whereas SIOPa plots closer to ocean water.

5.4.2 IBa and TJRw Have Significant Compositional Similarities

The ST2 analysis indicates significant overlap in the chemical species and bacteria communities found in TJRw and IBa. Figure 5.4 C and D show the fractional contribution of

each source to each aerosol sample ST2 calculated from the chemical and bacterial compositions. According to ST2, up to 45% of the chemical composition (Fig. 5.4 C) and 82% of the bacteria community (Fig. 5.4 D) found in IBa came from TJRw, with much smaller TJRw values for SIOPa.

5.4.3 Bacteria Are Effective Tracers of Airborne CWP

Evaluation of the top 40 bacteria identified by our tracer selection criteria supports that most are effective tracers of airborne CWP. Although amplicon sequencing is not appropriate for absolute quantitation, we used 16S read counts to estimate and compare the relative abundance of each tracer bacterium across the different sample types, with a focus on local particle origin (Fig. 5.5). In each feature we look for a tracer pattern: TJRw > SIOPw, and IBa-sea > IBa-land, SIOPw, and the blanks (Figs. 5.5, 5.6). Although in a few cases IBa-sea < IBa-land (# 27) or IBa-sea ≈ IBa-land (#s 10, 15, 17), in general these 40 bacteria show strongest associations with TJRw and IBa-sea and we consider them tracers of the polluted TJRw in IBa (Fig. 5.5). We present these data as direct observation of bacteria in the polluted TJR flowing into coastal waters, transferring to the atmosphere in SSA, and returning in onshore winds.

5.4.4 Tracer Bacteria Taxonomies Link Them to Sewage

Although mere library matches to the GreenGenes database, the taxonomic identities of the tracer bacteria link 26 of them to sewage (Table 5.1) (McDonald et al., 2012). These taxa include bacteria attributed specifically to Tijuana sewage and sewage foam, and taxa containing pathogenic and antimicrobial resistant members (Table 5.1 and references within). The *genus Arcobacter* appears eight times in the list and contains members that are pathogens, resistant to antimicrobials, and/or commonly found in sewage and sewage contaminated waters (Ho et al., 2006; Fera et al., 2004; Collado et al., 2008). *Acinetobacter spp*. are found in hospital infections

and sewage, and are increasingly resistant to antibiotics (Zhang et al., 2009; Dijkshoorn et al., 2007). Fifteen of the 40 tracer bacteria are nonfermenting gram-negative bacilli (NFGNB), a group of bacteria that contains many pathogens (Wisplinghoff, 2017). The *Bacteroides genus* contains the most common gene marker for human fecal pollution, HF183 (Bernard & Field, 2000; Ahmed et al., 2016). *Acinetobacter spp*. and *Alkanindiges spp*. combined appear seven times in the list and are dominant in biofoam at wastewater treatment plants (Klein et al., 2007). Their hydrophobic cell surfaces may cause their enrichment in foam and preferential aerosolization, as previously observed for *Actinobacteria* in SSA (Weber et al., 1983; Michaud et al., 2018).

5.4.5 Tracer Bacteria Independently Linked to TJR and TJ Sewage

The bacteria communities of the TJR and a sewage outfall South of Tijuana were characterized with 16S amplicon sequencing the same year we sampled (Zimmer-Faust et al., 2021). The most abundant taxa were *Acidovorax*, *Bacteroides*, *Cloacibacterium*, *Comamonas*, *Macellibacteroides*, and the potentially pathogenic *genera Acinetobacter*, *Aeromonas*, and *Arcobacter*. Nineteen of our 40 tracer bacteria match these taxa via their GreenGenes assignments (Table 5.1), further supporting that these bacteria are effective tracers of TJ sewage aerosolized in SSA.

5.4.6 Chemical Links Between CWP and IB Aerosol in Onshore Winds

Applying the same feature ranking criteria to the LC-MS/MS data identified chemical links between CWP and IB aerosol in onshore winds. As done for the tracer bacteria, we evaluated the selected LC-MS/MS features by comparing relative abundance, from MS1 peak areas, for each feature across the different sample types, and looking for compounds that meet our tracer criteria: TJRw > SIOPw and IBa-sea > IBa-land, SIOPa, and blanks (Fig. 5.6). We

report the top 40 chemical species with annotations (Level 2), excluding likely misannotations (n=2), compounds that did not return clear search results (n=8), and polyethylene glycols, because they are common sample contaminants (Table 5.2). Although some compounds show a weak tracer signal (#s 2, 8, 12, 17), most compounds show IBa-sea ≈ SIOPa and IBa-sea < IBa-land (Fig. 5.6). This implies these compounds in IBa have marine and continental sources and, therefore, we do not consider them explicit tracers of TJRw pollution in SSA. But they are chemical links shared between CWP and coastal aerosol in onshore winds, and we use them to provide chemical information on the same aerosol populations that contained our tracer bacteria.

5.4.7 Anthropogenic Compounds Dominate Chemical Links

Tentative Level 2 annotations for most of the selected chemical links are anthropogenic compounds, indicating a polluted aerosol population (Table 5.2). Industrial chemicals are common in the list, including flame retardants, paints, solvents, plasticizers, cleaning products, and personal care products, as well as known irritants and common environmental pollutants. These compounds may have reached the TJR by direct discharge from industrial facilities or from urban-industrial stormwater runoff. Other chemical species are human associated and indicative of sewage, such as caffeine and vitamin K2. Monopalmitolein (9c), lumichrome, and 5(Z),8(Z),11(Z)-eicosatrienoic acid methyl ester are marine associated, indicative of SSA. We annotated 160 drugs, 21 drug metabolites, 179 food compounds, 15 food additives, 36 biocides, 487 natural products, and 6 compounds from personal care products in our LC-MS/MS dataset as Level 2 IDs (n=497; list provided at https://doi.org/10.6075/J07944V3) and tested them as tracers (Fig. 5.7) (Sumner et al., 2007). Aerosols from the land appear to be the dominant source for all of them, and drugs have previously been detected in urban aerosol (Postigo et al., 2009; Cecinato et al., 2009).

5.4.8 Evaluating Bacteria vs. Chemicals as Tracers

This study found bacteria to be more effective than chemicals at identifying signs of TJRw aerosolizing in SSA. The chemical and bacterial ST2 source apportionments significantly differed (Fig. 5.4 C, D), likely because bacteria are only found in larger aerosols, whereas chemical compounds are present in all aerosols (Santander et al., 2021; Shaffer et al., 1997). Larger aerosols have shorter residence times in the atmosphere, so the airborne bacteria community is strongly influenced by local sources. In our tracer evaluations the chemicals are more ubiquitous across the sample types compared to the bacteria (Figs. 5.5 & 5.6). IBa-land samples yielded much more total LC-MS/MS signal than IBa-sea and IBa-mixed samples (Fig. 5.8 A), limiting the utility of chemicals as tracers of TJRw in IBa. Greater molecular diversity and abundance in polluted/continental aerosol vs. non-polluted/marine aerosol has been previously observed (Papazian et al., 2022). Normalization of microbiome and mass spectrometry data is often used to correct for variations in total signal strength across samples (Weiss et al., 2017; Wulff et al., 2018). Here, normalizing to total 16S read counts or LC-MS/MS peak area per sample (Figs. 5.9 & 5.10) yielded more tracer signatures in the LC-MS/MS data, but we feel usage of non-normalized data is more appropriate for this study in order to include differences in the contributions of marine vs. continental aerosol to IBa (Fig. 5.8). In comparison, 16S read counts were similar across the IBa samples (Fig. 5.8 B), and cell counts, a better measure of bacteria amount, were higher in IBa-sea and IBa-mixed vs. IBa-land (Fig. 5.11), suggesting bacteria are particularly useful as tracers of SSA.

5.4.9 Results in Context

Our findings are in agreement with the ability of SSA to transfer diverse chemical compounds and microorganisms from the ocean to the atmosphere, including naturally occurring

toxins, like brevetoxin from red tides, and artificial toxins, like perfluoroalkyl acids (Quinn et al., 2015; Johansson et al., 2019; Pierce et al., 2003; Backer et al., 2005; Patterson et al., 2016). Aerosolization of sewage by aeration and bubble bursting has been observed at wastewater treatment plants (WWTPs), open wastewater canals, spray irrigation, and the aeration of polluted waters, but not by SSA (Fanin et al., 1977; Carducci et al., 1995; Malakootian et al., 2013; Brisebois et al., 2018; Ginn et al., 2021; Teltsch & Katznelson, 1978; Dueker & O'Mullan, 2014). Direct aerosolization from the TJR may occur, but it is likely to be a much smaller source than SSA from the surf zone, a significant aerosol source, and from whitecaps in local waters (van Eijk et al., 2011). TJR aerosol would have been downwind during IBa-sea samples but could have been a minor contribution to IBa-mixed and IBa-land samples. The sequencing of Central California coastal aerosol and SSA isolated in the laboratory identified taxa that contain pathogenic strains, but of unknown origin (Michaud et al., 2018; Graham et al., 2018). We build on this work by linking bacteria and compounds in coastal aerosol to a major CWP source.

5.4.10 Significant Contributions of Airborne Bacteria

To investigate the magnitude of CWP's contribution to coastal aerosol, we examined the individual and combined fractional abundance of our 40 selected bacteria in the aerosol samples (Fig. 5.12). Like Figure 5.5, the tracer bacteria are most abundant in IBa-sea and IBa-mixed samples, most of which were collected at IBBFa. These bacteria are highest in IBa-mixed periods possibly because they encountered the most ideal conditions for transfer of CWP in SSA and collection, despite mixed winds: the highest bacterial pollution levels in the upwind waters and greatest SSA production. IBBFa shows higher levels than IBSCa, suggesting IBBFa was better located, possibly due to Northwest winds and IBBFa lying South of the TJR mouth (Figs. 5.1, 5.2, 5.3). Together these 40 bacteria comprise 41% on average, and up to 76% of the 16S

reads in the 12 total IBa-sea and IBa-mixed samples (Fig. 5.12 B). This demonstrates that a significant fraction of the airborne bacteria breathed by coastal communities can come from CWP, and this should be considered for public health along coastlines.

5.4.11 Implications

This study presents evidence of CWP transferring to the atmosphere in SSA and calls attention to potential public health impacts that need to be further explored. The multiple environmental conditions that transport pollution through this exposure pathway are under investigation (Grimes et al., 2020; Rodriguez et al., 2018). Future studies will focus on more comprehensive sampling and target specific chemicals and pathogens. This environmental and public health problem is expected to grow as our changing climate brings more extreme precipitation and CWP events (Curriero et al., 2001). This work provides further justification for improving and monitoring coastal water and air quality along the Tijuana-San Diego coastline and other populated coastlines worldwide.

5.5 Acknowledgements

This project was supported by the Understanding and Protecting the Planet (UPP) initiative from the University of California San Diego and by the German Research Foundation (DFG) with Grant PE 2600/1 to DP. We thank for accommodating our research: the city of Imperial Beach and IB lifeguards, including Robert Stabenow, Jason Lindquist, Art Ayala, Trevor Spence, Adam Wraight, Jesus Gonzalez; the Tijuana River National Estuary Research Reserve and CA State Parks, including Chris Peregrin, Jeff Crooks, Justin McCullough, Cara Stafford; CA Border Patrol Agents Amber Craig, Clinton Cox, and Paul Sheehan; UCSD-SIO: Monica Castrejón, Christian McDonald. We thank for research assistance: Kathryn Mayer, Gavin Cornwell, James Garrafa-Luna; TSRI: Brian Seegers, Alan Saluk. We thank three

anonymous reviewers for their feedback. We acknowledge that the site of this study and UC San Diego lie in the stolen territory of the Kumeyaay people.

Chapter 5, in full, has been submitted to Environmental Science & Technology for publication, where it is currently in review. Pendergraft, M. A., Belda-Ferre, P., Petras, D., Morris, C. K., Mitts, B. A., Aron, A. T., Bryant, M., Schwartz, T., Ackermann, G., Humphrey, G., Kaandorp, E., Dorrestein, P. C., Knight, R., Prather, K. A. Bacterial and chemical evidence of coastal water pollution from the Tijuana River in sea spray aerosol. The dissertation author is the primary author of the manuscript.

5.6 Figures

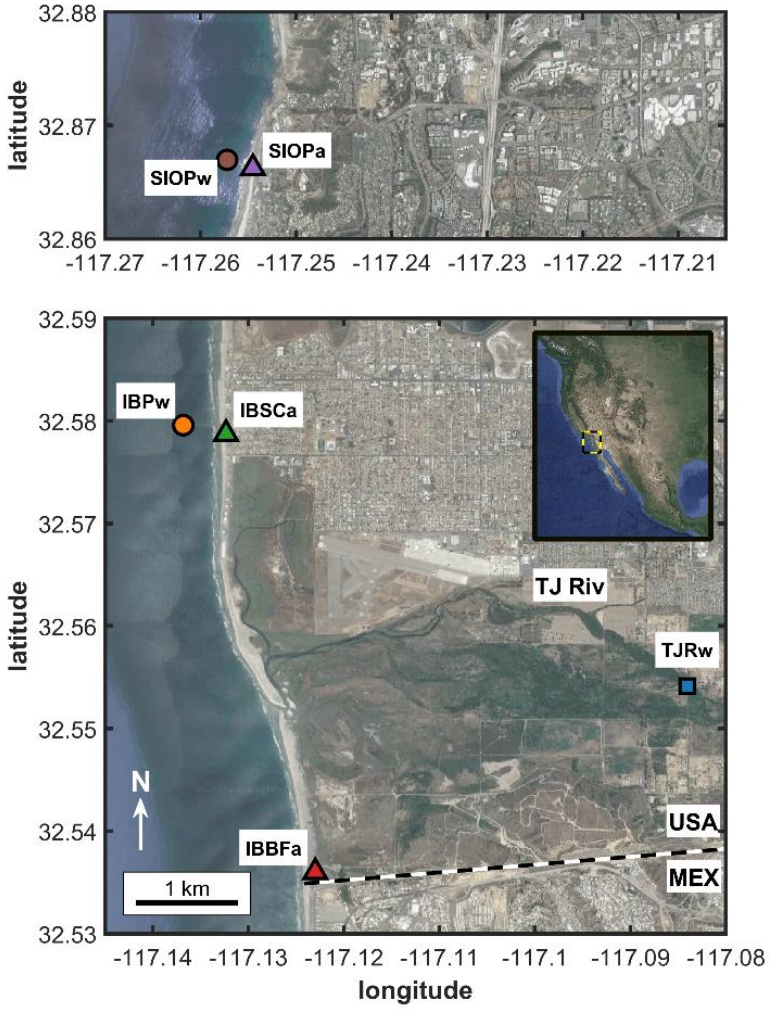

Figure 5.1. Site map with sampling locations. Produced using MATLAB version 9.10.0.1602886 (R2021a) 37 and additional resources [1-3]. Locations of aerosol and water sampling at Imperial Beach, CA, USA (bottom) and 35 km away at Scripps Institution of Oceanography (SIO) in La Jolla, CA, USA (top). Marker formatting is consistent in all figures. The dashed line denotes the Mexico-USA border. Also noted is the Tijuana River (TJ Riv). Also denoted are the Tijuana River and the Mexico-USA border. Sites of water sampling are denoted with a "w" and sites of aerosol sampling are denoted with an "a".
[1] Zohar Bar-Yehuda (2017). zoharby/plot_google_map (https://github.com/zoharby/plot_google_map), GitHub. Retrieved June 1, 2017.
[2] Map data: Imagery ©2021 Google. Data USGS, Data SIO, NOAA, U.S. Navy, NGA, GEBCO, Data LDEO-Columbia, NSF, NOAA, Imagery ©2021 TerraMetrics, Map data ©2021 INEGI.
[3] Jonathan Sullivan (2017). Automatic Map Scale Generation (https://www.mathworks.com/matlabcentral/fileexchange/33545-automatic-map-scale-generation), MATLAB Central File Exchange. Retrieved June 1, 2017.

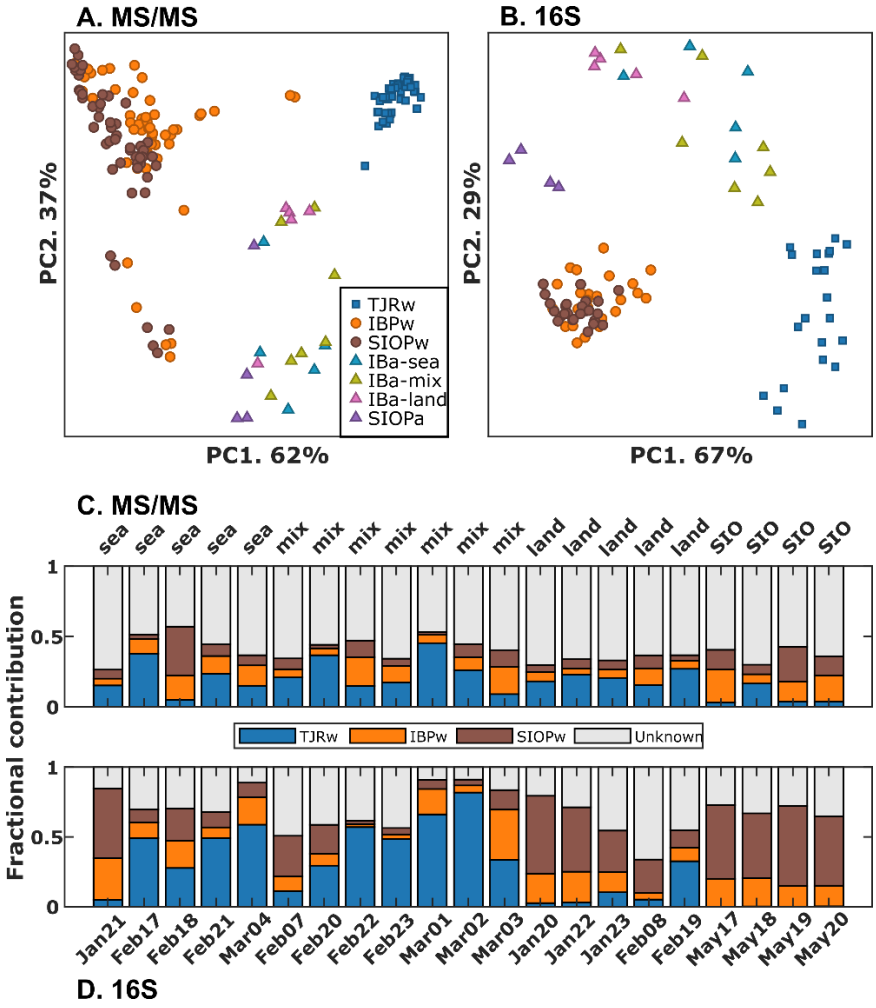

Figure 5.4. Robust Principal Component Analysis (RPCA) and and aerosol source apportionment from bacteria community and chemical composition. Panels (A) and (B) show RPCA (Aitchison distances) of non-targeted mass spectrometry (A) and 16S data (B). Panels (C) and (D) present ST2 results – the fractional contributions of different sources to each aerosol sample - for non-targeted mass spectrometry (C) and 16S data (D). Each bar represents one aerosol sample and is comprised of the fractional contribution of molecules (C) or bacteria (D) from TJRw (blue), IBPw (orange), SIOPw (brown), and Unknown (gray) as determined by ST2. Bars align vertically between (C) and (D) and are for the same aerosol sample.

Figure 5.5. Relative abundance across sample types for the 40 potential tracer bacteria of the polluted Tijuana River in IB aerosol. Each subplot represents a single bacterium (ASV). Each point is the read count of the bacterium in one sample. Sample types (and # of samples) are provided in the legend. Water samples plot on the left axes; aerosol samples and blanks plot on the right axes. Each black "+" denotes the sample type mean. For each bacterium/subplot, we look for the following tracer pattern: [TJRw] > [SIOPw] and [IBa-sea] > [IBa-land, SIOPa, and blanks]. Most bacteria here show a tracer pattern.

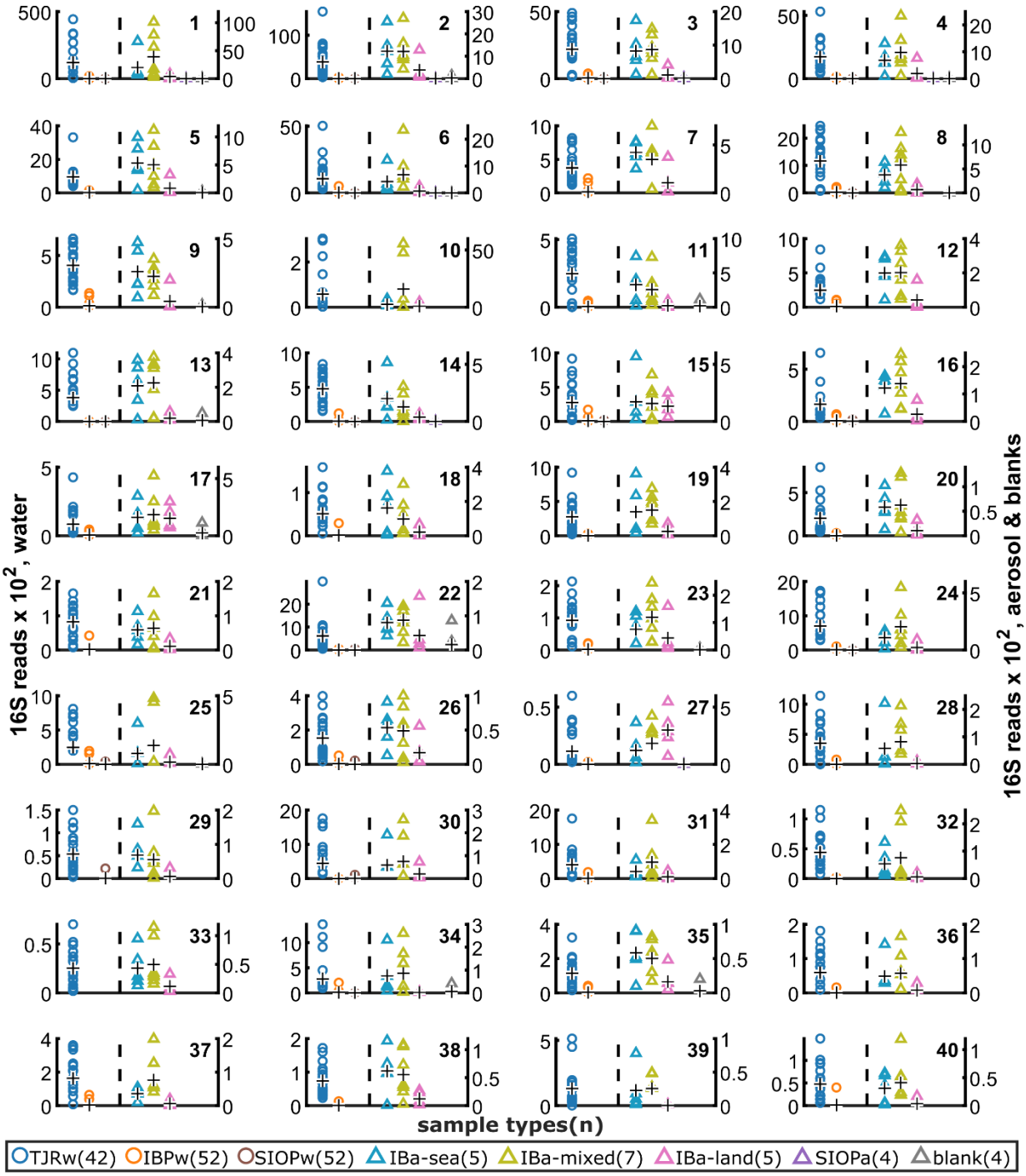
16S reads x 10^2, water
16S reads x 10^2, aerosol & blanks
sample types(n)
TJRw(42)
IBPw(52)
SIOPw(52)
IBa-sea(5)
IBa-mixed(7)
IBa-land(5)
SIOPa(4)
blank(4)

Figure 5.6. Relative abundance across sample types for the 40 chemical links between the polluted Tijuana River and IB aerosol. Each subplot represents a single compound Each point is the MS1 peak area of the compound in a sample. Sample types (and # of samples) are provided in the legend. Each black "+" denotes the sample type mean. Water samples plot on the left axes; aerosol samples and blanks plot on the right axes. Most compounds lack a tracer pattern of [TJRw] > [SIOPw] and [IBa-sea] > [IBa-land, SIOPa, & blanks] due to high IBa-land relative abundance. This implies they have multiple sources so we do not consider them as tracers but as chemical links between TJRW and IBa.

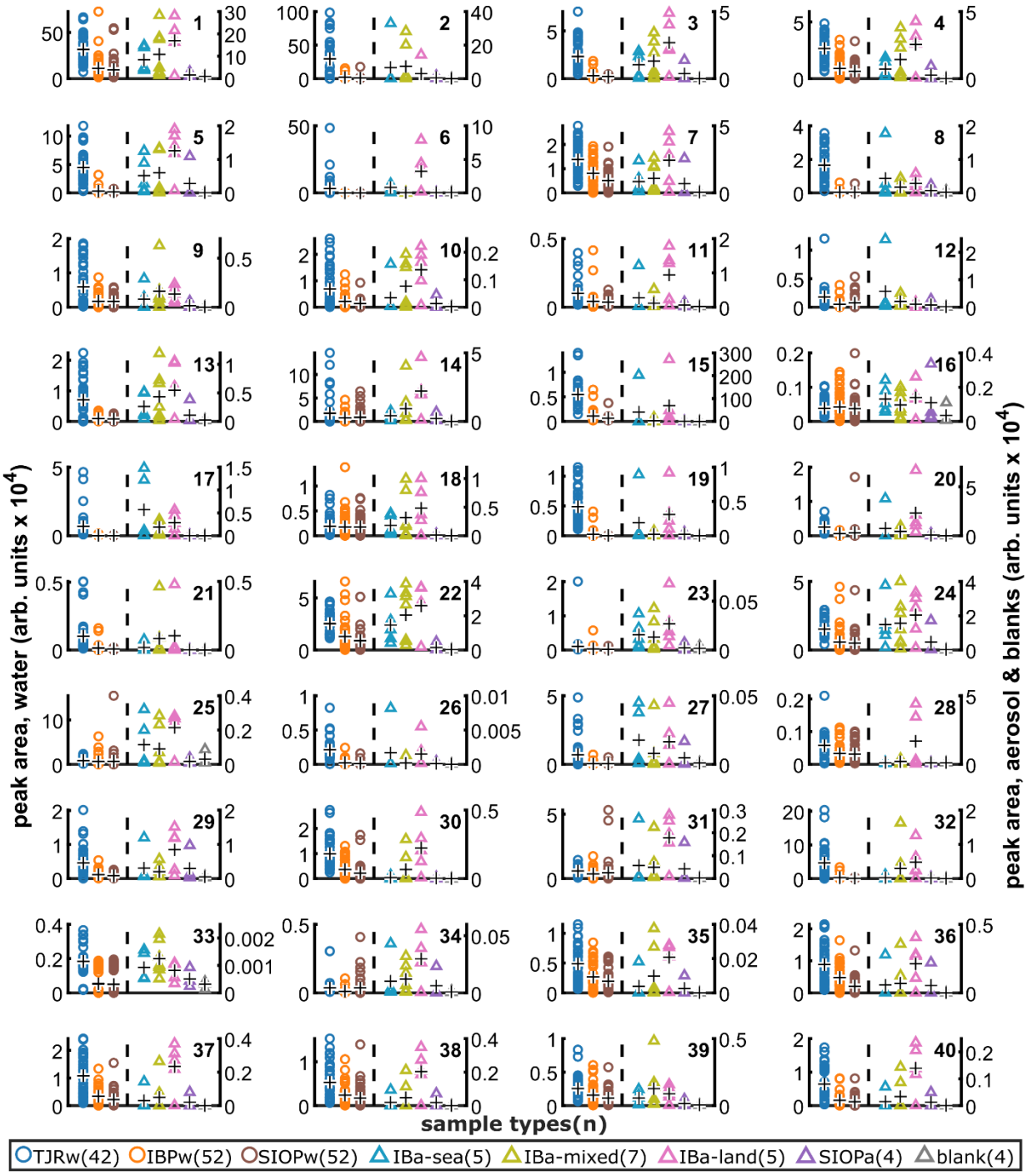
peak area, water (arb. units x 10^4)
peak area, aerosol & blanks (arb. units x 10^4)
sample types(n)
TJRw(42)
IBPw(52)
SIOPw(52)
IBa-sea(5)
IBa-mixed(7)
IBa-land(5)
SIOPa(4)
blank(4)

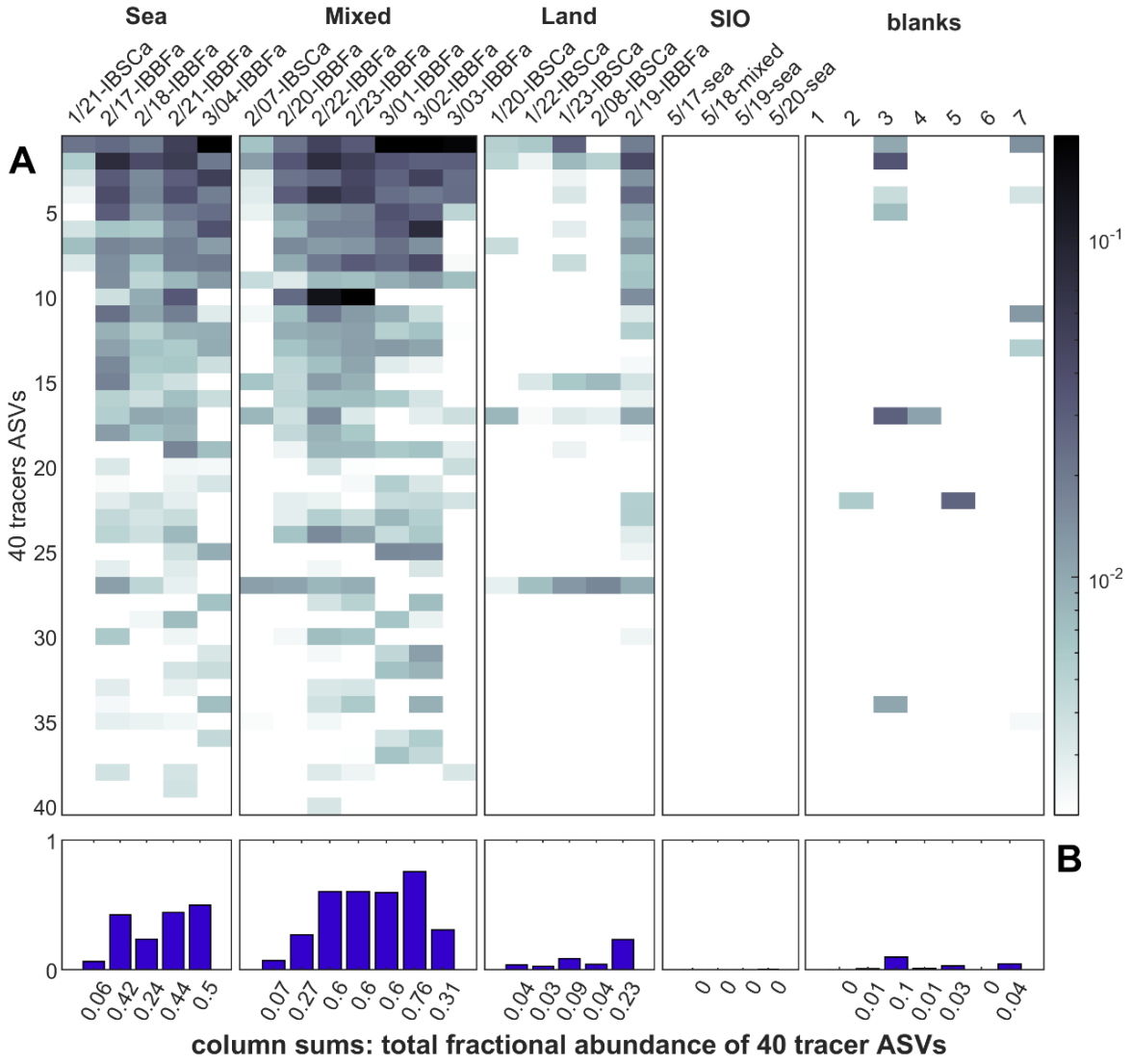

Figure 5.12. Individual and combined fractional abundance of the 40 tracer bacteria grouped by local particle origin. (A) is a heatmap of individual fractional abundances, with bacteria (ASVs) in rows and samples as columns. Fractional abundance was calculated by dividing the read count for each ASV in each sample by the total reads for that sample. (B) presents the sums of columns in (A), giving the combined fractional contribution of the 40 bacteria to the entire sample.

5.7 Supplementary Methods

5.7.1 Water Sampling

Water sampling occurred daily using an acid cleaned 5 gal high density polyethylene bucket (Home Depot, Atlanta, GA) with a rope attached to the handle. The bucket and rope were rinsed between sampling sites and thoroughly cleaned at the end of each day with solvent and acid. A separate bucket was used for sampling the heavily polluted Tijuana River. At each site a bucket was lowered into the water, raised, dumped to rinse, then lowered again to collect the sample. Coastal seawater was sampled from the West ends of the IB (IBPw) and SIO (SIOPw) piers (all 5 sampling rounds (SR)). Tijuana River water was sampled from the Hollister Street bridge (TJRw; SR 2-5). See Fig. 5.1 for sampling locations. We sampled the mouth of the Tijuana River on two occasions but do not use those data in the study because access was prohibitively difficult and because ocean influence was significant and variable there, changing with tides and surf. Sampling at the Hollister Street bridge avoided this problem and therefore better characterized the Tijuana River.

5.7.2 Aerosol Filter Sampling

Aerosol were sampled onto 47 mm QMA quartz fiber filters (Pall, Port Washington, NY) at 30 liters per minute. Quartz filters were precombusted at 500 °C for two hours and combusted filters were analyzed as blanks via mass spectrometry and 16S sequencing. Total suspended particles were collected, without any size exclusion, at ambient temperature and relative humidity.

5.7.3 Meteorological, Hydrological, and Oceanographic Data

Wind data for IB were acquired from the KNRS meteorological station (32° 33' 47" N, 117° 6' 39" W), retrieved from weather.gladstonefamily.net. Wind data for LJ were acquired

from cdip.ucsd.edu station 073 (SIO pier). Swell data were acquired from cdip.ucsd.edu. We use swell data from CDIP buoy 155 off IB because the primary purpose of the swell data is to determine if swell conditions were present that could have been driving alongshore currents. Elevated wave heights (>1 m) from the South or North can cause along shore currents that would transport pollution from the Tijuana River along the coast. Tijuana River flows at the international boundary (32° 32′ 36″ N, -117° 3′ 1″ W (WGS 84)) were acquired from the International Boundary and Water Commission at waterdata.ibwc.gov. Precipitation data for the locations of KNKX (MCAS Miramar; 32° 51' 52" N, 117° 8' 12" W), KSDM (Brown Field; 32° 34' 20" N, 116° 58' 49" W), KCZZ (Campo; 32° 37' 34" N, 116° 28' 06" W), KNRS (IB; 32° 33' 47" N, 117° 6' 39" W), from mesowest.utah.edu 73,74. Precipitation data at the Tijuana River estuary (32.57450, 117.12700) were acquired from the National Estuarine Research Reserve System (NERRS). Precipitation data for Los Penasquitos Lagoon (32° 56' 01" N, 117° 15' 26" W) were provided by J. McCullough and J. Crooks at the Tijuana River National Estuarine Research Reserve. Precipitation totals from KNKX (MCAS Miramar) and Los Penasquitos Lagoon were averaged for an estimate of precipitation in the LJ area. Precipitation data from KSDM, KCZZ, KNRS, and the Tijuana River estuary were averaged for an estimation of precipitation in the Tijuana River watershed. Aerosol particle volume was measured with the TSI 3321 aerodynamic particle sizer (TSI Inc, Shoreview, MN).

5.7.4 Sample Preparation for Mass Spectrometry

Sea water samples were taken with a 20 liter acid cleaned bucket (HomeDepot) at the water surface. 1 liter of seawater was then transferred to a 1 liter HD-PP bottle and stored on ice till extraction in the laboratory (within 5 h from sampling). For solid phase extraction, the samples were acidified to pH 2 with ~ 1.2 ml hydrochloric acid (38% p.a.; trace metal grade, J.T.

Baker, USA). The samples were then extracted through PPL cartridges with a bed mass of 200 mg. Before use, the cartridges were rinsed and activated with three cartridge volume of methanol (LC-MS grade, Fisher Scientific, San Diego, USA) and conditioned with two cartridge volumes of water (LC-MS grade, Fisher Scientific, San Diego, USA) at pH 2 (acidified with HCl, 37% p.a.; trace metal grade, J.T. Baker, USA). For extraction, acidified seawater was pulled through the PPL cartridge with a flow rate below 10 ml/min with the help of a vacuum SPE station. Subsequently, remaining salt was removed with three cartridge volumes of pH 2 water. After drying with nitrogen gas, DOM was eluted with 2 ml of methanol into glass vials. After elution, the extracts were dried in a vacuum centrifuge (Centrivap, Labconco, Kansas City, USA) and stored at -80° C until further analysis. For LC-MS/MS analysis, samples were re-suspended in 100 µL MeOH/H2O/Formic acid (80/19/1).

5.7.5 Tandem Mass Spectrometry Analysis

UHPLC-MS/MS analysis was performed as described before 75,90. In short, the extracted samples were re-dissolved in 100 µl methanol/water/formic acid (80:19:1, Fisher Scientific, San Diego, USA) of which 10 µl were injected into vanquish UHPLC system coupled to a Q-Exactive quadrupole orbitrap mass spectrometer (Thermo Fisher Scientific, Bremen, Germany) in two technical replicates. For the chromatographic separation, a reversed phase C18 porous core column (Kinetex C18, 150 x 2 mm, 1.8 µm particle size, 100 A pore size, Phenomenex, Torrance, USA) was used. For gradient elution a high-pressure binary gradient system was used. The mobile phase consisted of solvent A H2O + 0.1 % formic acid (FA) and solvent B acetonitrile (ACN) + 0.1 % FA. The flow rate was set to 0.5 mL/min. After injection, the samples were eluted with a linear gradient from 0-0.5 min, 5 % B, 0.5-8 min 5-50 % B, 8-10 min 50-99 % B, followed by a 2 min washout phase at 99% B and a 3 min re-equilibration phase

at 5 % B. Data dependent acquisition (DDA) of MS/MS spectra was performed in positive mode. Electrospray ionization (ESI) parameters were set to 52 L/min sheath gas flow, 14 L/min auxiliary gas flow, 0 L/min sweep gas flow and 400 °C auxiliary gas temperature. The spray voltage was set to 3.5 kV and the inlet capillary to 320 °C. 50 V S-lens level was applied. MS scan range was set to 150-1500 m/z with a resolution at m/z 200 (Rm/z 200) of 70,000 with one micro-scan. The maximum ion injection time was set to 100 ms with automated gain control (AGC) target of 1.0E6. Up to 5 MS/MS spectra per MS1 survey scan were recorded DDA mode with Rm/z 200 of 17,500 with one micro-scan. The maximum ion injection time for MS/MS scans was set to 100 ms with a AGC target of 3.0E5 ions and minimum 5 % C-trap filling. The MS/MS precursor isolation window were set to m/z 1. Normalized collision energy was set to a stepwise increase from 20 to 30 to 40 % with z = 1 as default charge state. MS/MS scans were triggered at the apex of chromatographic peaks within 2 to 15 s from their first occurrence. Dynamic precursor exclusion was set to 5 s. Ions with unassigned charge states were excluded from MS/MS acquisition as well as isotope peaks.

5.7.6 Mass Spectrometry Data Analysis

For MS/MS data analysis raw spectra were converted to .mzXML files using MSconvert (ProteoWizard) MS1 and MS/MS feature extraction was performed using MZmine2.37 IIMN enabled version 76. For peak picking an intensity threshold of 1E5 and for MS1 spectra and of 1E3 for MS/MS spectra was used. For MS1 chromatogram building a 5 ppm mass accuracy and a minimum peak intensity of 3E5 was set. Extracted Ion Chromatograms (XICs) were deconvoluted using the baseline cut-off algorithm with the baseline set to 1E5, a minimum peak intensity of 3E5 and a minimum peak duration of 0.01 min. After chromatographic deconvolution, MS1 features were linked to MS/MS spectra within 0.01 m/z mass and 0.2 min

retention time windows. Isotope peaks were grouped using the isotope grouper module and features from different samples were aligned with 5 ppm mass tolerance and 0.1 min retention time tolerance. MS1 features without MS2 features assigned were filtered out the resulting matrix as well as features which did not contain a minimum of 2 peak per isotope pattern and which did not occur at least in 2 samples. After filtering, gaps in the feature matrix were filled with the peak finder algorithm with a retention time tolerance of 0.1 min and 5 ppm mass tolerance. Finally, peak areas were exported in a feature table as .csv file and corresponding consensus MS/MS spectra as .mgf file. Contaminant features observed in the PPL process blanks with a relative peak area > 30% in comparison to the sample average were filtered out. For feature-based molecular networking and spectrum library matching the .mgf file was uploaded to GNPS (gnps.ucsd.edu) 77. For spectrum library matching (against the GNPS and NIS17 library) and spectral networking the minimum cosine score to define spectral similarity was set to 0.7. The Precursor and Fragment Ion Mass Tolerances were set to 0.01 Da and Minimum Matched Fragment Ions to 4, Minimum Cluster Size to 1 (MS Cluster off). When Analog Search was performed the maximum mass difference was set to 100 Da. The GNPS library currently contains 74044 MS/MS spectra (Dec 18, 2019) including Mass Bank, ReSpect and HMDB. RPCA of MS1 data, normalized to total ion current (TIC) were then created with using Aitchinson distances and organic matter compositional distance (Bray-Curtis) was correlated against different meta-data categories with ADONIS (999 permutation) using Qiime2 78.

5.7.7 Sample Preparation for 16S Amplicon Sequencing

Ocean and river water samples were prepared on site by transferring 400 µl into individual MoBio PowerSoil bead-beating tubes. Water samples and aerosol filters were stored at -80C until further processing. When all study samples were collected, samples were plated

using sterile technique and tools. A quarter of each aerosol filter sample was cut and placed into an individual MoBio PowerSoil bead-beating tube. To implement the KatharoSeq workflow for low biomass samples, each extraction plate contained a 10-fold serial dilution of ZymoBIOMICS™ Microbial Community Standard (D6300 Zymo, USA) ranging from 0.1 to 1 million cells per extraction. DNA was extracted using the Qiagen MagAttract PowerSoil DNA KF (384) Kit (Qiagen, Germany), following manufacturer's instructions. Briefly, 60 µl of SL solution was added to each bead-beating tube 79. Tubes were then beaten for 20 minutes at 20Hz using a TissueLyzer (Qiagen, Germany) and subsequently centrifuged at 3700xg for 5 mins. Lysates were transferred (400µL/tube) to a 96-deep well plate containing 450 µl of IR Solution. After vortexing for seconds, plates were incubated at 4C for 10 mins and centrifuged at 3700xg for 5 mins. Supernatants (850µL/well) were transferred to a clean 96-deep well plate and centrifuged at 3700xg for 5 mins. Supernatants (450µL/well) were transferred to a 96-deep well plate containing 470 µl of ClearMag Beads/ClearMag Binding Solution. This plate was further processed using the KingFisher Flex platform, using the protocol provided by the manufacturer. DNA was eluted in 65 µl and stored at -20C until further processing.

5.7.8 Amplicon Sequencing

Extracted DNA was amplified in triplicate 10 µl PCR reactions, containing 2 µl of gDNA, and using the Earth Microbiome Project standard 16S 515f/806rB bar-coded primers 79,80. Replicate reactions for each sample were pooled together, and 5 µl per pool was combined for the final library. Sequencing was performed on the Illumina MiSeq platform with 2x150bp paired-ends reads.

5.7.9 16S Amplicon Sequencing Data Analysis

Raw sequencing reads were demultiplexed, quality filtered and denoised using Deblur in QIITA under study ID 12758 91,72. Deblurred reads considered to be reagent contaminants were removed using the R package decontam 81. Downstream data processing was performed using QIIME2 78. Serially diluted mock communities were used to assess the sequencing depth needed to pass the KatharoSeq workflow, so that 80% of positive controls reads correctly aligned to the mock communities' composition. RPCA ordination plots were obtained using DEICODE 82. To assess the potential source of aerosol ASVs, SourceTracker2 was used setting ocean and river water samples as sources and aerosol samples as sinks .

5.7.10 Air Parcel Back Trajectories

A local particle origin for each sampling period was derived from local winds and running FLEXPART back trajectories initiated 24 hs prior to the initiation of each aerosol sampling period and terminating at the end of the sampling period (Fig. S2). We chose the period of 24 hs to capture short range transport of locally produced particles. Note particles from long range transport would also be present following those same trajectories. Simulated particles were released at 5 m elevation and allowed to travel horizontally and vertically, but we do not display the altitudes because we are only concerned with the horizontal (lat/lon) information (Fig. S2). Local particle origins were classified as from the sea or from the land when winds and back trajectories agreed on either; otherwise, a "mixed" local particle origin was assigned. Air parcel back trajectories were carried out using the Flexible Particle Dispersion Model (FLEXPART), a Lagrangian transport and dispersion model 83. The model was run using atmospheric circulation data from the National Centers for Environmental Prediction (NCEP) Climate Forecast System Reanalysis (CFSR) 6-hourly Products. For each aerosol sampling period, the simulation was run in back trajectory mode between the end of the sampling period and one day (24 h) prior to the

start of the ~1d sampling period. Each FLEXPART run simulated the release of 500 air parcels from the sampling coordinates and height, with convection activated, and outputs were generated and averaged every hour.

5.7.11 Bacteria Counts

Heterotrophic bacteria counts from aerosols collected into solution with the Series 100 Universal Spot Sampler (model SS110A; Aerosol Devices Inc, Fort Collins, CO) were determined by flow cytometry at The Scripps Research Institute Flow Core facility. Sample preservation and cell staining followed Noble & Fuhrman 87. Liquid samples were fixed with glutaraldehyde at a final concentration of 0.05%, incubated for 15 minutes at 5°C, then flash frozen with liquid nitrogen, and stored at 5°C. At the Flow Core, samples were thawed, diluted 1:10 in 1x TE buffer (pH 8), stained with SYBR Green I at a final dilution of 1:100 from the stock, and incubated for 10 minutes in the dark just before analysis by a Bio-Rad ZE5 Cell Analyzer. Heterotrophic bacteria were gated as a group in cytograms plotting fluorescence (488 nm laser; green fluorescence) against side scatter. Counts from this region from ultrapure water processed as a sample were subtracted as a blank.

5.7.12 Data Availability

All MS/MS data can be found on the Mass spectrometry Interactive Virtual Environment (MassIVE) at https://massive.ucsd.edu/ with the identifier MSV000083889. Molecular Networking and Spectrum Library Matching results can be found online at GNPS under the following links:

https://gnps.ucsd.edu/ProteoSAFe/result.jsp?task=fd75a1a473864a7ab6deb29875a9a82c&view=advanced_view

https://gnps.ucsd.edu/ProteoSAFe/status.jsp?task=2edebb51fbc34f8db8f5572666e4dde2

All 16S rRNA amplicon sequencing data and sample metadata are archived and available at the European Nucleotide Archive European Molecular Biology Laboratory European

Bioinformatics Institute (EMBL-EBI) under the primary accession number of PRJEB46560 and secondary accession number of ERP130752: https://www.ebi.ac.uk/ena/browser/view/PRJEB46560 and also on QIITA under project ID 12758 72

Data and code are in the University of California San Diego Library's Digital Collections and are available at https://doi.org/10.6075/J07944V3

5.8 Supplementary Figures

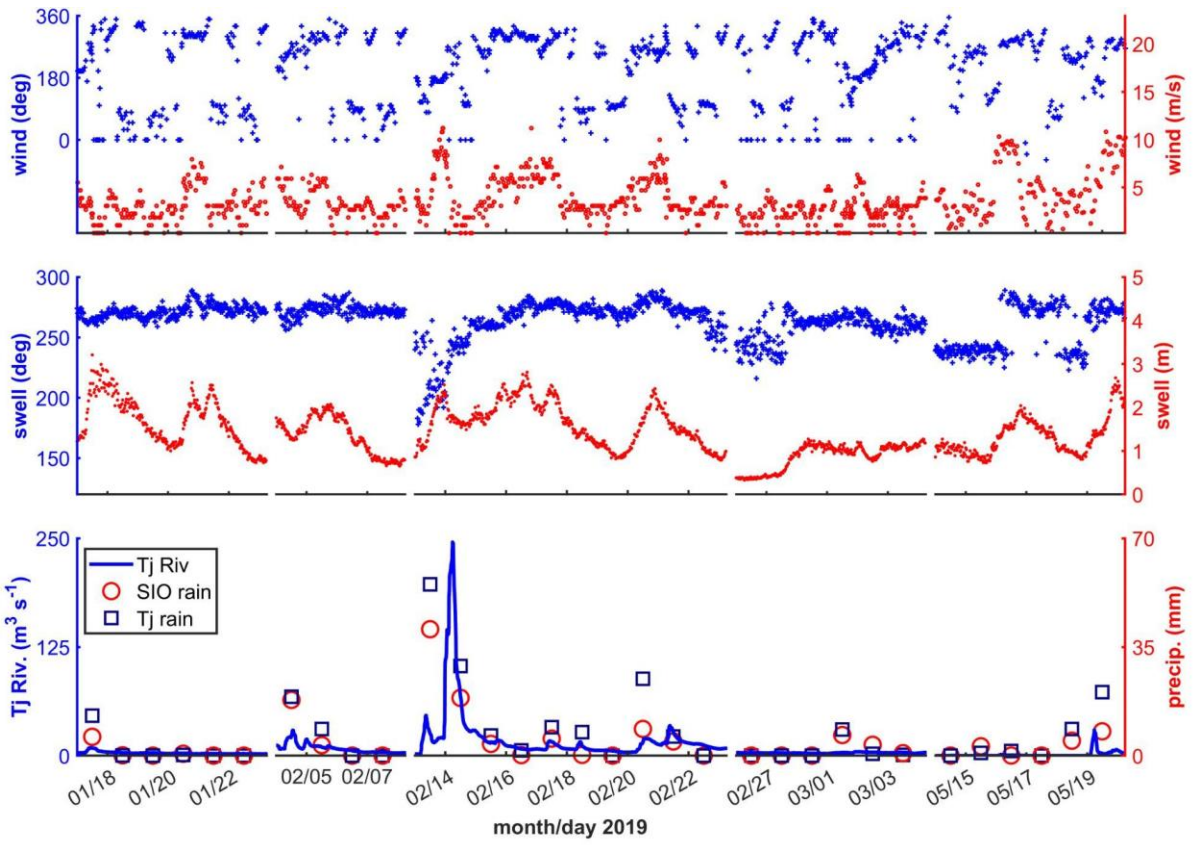

Figure 5.2. Environmental conditions. Sampling periods and aerosol sampling locations were: Jan. 19-23 IBSCa, Feb. 6-8 IBSCa, Feb. 16-23 IBBFa, Feb. 28 - Mar. 4 IBBFa, May 16-20 SIOPa. Aerosol sampling periods in Imperial Beach followed rain events to target coastal water pollution. The SIOPa aerosol sampling period in La Jolla included some light rain.

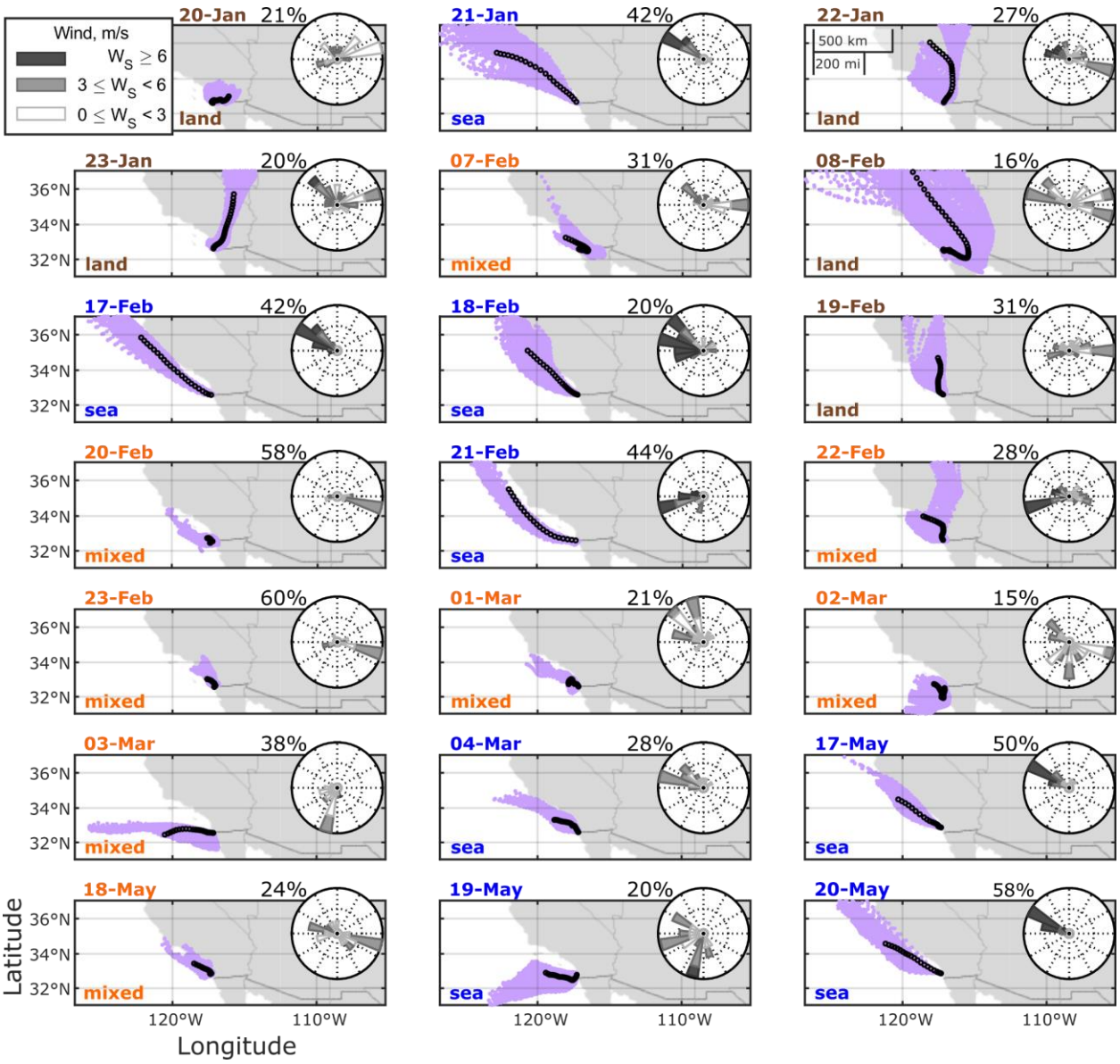

Figure 5.3. Local particle origins from local winds and FLEXPART back trajectories. Winds are from each sampling period, from a local meteorological station. FLEXPART back trajectories are from 24 hs prior to the initiation of each aerosol sampling period through to the end of the 22 hs sampling period. When both local winds and back trajectories agree on a land or sea origin, the corresponding classification was given. Otherwise, "mixed" was assigned. This is to characterize the origin of locally produced aerosols.

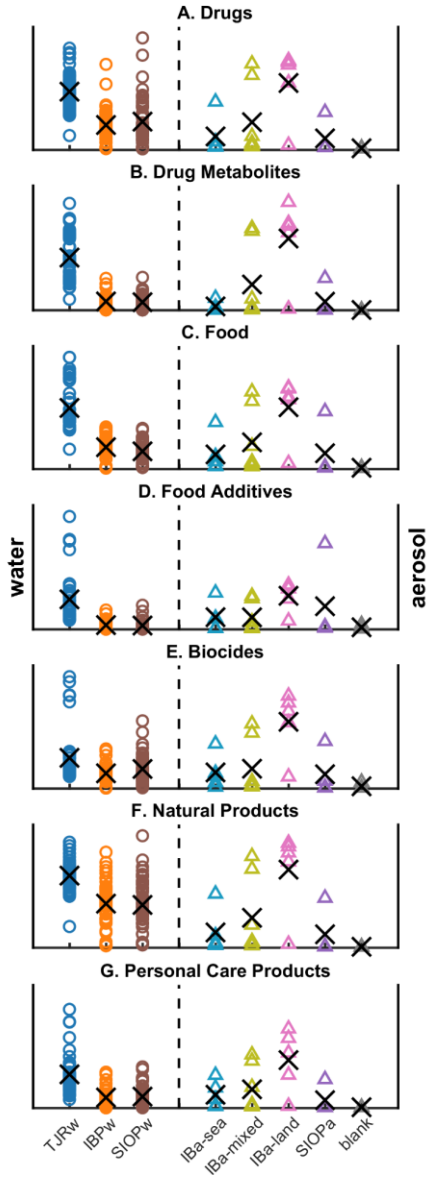

Figure 5.7. Relative abundance by sample type for annotated compound classes. We annotated 160 drugs, 21 drug metabolites, 179 food compounds, 15 food additives, 36 biocides, 487 natural products, and 6 compounds from personal care products in our MS/MS dataset as level 2 IDs (LIT; n=497). For each sample, we summed the peak area for all compounds in each group, and present them separated by sample type. Water samples are on the left of the dashed line and plot on the left axis. Aerosols and blanks are on the right of the dashed line and plot on the right axis. Black X's denote mean values.

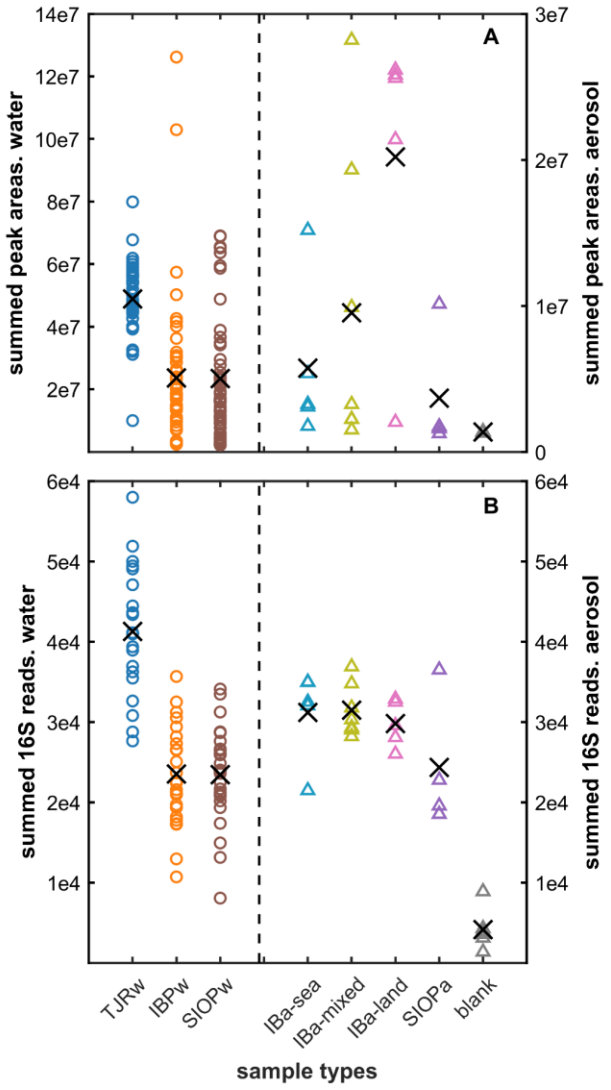

Figure 5.8. Relative signal strength across sample type. The total number of MS/MS peak areas (A, top) and 16S reads (B, bottom) were summed for each sample. Water samples, grouped by sample type, are on the left of the dotted line and aerosol samples, grouped by local particle origin and location, and blanks are on the right of the dotted line. X's denote means. Water and aerosol plot on separate y-axes in (A). Note the data plotted here are already blank corrected.

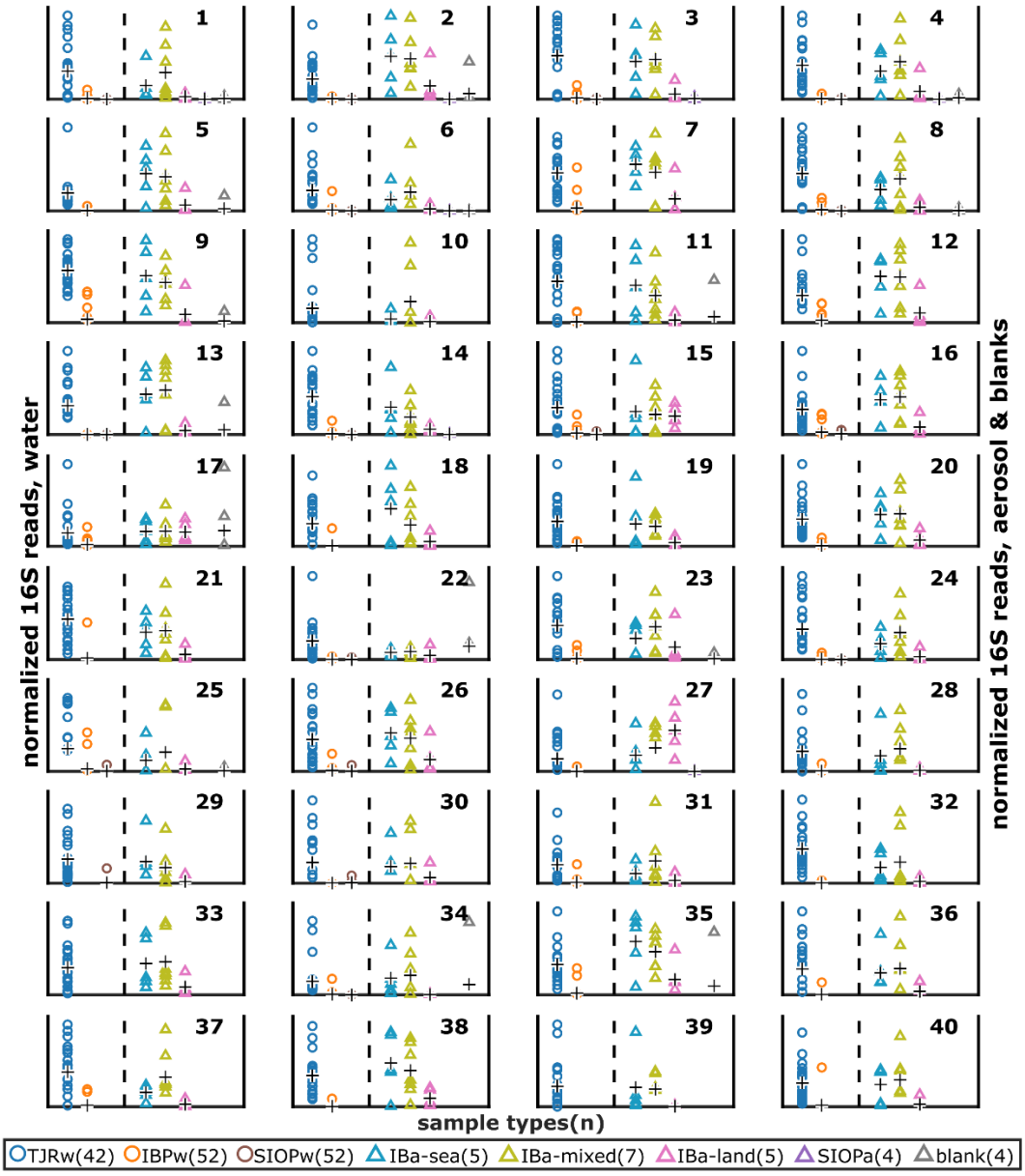

Figure 5.9. Relative normalized abundance across sample types for the 40 potential tracer bacteria of the polluted Tijuana River in IB aerosol. Each subplot represents a single bacterium (ASV). Each point is the read count of the bacterium in one sample, divided by the total reads of the sample. Sample types (and # of samples) are provided in the legend. Each black cross (+) denotes the sample type mean. Water samples plot on the left axes; aerosol samples and blanks plot on the right axes. For each bacterium/subplot, we look for the following tracer pattern: [TJRw] > [SIOPw] and [IBa-sea] > [IBa-land, SIOPa, and blanks].

Figure 5.10. Relative normalized abundance across sample types for the 40 chemical links between the polluted Tijuana River and IB aerosol. Each subplot represents a single compound. Each point is the MS1 peak area of the compound in a sample divided by total MS1 peak areas for the sample. Sample types (and # of samples) are provided in the legend. Each black cross (+) denotes the sample type mean. Water samples plot on the left axes; aerosol samples and blanks plot on the right axes. Most compounds lack a tracer pattern of [TJRw] > [SIOPw] and [IBa-sea] > [IBa-land, SIOPa, & blanks] due to high IBa-land relative abundance. This implies they have multiple sources so we do not consider them as tracers but as chemical links between TJRW and IBa.

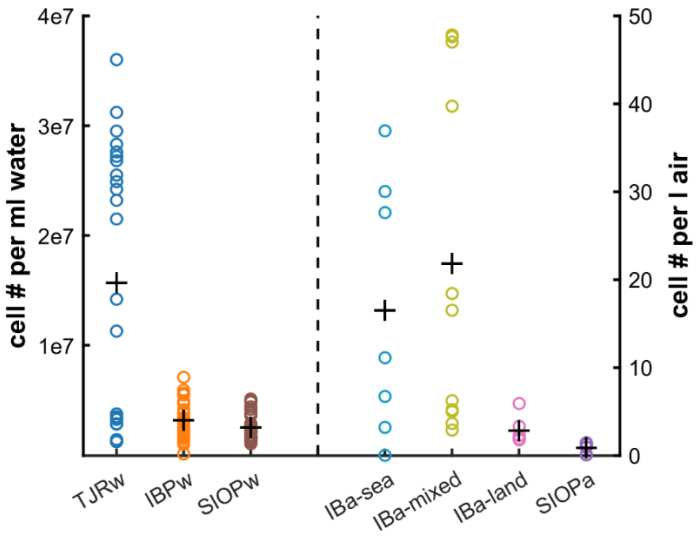

Figure 5.11. Cell counts of heterotrophic bacteria abundance in water and air. Aerosol samples were collected into liquid using the Series 100 Universal Spot Sampler (model SS110A; Aerosol Devices Inc, Fort Collins, CO). Cell counts were achieved using flow cytometry 92. Black crosses are means for each sample type.

5.9 Supplementary tables

Note: Sources are provided in the Supplementary References.

Table 5.1. Tracer bacteria of the polluted Tijuana River in IB aerosols coming from the sea. Notes: Sewage – sewage associated. Pathogens – taxon contains human pathogens. Foam – associated with sewage/wastewater foam. NFGNB – nonfermenting gram-negative bacilli. TJ – associated with Tijuana sewage. Sources are provided in the Supporting Information.

#	Taxonomy	Sewage	pathogens	Other	Sources
1	g_Arcobacter s_cryaerophilus	Yes, TJ	Yes	foodborne, antimicrobial resistance	1–4
2	g_Acinetobacter	Yes, dominant, TJ, foam	Yes	NFGNB	4,5
3	g_Arcobacter	Yes, dominant, TJ	Yes	foodborne, antimicrobial resistance	1–4
4	f_Aeromonadaceae	Yes, TJ	Yes	fresh & brackish water	6
5	g_Acidovorax	Yes, TJ	Yes	NFGNB	7
6	g_Arcobacter s_cryaerophilus	Yes, TJ	Yes	foodborne, antimicrobial resistance	1–4
7	g_Flavobacterium	No	No	ubiquitous; IB seawater	1,8
8	g_Arcobacter	Yes, dominant, TJ	Yes	foodborne, antimicrobial resistance	1–4
9	g_Comamonas	Yes, TJ	rarely	ubiquitous; NFGNB	1,4
10	g_Flectobacillus	No	No	freshwater , microplastic biofilms	9,10
11	g_Pseudomonas	ubiquitous	rarely	NFGNB	11
12	f_Pseudomonadaceae	ubiquitous	rarely	NFGNB	11
13	g_Hydrogenophaga	Yes, strongly	No	hydrogen-oxidizing aerobe	12–15
14	g_Aquabacterium	Yes	No	common to municipal water	16
15	g_Acinetobacter s_lwoffii	Yes, dominant, TJ, foam	Yes	NFGNB, antimicrobial resistance	4,16–18
16	g_Shewanella	ubiquitous	rarely	NFGNB	19,20
17	o_Clostridiales	Yes	Yes	common in gut	4,21–23
18	f_Pseudomonadaceae	ubiquitous	rarely	NFGNB	24
19	o_Fusobacteriales	No	Yes	humans, marine, terrestrial, infections	25–28
20	g_Bacteroides	Yes, TJ	Yes	fecal indicator, antimicrobial resistance	1,29–31
21	g_Rheinheimera	No	No	marine water & sediment; freshwater; soils	32
22	g_Acinetobacter s_johnsonii	Yes, dominant, TJ, foam	No	NFGNB , antimicrobial resistance	18
23	f_Pseudomonadaceae	ubiquitous	rarely	NFGNB	24
24	g_Acinetobacter	Yes, dominant, TJ, foam	Yes	NFGNB	4,5
25	g_Hydrogenophaga	Yes, strongly	No	hydrogen-oxidizing aerobe	12–15
26	g_Arcobacter	Yes, dominant, TJ	Yes	foodborne, antimicrobial resistance	1–4
27	g_Alkanindiges	Yes, foam	No	freshwater, terrestrial	33–35
28	g_Arcobacter	Yes, dominant, TJ	Yes	foodborne, antimicrobial resistance	1–4
29	f_Rhodocyclaceae g_C39	No	No	freshwater	36,37
30	g_Acinetobacter s_lwoffii	Yes, dominant, TJ, foam	Yes	NFGNB, antimicrobial resistance	4,17,18
31	g_Arcobacter	Yes, dominant, TJ	Yes	foodborne, antimicrobial resistance	1–4
32	f_Pseudomonadaceae	ubiquitous	rarely	NFGNB	24
33	g_Aeromonas s_sharmana	No	No	freshwater	38
34	g_Arcobacter	Yes, dominant, TJ	Yes	foodborne, antimicrobial resistance	1–4
35	f_Pseudomonadaceae	ubiquitous	rarely	NFGNB	24
36	g_Zoogloea	Yes	No	dominant in sewage at lower temps.	39
37	g_Acinetobacter	Yes, dominant, TJ, foam	Yes	NFGNB	4,5
38	f_Aeromonadaceae	Yes, TJ	Yes	fresh & brackish water	6
39	f_Comamonadaceae	some genii Yes, some No	rarely	aquatic, soil, natural & industrial environs	40
40	g_Paludibacter	Yes	No	rice field, sewage	41,42

Table 5.2. Chemical links between the Tijuana River and IB aerosols coming from the sea.

#	Annotation	Tags	Sources
1	Tris(2-butoxyethyl) phosphate	irritant; pollutant; flame retardant; polishes/waxes; water treatment	43,44
2	N-cyclohexylcyclohexanamine	irritant; used in paints, varnishes, detergents; xenobiotic metabolite	44
3	Tributyl phosphate	irritant; solvent; flame retardant; plasticizer; antifoaming agent	45,46
4	1-Oleoyl-2-acetyl-sn-glycerol	reagent chemical	47
5	Galaxolidone	fragrance metabolite; sewage associated	48,49
6	Lauramine oxide	industrial chemical (zwitterion surfactant)	50
7	2-Linoleoyl glycerol	natural product	44
8	2,4,7,9-Tetramethyl-5-decyne-4,7-diol (Surynol 104)	industrial surfactant; defoaming; adhesives; water-based coatings	51
9	Aleuritic acid	shellac; perfume; personal care	52
10	S-Hydroprene	insecticide	53
11	Conjugated linoleic acid (10E,12Z)	general metabolite; dietary supplement	53,54
12	Prostaglandin F2alpha-1,15 lactone	eicosanoid; hormone mimic; found in mammals	55
13	Acetyl tributyl citrate	plasticizer in drugs, food wrap, cosmetics, medical tubes, toys	56
14	Myristamine oxide	hair conditioner; soap; cleaners	44
15	Triphenylphosphine oxide	industrial chemical; catalyst	57
16	Monopalmitolein (9c)	cyanobacteria	72
17	Vitamin K2	essential vitamin; in bacteria, fermented foods, meat, dairy, eggs	58
18	Fesoterodine fumarate	drug	44
19	8-Acetyl-7-methoxycoumarin	reagent drug	44,59
20	11beta-Prostaglandin E2	common in mammalian tissue	60,61
21	Desbenzyldonepezil	drug metabolite	62
22	Butaprost free acid	reagent chemical	63
23	Di(3,7-dimethyl-1-octyl) phthalate	plasticizer, solvent	64
24	4alpha-Hydroxystanozolol	drug metabolite	65
25	N-Lauroylsarcosine	cleaning products, hair conditioner	44
26	17-Phenyltrinorprostaglandin A2	synthetic prostaglandin analog; reagent	66
27	Sorbitane monostearate	in-source fragment of Polysorbate 60, a food & drug emulsifier	44
28	Dibenzylamine	petroleum lubricants; synthetic rubber manufacturing	44
29	5(Z),8(Z),11(Z)-Eicosatrienoic acid methyl ester	algae	67
30	Biotin	general metabolite	68
31	3,5-bis(1,1-dimethylethyl)-4-hydroxy-Benzoic acid	flame retardants; adhesives; cables	44
32	Caffeine	human associated	44
33	Dibutyl phthalate	plasticizer; environmental contaminant; teratogen; metabolite	44
34	Adenosine	naturally occurring in humans, also a drug, metabolite	44
35	Lumichrome	marine; plant metabolite	44,69
36	Warfarin	drug; pesticide	44
37	17alpha-Dihydroequilin 3-sulfate	drug	70
38	(-)-Riboflavin	essential human nutrient	44
39	13,14-dihydro-15-keto-PGF1	human metabolite	71
40	Methyldopa	drug	44

5.10 References

Shuval, H. (2003). Estimating the global burden of thalassogenic diseases: human infectious diseases caused by wastewater pollution of the marine environment. *Journal of Water and Health*, 1, 53–64.

Arnold, B.F., Schiff, K.C., Ercumen, A., Benjamin-Chung, J., Steele, J.A., Griffith, J.F., Steinberg, S.J., Smith, P., McGee, C.D., Wilson, R., Nelsen, C., Weisberg, S.B., Colford, J.M., Jr. (2017). Acute illness among surfers after exposure to seawater in dry- and wet-weather conditions. *American Journal of Epidemiology*, 186, 866–875.

Haile, R.W., Witte, J.S., Gold, M., Cressey, R., McGee, C., Millikan, R.C., Glasser, A., Harawa, N., Ervin, C., Harmon, P., Harper, J., Dermand, J., Alamillo, J., Barrett, K., Nides, M., Wang, G. (1999). The health effects of swimming in ocean water contaminated by storm drain runoff. *Epidemiology*, 10, 355–363.

Kolpin, D.W., Furlong, E.T., Meyer, M.T., Thurman, E.M., Zaugg, S.D., Barber, L.B., Buxton, H.T. (2002). Pharmaceuticals, hormones, and other organic wastewater contaminants in U.S. streams, 1999-2000: a national reconnaissance. Environmental Science & Technology, 36, 1202–1211.

Petras, D., Minich, J.J., Cancelada, L.B., Torres, R.R., Kunselman, E.K., Wang, M., White, M.E., Allen, E.E., Prather, K.A., Aluwihare, L.I., Dorrestein, P.C. (2021). Non-targeted tandem mass spectrometry enables the visualization of organic matter chemotype shifts in coastal seawater. *Chemosphere*, 271, 129450.

Griffin, D.W., Donaldson, K.A., Paul, J.H., Rose, J.B. (2003). Pathogenic human viruses in coastal waters. *Clinical Microbiology Reviews*, 16(1), 129–143.

Gersberg, R.M., Rose, M.A., Robles-Sikisaka, R., Dhar, A.K. (2006). Quantitative detection of hepatitis a virus and enteroviruses near the United States-Mexico border and correlation with levels of fecal indicator bacteria. *Applied and Environmental Microbiology*, 72(12), 7438-7444.

Boehm, A.B., Yamahara, K.M., Love, D.C., Peterson, B.M., McNeill, K., Nelson, K.L. (2009). Covariation and photoinactivation of traditional and novel indicator organisms and human viruses at a sewage-impacted marine beach. *Environmental Science & Technology*, 43(21), 8046–8052.

Council Resolution R-2022-79. Council of the City of San Diego. 2021. available at: https://sandiego.hylandcloud.com/211agendaonlinecouncil/Documents/ViewDocument/R-2022-79_Sep_TJ_Emergency?meetingId=4550&documentType=Minutes&itemId=201741&publishId=520641&isSection=false. Date of access: 2021 October 8

Steele, J.A., Blackwood, A.D., Griffith, J.F., Noble, R.T., Schiff, K.C. (2018). Quantification of pathogens and markers of fecal contamination during storm events along popular surfing beaches in San Diego, California. *Water Research*, 136(2), 137-149.

Orozco-Borbón, M.V., Rico-Mora, R., Weisberg, S.B., Noble, R.T., Dorsey, J.H., Leecaster, M.K., McGee, C.D. (2206). Bacteriological water quality along the Tijuana–Ensenada, Baja California, México shoreline. *Marine Pollution Bulletin*, 52, 1190–1196.

Zimmer-Faust, A.G., Steele, J.A., Xiong, X., Staley, C., Griffith, M., Sadowsky, M.J., Diaz, M., Griffith, J.F. (2021). A combined digital PCR and next generation DNA-sequencing based approach for tracking nearshore pollutant dynamics along the Southwest United States/Mexico Border. *Frontiers in Microbiology*, 12, 674214.

Feddersen, F., Boehm, A.B., Giddings, S.N., Wu, X., Liden, D. (2021). Modeling untreated wastewater evolution and swimmer illness for four wastewater infrastructure scenarios in the San Diego-Tijuana (US/MX) border region. *Geohealth*, 5, e2021GH000490.

Smith, J.E., Fry, W. "Tijuana sewage pounded South Bay beaches last year. EPA says help is on the way". San Diego Union-Tribune 2021. (accessed 12 April 2022)

Curriero, F.C., Patz, J.A., Rose, J.B., Lele, S. (2001). The association between extreme precipitation and waterborne disease outbreaks in the United States, 1948–1994. *American Journal of Public Health*, 91, 1194–1199.

Pendergraft, M.A. Grimes, D.J., Giddings, S.N., Feddersen, F., Beall, C.M., Lee, C., Santander, M.V., Prather, K.A. (2021). Airborne transmission pathway for coastal water pollution. *PeerJ*, 9, e11358.

Lewis, E.R., Schwartz, S.E. (2004). Sea Salt Aerosol Production: Mechanisms, Methods, Measurements, and Models; American Geophysical Union: New York, USA.

Baylor, E.R., Baylor, M.B., Blanchard, D.C., Syzdek, L.D., Appel, C. (1977). Virus transfer from surf to wind. *Science*, 198, 575–580.

Quinn, P.K., Collins, D.B., Grassian, V.H., Prather, K.A., Bates, T. S. (2015). Chemistry and related properties of freshly emitted sea spray aerosol. *Chemical Reviews*, 115(10), 4383–4399.

Blanchard, D.C., Syzdek, L. (1970). Mechanism for the water-to-air transfer and concentration of bacteria. *Science*, 170(3958), 626–628.

Aller, J.Y., Kuznetsova, M.R., Jahns, C.J., Kemp, P.F. (2005). The sea surface microlayer as a source of viral and bacterial enrichment in marine aerosols. *Journal of Aerosol Science*, 36(5-6), 801–812.

Wurl, O., Wurl, E., Miller, L., Johnson, K., Vagle, S. (2011). Formation and global distribution of sea-surface microlayers. *Biogeosciences*, 8, 121–135.

Wu, X., Feddersen, F., Giddings, S.N. (2021). Diagnosing surfzone impacts on inner-shelf flow spatial variability using realistic model experiments with and without surface gravity waves. *Journal of Physical Oceanography*, doi.org/10.1175/jpo-d-20-0324.1

van Eijk, A.M.J., Kusmierczyk-Michulec, J.T., Francius, M.J., Tedeschi, G., Piazzola, J., Merrittm D.L., Fontana, J.D. (2011). Sea-spray aerosol particles generated in the surf zone. *Journal of Geophysical Research Atmospheres*, 116(19), 1-20.

Cancelada, L., Torres, R.R., Luna, J.G., Dorrestein, P.C., Aluwihare, L.I., Prather, K.A., Petras, D. (2022). Assessment of styrene-divinylbenzene polymer (PPL) solid-phase extraction and non-targeted tandem mass spectrometry for the analysis of xenobiotics in seawater. *Limnology and Oceanography: Methods*, 20, 89–101.

Minich, J.J., Zhu, Q., Janssen, S., Hendrickson, R., Amir, A., Vetter, R., Hyde, J., Doty, M.M., Stillwell, K., Benardini, J., Kim, J.H., Allen, E.E., Venkateswaran, K., Knight, R. (2018). KatharoSeq enables high-throughput microbiome analysis from low-biomass samples. *mSystems*, 3.

Bolyen, E., Rideout, J.R., Dillon, M.R., Bokulich, N.A., Abnet, C.C., Al-Ghalith, G.A., Alexander, H., Alm, E.J., Arumugam, M., Asnicar, F., Bai, Y., Bisanz, J.E., Bittinger, K., Brejnrod, A., Brislawn, C.J., Brown, C.T., Callahan, B.J., Caraballo-Rodríguez, A.M., Chase, J., Cope, E.K., DaSilva, R., Diener, C., Dorrestein, P.C., Douglas, G.M., Durrall, D.M., Duvallet, C., Edwardson, C.F., Ernst, M., Estaki, M., Fouquier, J., Gauglitz, J.M., Gibbons, S.M., Gibson, D.L., Gonzalez, A., Gorlick, K., Guo, J., Hillmann, B., Holmes, S., Holste, H., Huttenhower, C., Huttley, G.A., Janssen, S., Jarmusch, A.K., Jiang, L., Kaehler, B.D., Kang, K.B., Keefe, C.R., Keim, P., Kelley, S.T., Knights, D., Koester, I., Kosciolek, T., Kreps, J., Langille, M.G.I., Lee, J., Ley, R., Liu, Y.-X., Lotfield, E., Lozupone, C., Maher, M., Marotz, C., Martin, B.D., McDonald, D., McIver, L.J., Melnik, A.V., Metcalf, J.L., Morgan, S.C., Morton, J.T., Naimey, A.T., Navas-Molina, J.A., Nothias, L.F., Orchanian, S.B., Pearson, T., Peoples, S.L., Petras, D., Preuss, M.L., Pruesse, E., Rasmussen, L.B., Robeson 2nd, M.S., Rosenthal, P., Segata, N., Shaffer, M., Shiffer, A., Sinha, R., Song, S.J., Spear, J.R., Swafford, A.D., Thompson, L.R., Torres, P.J., Trinh, P., Tripathi, A., Turnbaugh, P.J., Ul-Hassan, S., vander Hooft, J.J.J., Vargas, F., Vazquez-Baeza, Y., Vogtmann, E., von Hippel, M., Walters, W., Wan, Y., Wang, M., Warren, J., Weber, K.C., Williamson, C.H.D., Willis, A.D., Xu, Z.Z., Zaneveld, J.R., Zhang, Y., Zhu, Q., Knight, R., Caporaso, J. G. (2019). Reproducible, interactive, scalable and extensible microbiome data science using QIIME 2. *Nature Biotechnology*, 37(8), 852–857.

Gonzalez, A., Navas-Molina, J.A., Kosciolek, T., McDonald, D., Vázquez-Baeza, Y., Ackermann, G., DeReus, J., Janssen, S., Swafford, A.D., Orchanian, S.B., Sanders, J.G., Shorenstein, J., Holste, H., Petrus, S., Robbins-Pianka, A., Brislawn, C.J., Wang, M., Rideout, J.R., Bolyen, E., Dillon, M., Caporaso, J.G., Dorrestein, P.C., Knight, R. (2018). Qiita: rapid, web-enabled microbiome meta-analysis. *Nature Methods*, 15(10), 796–798.

McDonald, D., Price, M.N., Goodrich, J., Nawrocki, E.P., DeSantis, T.Z., Probst, A., Andersen, G.L., Knight, R., Hugenholtz, P. (2012). An improved Greengenes taxonomy with explicit ranks for ecological and evolutionary analyses of bacteria and archaea. *ISME Journal*, 6, 610–618.

Amir, A., McDonald, D., Navas-Molina, J.A., Kopylova, E., Morton, J.T., Zech Xu, Z., Kightley, E.P., Thompson, L.R., Hyde, E.R., Gonzalez, A., Knight, R. (2017). Deblur rapidly resolves single-nucleotide community sequence patterns. mSystems, 2(2). doi.org/10.1128/mSystems.00191-16

Schmid, R., Petras, D., Nothias, L.F., Wang, M., Aron, A.T., Jagels, A., Tsugawa, H., Rainer, J., Garcia-Aloy, M., Duhrkop, M., Korf, A., Pluskal, T., Kamenik, Z., Jarmusch, A.K., Caraballo-Rodriguez, A.M., Weldon, K.C., Nothias-Esposito, M., Akssenov, A.A., Bauermeister, A., Albarracin Orio, A., Grundmann, C.O., Vargas, F., Koester, I., Gauglitz, J.M., Gentry, E.C., Hovelmann, Y., Kalinina, S.A., Pendergraft, M.A., Panitchpakdi, M., Tehan, R., Le Gouellec, A., Aleti, G., Mannochio Russo, H., Arndt, B., Hubner, F., Hayen, H., Zhi, H. Raffatellu, M., Prather, K.A., Aluwihare, L.I., Bocker, S., McPhail, K.L., Humpf, H.U., Karst, U., Dorrestein, P.C. (2021). Ion identity molecular networking for mass spectrometry-based metabolomics in the GNPS environment. *Nature Communications*, 12, 3832.

Sumner, L. W.; Amberg, A.; Barrett, D.; Beale, M. H.; Beger, R.; Daykin, C. A.; Fan, T. W.-M.; Fiehn, O.; Goodacre, R.; Griffin, J. L.; Hankemeier, T.; Hardy, N.; Harnly, J.; Higashi, R.; Kopka, J.; Lane, A. N.; Lindon, J. C.; Marriott, P.; Nicholls, A. W.; … Viant, M. R.. Proposed minimum reporting standards for chemical analysis Chemical Analysis Working Group (CAWG) Metabolomics Standards Initiative (MSI). Metabolomics 2007, 3, 211–221.

Sumner, L.W., Amberg, A., Barrett, D., Beale, M.H., Beger, R., Daykin, C.A., Fan, T.W., Fiehn, O., Goodacre, R., Griffin, J.L., Hankemeier, T., Hardy, N., Harnly, J., Higashi, R., Kopka, J., Lane, A.N., Lindon, J.C., Marriott, P., Nicholls, A.W., Reily, M.D., Thaden, J.J., Viant, M.R. (2007). Proposed minimum reporting standards for chemical analysis Chemical Analysis Working Group (CAWG) Metabolomics Standards Initiative (MSI). Metabolomics. 3(3), 211-221. doi.org/10.1007/s11306-007-0082-2

Schymanski, E.L., Jeon, J., Gulde, R., Fenner, K., Ruff, M., Singer, H.P., Hollender, J. (2014). Identifying small molecules via high resolution mass spectrometry: communicating confidence. *Environmental Science & Technology*, 48, 2097–2098.

Knights, D., Kuczynski, J., Charlson, E.S., Zaneveld, J., Mozer, M.C., Collman, R.G., Bushman, F.D., Knight, R., Kelley, S.T. (2011). Bayesian community-wide culture-independent microbial source tracking. *Nature Methods*, 8, 761–763.

Stohl, A. (2003). A backward modeling study of intercontinental pollution transport using aircraft measurements. *Journal of Geophysical Research*, 108.

Stohl, A., Hittenberger, M., Wotawa, G. (1998). Validation of the lagrangian particle dispersion model FLEXPART against large-scale tracer experiment data. *Atmospheric Environment*, 32, 4245–4264.

MATLAB. 9.10.0.1602886 (R2021a). The MathWorks Inc: Natick, USA, 2021.

Martino, C., Morton, J.T., Marotz, C.A., Thompson, L.R., Tripathi, A., Knight, R., Zengler, K. (2019). A novel sparse compositional technique reveals microbial perturbations. *mSystems*, 4.

Santander, M.V., Mitts, B.A., Pendergraft, M.A., Dinasquet, J., Lee, C., Moore, A.N., Cancelada, L.B., Kimble, K.A., Malfatti, F., Prather, K.A. (2021). Tandem fluorescence measurements of organic matter and bacteria released in sea spray aerosols. *Environmental Science & Technology*, 55, 5171–5179.

Shaffer, B.T., Lighthart, B. (1997). Survey of culturable airborne bacteria at four diverse locations in Oregon: urban, rural, forest, and coastal. *Microbial Ecology*, 34, 167–177.

Ho, H.T.K., Lipman, L.J.A., Gaastra, W. (2006). Arcobacter, what is known and unknown about a potential foodborne zoonotic agent! *Veterinary Microbiology*, 115, 1–13.

Fera, M.T., Maugeri, T.L., Gugliandolo, C., Beninati, C., Giannone, M., La Camera, E., Carbone, M. (2004). Detection of Arcobacter spp. in the coastal environment of the Mediterranean Sea. *Applied Environmental Microbiology*, 70, 1271–1276.

Collado, L., Inza, I., Guarro, J., Figueras, M.J. (2008). Presence of Arcobacter spp. in environmental waters correlates with high levels of fecal pollution. *Environmental Microbiology*, 10, 1635–1640.

Zhang, Y., Marrs, C.F., Simon, C., Xi, C. (2009). Wastewater treatment contributes to selective increase of antibiotic resistance among Acinetobacter spp. *Science of the Total Environment*, 407, 3702–3706.

Dijkshoorn, L., Nemec, A., Seifert, H. (2007). An increasing threat in hospitals: multidrug-resistant Acinetobacter baumannii. *Nature Reviews Microbiology*, 5, 939–951.

Wisplinghoff, H. Pseudomonas spp., Acinetobacter spp. and miscellaneous Gram-negative bacilli. In Infectious Diseases. Cohen, J.; Powderly, W. G.; Opal, S. M. Elsevier. 2017, 1579–1599.

Bernhard, A.E., Field, K.G. (2000). A PCR assay to discriminate human and ruminant feces on the basis of host differences in Bacteroides-Prevotella genes encoding 16S rRNA. *Applied Environmental Microbiology*, 66, 4571–4574.

Ahmed, W., Hughes, B., Harwood, V. (2016). Current status of marker genes of Bacteroides and related taxa for identifying sewage pollution in environmental waters. *Water*, 8, 231.

Klein, A.N., Frigon, D., Raskin, L. (2007). Populations related to Alkanindiges, a novel genus containing obligate alkane degraders, are implicated in biological foaming in activated sludge systems. *Environmental Microbiology*, 9, 1898–1912.

Weber, M.E., Blanchard, D.C., Syzdek, L.D. (1983). The mechanism of scavenging of waterborne bacteria by a rising bubble. *Limnology and Oceanography*, 28, 101–105.

Michaud, J.M., Thompson, L.R., Kaul, D., Espinoza, J.L., Richter, R.A., Xu, Z.Z., Lee, C., Pham, K.M., Beall, C.M., Malfatti, F., Azam, F., Knight, R., Burkart, M.D., Dupont, C. L., Prather, K.A. (2018). Taxon-specific aerosolization of bacteria and viruses in an experimental ocean-atmosphere mesocosm. *Nature Communications*, 9(1), 2017.

Papazian, S., D'Agostino, L.A., Sadiktsis, I., Froment, J., Bonnefille, B., Sdougkou, K., Xie, H., Athanassiadis, I., Budhavant, K., Dasari, S., Andersson, A., Gustafsson, Ö., Martin, J.W. (2022). Nontarget mass spectrometry and in silico molecular characterization of air pollution from the Indian subcontinent. *Communications Earth & Environment*, 3.

Postigo, C., Lopez de Alda, M.J., Viana, M., Querol, X., Alastuey, A., Artiñano, B., Barceló, D. (2009). Determination of drugs of abuse in airborne particles by pressurized liquid extraction and liquid chromatography-electrospray-tandem mass spectrometry. Analytical Chemistry, 81, 4382–4388.

Cecinato, A., Balducci, C., Nervegna, G. (2009). Occurrence of cocaine in the air of the World's cities. An emerging problem? A new tool to investigate the social incidence of drugs? *Science of the Total Environment*, 407, 1683–1690.

Johansson, J.H., Salter, M.E., Acosta Navarro, J.C., Leck, C., Nilsson, E.D., Cousins, I.T. (2019). Global transport of perfluoroalkyl acids via sea spray aerosol. *Environmental Science: Process & Impacts*, 21, 635–649.

Pierce, R.H., Henry, M.S., Blum, P.C., Lyons, J., Cheng, Y.S., Yazzie, D., Zhou, Y. (2003). Brevetoxin concentrations in marine aerosol: human exposure levels during a Karenia brevis harmful algal bloom. *Bulletin of Environmental Contamination and Toxicology*, 70, 161–165.

Backer, L.C., Kirkpatrick, B., Fleming, L.E., Cheng, Y.S., Pierce, R., Bean, J.A., Clark, R., Johnson, D., Wanner, A., Tamer, R., Zhou, Y., Baden, D.G. (2005). Occupational exposure to aerosolized brevetoxins during Florida red tide events: effects on a healthy worker population. *Environmental Health Perspectives*, 113, 644–649.

Patterson, J.P., Collins, D.B., Michaud, J.M., Axson, J.L., Sultana, C.M., Moser, T., Dommer, A. C., Conner, J., Grassian, V.H., Stokes, M.D., Deane, G.B., Evans, J.E., Burkart, M.D., Prather, K.A., Gianneschi, N.C. (2016). Sea spray aerosol structure and composition using cryogenic transmission electron microscopy. *ACS Central Science*, 2(1), 40–47.

Fannin, K.F., Gannon, J.J., Cochran, K.W., Spendlove, J.C. (1977). Field studies on coliphages and coliforms as indicators of airborne animal viral contamination from wastewater treatment facilities. *Water Research*, 11(2), 181-188.

Carducci, A., Arrighi, S., Ruschi, A. (1995). Detection of coliphages and enteroviruses in sewage and aerosol from an activated sludge wastewater treatment plant. *Letters in Applied Microbiology*, 21(3), 207-209.

Malakootian, M., Radhakrishna, N., Mazandarany, M.P., Hossaini, H. (2013). Bacterial-aerosol emission from wastewater treatment plant. *Desalination and Water Treatment*, 51(22–24), 4478-4488.

Brisebois, E., Veillette, M., Dion-Dupont, V., Lavoie, J., Corbeil, J., Culley, A., Duchaine, C. (2018). Human viral pathogens are pervasive in wastewater treatment center aerosols. *Journal of Environmental Sciences (China)*, 67(10), 45-53.

Ginn, O., Rocha-Melogno, L., Bivins, A., Lowry, S., Cardelino, M., Nichols, D., Tripathi, S.N., Soria, F., Andrade, M., Bergin, M., Deshusses, M.A., Brown, J. (2021). Detection and quantification of enteric pathogens in aerosols near open wastewater canals in cities with poor sanitation. *Environmental Science & Technology*, 55, 14758–14771.

Teltsch, B., Katzenelson, E. (1978). Airborne enteric bacteria and viruses from spray irrigation with wastewater. *Applied and Environmental Microbiology*, 35(2), 290-296.

Dueker, M.E., O'Mullan, G.D. (2014). Aeration remediation of a polluted waterway increases near-surface coarse and culturable microbial aerosols. *Science of the Total Environment*, 478, 184-189.

Graham, K.E., Prussin, A.J., 2nd, Marr, L.C., Sassoubre, L.M., Boehm, A. B. (2018). Microbial community structure of sea spray aerosols at three California beaches. *FEMS Microbiology Ecology*, 94(3). doi.org/10.1093/femsec/fiy005

Grimes, D.J., Feddersen, F., Giddings, S.N., Pawlak, G. (2020). Cross-shore deformation of a surfzone released dye plume by an internal tide on the inner-shelf. *Journal of Physical Oceanography*, 50(1), 35-54.

Rodriguez, A.R., Giddings, S.N., Kumar, N. (2018). Impacts of nearshore wave-current interaction on transport and mixing of small-scale buoyant plumes. *Geophysical Research Letters*, 45(16), 8379-8389.

Rocha, A.Y., Verbyla, M.E., Sant, K.E., Mladenov, N. (2022). Detection, quantification, and simplified wastewater surveillance model of SARS-CoV-2 RNA in the Tijuana River. *ACS ES&T Water*, 2(11), 2134–2143.

Weiss, S., Xu, Z.Z., Peddada, S., Amir, A., Bittinger, K., Gonzalez, A., Lozupone, C., Zaneveld, J.R., Vázquez-Baeza, Y., Birmingham, A., Hyde, E.R., Knight, R. (2017). Normalization and microbial differential abundance strategies depend upon data characteristics. *Microbiome*, 5, 27.

Wulff, J., Mitchell, M.A. (2018). Comparison of various normalization methods for LC/MS metabolomics data. *Advances in Bioscience and Biotechnology*, 9(8), 339-351.

Hernandez, D. (2017). 143 Million Gallons of Sewage Spill into Tijuana River. San Diego Union Tribune. (accessed 6 June 2018).

Supplementary References

1. Zimmer-Faust, A.G., Steele, J.A., Xiong, X., Staley, C., Griffith, M., Sadowsky, M.J., Diaz, M., Griffith, J.F. (2021). A combined digital PCR and next generation DNA-sequencing based approach for tracking nearshore pollutant dynamics along the Southwest United States/Mexico Border. *Frontiers in Microbiology*, 12, 674214.

2. Barboza, K., Cubillo, Z., Castro, E., Redondo-Solano, M., Fernandez-Jaramillo, H., Arias Echandi, M.L. (2017). First isolation report of Arcobacter cryaerophilus from a human diarrhea sample in Costa Rica. *Revista do Instituto de Medicina Tropical de São Paulo*, 59, e72.

3. Collado, L., Figueras, M.J. (2011). Taxonomy, epidemiology, and clinical relevance of the genus Arcobacter. *Clinical Microbiology Reviews*, 24, 174–192.

4. Numberger, D., Ganzert, L., Zoccarato, L., Mühldorfer, K., Sauer, S., Grossart, H.-P., Greenwood, A.D. (2019). Characterization of bacterial communities in wastewater with enhanced taxonomic resolution by full-length 16S rRNA sequencing. *Scientific Reports*, 9, 9673.

5. Encyclopedia of Food Microbiology (2014). doi:10.1016/c2009-1-61842-6.

6. Lowry, R., Balboa, S., Parker, J.L., Shaw, J.G. (2014). Aeromonas flagella and colonisation mechanisms. *Advances in Microbial Physiology*, 65, 203–256.

7. Wisplinghoff, H. Pseudomonas spp., Acinetobacter spp. and miscellaneous Gram-negative bacilli. In Infectious Diseases. Cohen, J.; Powderly, W. G.; Opal, S. M. Elsevier. 2017, 1579–1599.

8. Guérin, C., Lee, B.-H., Fradet, B., Dijk, E. v., Mirauta, B. (2021). Transcriptome architecture and regulation at environmental transitions in flavobacteria: the case of an important fish pathogen. *ISME Communications*, 1.

9. Bergey's Manual of Systematics of Archaea and Bacteria. (2015). doi:10.1002/9781118960608.

10. Pham, D.N.; Clark, L., Li, M. (2021). Microplastics as hubs enriching antibiotic-resistant bacteria and pathogens in municipal activated sludge. *Journal of Hazardous Materials Letters*, 2, 100014.

11. Bergan, T. (1981). Human- and animal-pathogenic members of the genus Pseudomonas. The Prokaryotes, 666–700. doi:10.1007/978-3-662-13187-9_59.

12. Amann, R., Ludwig, W., Schulze, R., Spring, S., Moore, E., Schleifer, K.-H. (1996). rRNA-targeted oligonucleotide probes for the identification of genuine and former Pseudomonads. *Systematic and Applied Microbiology*, 19, 501–509.

13. Kämpfer, P., Schulz, R., Jäckel, U., Malik, A.K., Aman, R.; Spring, S. (2005).

Hydrogenophaga defluvii sp. nov. and Hydrogenophaga atypica sp. nov.; isolated from activated sludge. *International Journal of Systematic and Evolutionary Microbiology*, 55, 341–344.

14. Li, W., Zheng, T., Ma, Y., Liu, J. (2020). Influences of flow conditions on bacterial communities in sewage and greywater small diameter gravity sewer biofilms. *Environmental Research*, 183, 109289.

15. Wolff, D., Krah, D., Dotsch, A., Ghattas, A.-K., Wick, A., Ternes, T.A. (2018). Insights into the variability of microbial community composition and micropollutant degradation in diverse biological wastewater treatment systems. *Water Research*, 143, 313–324.

16. Kalmbach, S. (2000). In situ probing reveals Aquabacterium commune as a widespread and highly abundant bacterial species in drinking water biofilms. *Water Research*, 34, 575–581.

17. Regalado, N.G., Martin, G., Antony, S.J. (2009). Acinetobacter lwoffii: bacteremia associated with acute gastroenteritis. *Travel Medicine and Infectious Disease*, 7, 316–317.

18. Kozińska, A., Paździor, E., Pękala, A., Niemczuk, W. (2014). Acinetobacter johnsonii and Acinetobacter lwoffii - the emerging fish pathogens. *Bulletin of the Veterinary Institute in Pulawy*, 58 193–199.

19. Lemaire, O.N.; Méjean, V., Iobbi-Nivol, C. (2020). The Shewanella genus: ubiquitous organisms sustaining and preserving aquatic ecosystems. *FEMS Microbiology Reviews*, 44, 155–170.

20. Vignier, N., Barreau, M., Olive, C., Baubion, B., Theodose, R., Hochedez, P., Cabié, A. (2013). Human infection with Shewanella putrefaciens and S. algae: report of 16 cases in Martinique and review of the literature. *American Journal Tropical Medicine Hygiene*, 89, 151–156.

21. Jones, R.L. (2000). Clostridial Enterocolitis. *Veterinary Clinics of North America: Equine Practice*, 16 471–485.

22. Labus, J.S. , Osadchiy, V., Hsiao, E.Y., Tap, J., Derrien, M., Gupta, A., Tillisch, K., Le Nevé, B., Grinsvall, C., Ljungberg, M., Öhman, L., Törnbom, H., Simren, M., Mayer, E.A. (2019). Evidence for an association of gut microbial Clostridia with brain functional connectivity and gastrointestinal sensorimotor function in patients with irritable bowel syndrome, based on tripartite network analysis. *Microbiome*, 7, 45.

23. Borriello, S.P. (1995). Clostridial disease of the gut. *Clinical Infectious Diseases*, 20 S242–S250.

24. Palleroni, N.J. (1981). Introduction to the family Pseudomonadaceae. The Prokaryotes, 655–665 doi:10.1007/978-3-662-13187-9_58.

25. Bennett, K.W., Eley, A. (1993). Fusobacteria: new taxonomy and related diseases.

Journal of Medical Microbiology, 39, 246–254.

26. Hong, P.-Y., Li, X., Yang, X., Shinkai, T., Zhang, Y., Wang, X., Mackie, R.I. (2012). Monitoring airborne biotic contaminants in the indoor environment of pig and poultry confinement buildings. *Environmental Microbiology*, 14, 1420–1431.

27. Guiry, M.D., Guiry, G.M., Morrison, L., Rindi, F., Miranda, S.V., Mathieson, A.C., Parker, B.C., Langangen, A., John, D.M., Barbara, I., Carter, C.F., Kuipers, P., Garbary, D.J. (2014). AlgaeBase: an on-line resource for algae. *Cryptogamie, Algologie*, 35(2), 105–115.

28. Vandepitte, L., Vanhoorne, B., Decock, W., Vranken, S., Lanssens, T., Dekeyzer, S., Verfaille, K., Horton, T., Kroh, A., Hernandez, F., Mees, J. (2018). A decade of the World Register of Marine Species - general insights and experiences from the Data Management Team: where are we, what have we learned and how can we continue? *PLoS One*, 13, e0194599.

29. Wexler, H.M. (2007). Bacteroides: the good, the bad, and the nitty-gritty. *Clinical Microbiology Reviews*, 20, 593–621.

30. Bernhard, A.E., Field, K.G. (2000). A PCR assay to discriminate human and ruminant feces on the basis of host differences in Bacteroides-Prevotella genes encoding 16S rRNA. *Applied Environmental Microbiology*, 66, 4571–4574.

31. Ahmed, W., Hughes, B., Harwood, V. (2016). Current status of marker genes of bacteroides and related taxa for identifying sewage pollution in environmental waters. *Water*, 8, 231.

32. Baek, K., Jeon, C.O. (2015). Rheinheimera aestuari sp. nov.; a marine bacterium isolated from coastal sediment. *International Journal of Systematic and Evolutionary Microbiology*, 65, 2640–2645.

33. Klein, A.N., Frigon, D., Raskin, L. (2007). Populations related to Alkanindiges, a novel genus containing obligate alkane degraders, are implicated in biological foaming in activated sludge systems. *Environmental Microbiology*, 9, 1898–1912.

34. Guðmundsdóttir, R., Kreiling, A.-K., Kristjánsson, B. K., Marteinsson, V. Þ., Pálsson, S. (2019). Bacterial diversity in Icelandic cold spring sources and in relation to the groundwater amphipod Crangonyx islandicus. *PLoS One*, 14, e0222527.

35. Erlacher, A., Cardinale, M., Grosch, R., Grube, M., Berg, G. (2014). The impact of the pathogen Rhizoctonia solani and its beneficial counterpart Bacillus amyloliquefaciens on the indigenous lettuce microbiome. *Frontiers in Microbiology*, 5, 175.

36. Carney, R.L., Mitrovic, S.M., Jeffries, T., Westhorpe, D., Curlevski, N., Seymour, J.R. (2015). River bacterioplankton community responses to a high inflow event. *Aquatic Microbial Ecology*, 75, 187–205.

37. Alfano, N., Tagliapietra, V., Rosso, F., Manica, M., Arnoldi, D., Pindo, M., Rizzoli, A. (2019). Changes in microbiota across developmental stages of Aedes koreicus, an invasive mosquito vector in Europe: indications for microbiota-based control strategies. *Frontiers in Microbiology*, 10.

38. Padakandla, S.R., Chae, J.-C. (2017). Reclassification of Aeromonas sharmana to a new genus as Pseudaeromonas sharmana gen. nov.; comb. nov.; and description of Pseudaeromonas pectinilytica sp. nov. isolated from a freshwater stream. *International Journal of Systematic and Evolutionary Microbiology*, 67, 1018–1023.

39. Wang, Z., Li, W., Li, H., Zheng, W., Guo, F. (2020). Phylogenomics of Rhodocyclales and its distribution in wastewater treatment systems. *Scientific Reports*, 10, 3883.

40. Willems, A. (2014). The Family Comamonadaceae. *The Prokaryotes*, 777–851 doi:10.1007/978-3-642-30197-1_238.

41. Ueki, A. (2006). Paludibacter propionicigenes gen. nov.; sp. nov.; a novel strictly anaerobic, Gram-negative, propionate-producing bacterium isolated from plant residue in irrigated rice-field soil in Japan. International Journal of Systematic and Evolutionary Microbiology, 56, 39–44.

42. McLellan, S.L., Huse, S.M., Mueller-Spitz, S.R., Andreishcheva, E.N., Sogin, M.L. (2010). Diversity and population structure of sewage-derived microorganisms in wastewater treatment plant influent. *Environmental Microbiology*, 12, 378–392.

43. van Esch, G.J. (2000). World Health Organization & International Program on Chemical Safety. Flame Retardants: Tris(2-butoxyethyl) Phosphate, Tris(2-ethylhexyl) Phosphate and Tetrakis(hydroxymethyl) Phosphonium Salts.

44. Kim, S. (2021). Exploring Chemical Information in PubChem. *Current Protocols*, 1, e217.

45. Pagel, H.A., McLafferty, F.W. (1948). Use of Tributyl Phosphate for Extracting Organic Acids from Aqueous Solution. *Analytical Chemistry*, 20, 272–272.

46. Davankov, V., Tsyurupa, M. (2011). Sorption of Organic Compounds from Aqueous Solutions. in *Comprehensive Analytical Chemistry*. Elsevier, 56, 411–444.

47. Marchetti, C., Brown, A.M. (1988). Protein kinase activator 1-oleoyl-2-acetyl-sn-glycerol inhibits two types of calcium currents in GH3 cells. *American Journal of Physiology*, 254, C206–10.

48. Sardar, S.W., Choi, Y., Park, N., Jeon, J. (2019). Occurrence and concentration of chemical additives in consumer products in Korea. *International Journal of Environmental Research and Public Health*, 16.

49. Tasselli, S., Guzzella, L. (2020). Polycyclic musk fragrances (PMFs) in wastewater and activated sludge: analytical protocol and application to a real case study. *Environmental Science and Pollution Research International*, 27, 30977–30986.

50. Friedli, F. (2001). Detergency of Specialty Surfactants. CRC Press: Boca Raton, USA.

51. Guedez, A.A., Frömmel, S., Diehl, P., Püttmann, W. (2010). Occurrence and temporal variations of TMDD in the river Rhine, Germany. *Environmental Science and Pollution Research International*, 17, 321–330.

52. Nagappayya, S.K., Gaikar, V.G. (2010). Extraction of aleuritic acid from seedlac and purification by reactive adsorption on functionalized polymers. *Industrial & Engineering Chemistry Research*, 49, 6547–6553.

53. Stone, D., Ross, S. (2014). At your fingertips: rapid retrieval of product information from the National Pesticide Information Center. *Proceedings of the Vertebrate Pest Conference*, 26.

54. den Hartigh, L.J. (2019). Conjugated linoleic acid effects on cancer, obesity, and atherosclerosis: a review of pre-clinical and human trials with current perspectives. *Nutrients*, 11.

55. Ricciotti, E.; FitzGerald, G. A. (2011). Prostaglandins and inflammation. *Arteriosclerosis, Thrombosis, and Vascular Biology*, 31, 986–1000

56. Takeshita, A., Igarishi-Migitaka, J., Takahashi, H., Takeushi, Y., Koibuchi, N. (2011). Acetyl tributyl citrate, the most widely used phthalate substitute plasticizer, induces cytochrome p450 3a through steroid and xenobiotic receptor. *Toxicological Sciences*, 123, 460–470.

57. Triphenylphosphine oxide, 99%, Thermo ScientificTM. https://www.thermofisher.com/order/catalog/product/A12455.36.

58. Maresz, K. (2015). Proper Calcium Use: Vitamin K2 as a Promoter of Bone and Cardiovascular Health. Journal of Integrative Medicine, 14, 34–39.

59. Amin, K.M., Abou-Seri, S.M., Awadallah, F.M., Eissa, A.A.M., Hassan, G.S., Abdulla, M.M. (2015). Synthesis and anticancer activity of some 8-substituted-7-methoxy-2H-chromen-2-one derivatives toward hepatocellular carcinoma HepG2 cells. *European Journal of Medicinal Chemistry*, 90, 221–231.

60. Brose, S.A., Thuen, B.T., Golovko, M.Y. (2011). LC/MS/MS method for analysis of E2 series prostaglandins and isoprostanes. *Journal of Lipid Research*, 52, 850–859.

61. Van Elssen, C.H.M.J., Vanderlocht, J., Oth, T., Senden-Gijsbers, B.L.M.G., Germeraad, W.T.V., Bos, G.M.J. (2011). Inflammation restraining effects of prostaglandin E2 on natural killer–dendritic cell (NK-DC) interaction are imprinted during DC maturation. *Blood*, 118, 2473–2482.

62. Ramanathan, R., Chowdhury, S.K., Alton, K.B. (2005). Chapter 10. Oxidative metabolites of drugs and xenobiotics: LC-MS methods to identify and characterize in biological matrices. In *Identification and Quantification of Drugs, Metabolites and Metabolizing Enzymes by LC-MS*, 225–276 doi.org/10.1016/s1464-3456(05)80012-2.

63. Duckworth, N., Marshall, K., Clayton, J.K. (2002). An investigation of the effect of the prostaglandin EP2 receptor agonist, butaprost, on the human isolated myometrium from pregnant and non-pregnant women. *Journal of Endocrinology*, 172, 263–269.

64. Consumer Product Safety Commission (CPSC). (2010). Overview of Phthalates Toxicity. U.S. CPSC, Bethesda, MD 20814. https://www.cpsc.gov/s3fs-public/phthalover.pdf.

65. Schänzer, W., Opfermann, G., Donike, M. (1990). Metabolism of stanozolol: identification and synthesis of urinary metabolites. *The Journal of Steroid Biochemistry and Molecular Biology*, 36, 153–174.

66. Santa Cruz Biotechnology. 17-phenyl trinor Prostaglandin A2. https://www.scbt.com/p/17-phenyl-trinor-prostaglandin-a2-38315-51-4.

67. Knothe, G. (2012). Fuel properties of highly polyunsaturated fatty acid methyl esters. Prediction of fuel properties of algal biodiesel. *Energy & Fuels*, 26, 5265–5273.

68. Zempleni, J., Mock, D.M. (1999). Biotin biochemistry and human requirements. *Journal of Nutritional Biochemistry*, 10, 128–138.

69. Tsukamoto, S., Kato, H., Hirota, H., Fusetani, N. (1999). Lumichrome. A larval metamorphosis-inducing substance in the ascidian Halocynthia roretzi. *European Journal of Biochemistry*, 264, 785–789.

70. Sulistiyani, S., Adelman, J., Chandrasekaran, A., Jayo, J., St. Clair, R.W. (1995). Effect of 17α-dihydroequilin sulfate, a conjugated equine estrogen, and ethynylestradiol on atherosclerosis in cholesterol-fed rabbits. *Arteriosclerosis, Thrombosis, and Vascular Biology*, 15, 837–846.

71. 13,14-dihydro-15-keto Prostaglandin F1α (CAS 29044-75-5). https://www.caymanchem.com/product/15670.

72. Gonzalez, A., Navas-Molina, J.A., Kosciolek, T., McDonald, D., Vázquez-Baeza, Y., Ackermann, G., DeReus, J., Janssen, S., Swafford, A.D., Orchanian, S.B., Sanders, J.G., Shorenstein, J., Holste, H., Petrus, S., Robbins-Pianka, A., Brislawn, C.J., Wang, M., Rideout, J.R., Bolyen, E., Dillon, M., Caporaso, J.G., Dorrestein, P.C., Knight, R. (2018). Qiita: rapid, web-enabled microbiome meta-analysis. *Nature Methods*, 15(10), 796–798.

73. Horel, J., Splitt, M., Dunn, L., Pechmann, J., White, B., Ciliberti, C., Lazarus, S., Slemmer, J., Zaff, D., Burks, J. (2002). Mesowest: Cooperative Mesonets in the Western United States. *Bulletin of the American Meteorological Society*, 83, 211–225.

74. Horel, J., Potter, T., Dunn, L., Steenburgh, W.J., Eubank, M., Splitt, M., Onton, D.J. (2002). Weather support for the 2002 Winter Olympic and Paralympic Games. *Bulletin of the American Meteorological Society*, 83, 227–240.

75. Petras, D., Loester, I., Da Silva, R., Stephens, B.M., Haas, A.F., Nelson, C.E., Kelly, L.W., Aluwihare, L.I., Dorrestein, P.C. (2017). High-resolution liquid chromatography tandem mass spectrometry enables large scale molecular characterization of dissolved organic matter. *Frontiers in Marine Science*, 4.

76. Schmid, R., Petras, D., Nothias, L.F., Wang, M., Aron, A.T., Jagels, A., Tsugawa, H., Rainer, J., Garcia-Aloy, M., Duhrkop, M., Korf, A., Pluskal, T., Kamenik, Z., Jarmusch, A.K., Caraballo-Rodriguez, A.M., Weldon, K.C., Nothias-Esposito, M., Akssenov, A.A., Bauermeister, A., Albarracin Orio, A., Grundmann, C.O., Vargas, F., Koester, I., Gauglitz, J.M., Gentry, E.C., Hovelmann, Y., Kalinina, S.A., Pendergraft, M.A., Panitchpakdi, M., Tehan, R., Le Gouellec, A., Aleti, G., Mannochio Russo, H., Arndt, B., Hubner, F., Hayen, H., Zhi, H. Raffatellu, M., Prather, K.A., Aluwihare, L.I., Bocker, S., McPhail, K.L., Humpf, H.U., Karst, U., Dorrestein, P.C. (2021). Ion identity molecular networking for mass spectrometry-based metabolomics in the GNPS environment. *Nature Communications*, 12, 3832.

77. Nothias, L.-F., Petras, D., Schmid, R., Dührkop, K., Rainer, J., Sarvepalli, A., Protsyuk, I., Ernst, M., Tsugawa, H., Fleischauer, M., Aicheler, F., Aksenov, A. A., Alka, O., Allard, P.-M., Barsch, A., Cachet, X., Caraballo-Rodriguez, A. M., Da Silva, R. R., Dang, T., Garg, N., Gauglitz, J.M., Gurevich, A., Isaac, G., Jarmusch, A.K., Kameník, Z., Kang, K.B., Kessler, N., Koester, I., Korf, A., Le Gouellec, A., Ludwig, M., Martin H., C., McCall, L.-I., McSayles, J., Meyer, S.W., Mohimani, H., Morsy, M., Moyne, O., Neumann, S., Neuweger, H., Nguyen, N.H., Nothias-Esposito, M., Paolini, J., Phelan, V.V., Pluskal, T., Quinn, R.A., Rogers, S., Shrestha, B., Tripathi, A., van der Hooft, J.J.J, Vargas, F., Weldon, K.C., Witting, M., Yang, H., Zhang, Z., Zubeil, F., Kohlbacher, O., Böcker, S., Alexandrov, T., Bandeira, N., Wang, M., Dorrestein, P.C. (2020). Feature-based molecular networking in the GNPS analysis environment. Nature Methods, 17(9), 905–908. doi.org/10.1038/s41592-020-0933-6

78. Bolyen, E., Rideout, J.R., Dillon, M.R., Bokulich, N.A., Abnet, C.C., Al-Ghalith, G.A., Alexander, H., Alm, E.J., Arumugam, M., Asnicar, F., Bai, Y., Bisanz, J.E., Bittinger, K., Brejnrod, A., Brislawn, C.J., Brown, C.T., Callahan, B.J., Caraballo-Rodríguez, A.M., Chase, J., Cope, E.K., DaSilva, R., Diener, C., Dorrestein, P.C., Douglas, G.M., Durrall, D.M., Duvallet, C., Edwardson, C.F., Ernst, M., Estaki, M., Fouquier, J., Gauglitz, J.M., Gibbons, S.M., Gibson, D.L., Gonzalez, A., Gorlick, K., Guo, J., Hillmann, B., Holmes, S., Holste, H., Huttenhower, C., Huttley, G.A., Janssen, S., Jarmusch, A.K., Jiang, L., Kaehler, B.D., Kang, K.B., Keefe, C.R., Keim, P., Kelley, S.T., Knights, D., Koester, I., Kosciolek, T., Kreps, J., Langille, M.G.I., Lee, J., Ley, R., Liu, Y.-X., Lotfield, E., Lozupone, C., Maher, M., Marotz, C., Martin, B.D., McDonald, D., McIver, L.J., Melnik, A.V., Metcalf, J.L., Morgan, S.C., Morton, J.T., Naimey, A.T., Navas-Molina, J.A., Nothias, L.F., Orchanian, S.B., Pearson, T., Peoples, S.L., Petras, D., Preuss, M.L., Pruesse, E., Rasmussen, L.B., Robeson 2nd, M.S., Rosenthal, P., Segata, N., Shaffer, M., Shiffer, A., Sinha, R., Song, S.J., Spear, J.R., Swafford, A.D., Thompson, L.R., Torres, P.J., Trinh, P., Tripathi, A., Turnbaugh, P.J., Ul-Hassan, S., vander Hooft, J.J.J., Vargas, F., Vazquez-Baeza, Y., Vogtmann, E., von Hippel, M., Walters, W., Wan, Y., Wang, M.,

Warren, J., Weber, K.C., Williamson, C.H.D., Willis, A.D., Xu, Z.Z., Zaneveld, J.R., Zhang, Y., Zhu, Q., Knight, R., Caporaso, J. G. (2019). Reproducible, interactive, scalable and extensible microbiome data science using QIIME 2. *Nature Biotechnology*, 37(8), 852–857.

79. Minich, J.J., Humphrey, G., Benitez, R.A.S., Sanders, J., Swafford, A., Allen, E.E., Knight, R. (2018b). High-throughput miniaturized 16S rRNA amplicon library preparation reduces costs while preserving microbiome integrity. mSystems, 3(6). doi.org/10.1128/msystems.00166-18.

80. Thompson, L.R., Sanders, J.G., McDonald, D., Amir, A., Ladau, J., Locey, K.J., Prill, R.J., Tripathi, A., Gibbons, S.M., Ackermann, G., Navas-Molina, J.A., Janssen, S., Kopylova, E., Vázquez-Baeza, Y., González, A., Morton, J.T., Mirarab, S., Xu, Z.Z., Jiang, L., Haroon, M.F., Kanbar, J., Zhu, Q., Song, S.E., Kosciolek, T., Bokulich, N.A., Lefler, J., Brislawn, C.J., Humphrey, G., Owens, S.M., Hampton-Marcell, J., Berg-Lyons, D., McKenzie, V., Fierer, N., Fuhrman, J.A., Clauset, A., Stevens, R.L., Shade, A., Pollard, K.S., Goodwin, K.D., Jansson, J.K., Gilbert, J.A., Knight, R., The Earth Microbiome Project Consortium. (2017). A communal catalogue reveals Earth's multiscale microbial diversity. *Nature*, 551(7681), 457–463. doi.org/10.1038/nature24621

81. Davis, N.M., Proctor, D.M., Holmes, S.P., Relman, D.A., Callahan, B.J. (2018). Simple statistical identification and removal of contaminant sequences in marker-gene and metagenomics data. *Microbiome*, 6, 1–14.

82. Martino, C., Morton, J.T., Marotz, C.A., Thompson, L.R., Tripathi, A., Knight, R., Zengler, K. (2019). A novel sparse compositional technique reveals microbial perturbations. *mSystems*, 4.

83. Stohl, A., Forster, C., Frank, A., Seibert, P., Wotawa, G. (2005). Technical note: The Lagrangian particle dispersion model FLEXPART version 6.2. *Atmospheric Chemistry and Physics*, 5, 2461–2474.

84. Hager, S.W., Atlas, E.L., Gordon, L.I., Mantyla, A.W., Park, P.K. (1972). A comparison at sea of manual and autoanalyzer analyses of phosphate, nitrate, and silicate1. *Limnology & Oceanography*, 17, 931–937.

85. Atlas, E.L., Hager, S.W., Gordon, L.I., Kilho Park, P. (1971). Oregon State University Corvallis Department of Oceanography. A practical manual for use of the technicon autoanalyzer in seawater nutrient analyses; revised.

86. Becker, S. et al. (2019). GO-SHIP Repeat Hydrography Nutrient Manual: The precise and accurate determination of dissolved inorganic nutrients in seawater, using Continuous Flow Analysis methods. doi:10.25607/OBP-555.

87. Noble, R.T., Fuhrman, J.A. (1998). Use of SYBR Green I for rapid epifluorescence counts of marine viruses and bacteria. *Aquatic Microbial Ecology*, 14, 113-118.

88. SIO-CalCOFI. Scripps Institution of Oceanography. California Cooperative Oceanic Fisheries Investigations Technical Group. Chlorophyll Methods. https://calcofi.org/references/methods/8-chlorophyll-methods.html.

89. Sousa, M.L. (2020). Assessing promising bioactivity of cyanobacterial strains on a 3D in vitro model of solid tumours. Mechanisms in physiologically relevant 3D cell culture. https://repositorio-aberto.up.pt/bitstream/10216/126888/2/393006.pdf

90. Cancelada, L., Torres, R.R., Luna, J.G., Dorrestein, P.C., Aluwihare, L.I., Prather, K.A., Petras, D. (2022). Assessment of styrene-divinylbenzene polymer (PPL) solid-phase extraction and non-targeted tandem mass spectrometry for the analysis of xenobiotics in seawater. *Limnology and Oceanography: Methods*, 20, 89–101.

91. Amir, A., McDonald, D., Navas-Molina, J.A., Kopylova, E., Morton, J.T., Zech Xu, Z., Kightley, E.P., Thompson, L.R., Hyde, E.R., Gonzalez, A., Knight, R. (2017). Deblur rapidly resolves single-nucleotide community sequence patterns. mSystems, 2(2). doi.org/10.1128/mSystems.00191-16

92. Gasol, J.M., Del Giorgio, P.A. (2000). Using flow cytometry for counting natural planktonic bacteria and understanding the structure of planktonic bacterial communities, *Scientia Marina*, 197–224. doi:10.3989/scimar.2000.64n2197.

Chapter 6. Conclusions

6.1 Synopsis

This dissertation investigates the aerosolization of bacteria and associated chemical compounds in sea spray aerosol in the field and laboratory and under varying seawater conditions. Chapter 2 illustrates how the enzyme activity of SSA is qualitatively distinct from the enzyme activity of its source waters. Chapter 3 demonstrates that distinct bacteria communities in seawater produce different bacteria communities in SSA. Chapter 4 uses a water pollution mimic to simulate coastal water pollution in the environment at full scale and demonstrates the potential for CWP to transfer to the atmosphere in SSA. Chapter 5 uses bacterial and chemical signals to identify CWP aerosolizing in sea spray aerosol.

6.2 Conclusions

6.2.1 Enhanced Lipase and Alkaline Phosphatase Enzyme Activities in Sea Spray Aerosol

This study demonstrated qualitative differences between the enzyme activities of sea spray aerosol and its source waters. Phytoplankton blooms were stimulated with nutrient addition to Southern California coastal waters. Nascent, isolated SSA was generated from isolated source waters using the MART (Stokes et al., 2013). Enzyme activities in seawater and sea spray aerosol were tracked using the fluorogenic substrate method (Hoppe, 1983; Malfatti & Lee et al., 2019; Martinez et al., 1996). In the seawater, aminopeptidase activity was consistently much stronger than lipase activity, in agreement with previous observations (Arnosti, 2011; Martinez et al., 1996; Smith et al., 1992). In the SSA, lipase and aminopeptidase showed similar activities, with higher lipase activity in 2 of three experiments. Comparing lipase:aminopeptidase ratios across water and aerosol revealed consistent lipase enhancement in SSA across all three

experiments. Alkaline phosphatase activity also showed enrichment in SSA across all three experiments. Whereas aminopeptidase activity accounted for 82% of total EA in SW, alkaline phosphatase, lipase, and aminopeptidase show similar activities in SSA. Possible mechanisms include selective transfer of bacteria with cell-bound enzymes and/or selective transfer of free enzymes into SSA, such as lipases embedded in lipids that enrich in SSA.

6.2.2 Advances in Sea Spray Aerosol 16S Sequencing Reveal a Dynamic Community

In this research, a low biomass 16S amplicon sequencing workflow was coupled to high efficiency aerosol collection in order to improve the sensitivity of sequencing the bacteria in SSA. The amplicon sequencing methodology uses contamination in positive controls to estimate contamination in the workflow and to establish a minimum read cutoff for accepting or rejecting sequencing results, on a sample by sample basis. Sequencing detection limits were achieved at $4.1x10^6$ supermicron SSA and 1046 heterotrophic bacteria in SSA. A correlation of $R^2=0.7170$ was found between sequencing reads and bacteria cell counts in SSA determined by flow cytometry, supporting the hypothesis that SSA sequencing success is determined by the amount of bacteria cells sequenced. In the resulting dataset, relationships were explored between the SSA and SW bacteria communities. It was found that both the SW and SSA communities differed across the three sampling rounds using three different water masses. This demonstrated for the first time that changes in the SW bacteria community produces changes in the SSA bacteria community.

Taxon specific aerosolization, which states that taxonomically similar bacteria have similar tendencies to aerosolize in SSA, was investigated as a possible mechanism. Bacteria can show constitutive (consistent) or intermittent (variable) aerosolization rates. TSA was found to

vary within taxa and across the three water masses investigated. Therefore different SSA communities emerging from different SW communities was the result of intermittent bacteria aerosolization. These findings are in agreement with the body of literature that shows many, variable aspects of SW and bacteria cells can influence the transfer rates of bacteria in SSA, including bacteria growth phase, cell surface hydrophobicity, and SW salinity (Harb et al., 2021; Hejkal et al., 1980; Schäfer et al., 1998).

6.2.3 Airborne Transmission Pathway for Coastal Water Pollution

This research investigated the potential of coastal water pollution (CWP) to transfer to the atmosphere in SSA. Three dye releases in the coastal waters of Imperial Beach, CA reproduced CWP events at full scale in the environment. Aerial imagery tracked the dye hourly at 2 m x 2 m spatial resolution over 5+ km of coastline. These observations of SW dye concentrations demonstrated pollution transport in the coastal waters, which varied significantly between the three dye releases. Aerosol sampling along the coast tested for the transfer of the dye in SSA. Dye release 2 rapidly transported the dye in the coastal waters out of the range for the aerosol sampling, and was valuable in demonstrating the extent of alongshore transport of CWP. Dye was detected for two days following dye releases 1 and 3, as far as 668 m inland and 720 m downwind of the source waters. Detecting a dye in the air that could only come from coastal waters provided a clear demonstration of the potential for CWP to transfer to the atmosphere in SSA and reach many people on land. These findings are in agreement with the well established ability of SSA to carry naturally occurring chemical compounds and microorganisms (Bertram et al., 2018; Quinn et al., 2015). Other research has identified natural toxins in the coastal air and anthropogenic compounds in SSA, but with unconstrained source regions (Cheng et al., 2005; Johansson et al., 2019). This research builds on that work by

identifying in the atmosphere an anthropogenic input released into coastal waters, with quantitative measurements of well-constrained source waters.

6.2.4 Bacterial and Chemical Evidence of Coastal Water Pollution from the Tijuana River in Sea Spray Aerosol

This investigation tested coastal aerosol for bacterial and chemical signs of CWP transferring to the atmosphere in SSA. The Tijuana River was sampled as a known source of pollution to the coastal waters of Tijuana, Mexico and Imperial Beach, USA. Coastal aerosol was sampled in IB during four periods of CWP following rains. Coastal water and aerosol were also sampled at Scripps Institution of Oceanography for the sake of comparison. 16S rRNA gene amplicon sequencing and non-targeted high resolution tandem mass spectrometry were used to describe the bacteria community and chemical composition of the TJR, coastal waters, and coastal aerosol. Robust Aitchinson principal component analysis showed compositional similarity between IB aerosol and the TJR. The SourceTracker2 Bayesian statistical method indicated up to 45% of chemical compounds and up to 82% of bacteria in IBa were shared with the TJR. Each aerosol sample was categorized as having come from the ocean, land, or mixed, by using local winds and the FLEXPART particle dispersion model. Features associated with the TJR were identified in IBa by comparing ST2 source apportionments and relative abundances between TJR and SIO waters. 16S reads and MS/MS peak areas were used for relative abundance estimates. This identified bacteria from the TJR in IBa from the ocean. Taxonomic assignments from GreenGenes for the top 40 bacteria included bacteria independently linked to the TJR and TJ sewage. The identified bacteria comprised up to 76% of the airborne bacteria community in IB. The MS/MS data identified chemical pollutants found both in the TJR and in IBa from the ocean, although they were not exclusive to that source. Previous work identified

bacteria evidence of possible CWP in coastal air, but without a clear source (Graham et al., 2018). The present study built upon that work by targeting a known source of CWP and detecting associated bacteria and chemicals in aerosols coming from the ocean that make significant contributions to coastal air.

6.3 Future Directions

6.3.1 Advancing Our Understanding of Enzyme Activity in SSA

Chapter 2 demonstrates that SSA has a distinct enzyme activity profile from that of its source waters. Investigations into enzymes and enzyme activity in SSA stand to benefit from advances in methodology. Conducting proteomics investigations of SSA could identify the diversity of enzymes present and provide a comparison between enzymes in SW and SSA. The successful application of non-targeted high resolution tandem mass spectrometry accomplished in Chapter 5 is encouraging for this endeavor. Coupling proteomics to size-resolved SSA sampling could be used to relate SSA enzyme composition to SSA particle size and indicate the relative importance of cell-attached enzymes vs. free enzymes in SSA. It is possible to measure the activities of enzymes isolated in a proteomics workflow, which could be applied to SSA (Mazzotta et al., 2020). But that approach would not get the total, *in situ* enzyme activity achieved by the fluorometric substrate method, and development of a novel method for that would be beneficial. Also worthy of further investigation is how marine microbial processes in the seawater affect bacteria aerosolization, explored in Chapters 2 and 3. Bacteria constitute a significant fraction of organic material in seawater but the fraction of SSA organic material they comprise is unknown (Cho & Azam, 1988). Furthermore, it would be interesting to see how fluctuations in the ratio of free-living bacteria to particle-attached bacteria in the SW could impact bacteria aerosolization. In addition, proteins and amino acids are important in ice

nucleation (Hudait et al., 2018). Marine proteases, other enzymes, and other proteins and amino acids should be investigated for their roles in ice nuclei formation and destruction.

6.3.2 Avenues for Progress in the Genetic Sequencing of SSA

Chapter 3 develops a workflow for the 16S sequencing of SSA and demonstrates that seawater with different bacteria communities produce SSA with different bacteria communities. New methods for sampling aerosol and for genetic sequencing continually emerge and merit application to SSA. Droplet-based sequencing methods coupled to microfluidics are bringing online SSA sequencing closer to reality (Zilionis et al., 2017). Such advances stand to provide greater sensitivity and temporal insight into SSA community dynamics. How basic factors such as bacteria cell size affect bacteria transfer in SSA merit further investigation. If all factors that determine bacteria transfer rates in SSA could be resolved, then bacteria in SSA could be predicted and modeled from the SW community. If the climate roles bacteria play in the atmosphere could be resolved, then both the transfer of bacteria in SSA and their atmospheric roles could be predicted.

6.3.3 Gaining Further Insight in Coastal SSA Production, Transport, and Deposition

Chapter 4 utilizes a tracer dye to simulate coastal water pollution and to track its transport in the water, its transfer to the atmosphere in SSA, and its atmospheric transport. Additional tracer dye releases in the coastal waters could be tracked in the coastal aerosol with an emphasis on gaining spatio-temporal information. Online dye detection in the aerosol could potentially be accomplished with a modified Waveband Integrated Bioaerosol Sensor (WIBS) (Toprak & Schnaiter, 2013). A vertical sampling array could further detail the SSA population produced by the surfzone (de Leeuw et al., 2011). Multiple vertical sampling arrays could detail the coastal

aerosol population in three dimensions, but may be hindered by significant instrumentation requirements. Dye releases could be planned to coincide with CWP events that can be anticipated from weather forecasts. But tagging pollution sources with a dye would be difficult because turbidity in CWP plumes inhibits dye detection and it would be difficult to tag multiple pollution sources (Clark et al., 2009). Hyperspectral imaging, LIDAR, and related methods perhaps have greater potential for describing the spatial distribution of CWP transport and transfer in the ocean and atmosphere (Dierssen et al., 2021; Dreischuh et al., 2016; Knobelspiesse et al., 2020). A better understanding of spatio-temporal trends of SSA transport in the coastal environment would be useful in understanding atmospheric transport of polluted SSA and assessing associated risks.

6.3.4 Answering Unknowns About Coastal Water Pollution in SSA

Chapter 5 utilized 16S gene amplicon sequencing and non-targeted tandem mass spectrometry to identify bacterial and chemical evidence of coastal water pollution transferring to the atmosphere in SSA. Levels of exposure to CWP in SSA and associated risks need to be addressed. This evaluation requires quantitative measurements of pathogens and chemical contaminants in the ocean and atmosphere (Toze, 1999; Cancelada et al., 2022). More non-targeted chemical and biological analyses would also be beneficial to keeping a broad view of types of contaminants present. Linking toxins and pathogens to the CWP source would be valuable, and so would be comparisons between sites, with or without direct links to sources. These evaluations should be long enough in duration to cover variable environmental conditions and pollutant loadings in order to evaluate total exposure levels and fluctuations. Ideally, the efforts within this dissertation to identify tracers of CWP could be extended into quantitative measures of pollutant loadings in the ocean and air tied to specific sources. Much progress can

be made in the spatio-temporal characterization of pollutants in the Tijuana River, and other pollution sources in the region and elsewhere merit investigation (Zimmer-Faust et al., 2021). Ini addition, tracking pollution levels in the ocean and atmosphere will be necessary to evaluate the effectiveness of implemented infrastructure (Feddersen et al., 2021).

6.4 References

Arnosti, C. (2011). Microbial extracellular enzymes and the marine carbon cycle. *Annual Review of Marine Science*, 3, 401–425.

Bertram, T. H., Cochran, R. E., Grassian, V. H., & Stone, E. A. (2018). Sea spray aerosol chemical composition: elemental and molecular mimics for laboratory studies of heterogeneous and multiphase reactions. *Chemical Society Reviews*, 47(7), 2374–2400.

Cheng, Y. S., Zhou, Y., Irvin, C. M., Pierce, R. H., Naar, J., Backer, L. C., Fleming, L. E., Kirkpatrick, B., & Baden, D. G. (2005). Characterization of marine aerosol for assessment of human exposure to brevetoxins. *Environmental Health Perspectives*, 113(5), 638–643.

Cho, B. C., & Azam, F. (1988). Major role of bacteria in biogeochemical fluxes in the ocean's interior. *Nature*, 332(6163), 441–443. https://doi.org/10.1038/332441a0

Clark, D. B., Feddersen, F., Omand, M. M., & Guza, R. T. (2009). Measuring Fluorescent Dye in the Bubbly and Sediment-Laden Surfzone. Water, Air, and Soil Pollution, 204(1-4), 103–115.

de Leeuw, G., Andreas, E. L., Anguelova, M. D., Fairall, C. W., Lewis, E. R., O'Dowd, C., Schulz, M., & Schwartz, S. E. (2011). Production flux of sea spray aerosol. *Reviews of Geophysics*, 49(2). https://doi.org/10.1029/2010rg000349

Dierssen, H. M., Ackleson, S. G., Joyce, K. E., Hestir, E. L., Castagna, A., Lavender, S., & McManus, M. A. (2021). Living up to the hype of hyperspectral aquatic remote sensing: Science, resources and outlook. *Frontiers of Environmental Science & Engineering in China*, 9. https://doi.org/10.3389/fenvs.2021.649528

Dreischuh, T., Grigorov, I., Peshev, Z., Deleva, A., Kolarov, G., & Stoyanov, D. (2016). Lidar mapping of near-surface aerosol fields. In *Aerosols - Science and Case Studies*. InTech.

Feddersen, F., Boehm, A. B., Giddings, S. N., Wu, X., & Liden, D. (2021). Modeling Untreated Wastewater Evolution and Swimmer Illness for Four Wastewater Infrastructure Scenarios in the San Diego-Tijuana (US/MX) Border Region. *GeoHealth*, 5(11), e2021GH000490.

Graham, K. E., Prussin, A. J., 2nd, Marr, L. C., Sassoubre, L. M., & Boehm, A. B. (2018). Microbial community structure of sea spray aerosols at three California beaches. *FEMS Microbiology Ecology*, 94(3). https://doi.org/10.1093/femsec/fiy005

Harb, C., Pan, J., DeVilbiss, S., Badgley, B., Marr, L. C., Schmale, D. G., 3rd, & Foroutan, H. (2021). Increasing Freshwater Salinity Impacts Aerosolized Bacteria. *Environmental Science & Technology*, 55(9), 5731–5741.

Hejkal, T. W., Larock, P. A., & Winchester, J. W. (1980). Water-to-Air Fractionation of Bacteria. *Applied and Environmental Microbiology*, 39(2), 335–338.

Hoppe, H.-G. (1983). Significance of exoenzymatic activities in the ecology of brackish water: measurements by means of methylumbelliferyl-substrates. *Marine Ecology Progress Series*, 11, 299–308. DOI: 10.3354/meps011299

Hudait, A., Odendahl, N., Qiu, Y., Paesani, F., & Molinero, V. (2018). Ice-Nucleating and Antifreeze Proteins Recognize Ice through a Diversity of Anchored Clathrate and Ice-like Motifs. *Journal of the American Chemical Society*, 140(14), 4905–4912.

Johansson, J. H., Salter, M. E., Acosta Navarro, J. C., Leck, C., Nilsson, E. D., & Cousins, I. T. (2019). Global transport of perfluoroalkyl acids via sea spray aerosol. *Environmental Science. Processes & Impacts*, 21(4), 635–649.

Knobelspiesse, K., Barbosa, H. M. J., Bradley, C., Bruegge, C., Cairns, B., Chen, G., Chowdhary, J., Cook, A., Di Noia, A., van Diedenhoven, B., Diner, D. J., Ferrare, R., Fu, G., Gao, M., Garay, M., Hair, J., Harper, D., van Harten, G., Hasekamp, O., Helmlinger, M., Hostetler, C., Kalashnikova, O., Kupchok, A., De Freitas, K. L., Maring, H., Martins, J. L., McBride, B., McGill, M., Norlin, K., Puthukkudy, A., Rheingans, B., Rietjens, J., Seidel, F. C., da Silva, A., Smit, M., Stammes, S., Tan, Q., Val, S., Wasilewski, A., Xu, F., Xu., X., & Yorks, J. (2020). The Aerosol Characterization from Polarimeter and Lidar (ACEPOL) airborne field campaign. *Earth System Science Data*, 12(3), 2183–2208.

Malfatti, F., Lee, C., Tinta, T., Pendergraft, M. A., Celussi, M., Zhou, Y., Sultana, C. M., Rotter, A., Axson, J. L., Collins, D. B., Santander, M. V., Anides Morales, A. L., Aluwihare, L. I., Riemer, N., Grassian, V. H., Azam, F., & Prather, K. A. (2019). Detection of active microbial enzymes in nascent sea spray aerosol: Implications for atmospheric chemistry and climate. *Environmental Science & Technology Letters*, 6(3), 171–177.

Martinez, J., Smith, D. C., Steward, G. F., & Azam, F. (1996). Variability in ectohydrolytic enzyme activities of pelagic marine bacteria and its significance for substrate processing in the sea. *Aquatic Microbial Ecology: International Journal*, 10(3), 223–230.

Mazzotta, M. G., McIlvin, M. R., & Saito, M. A. (2020). Characterization of the Fe metalloproteome of a ubiquitous marine heterotroph, Pseudoalteromonas (BB2-AT2): multiple bacterioferritin copies enable significant Fe storage. *Metallomics: Integrated Biometal Science*, 12(5), 654–667.

Quinn, P. K., Collins, D. B., Grassian, V. H., Prather, K. A., & Bates, T. S. (2015). Chemistry and related properties of freshly emitted sea spray aerosol. *Chemical Reviews*, 115(10), 4383–4399.

Schäfer, A., Harms, H., & Zehnder, A. J. B. (1998). Bacterial Accumulation at the Air−Water Interface. *Environmental Science & Technology*, 32(23), 3704–3712). DOI: 10.1021/es980191u

Smith, D. C., Simon, M., Alldredge, A. L., & Azam, F. (1992). Intense hydrolytic enzyme activity on marine aggregates and implications for rapid particle dissolution. *Nature*, 359(6391), 139–142.

Stokes, M. D., Deane, G. B., Prather, K., Bertram, T. H., Ruppel, M. J., Ryder, O. S., Brady, J. M., & Zhao, D. (2013). A Marine Aerosol Reference Tank system as a breaking wave analogue for the production of foam and sea-spray aerosols. *Atmospheric Measurement Techniques*, 6(4), 1085–1094.

Toprak, E., & Schnaiter, M. (2013). Fluorescent biological aerosol particles measured with the Waveband Integrated Bioaerosol Sensor WIBS-4: laboratory tests combined with a one year field study. *Atmospheric Chemistry and Physics*, 13(1), 225–243.

Toze, S. (1999). PCR and the detection of microbial pathogens in water and wastewater. *Water Research*, 33(17), 3545–3556. DOI: 10.1016/s0043-1354(99)00071-8

Zilionis, R., Nainys, J., Veres, A., Savova, V., Zemmour, D., Klein, A. M., & Mazutis, L. (2017). Single-cell barcoding and sequencing using droplet microfluidics. *Nature Protocols*, 12(1), 44–73.

Zimmer-Faust, A. G., Steele, J. A., Xiong, X., Staley, C., Griffith, M., Sadowsky, M. J., Diaz, M., & Griffith, J. F. (2021). A Combined Digital PCR and Next Generation DNA-Sequencing Based Approach for Tracking Nearshore Pollutant Dynamics Along the Southwest United States/Mexico Border. *Frontiers in Microbiology*, 12, 674214.